

**ANALYTICAL APPLICATIONS OF THE PEROXYOXALATE
CHEMILUMINESCENCE REACTION**

By

MATTHEW GRAHAM SANDERS

A thesis submitted to the University of Plymouth

in partial fulfilment for the degree of

DOCTOR OF PHILOSOPHY

Department of Environmental Sciences

Faculty of Science

In collaboration with

Shell Research Limited,

Shell Research and Technology Centre, Thornton, Chester.

June 1999

REFERENCE ONLY

LIBRARY STORE

UNIVERSITY OF PLYMOUTH	
Item No.	9004013645
Date	24 SEP 1999 S
Class No.	T 547.83046 SAN
Contl. No.	X703934383
LIBRARY SERVICES	

90 0401364 5



ABSTRACT

ANALYTICAL APPLICATIONS OF THE PEROXYOXALATE CHEMILUMINESCENCE REACTION

Matthew Graham Sanders

The overall objectives of this thesis were to investigate the potential of the peroxyoxalate chemiluminescence (POCL) reaction for the quantitative detection of target analytes in non-aqueous matrices and to compare quantitative performance with fluorescence detection. The target analytes investigated were polycyclic aromatic hydrocarbons (PAHs) and aliphatic amines. These were selected as an important class of compounds in engine exhaust emissions and a detergent additive in diesel fuel respectively.

Chapter one outlines the challenges of analysing petroleum products and engine exhaust emissions and discusses the potential of luminescence techniques, particularly chemiluminescence (CL), for the quantification of trace components. The chapter also reviews the technique of flow injection (FI) as a means of sample delivery for CL detection and as a potential technique for field deployment. Liquid chromatography techniques are described as a means of separation of complex matrices, e.g. fuels and engine exhaust particulates, in the laboratory prior to CL detection.

The luminescence properties of several PAHs were investigated in Chapter Two. Optimum excitation and emission wavelengths for eleven PAHs in four different solvents were determined using a batch fluorescence technique. A FI approach was used to determine PAH concentrations using fluorescence and POCL detection. Two aryl oxalates; bis(2,4-dinitrophenyl)oxalate and bis(2,4,6-trichlorophenyl)oxalate were compared for their suitability for PAH determinations and an investigation of the key variables (e.g. concentration of aryl oxalate and hydrogen peroxide, mobile phase composition and pH) affecting POCL was performed. Recommendations for the optimum conditions for the determination of PAHs by POCL detection were determined. A comparison between a photodiode based detection device and a low power (12V) photomultiplier tube was also described.

In Chapter Three the procedure of using POCL detection as a post column liquid chromatography (LC) detector for PAHs has been considered. The performance of the POCL detection system was compared with wavelength programmed fluorescence. Both reversed and normal phase LC was investigated and the suitability of POCL detection with each approach was discussed. Additionally the procedure for the LC separation and analysis of SRM 1649 (*Urban Dust/Organics*) and SRM 1650 (*Diesel Particulate Matter*) was described. The relative performance of fluorescence and CL detection are discussed.

Chapter four describes the principles of multivariate calibration of spectrophotometric data, and three commonly applied techniques (PCR, PLS1 and PLS2). Fluorescence data was obtained for synthetic mixtures of PAHs containing two, three, four and five components. A procedure whereby individual spectra were 'glued' together before undergoing data analysis has been developed and the results obtained discussed. POCL emission spectra for five PAHs were acquired using a two-dimensional charge coupled device (CCD). The sensitivity of the CCD system toward POCL detection of PAHs and a multivariate investigation using benzo[*a*]pyrene and benzo[*k*]fluoranthene has been described. The potential of the fluorescence and CL approaches used has been discussed.

Chapter five describes the aryl oxalate sulphorhodamine-101 CL reaction and its application to the determination of amines. A FI optimisation of the reaction parameters is presented together with some quantitative data for the detection of a homologous series of amines and dodecylamine (a commonly added detergent compound in diesel fuels). The application of the technique toward the detection of dodecylamine in a diesel fuel matrix and the potential as a field deployable technique was also considered.

ACKNOWLEDGEMENTS

First and foremost, I would like to offer my sincere thanks to Professor Paul Worsfold for his guidance and support during the course of this research and for the pressure applied in order to make this thesis a reality. Many thanks are also due to the other members of my academic supervisory team, Dr Kevin Andrew and Dr Mike Rhead.

I would like to register my gratitude to Shell Research and Technology Centre, Thornton, Shell Research Limited, for the provision of the extramural research grant that funded this work. A very big thank you to my industrial supervisors, Dr Stuart Forbes and Mr Euan McKerrell, and to all that I had the pleasure of meeting during my visits to Thornton.

I would like to thank my colleagues from Davy 102, but being the only one sent into exile within its four walls this is not possible. Instead, thanks to everyone I have worked with during my time in Plymouth, past and present, including Robby Rob (boro boy!), Trevy Trev (ginger warrior!), Phil (cobblers!), Neil, Hefty, Daz, Andy, Rich, and Simon. To those of you following in my writing up footsteps I must apologise, as I seem to have worn the thumbscrews out.

Thanks also to all the foreigners that introduced a somewhat international flavour to the lab, especially Manuel, Crispy Cris, Cristina (chorizo chica) and Paulo. I must also thank everyone else in the Department of Environmental Sciences, especially the support staff.

Thank you to my parents for all their love and support, and to my sister who always lands on her feet. By the way Mum, whatever happened to that rest I was supposed to be working towards, right back when studying for my GCSE exams?

Finally I would like to thank Claire who has stuck by me through thick and thin. You must have worried about what you had let yourself in for when you said yes that November night in Paris. I would never have made it through the storm without your guiding light.

AUTHORS DECLARATION

At no time during the registration for the degree of Doctor of Philosophy has the author been registered for any other University award.

The study was financed with the aid of an extramural research grant from Shell Research Limited, Shell Research and Technology Centre, Thornton, Chester.

The work described in this thesis has entirely been carried out by the author. Relevant scientific seminars and conferences were regularly attended at which work was presented, external institutions were visited for consultation purposes, and several papers were prepared for publication.

Signed.....*M. Sanders*.....

Date.....10TH JUNE 1999.....

TABLE OF CONTENTS

<i>Abstract</i>	i
<i>Acknowledgements</i>	ii
<i>Authors declaration</i>	iii
<i>List of tables</i>	viii
<i>List of figures</i>	xi

Chapter 1 INTRODUCTION

1.1 ANALYSIS OF PETROLEUM PRODUCTS.....	1
1.2 LUMINESCENCE SPECTROMETRY.....	4
1.2.1 Photoluminescence.....	4
1.2.2 Fluorescence.....	6
1.2.3 Phosphorescence.....	7
1.2.4 Structural and environmental effects on photoluminescence.....	7
1.2.5 Chemiluminescence.....	10
1.2.6 Bioluminescence.....	13
1.2.7 Instrumentation for CL detection.....	14
1.3 FLOW INJECTION ANALYSIS.....	17
1.3.1 Basic principles.....	17
1.3.2 Dispersion coefficient (D).....	19
1.3.3 Factors affecting dispersion.....	20
1.3.4 Detectors for FI applications.....	21
1.3.5 Applications of FI-CL to inorganic species.....	22
1.3.6 Applications of FI-CL to organic species.....	29
1.4 CHROMATOGRAPHY.....	38
1.4.1 Basic principles.....	38
1.4.2 High performance liquid chromatography.....	39

1.4.3	Chromatographic parameters.....	41
1.4.4	Detectors for HPLC.....	44
1.4.5	Analytical applications of LC with CL detection.....	47
1.5	RESEARCH OBJECTIVES.....	55

Chapter 2 DETERMINATION OF PAHs USING FLOW INJECTION WITH FLUORESCENCE AND PEROXYOXALATE CHEMILUMINESCENCE DETECTION

2.1	INTRODUCTION.....	56
2.2	EXPERIMENTAL.....	56
2.2.1	Reagents.....	56
2.2.2	Instrumentation and procedures.....	57
2.3	RESULTS AND DISCUSSION.....	61
2.3.1	Fluorescence properties of PAHs obtained using a batch fluorimeter.....	61
2.3.2	FI determination of PAHs using FL detection.....	69
2.3.3	FI determination of PAHs using POCL detection.....	70
2.3.4	A comparison of FL and POCL detection methods.....	85
2.4	CONCLUSIONS.....	85

Chapter 3 DETERMINATION OF PAHs USING LIQUID CHROMATOGRAPHY WITH FLUORESCENCE AND PEROXYOXALATE CHEMILUMINESCENCE DETECTION

3.1	INTRODUCTION.....	87
3.2	EXPERIMENTAL.....	87
3.2.1	Reagents.....	87
3.2.2	Instrumentation and procedures.....	88
3.3	RESULTS AND DISCUSSION.....	93

3.3.1	Occurrence and properties of polycyclic aromatic hydrocarbons.....	93
3.3.2	RP-LC determination of PAHs with FL detection.....	97
3.3.3	RP-LC determination of PAHs in SRMs with FL detection.....	103
3.3.4	RP-LC analysis of PAHs with POCL detection.....	110
3.3.5	NP-LC analysis of PAHs with POCL detection.....	115
3.3.6	Comparison of the detection systems.....	117
3.4	CONCLUSIONS.....	118

Chapter 4 DETERMINATION OF PAHs USING MULTIVARIATE CALIBRATION WITH FLUORESCENCE AND PEROXYOXALATE CHEMILUMINESCENCE DETECTION

4.1	INTRODUCTION.....	119
4.2	EXPERIMENTAL.....	120
4.2.1	Reagents.....	120
4.2.2	Instrumentation and procedures.....	120
4.3	RESULTS AND DISCUSSION.....	125
4.3.1	Data pre-processing techniques.....	125
4.3.2	Multivariate calibration routines.....	126
4.3.3	FL investigation.....	131
4.3.4	CL investigation.....	141
4.4	CONCLUSIONS.....	151

Chapter 5 DETERMINATION OF AMINES USING FLOW INJECTION WITH ARYL-OXALATE SULPHORHODAMINE 101 CHEMILUMINESCENCE DETECTION

5.1	INTRODUCTION.....	152
5.2	EXPERIMENTAL.....	153
5.2.1	Reagents.....	153
5.2.2	Instrumentation and procedures.....	154

5.3	RESULTS AND DISCUSSION.....	156
5.3.1	The aryl oxalate-sulphorhodamine 101 reaction.....	156
5.3.2	Optimisation of reaction conditions for CL emission.....	158
5.3.3	Limits of detection.....	168
5.3.4	Application to a diesel fuel matrix.....	170
5.4	CONCLUSIONS.....	172

Chapter 6 CONCLUSIONS AND FUTURE WORK

6.1	GENERAL CONCLUSIONS.....	173
6.2	SUGGESTIONS FOR FUTURE WORK.....	175

REFERENCES.....	177
------------------------	------------

APPENDICES

1	Concentration (mg l ⁻¹) data for the 2 component FL calibration and test set.....	190
2	Concentration (mg l ⁻¹) data for the 3 component FL calibration and test set.....	191
3	Concentration (mg l ⁻¹) data for the 4 component FL calibration and test set.....	192
4	Concentration (mg l ⁻¹) data for the 5 component FL calibration and test set.....	193
5	Concentration (mg l ⁻¹) data for the 5 component sample simulation FL calibration and test set.....	195
6	Concentration (mg l ⁻¹) data for the 2 component CL calibration and test set.....	197
7	Publications.....	198
8	Presentations.....	199
9	Conferences and courses attended.....	200

LIST OF TABLES

1.1	Glossary of luminescence.....	5
1.2	Spectroscopic parameters of η , π^* and π , π^* transitions.....	8
1.3	Effect of substituents on fluorescence of benzene.....	9
1.4	Properties of chemiluminescence reactions.....	11
1.5	Commonly used detectors for FI.....	21
1.6	Flow injection chemiluminescence applications for the determination of inorganic species.....	23
1.7	Flow injection chemiluminescence applications for the determination of organic species.....	30
1.8	Classification of chromatographic methods.....	38
1.9	Chromatographic parameters.....	42
1.10	Sources of band broadening in LC.....	43
1.11	Characteristics of common detectors for HPLC.....	46
1.12	Liquid chromatography chemiluminescence applications.....	49
2.1	Instrument parameter settings for F-4500.....	58
2.2	Optimum excitation and emission wavelengths for PAHs in ACN.....	61
2.3	Excitation wavelengths, emission wavelengths and intensities for 11 PAHs in four different solvents.....	68
2.4	Selected wavelengths for monitoring PAHs in ACN by FL detection.....	69
2.5	Limits of detection for six PAH compounds by FI-FL.....	69
2.6	Structures of analytically useful aryl oxalates.....	72
2.7	Comparison of DNPO and TCPO reagents.....	73
2.8	Experimentally optimised conditions for the PO-CL detection of PAHs.....	82
2.9	Limits of detection for six PAH compounds by FI-CL.....	83
2.10	LODs of PAHs using FI with FL and CL detection.....	85

3.1	Certified values for PAHs in SRM 1649 and SRM 1650.....	88
3.2	Characteristics of the columns used for RP-LC separation of PAHs.....	90
3.3	Mobile phase gradient used for RP separation.....	90
3.4	Wavelength programme used for programmed FL detection.....	92
3.5	Major anthropogenic sources of PAH.....	93
3.6	Relative carcinogenicity index for some PAHs.....	95
3.7	Retention times of PAHs using three different columns.....	101
3.8	Summary of results obtained for extraction of SRM 1649.....	104
3.9	Concentrations of PAHs found for SRM 1649 using LC-FL.....	106
3.10	Summary of results obtained for extraction of SRM 1650.....	107
3.11	Concentrations of PAHs found for SRM 1650 using LC-FL.....	109
3.12	Response data for the seven PAHs detected using post column PO-CL detection (1000 $\mu\text{g l}^{-1}$).....	111
3.13	Response data for the five PAHs detected in SRM 1649 using post column PO-CL detection.....	112
3.14	Concentrations of PAHs found for SRM 1649 using LC-CL.....	113
3.15	Response data for the five PAHs detected in SRM 1650 using post column PO-CL detection.....	114
3.16	Concentrations of PAHs found for SRM 1650 using LC-CL.....	114
3.17	Mobile phase gradient used for NP separation.....	115
3.18	Response data for the PAHs detected using post column PO-CL detection with NP-LC separation (1000 $\mu\text{g l}^{-1}$).....	116
4.1	Instrument settings for fluorescence spectrophotometer.....	121
4.2	Summary of the design of factorial models.....	121
4.3	Optimum excitation and emission wavelengths for PAHs in ACN.....	131
4.4	Calibration and test set design for solutions used to simulate a real sample (SRM 1650 values shown for reference).....	141

4.5	Peak maxima and peak1:peak2 height ratio for the five PAH compounds in acetonitrile and hexane solutions.....	145
4.6	Limits of detection for three PAHs in hexane solution, using the continuous flow system with CCD detection.....	146
5.1	Common additive types and typical composition.....	152
5.2	Parameter settings for F-4500 fluorescence spectrophotometer.....	154
5.3	Optimum conditions determined for detection of amines.....	167
5.4	Comparison of experimentally obtained reaction conditions with literature values.....	168
5.5	Details of amines investigated.....	168
5.6	Detection limits of amines investigated.....	169
5.7	Comparison of experimentally obtained LODs with literature.....	169

LIST OF FIGURES

1.1	Typical uses of petrochemicals.....	1
1.2	Typical fractions of crude oil.....	2
1.3	Partial energy diagram for a photoluminescent system.....	6
1.4	Structural comparison of fluorene and biphenyl.....	9
1.5	Schematic of the luminol CL reaction.....	12
1.6	Schematic of the peroxyoxalate CL reaction.....	13
1.7	Firefly bioluminescence reaction.....	13
1.8	Schematic diagram of the bacterial luciferase/NAD(P)H reaction.....	14
1.9	Schematic layout of a typical CCD chip.....	15
1.10	General scheme of a simple FI manifold.....	17
1.11	Chart recorder output; where I is the point of injection, H is the peak height, W is the peak width and T is the residence time.....	18
1.12	Typical flow injection manifold for chemiluminescence applications.....	22
1.13	Typical layout of major components for HPLC.....	39
1.14	Typical liquid chromatography manifold for PO-CL applications.....	48
2.1	FI manifold with FL detection for the determination of PAHs.....	59
2.2	FI manifold for the investigation of the POCL reaction.....	60
2.3	(a-c) Experimentally acquired emission and excitation fluorescence spectra of PAHs dissolved in ACN solvent at a concentration of 100ppb.....	62
2.4	Structures of the 12 PAHs used for the FL investigation.....	65
2.5	Spectra observed for benzo[<i>k</i>]fluoranthene in four different solvents.....	66
2.6	Spectra observed for benzo[<i>a</i>]anthracene in four different solvents.....	67
2.7	POCL mechanism as originally proposed by Rauhut <i>et al</i>	70
2.8	The proposed CIEEL mechanism for energy transfer.....	71

2.9	Effect of water on the CL emission intensity for the two reagents (a) DNPO and (b) TCPO.....	74
2.10	Effect of water on the CL emission intensity for DNPO and TCPO.....	75
2.11	Reported structures of disulfide oxamides.....	76
2.12	Scheme of the proposed reaction between imidazole and an aryl oxalate ester to form the intermediate 1,2-dioxetanedione.....	76
2.13	Effect of imidazole on the CL emission intensity for DNPO.....	77
2.14	Effect of imidazole on the CL emission intensity for TCPO.....	78
2.15	Effect of imidazole on the CL emission intensity for DNPO and TCPO plotted as imidazole concentration against signal-to-noise.....	78
2.16	Effect of H ₂ O ₂ on the CL emission intensity for DNPO and TCPO plotted as H ₂ O ₂ concentration against signal-to-noise.....	79
2.17	Effect of pH on the CL emission intensity for DNPO.....	80
2.18	Effect of pH on the CL emission intensity for TCPO.....	81
2.19	Effect of pH on the CL emission intensity for DNPO and TCPO plotted as pH against signal-to-noise.....	81
2.20	Typical spectral response of (a) photodiodes and (b) low power PMT that are commercially available.....	82
3.1	LC manifold for the detection of PAHs with FL and POCL detection.....	91
3.2	Pyrosynthesis of benzo[<i>a</i>]pyrene.....	94
3.3	Enzymatic activation of benzo[<i>a</i>]pyrene.....	95
3.4	Bay region containing PAHs and related dihydrodiol epoxides.....	96
3.5	Separation of 16 PAH test mixture using Spherisorb S5 PAH column using System I.....	97
3.6	Structures of the 16 PAHs identified as priority pollutants by the EPA.....	98
3.7	Chromatogram of 16 PAH test mixture using programmed FL detection.....	99
3.8	Chromatogram of 16 PAH test mixture using UV ($\lambda=230\text{nm}$) detection.....	100

3.9	Synthesis of a) monomeric and b) polymeric type bonded phases	102
3.10	LC chromatogram of SRM 1649 using programmed FL detection	105
3.11	Chromatogram of SRM 1650 (Diesel Particulate Matter) using programmed FL detection	108
3.12	Chromatogram of background signal (blank) using RPLC with post column PO-CL detection	110
3.13	Chromatogram of 16 PAH test mixture using post column PO-CL detection	111
3.14	Chromatogram of SRM 1649 (Urban Dust Organic Extract) using post column PO-CL detection	112
3.15	Structure of the tetrachlorophthalimidopropyl bonded silica support	115
3.16	Chromatogram of 16 PAH test mixture using NP-LC and CL detection	116
4.1	Schematic to show the process of joining spectra together in series	122
4.2	Schematic diagram of the continuous flow manifold used for CL-CCD determination of PAHs	123
4.3	Display of regression overview (a) standard Unscrambler overview (b) preferred overview used	130
4.4	Prediction errors for the two-component system using single wavelength (250 nm) excitation method	132
4.5	Prediction errors for the two-component system using dual wavelength (250 nm and 306 nm) excitation method with spectral gluing	133
4.6	Prediction errors for the three-component system using single compromise wavelength (252 nm) excitation method	134
4.7	Prediction errors for the three-component system using multiple wavelength (247 nm, 306 nm and 264 nm) excitation method with spectral gluing	135
4.8	Prediction errors for the four-component system	136

4.9	Overlay of 'glued' emission spectra for the 2 ⁵ factorial 5-component calibration samples.....	137
4.10	Prediction errors for the five-component system using PCs as recommended by the software.....	138
4.11	Prediction errors for the five-component system using PCs giving the lowest RRMSEP value.....	139
4.12	Prediction errors for the five-component system based on concentrations expected in a real sample.....	141
4.13	Structural formulae of benzo[<i>b</i>]fluoranthene, benzo[<i>k</i>]fluoranthene, benzo[<i>a</i>]pyrene, benzo[<i>g,h,i</i>]perylene and perylene.....	142
4.14	Chemiluminescence spectra for benzo[<i>b</i>]fluoranthene (i), benzo[<i>k</i>]fluoranthene (ii), benzo[<i>a</i>]pyrene (iii), benzo[<i>g,h,i</i>]perylene (iv) and perylene (v): (a) 20 mg l ⁻¹ solutions in acetonitrile; (b) 1 mg l ⁻¹ solutions (0.1 mg l ⁻¹ for perylene) in hexane.....	143
4.15	CL spectra of a 2 component mixture showing effect of different degrees of smoothing.....	146
4.16	PCR prediction errors for a two-component system showing the effects of different degrees of smoothing.....	147
4.17	Chemiluminescence spectra for the benzo[<i>a</i>]pyrene/ benzo[<i>k</i>]fluoranthene two-component system: (a) calibration set; (b) test set.....	148
4.18	Prediction errors for the two-component system.....	149
4.19	Scores plot for the PCR calibration model showing two possible outliers....	149
4.20	Prediction errors for the two-component system with 'outliers' removed from the calibration model.....	150
5.1	FI manifold for the investigation of the sulphorhodamine 101 POCL reaction.....	155
5.2	The structure and properties of sulphorhodamine 101.....	156

5.3	Spectra of sulphorhodamine 101 in ACN showing a) 3D scanning FL spectrum, b) FL excitation spectrum and c) FL emission spectrum.....	157
5.4	Effect of mixing coil length on the CL signal and peak-to-peak noise.....	159
5.5	Effect of mixing coil length on the CL signal-to-noise and relative standard deviation.....	159
5.6	Time/intensity profile to illustrate the time window concept and how this is related to the length of the mixing coil.....	160
5.7	Effect of water content of mobile phase on the CL signal and peak-to-peak noise.....	161
5.8	Effect of water content of mobile phase on the CL signal-to-noise and relative standard deviation.....	162
5.9	Effect of H ₂ O ₂ on the CL signal and peak-to-peak noise.....	163
5.10	Effect of H ₂ O ₂ on the CL signal-to-noise and relative standard deviation....	164
5.11	Effect of DNPO concentration on the CL signal and peak-to-peak noise.....	165
5.12	Effect of DNPO concentration on the CL signal-to-noise and relative standard deviation.....	165
5.13	Effect of sulphorhodamine 101 concentration on the observed CL signal and peak-to-peak noise.....	166
5.14	Effect of sulphorhodamine 101 concentration on the CL signal-to-noise and relative standard deviation.....	167
5.15	Typical SPE sequence.....	171
5.16	Commercially available polar SPE cartridges.....	172

CHAPTER 1

Introduction

1. INTRODUCTION

1.1. ANALYSIS OF PETROLEUM PRODUCTS

Crude oil or 'petroleum' is perhaps the most useful and versatile natural resource that has become available for exploitation. The price of crude oil and ensuring a supply of crude oil have come to dominate modern economic thinking and modern industrial planning. Oil accounts for approximately 40 per cent of the world energy market. In 1997 the average total world oil supply was 74.1 million barrels per day (b/d) [1]. Modern industrial societies use it primarily to achieve a degree of motability – on land, at sea, and in the air - that was barely imaginable less than one hundred years ago. As well as being a major source of fuels, the chemical industry it supplies is responsible for the manufacture of thousands of products, which satisfy the basic needs of modern society and also provide its luxury and leisure consumer items (Figure 1.1.).

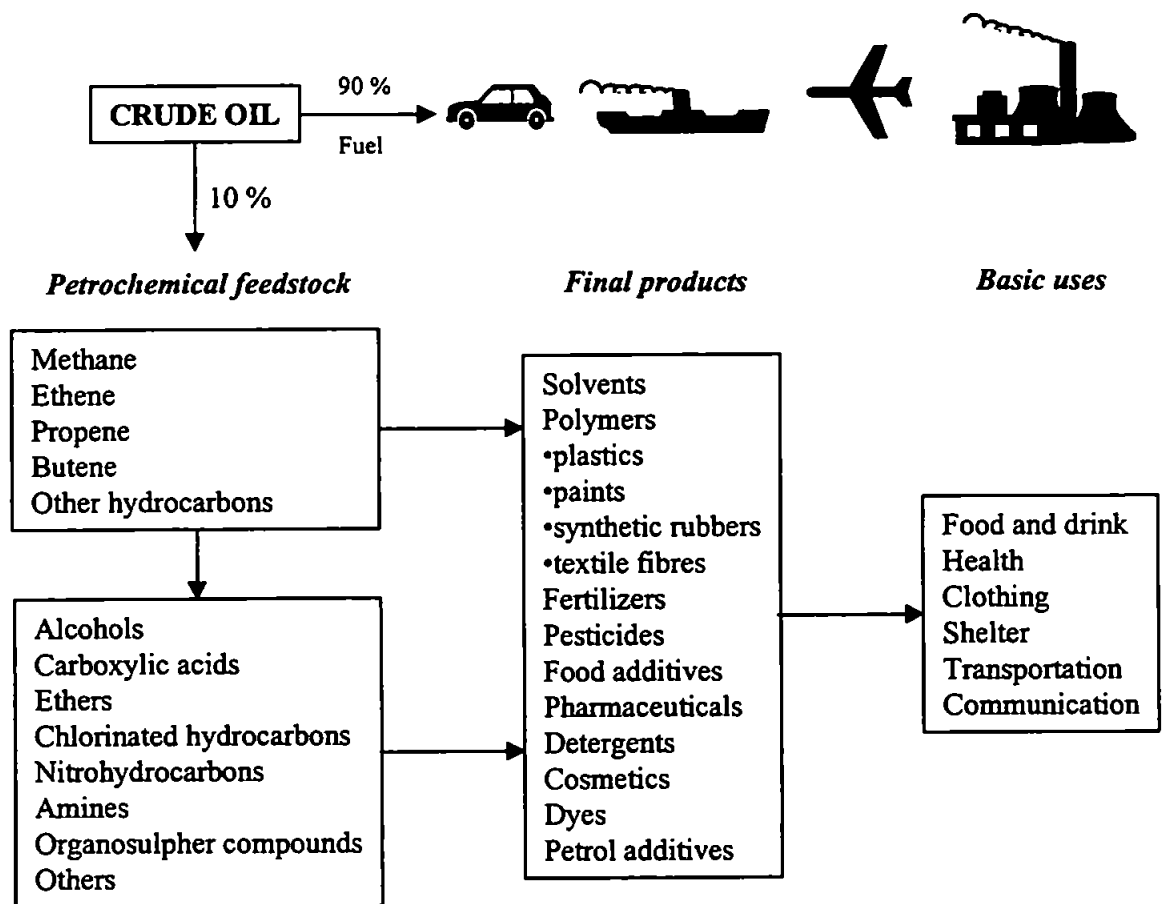


Figure 1.1. Typical uses of petrochemicals [2].

Petroleum is a complex mixture of hydrocarbons and other compounds and has to be refined into products that are useful for downstream processing (Figure 1.2.); including petrol and diesel fuels. Refining oil involves a number of physical and chemical processes including; fractional distillation, cracking, reforming and sulfur removal.

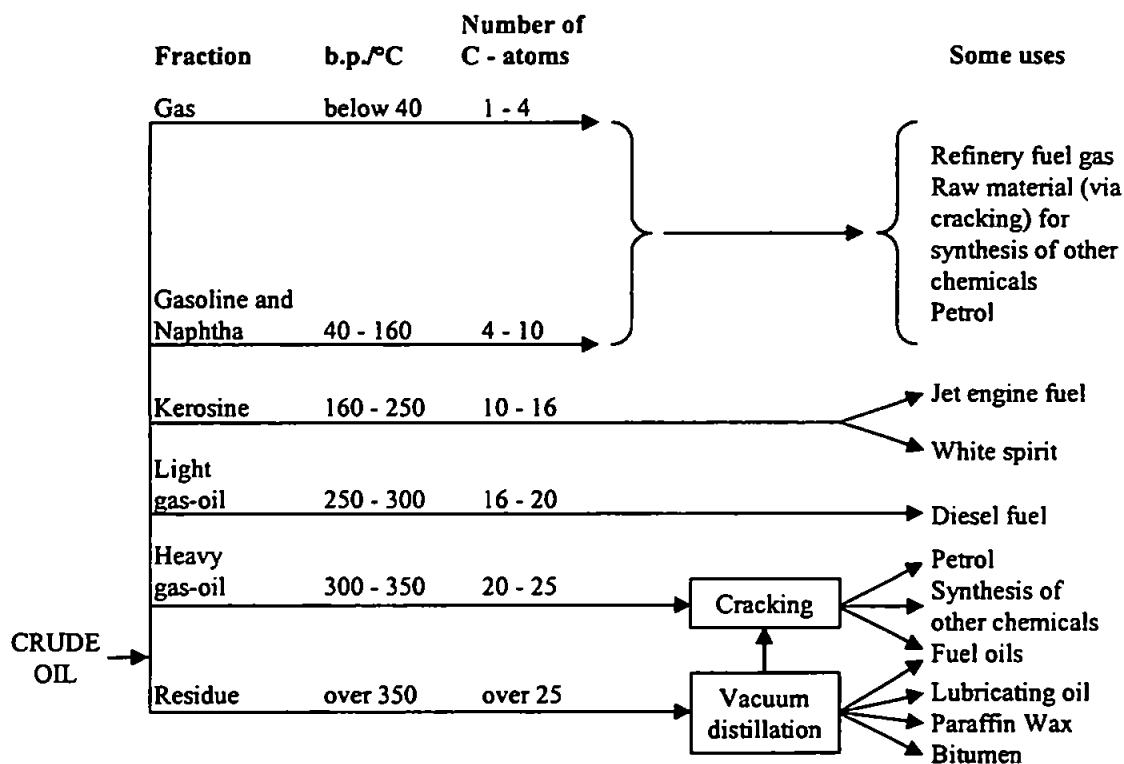


Figure 1.2. Typical fractions of crude oil [2].

In order to maximise the efficiency of fuels it is often necessary to introduce performance enhancing additives, such as detergents, ignition improvers, corrosion inhibitors, lubricity agents and foam inhibitors. The end products of the petroleum industry are therefore a wide range of complex, non-aqueous matrices. Whilst the major hydrocarbon components are relatively easy to determine, the characterisation and quantification of additives in fuels and other downstream products presents a major analytical challenge for the following reasons:

1. Most additives are present at relatively low concentrations in the fuel. Detergents and ignition improvers will typically be dosed in fuel at 200-500 ppm levels, lubricity agents at 100-200 ppm levels and corrosion inhibitors, antifoams and dehazers at 5-10 ppm levels.

2. Most additives are not single chemical entities but mixtures of compounds having broadly similar structures.
3. Fuel is not a standard matrix because its composition is clearly dependent on the source of crude oil from which the fuel is derived and the refining processes used to manufacture the fuel. For example, heavily cracked fuel is very different from straight run distillate.

It is also important to be able to monitor the impact of using petroleum based fuels, particularly with regard to the emission of combustion products into the atmosphere from engines. Major components of engine exhausts, e.g. nitrous oxides (NO_x) and sulfur dioxide (SO_2), are relatively easy to determine and are extensively monitored, particularly in urban areas, due to their impact on air quality and global warming. Other parameters such as lead compounds and particulate matter (PM_{10}) are also widely monitored due to their implication on air quality and health.

Trace components of the emissions, such as polycyclic aromatic hydrocarbons (PAHs) and their metabolites, are more difficult to determine for the following reasons:

1. PAHs are present at low concentrations in the combustion products of fuels compared with the other components present in the emissions. Typical concentrations would be in the low ppm range.
2. Due to the large number of chemical reactions that take place in a combustion process the mixtures of PAHs produced are extremely complex. The PAHs encountered in air particulate samples would typically include numerous isomeric structures and various other substituted PAH.
3. Sample handling presents difficulties due to the toxicity and potential carcinogenicity of the sample.

A wide spectrum of analytical techniques is used to meet the challenges described above. For quantification luminescence techniques, e.g. fluorescence and CL, provide relatively selective and sensitive detection. FI techniques can be used to provide rapid, reproducible sample presentation to the detector and are potentially suited to field deployment. More complex matrices require liquid chromatographic techniques for the separation of trace components prior to fluorescence or CL detection.

1.2. LUMINESCENCE SPECTROMETRY

Luminescence spectrometry is a widely used technique in analytical chemistry and is defined as [3],

“the emission of ultraviolet (UV), visible or near infrared (NIR) radiation from a molecule or an atom resulting from the transition of an electronically excited state to a lower energy state (usually the ground state).”

The procedure by which this excited state is reached defines the type of luminescence occurring, as summarised in Table 1.1.

Fluorescence, phosphorescence, chemiluminescence and bioluminescence are the four most common types of luminescence techniques used for analytical purposes. Fluorescence continues to be used most often although other luminescence techniques are finding more widespread application. The theory and applications of luminescence spectrometry have been reviewed in a number of publications [4-6].

It is due to their inherent sensitivity and wide dynamic ranges that luminescence methods are analytically attractive. The main disadvantage is their low applicability compared with absorbance methods because of the relatively limited number of species that show luminescence. Detection therefore often requires the derivatisation of the analyte species in order that luminescence methods can be applied.

1.2.1. Photoluminescence

The electronic transitions occurring in a molecule after absorption of UV or visible radiation can be represented by a Jablonski diagram (Figure 1.3.).

Most organic compounds in the ground state contain a pair of electrons in the occupied orbitals. Each of the electrons has opposing spin, according to the Pauli Exclusion Principle, and is said to be in a condition known as the singlet state. The molecule is raised to an excited singlet state on absorption of UV or visible radiation. The nuclei of the molecule are considered to be stationary (Franck-Condon Principle) due to the speed of this transition (10^{-15} s).

Table 1.1 Glossary of luminescence.

Luminescence	The emission of UV, visible or NIR radiation from a molecule or atom resulting from the transition of an electronically excited state to a lower energy state.
Photoluminescence	Luminescence in which absorption of UV, visible or NIR radiation forms the mode of excitation.
Fluorescence	Photoluminescence from a singlet electronically excited state.
Phosphorescence	Photoluminescence from a triplet electronically excited state.
Chemiluminescence	Luminescence in which the electronically excited state is produced by a chemical reaction.
Bioluminescence	Similar to chemiluminescence although visible radiation is emitted from living organisms.
Electrochemiluminescence	Chemiluminescence occurring in solution in which the electronically excited state is produced by high energy transfer reactions.
Thermoluminescence	Luminescence from solids on gentle heating.
Pyroluminescence	Luminescence from metal atoms within a flame.
Sonoluminescence	Luminescence from the exposure of solution to ultrasonic sound waves.
Electroluminescence	Luminescence from electrical discharges.
Triboluminescence	Luminescence from structural rearrangement.
Anodoluminescence	Luminescence from irradiation by α particles.
Cathodoluminescence	Luminescence from irradiation by β particles.
Candoluminescence	Luminescence from incandescent solids.
Radioluminescence	Luminescence from irradiation by X- or γ - rays.

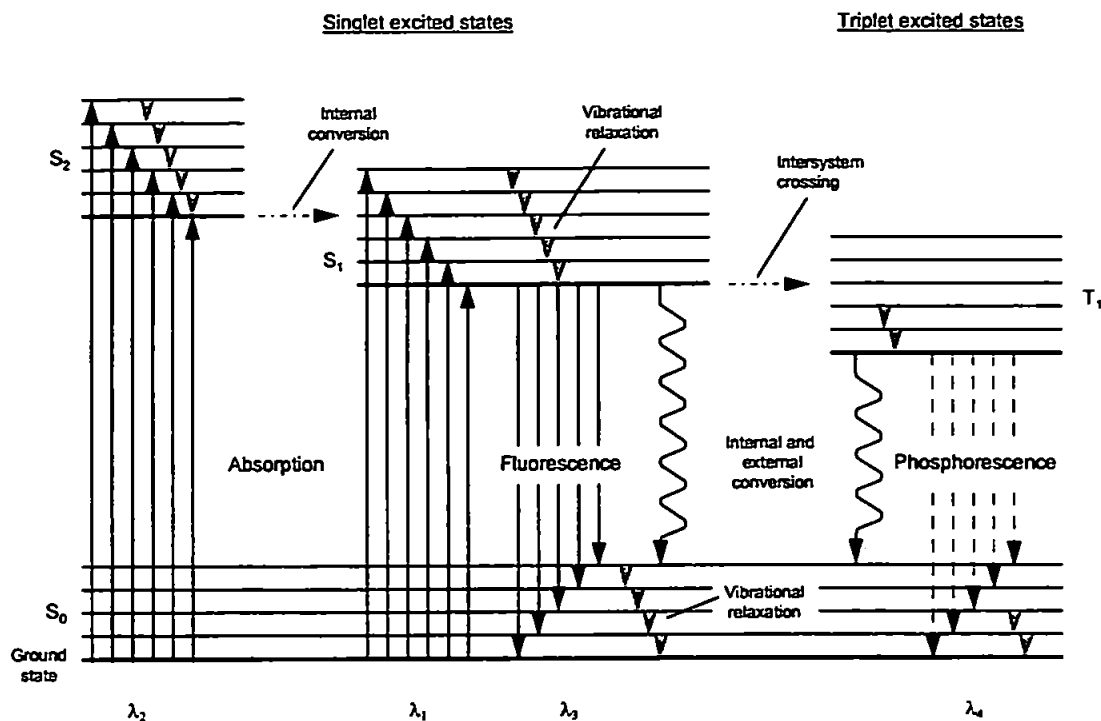


Figure 1.3. Partial energy diagram for a photoluminescent system.

Several mechanistic pathways allow the relaxation of an excited species, both radiative and non-radiative. The route that keeps the lifetime of the excited state species to a minimum is the most favoured. In order that photoluminescence can be observed deactivation by radiative pathways must be rapid compared with the non-radiative pathways.

1.2.2. Fluorescence

For fluorescence, before relaxing to the ground state emitting photons, the molecule first relaxes to the lowest vibrational energy level within the lowest singlet excited state (10^{-12} s). The lifetime of a singlet excited state is of the order of 10^{-9} - 10^{-7} s and as the process does not involve a change in spin it is termed an allowed transition.

In the simplest type of fluorescence, exhibited by dilute atomic vapours, the excited state relaxes to the lowest level in the ground state with the radiation being emitted without alteration of wavelength (resonance fluorescence). For molecules in solution the emitted radiation for a particular transition is displaced to a longer wavelength. This displacement is known as the Stokes Shift and is due to the loss of vibrational and rotational energy by collision of the excited state molecules with solvent molecules.

Internal conversion, external conversion and inter system crossing are all non-radiative transitions that compete with fluorescence. If two energy levels are close enough for vibrational energy levels to overlap internal conversion, a very efficient deactivation pathway exists. Energy transfer between the excited state molecule and solvent molecules results in external conversion.

The non-radiative transfer from a singlet excited state to a triplet state, where the spins of the electron pair are parallel, leads to deactivation by inter-system crossing and as it involves a change in spin this process is termed spin-forbidden.

1.2.3. Phosphorescence

Phosphorescence arises from relaxation to the ground state from a triplet excited state. This has a low probability of occurring, as it is a forbidden transition, and because of this the rate of relaxation for phosphorescence is slow with lifetimes in the range 10^{-4} to 10 s. Excitation to the triplet state from the ground state rarely happens, the singlet excited state passes to a lower triplet excited state by inter-system crossing. Phosphorescence is observed at longer wavelengths than fluorescence because the lowest triplet excited state has a lower energy than the lowest singlet excited state.

In relation to the rate of deactivation through phosphorescence the non-radiative deactivation processes are very fast and unless they are slowed down phosphorescence is not usually observed. Analytically useful phosphorescence can be achieved by cooling to very low temperatures and by use of viscous media, micellar media or adsorption onto solid surfaces to trap the excited state molecule [7,8].

1.2.4. Structural and environmental effects on photoluminescence

Both molecular structure and chemical environment are influential in determining whether a substance will or will not photoluminesce. It is these same factors that also determine the emission intensity when photoluminescence does occur.

Fluorescence quantum efficiency, or quantum yield, is the term used to describe the efficiency of a fluorescent process. This is described simply as the ratio of the number of molecules that fluoresce to the total number of excited molecules and can be represented as;

$$\Phi_F = \Phi_{F_p} / \Phi_{A_p}$$

where Φ_F represents the fluorescence quantum efficiency and Φ_{F_p} and Φ_{A_p} are the number of photons emitted due to fluorescence and the number of photons absorbed respectively.

Photoluminescence resulting from absorption of wavelengths below 200 nm is not common since such radiation is sufficiently energetic to cause deactivation of the excited states by dissociation or predissociation. It is therefore not surprising that luminescence arising from $\sigma^* \rightarrow \sigma$ transitions are virtually non-existent. Therefore, most fluorescent compounds emission arises from π bonding and π antibonding ($\pi^* \rightarrow \pi$) transitions and less frequently $\pi^* \rightarrow \eta$ transitions depending upon which is the less energetic. Transitions of the type $\pi^* \rightarrow \pi$ have greater quantum efficiencies than $\pi^* \rightarrow \eta$ transitions as they have shorter lifetimes and competing deactivation processes are less likely to occur (Table 1.2.).

Table 1.2 Spectroscopic parameters of η , π^* and π , π^* transitions.		
Parameter	η , π^*	π , π^*
Molar absorptivity (ϵ)	10 to 10^3	10^3 to 10^5
Lifetime (s)	10^{-7} to 10^{-5}	10^{-10} to 10^{-7}
Energy difference between S_1 and T_1	small	large
Rate constant for intersystem crossing (k_i)	$>k_f$	$<k_f$

Hence compounds exhibiting the most intense fluorescence will contain low energy π to π^* transitions, the largest group of these are aromatic compounds. A small number of aliphatic and alicyclic carbonyl structures and species with highly conjugated double bond structures are also fluorescent. Most unsubstituted aromatic hydrocarbons fluoresce when in solution, the quantum efficiency usually increasing with the number of rings and the degree of condensation. Substituents attached to aromatic rings can dramatically influence emission wavelengths and quantum efficiencies. Electron donating functional groups, such as $-\text{OR}$ and $-\text{NR}_2$, enhance fluorescence intensity, while electron withdrawing groups such as halides (except F), $-\text{NO}_2$ or $-\text{COOH}$ often yield a compound with decreased fluorescence intensity, as shown in Table 1.3.

Table 1.3. Effect of substituents on fluorescence of benzene.			
Compound	Substituent	Wavelength (nm)	Relative intensity
Benzene	H	270-310	10
Aniline	NH ₂	310-405	20
Fluorobenzene	F	270-320	10
Chlorobenzene	Cl	275-345	7
Phenol	OH	285-365	18
Benzoic acid	COOH	310-390	3
Nitrobenzene	NO ₂	-	0

Structural rigidity has a strong effect on fluorescence, with luminescence being favoured in molecules with rigid planar structures. These characteristics increase the interaction and conjugation of the π -electron system with a resultant decrease in vibrational amplitudes that promote radiationless losses. For example, the quantum efficiencies for fluorene and biphenyl (Figure 1.4.) are nearly 1.0 and 0.2, respectively, under similar conditions of measurement. The only difference being the methylene bridge, which forces planarity, in fluorene [9].

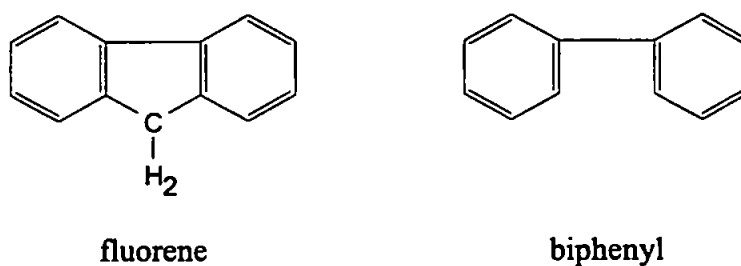


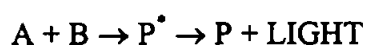
Figure 1.4. Structural comparison of fluorene and biphenyl.

Environmental factors can have great effect upon the intensity of emission observed from a luminescent species. Increasing temperature and decreasing solvent viscosity increase the likelihood of deactivation by external conversion, due to the higher frequency of collisions between solvent molecules and the excited species. Halogenated solvents e.g. carbon tetrabromide and ethyl iodide cause a decrease in fluorescence due to orbital spin interactions resulting in an increase in the rate of triplet formation. Dissolved oxygen also assists non-radiative deactivation by inter-system crossing as a consequence of the paramagnetic properties of molecular oxygen.

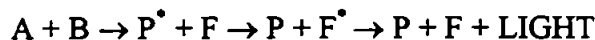
The pH of solutions can be critical for compounds with acidic or basic functional groups (e.g. phenols, amines), as the excitation and emission wavelengths of the ionised and free forms are likely to differ. For example, different excitation and emission spectra are observed for 2-naphthol and the 2-naphtholate anion. Fluorescence from the unprotonated form is observed at pHs less than 9.5 because after excitation of 2-naphthol, rapid deprotonation to the anion form occurs before emission.

1.2.5. Chemiluminescence

Chemiluminescence (CL) is luminescence in which the source of the excitation is a chemical reaction. It can occur in the gas-, liquid-, or solid-phase. In its simplest form a CL reaction can be represented by;



where P^* is an excited state product (direct CL). In some cases the excited state product is either weakly or non-fluorescent and the emission is enhanced by addition of a sensitiser, which becomes the emitting species after energy transfer;



where F is the sensitiser. This indirect CL is often termed energy transfer or sensitised CL [3]. A special type of CL is electrochemiluminescence, i.e., light emission produced by the electrolytes of solutions of analytes. Many classes of aromatic compounds emit light during electrolysis with detection limits in the ng range. Examples include naphthalene, pyrene, carbazole, chrysene [10,11], phthalates [12] and derivatives of amino acids[13].

For the generation of CL in the visible region of the spectrum three conditions must be met;

1. An energetically favourable reaction pathway should be available for the production of the excited state species. A significant number of molecules participating in the reaction should reach the excited state.
2. The reaction is required to be exothermic, with the free energy change being in the range 170-300 kJ mol⁻¹.
3. There should be a favourable deactivation pathway for CL emission. In this regard the competing processes are the same as those for molecular fluorescence.

Table 1.4. Properties of chemiluminescence reactions.		
Reaction	Colour (λ_{\max})	Quantum yield
Solid-phase		
Rubrene peroxide dissociation by heat	red	
Oxidation of siloxane	red	
Liquid-phase		
Oxidation of <i>p</i> -chlorophenyl magnesium bromide (Grignard reagent)	blue (475 nm)	10^{-6} - 10^{-8}
Oxidation of luminol in dimethyl sulphoxide	blue-violet (480-502 nm)	0.05
Oxidation of luminol in aqueous alkali	blue (425 nm)	
Oxidation of lucigenin in alkaline H ₂ O ₂	blue-green (440 nm)	0.016
Oxidation of lophine in alcoholic NaOH	yellow (525 nm)	
Pyrogallol in alkaline H ₂ O ₂	reddish pink	
Peroxyoxalate reaction	sensitiser dependant	0.05-0.5
ATP-dependant oxidation of D-luciferin with firefly luciferase at pH 8.6	yellow-green (560 nm)	0.88
ATP-dependant oxidation of D-luciferin with firefly luciferase at pH 7.0	red (615 nm)	
Bacterial luciferase/oxidoreductase	blue-green (480-490 nm)	0.1-0.2
Gas-phase		
Nitric oxide + ozone	(600nm)	
Reduced sulphur compounds + ozone	(300-400 nm)	

The values for the free-energy change in the visible region (400-700 nm) are calculated from the Planck-Einstein equation:

$$E = hc/\lambda$$

Where E is the energy of the photon, h is Planck's constant (6.63×10^{-34} J s), c is the velocity of light (3×10^8 m s⁻¹ in a vacuum) and λ is the wavelength of light.

Four parameters characterise CL emission; colour, intensity, rate of production and rate of decay [14]. Table 1.4. summarises the properties of several CL reactions in the solid-, liquid-, and gas-phase [3]. The intensity of a CL reaction is highly variable and is dependent on both the rate of reaction and the efficiency with which molecules in the excited state are generated. The efficiency is measured by the quantum yield:

$$\begin{aligned} \text{quantum yield } (\Phi_{\text{CL}}) &= \sum \text{photons emitted} / \sum \text{molecules reacting} \\ &= \Phi_{\text{C}} \Phi_{\text{EX}} \Phi_{\text{F}} \end{aligned}$$

where:

Φ_{C} = fraction of molecules going through the CL pathway.

Φ_{EX} = fraction of pathway molecules that produce an excited state product.

Φ_{F} = fraction of excited state molecules which generate a photon.

Values between 10^{-15} and nearly 1 have been observed but even inefficient CL reactions can be utilised due to the extremely low background emission [14].

Luminol (5-amino-2,3-dihydro-1,4-phthalazinedione) is one of the most commonly used liquid-phase CL reagents. The reaction involves the aqueous alkaline oxidation of luminol, in the presence of a catalyst, to produce an excited state 3-aminophthalate anion that subsequently decays to the ground state (Figure 1.5.).

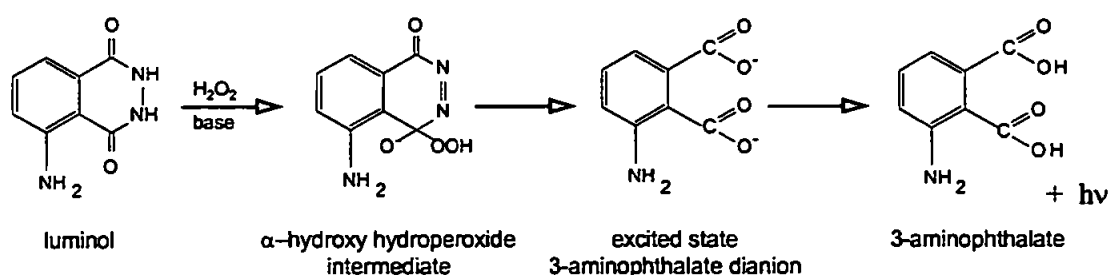


Figure 1.5. Schematic of the luminol CL reaction.

The peroxyoxalate reaction is based on the hydrogen peroxide oxidation of aryl oxalate esters in the presence of a suitable fluorophore (F) (Figure 1.6.). The CL emission profile is characteristic of the fluorophore rather than the CL reagents. These reactions are among the most efficient of non-biological CL reactions, with quantum efficiencies as high as 20-30%.

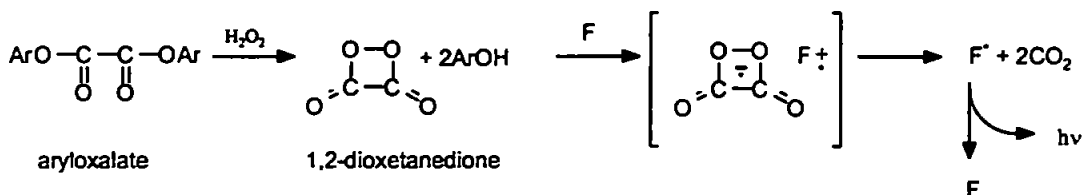


Figure 1.6. Schematic of the peroxyoxalate CL reaction.

1.2.6. Bioluminescence

A number of biological systems undergo chemiluminescent reactions. Here the reactants and catalysts are all naturally occurring molecules and thus the luminescence is termed bioluminescence.

Generally these reactions involve the interaction of a catalytic enzyme luciferase, and a luciferin, (a substrate). Oxygen is usually the oxidising agent, but as with many chemiluminescent reactions, the chemistry is not completely understood. One of the most familiar experiences of a bioluminescent reaction is the light produced by a firefly, caused by the enzymatic oxidation of firefly luciferin (Figure 1.7.).

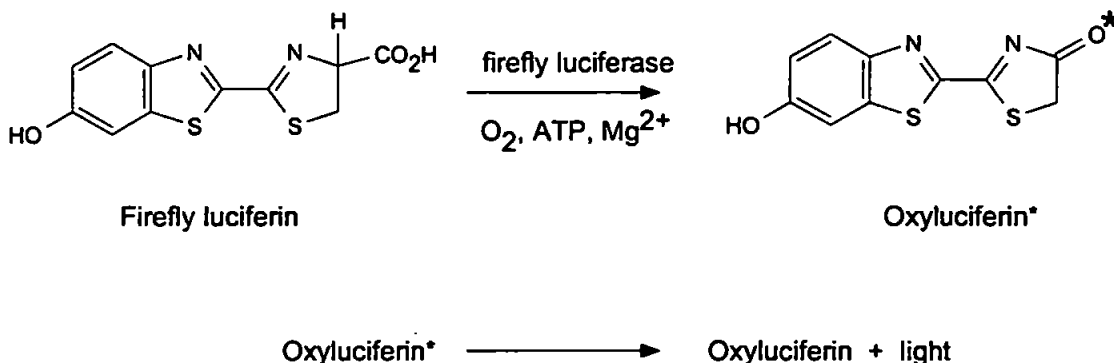


Figure 1.7. Firefly bioluminescence reaction.

These systems are of interest in analytical applications because of their high light yields, which allow low limits of detection to be obtained with their use and are particularly useful

in clinical analysis for immunoassay studies. Luciferases, however, are expensive and not very stable and are often stabilised by immobilisation on solid supports [15,16].

Applications of bioluminescent reactions have included the determination of ATP (firefly luciferase), NAD/NADH (marine bacterial reaction) (Figure 1.8.) and metal ions such as calcium (aequorin).

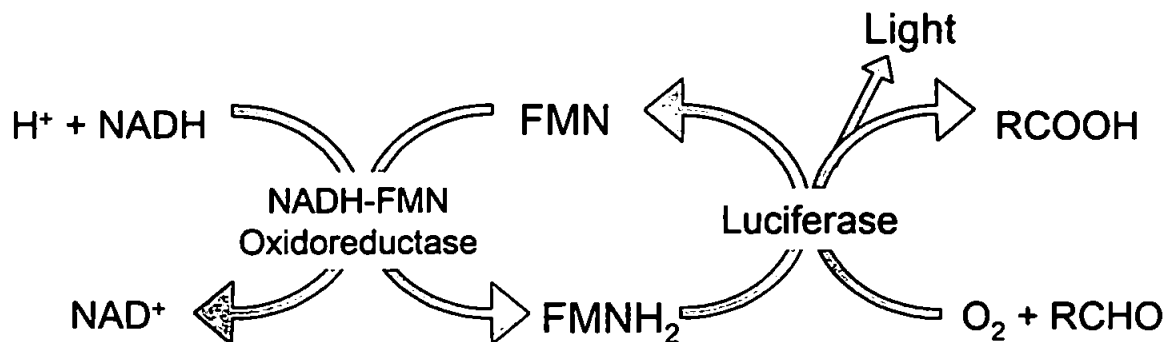


Figure 1.8. Schematic diagram of the bacterial luciferase/NAD(P)H reaction. Where FMN and FMNH₂ are the oxidised and reduced forms of flavin mononucleotide.

1.2.7. Instrumentation for CL detection

The instrumentation required for monitoring CL reactions is relatively simple and inexpensive. The most important component of the instrument is the light detector, which traditionally has been the photo-multiplier tube (PMT).

A PMT consists of a photo cathode and a series of dynodes at progressively higher positive potentials contained in a glass vacuum tube, exposure to light causes the emission of electrons from the photo cathode by the photoelectric effect which are amplified down the chain of dynodes to an anode. The resulting current is proportional to the light intensity impinging on the cathode surface. PMTs have fast response times (typically nanoseconds), good linearity and low noise (particularly if cooled) and are supplied with a variety of photo cathode materials sensitive to different sections of the visible spectrum. The PMT selected for CL detection should give a very low background signal and high sensitivity at the most common CL emission wavelengths (400-550 nm). Major drawbacks in the use of PMTs are their fragility, high voltage supply requirements (>1.0 kV) and the length of time to return to maximum sensitivity after exposure to daylight [17].

Solid state devices for the detection of light, e.g. the photodiode and the charge coupled device (CCD) are more robust than PMTs. Photodiodes consist of a silicon pn junction

that is reverse biased creating a depletion layer that reduces the conductance of the junction to near zero. When light falls on the junction, free electrons are formed which under the influence of an external potential produce a current proportional to the intensity of light. Photodiodes are inexpensive, small, rugged and have low power requirements (<15 V DC) [18]. Red and blue/UV sensitive photodiodes are available and with careful instrument design they can give sensitivity comparable to PMTs. A photo diode based detector has been applied to CL detection in FI and LC [19-21].

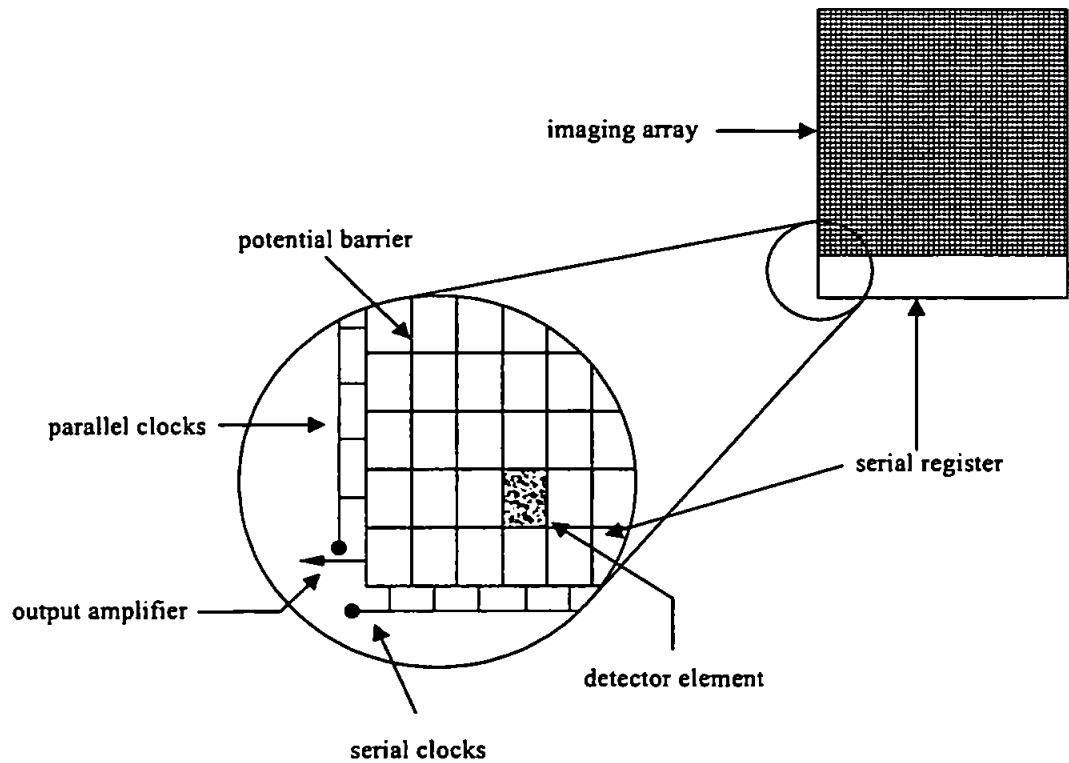


Figure 1.9. Schematic layout of a typical CCD chip.

CCDs are ultra-sensitive light detectors that have found application for imaging, particularly in astronomy, and their use for spectroscopy is increasing [22, 23]. They consist of arrays of metal oxide semiconductor capacitors on a single silicon chip (Figure 1.9.). Photo generated electrons are collected in detector elements (pixels) as charge packets which are transferred to an on-chip amplifier by passing them vertically in sequence from one pixel to the next adjacent pixel into a serial register and then horizontally into the amplifier [22]. Electrodes control the transfer, which are held at different potentials and when the CCD is exposed, photons of light incident on the surface of the CCD pass through the electrodes and cause electrons to be generated in a doped depletion layer of the silicon substrate. These generated electrons are held in position by the applied voltages on the electrodes and are stored in potential wells. After the CCD has been exposed to light, the accumulated charge in each potential well is then transferred (or

coupled) to adjacent electrodes by altering their relative potentials. In this way the charge pattern, corresponding to the intensity of incident photons of light, can be moved along the CCD and into an output register and amplifier at the edge of the CCD for digitisation.

CCDs exhibit good signal to noise ratios due to the on-chip amplifier and the multiplex advantage of an array detector [22]. The dark current of a CCD when cooled with liquid nitrogen (140 K) can be as low as $1 e^-/\text{pixel}/\text{h}$ and dynamic ranges are wide ($1-10^5$).

It is possible to read the CCD by a process called binning where the charge contained in several vertical elements is summed before passing to the amplifier. The noise associated with this is of the level of reading a single pixel in contrast to summation in computer memory where the noise associated with each pixel reading contributes separately to the total noise [22]. CCDs show excellent sensitivity at the red/infrared end of the spectrum and their overall sensitivity at the blue/UV end can be improved by using UV sensitive dye coatings. One distinct advantage over a PMT is that as a CCD is an array detector it is possible to measure an entire spectrum simultaneously. CCDs therefore have the potential to be used as sensitive and selective detection systems for chemiluminescence methods.

A number of batch luminometers, for measurements on static solutions, are commercially available. These operate by the injection of a fixed volume of reagents into a cuvette containing the sample and a photomultiplier tube (PMT) directly detects the CL emission. However, the majority of CL reactions are neither long-lived nor highly selective (the ideal conditions for batch luminometers) and additional chemical and/or physical sample treatment is often needed, which is best achieved in a flow-through system.

Instrumentation for flow-through applications (e.g. flow injection analysis, FI, and liquid chromatography, LC) of CL is generally custom built or an adaptation of other instrumentation, e.g. spectrophotometers or fluorimeters with the radiation source removed. PMT-based flow-through detectors are now commercially available. A review by Stanley [24] surveys commercially available luminometers and imaging devices for low light measurements and kits and reagents for CL. It includes technical details together with company addresses and contact information for such items as luminometers, low-light imaging systems and CCD cameras.

1.3. FLOW INJECTION ANALYSIS

1.3.1. Basic Principles

Flow injection analysis (FI) is based on the injection of a highly precise liquid sample volume into a moving, unsegmented stream. The injected sample forms a zone that is transported towards a detector, which continuously records the fluorescence, absorbance or other parameter as the sample passes through a flow cell [25-27]. FI has gained widespread use, especially in the last decade, in which it has been the subject of a number of papers [28, 29]. The technique is finding increasing applications in research, routine analysis, monitoring of chemical processes and enhancing the performance of various instruments as well as measurement of diffusion coefficients, stability constants, reaction rates, composition of complexes and extraction constants and solubility constants [30-35]. Optimisation and design of the flow channels to achieve maximum sampling frequency, best reagent and sample economies, and proper exploitation of the chemistries is possible through the understanding of the chemical and physical processes occurring during the movement of the fluids through the FI channel. A typical FI manifold is comprised of a pump, injection valve, detector, and tubing manifold (Figure 1.10.).

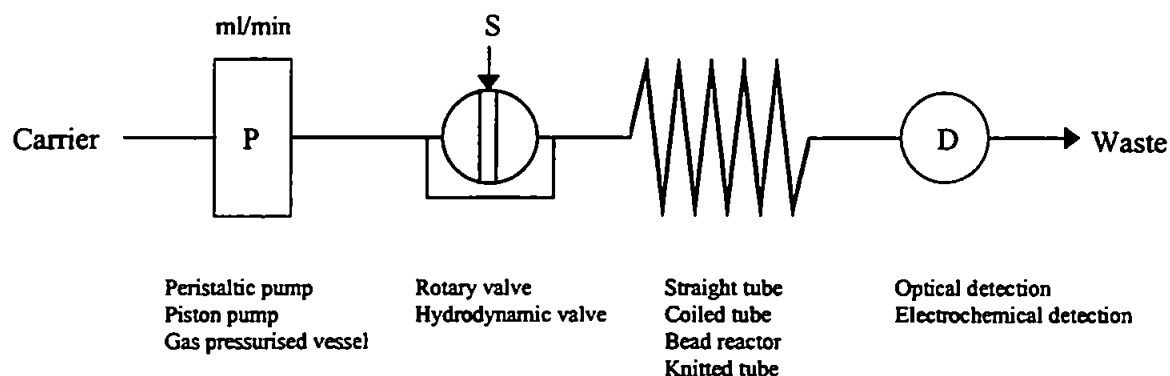


Figure 1.10. General scheme of a simple FI manifold.

The pump is used to propel one or more streams through the detector via narrow bore (0.5 - 0.8 mm ID) tubing. These streams may be reagents, simple buffers, or solvent. The injection valve is used to periodically introduce a small volume (<100 μ l) of sample into the carrier stream. As this sample is carried to the detector, axial dispersion mixes sample and reagent, leading to chemical reaction to form a detectable species. This species is observed by the detector as a transient peak (Figure 1.11.). Of course, the described manifold is the simplest case, and innovative researchers have integrated a wide range of

different sample processing steps into FI methodologies. These include dilution, trace enrichment, solvent extraction [36], matrix modification, gas permeation, dialysis [37], and reactions with immobilized reagents.

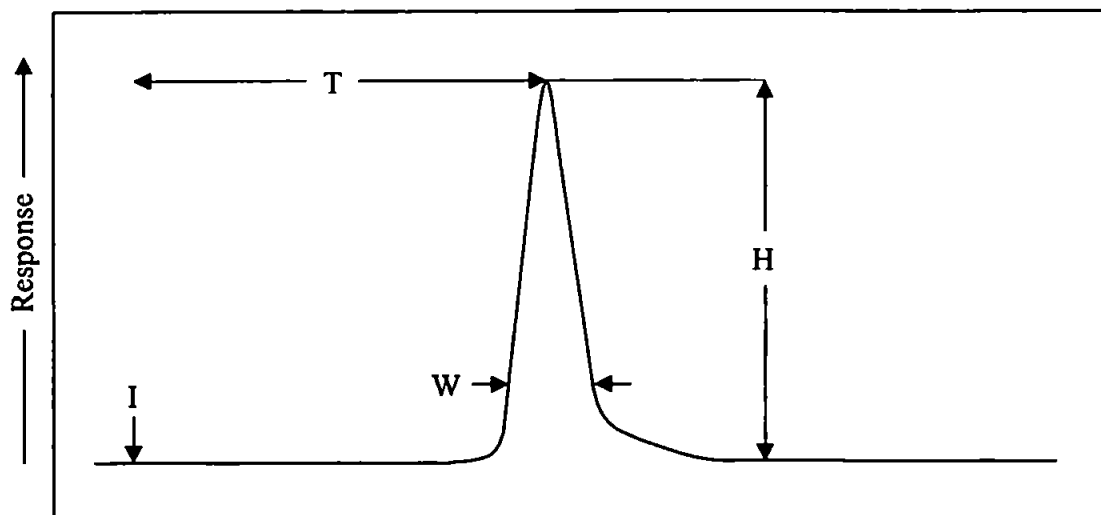


Figure 1.11. Chart recorder output; where I is the point of injection, H is the peak height, W is the peak width and T is the residence time.

The height and area of the peak are proportional to concentration, and are used for quantitation by comparison to samples of known concentration. The time span between the sample injection I, and the peak height H is the residence time T during which the chemical reaction takes place. With rapid response times, typically in the range 5-20 seconds, a sampling frequency of 100-300 samples per hour can be achieved. FI is based on a combination of three principles. First is sampling, where the sample is measured out and injected into the flowing carrier stream. The second stage is termed controlled dispersion of the injected sample zone. The chemical reactions take place whilst the sample material is dispersing within the reagent, the concentration of the sample zone being formed by the physical dispersion process, where the sample zone broadens as it moves down stream and changes from the original asymmetrical shape to a more symmetrical and eventually Gaussian form [27]. The third stage is reproducible timing of its movement from point of injection to the detector. What happens to one injected sample happens in exactly the same fashion to all subsequent sample injections. The power of FI as an analytical tool lies in its ability to combine these functions in a wide variety of different ways to create a broad range of different methodologies, and perform these methodologies rapidly and automatically with small volumes of sample (typically 10-200 μ l) and reagents.

1.3.2. Dispersion Coefficient (D)

Dispersion can be defined as the dynamic but reproducible intermingling of sample zone with a reagent zone and/or carrier caused by flow patterns created by the dynamics of fluid flow through narrow bore tubing. A key word in the definition of dispersion is reproducible. While the dispersion is dynamic and never reaches equilibrium before the sample zone reaches the detector, it is reproducible at any given instant in time if the factors that affect dispersion are held constant. These factors include flow rate, tubing ID, type of reactor (e.g. coil, knotted, static mixer, straight, serpentine), length of tubing, and internal architecture of components such as valves, detectors, and connectors, all of which are readily controlled. Thus, the degree of dilution and chemistry caused by the dispersion process during transport of the sample zone from injector to detector can be controlled so that it is reproducibly the same for calibrants and samples. This allows calibration of the system and use of the calibration to quantitate samples.

The dispersion coefficient, D is defined as the ratio of concentrations of sample material before and after the dispersion process.

$$D = C^0/C^{max}$$

Where C^0 is the concentration of an analyte in the sample prior to dispersion and C^{max} is the maximum concentration in the dispersed sample zone at the time of detection. If $D=2$, the sample has been diluted 1:1 with the carrier stream. For convenience, sample dispersion is defined as limited for $D=1-3$, medium for $D=3-10$, and large if $D>10$ [38]. In developing a new methodology a set of conditions must therefore be found which gives the optimum balance between enhancement of chemistry and dilution for the application of interest.

There are actually two types of dispersion in FI, axial and radial. Axial dispersion occurs in the direction of stream flow and causes greater dilution and peak broadening than radial dispersion. Axial dispersion predominates in a straight tube. Radial dispersion is caused by flow patterns in the stream, which circulate normal to the direction of flow, and thus cause mixing with minimum dilution and peak broadening.

1.3.3. Factors affecting dispersion

Dispersion within an FI manifold can be manipulated by acting on the hydrodynamic and/or geometric variables involved.

In general, on increasing the sample volume the value of D decreases. By injecting increasing volumes of solution, a series of curves will be recorded, all starting from the same point of injection, where the height of the individual peaks will increase until an upper limit has been reached. Changing the sample volume injected is the single most powerful method of changing the value of D . An increase in peak height and in sensitivity of measurement is achieved by increasing the volume of the injected sample solution. Dilution of overly concentrated samples is best achieved by reduction of the injection volume.

The length of tubing along which the sample zone travels prior to detection can vary in length, diameter and geometry. The influence of tube length and internal diameter has been extensively studied [25]. In general the value of D increases with increasing tube length and internal diameter. There are practical considerations for using tubing with too narrow a bore because the flow resistance will increase and the system might easily become blocked by any solid particles in the flow stream. For this reason the most common tubing I.D. is 0.5 mm although 0.75 mm and 0.3 mm I.D. tubing has also found use [39] depending on the dispersion characteristics of the system. Tube geometry also has a marked effect on the value of D and in general the greater the tortuosity of the tubing the smaller the value of D . Turns in the flow path, e.g. coiling the tubing, and in particular where frequent and sharp changes in the direction of the turns occurs, e.g. knotted tubing, promote radial dispersion. For this reason, knotted reactors are more widely used than coiled reactors since they lead to greater sensitivity and narrower peaks.

Increasing the flow rate leads to an increase in the dispersion coefficient due to an increase in the axial dispersion owing to the frictional forces generated between the flowing stream and the tubing. The residence time (T) is dependent on the tube length (L), the tube internal diameter, and the pumping rate. For systems of medium dispersion where the sample requires mixing for reactions to occur one would tend to increase the tube length in order to increase T . This however leads to band broadening and hence loss of sensitivity due to the increased dispersion. It is therefore more practical to keep L as short as possible and decrease the pumping rate.

1.3.4. Detectors for FI applications

The versatility of FI has allowed the method to be adapted to any detection system that is capable of accepting a flowing stream. Thus, all the detectors that have long been used for liquid chromatography have been investigated for use in FI using a variety of manifold configurations. Detection systems used can be broadly classed as one of two types, optical or electrochemical, as summarised in Table 1.5.

Detection system	
Optical	Electrochemical
<i>e.g.</i> UV-visible spectrophotometry; solid-state photometry; IR spectrophotometry; diode array spectrophotometry; atomic spectrometry; luminescence.	<i>e.g.</i> Potentiometry (ion-selective and pH electrodes); conductimetry; amperometry; coulometry; voltammetry.

In the case of electrochemical methods, potentiometry with ion selective electrodes, voltammetric and amperometric methods are the most frequently used. Spectrophotometric detectors however, are by far the most widely used systems in FI, because of the numerous selective reactions available for almost every type of compound and element. UV-visible spectrophotometry is most commonly employed, and since the development of solid-state photometers, using light emitting diode (LED) light sources and photodiode (PD) detectors, it has become even more common [40]. More recently FI has been used for the on-line preconcentration of analytes and sample delivery to atomic spectrometry detectors [41].

FI methods that combine on-line derivatisation procedures with fluorescence or chemiluminescence detection can provide a high degree of selectivity and sensitivity for some analytes. FI is ideally suited to monitoring CL reactions because of the rapid and reproducible mixing of the sample and reagent that can be achieved in close proximity to the detector, thus resulting in maximum sensitivity and reproducibility when only weak and short lived emissions are observed.

A simple FI-CL manifold is shown in Figure 1.12. The sample is injected into a flowing stream and mixed with the reagent in close proximity to the detector. Emission occurs in a

flat spiral coil placed in front of the optical window of a photomultiplier tube (PMT), with no wavelength discrimination. The PMT housing can be cooled (typically -10 to -20°C) to reduce the dark current and minimise baseline noise, and either photon-counting or analog measurement employed to process the PMT output.

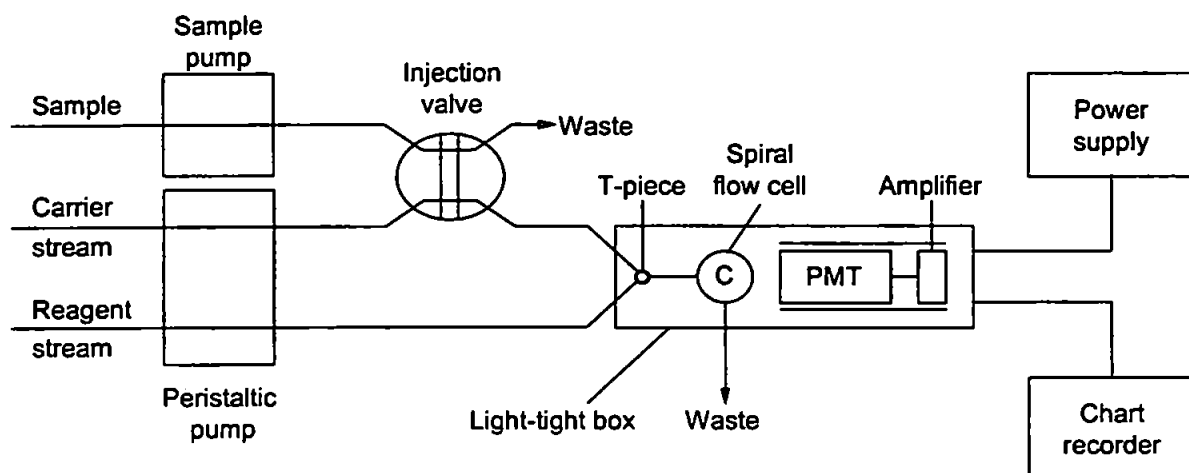


Figure 1.12. Typical flow injection manifold for chemiluminescence applications.

The dimensions of the mixing and detector coils, flow rates, pH, temperature and reagent concentrations can easily be optimised (e.g. using simplex optimisation) to maximise the CL emission intensity seen by the detector. The instrumentation is compact, inexpensive and allows rapid and reproducible mixing, providing good precision and allowing high sample throughput.

1.3.5. Applications of FI-CL to Inorganic Species

Historically, the catalytic effect of inorganic ions on the oxidation of luminol (5-amino-2,3-dihydrophthalazine-1,4-dione) in basic aqueous solution, giving rise to a characteristic blue emission, has been used to determine such species. This is one of the most efficient CL reactions known and several oxidants, e.g., hydrogen peroxide and potassium periodate, and co-oxidants, e.g., haem-containing enzymes such as horseradish peroxidase, and iron hexacyanoferrate(III) have also been used. FI applications incorporating inorganic species [42 – 84] are shown in Table 1.6.

Table 1.6. Flow injection chemiluminescence applications for the determination of inorganic species.

Analyte	CL reaction	Sample matrix	LOD (as specified in original paper)	Reference
METAL IONS				
Co(II)	catalysed oxidation of dibromoalizarin violet by H ₂ O ₂ in alkaline solution; enhanced using cationic surfactant	natural waters	4 pg ml ⁻¹	[42]
Co(II), Mn(II)	luminol oxidation by potassium periodate	fresh, polluted waters, vitamin B12	0.01 ng ml ⁻¹ Co(II) 0.02 ng ml ⁻¹ Mn(II)	[43]
Co(II), Fe(II)	decomposition of peroxymonosulfate; use of brilliant sulfoflavin sensitizer in micellar solution	pepperbush, pond sediment	5 x 10 ⁻⁹ M Co(II) 6 x 10 ⁻⁹ M Fe(II)	[44]
Co(II), Fe(II), [VO] ²⁺	transition metal ion decompositions of peroxymonosulfate ion	synthetic	1 x 10 ⁻⁸ M Co(II) 2 x 10 ⁻⁷ M Fe(II) 6 x 10 ⁻⁷ M [VO] ²⁺	[45]
Cu(II)	oxidation of copper(II) - 1,10-phenanthroline chelates by H ₂ O ₂ at alkaline pH	sea water	0.05-0.1 nM	[46]
Cu(II)	oxidation of copper - 1,10-phenanthroline complex by H ₂ O ₂ ; separation of copper from matrix on immobilized 8-hydroxyquinoline	sea water	0.4 nM	[47]
Cr(III)	luminol - H ₂ O ₂ system	distilled, drinking, mineral, waste waters, food samples	0.01 ppb	[48]
Cr(III)	oxidation of pyrogallol with periodate at neutral pH; increased intensity with 3-(N-morpholino) propanesulphonic acid	synthetic	1 ng ml ⁻¹	[49]
Cr(III), Cr(IV)	separation by cation-exchange column; reduction of Cr(IV) by potassium sulfite; detection by luminol - H ₂ O ₂ system	synthetic	0.5 µg l ⁻¹	[50]

Analyte	CL reaction	Sample matrix	LOD (as specified in original paper)	Reference
Cr(III), Cr(IV)	separation by anion-exchange column; reduction by sulfur dioxide solution; detection by luminol oxidation	fresh water	0.05 $\mu\text{g l}^{-1}$ Cr(III) 0.1 $\mu\text{g l}^{-1}$ Cr(IV)	[51]
Au(III)	tetrachloroaurate(III) - luminol system in reversed micellar system	chloroform	10 pg ml^{-1}	[52]
Au(III)	luminol in reversed micellar medium after solvent extraction	industrial samples of silver-based alloy	not reported	[53]
Au(III)	tetrachloroaurate(III) with luminol in reversed micellar medium	silver based alloy	10 fg l^{-1}	[54]
Fe(II), total dissolved iron	brilliant sulfoflavin - H_2O_2 in neutral medium; preconcentration on 8-hydroxyquinoline column	sea water	0.45 nM	[55]
Fe(III)	luminol - aqueous ammonia - hydrogen peroxide reaction; selective column extraction using 8-HQ chelating resin	sea water	0.05 nM	[56]
Mn(II)	oxidation of 7,7,8,8-tetracyanoquinodimethane in alkaline solution; preconcentration on immobilized 8-hydroxyquinoline	sea water	0.1 nM	[57]
Mn(II)	oxidation of 7,7,8,8-tetracyanoquinodimethane in alkaline solution; eosin Y sensitization in surfactant bilayer vesicles	raw, processed water	4.5 ppb	[58]
Rh(III)	oxidation of luminol by dissolved oxygen in reverse micellar medium	chloroform	50 ng ml^{-1}	[59]
Ag(I)	hydrophilic cation-exchange resin; detection based on oxidation by luminol with peroxodisulfate	synthetic	0.5 $\mu\text{g l}^{-1}$	[60]
Ti(IV)	reaction of Ti(III) with carbonate buffer; on-line Jones reductor column	synthetic	1 x 10^{-6}M	[61]

Analyte	CL reaction	Sample matrix	LOD (as specified in original paper)	Reference
rare earth metals	reaction of analyte - edta complex with H ₂ O ₂ in alkaline solution to produce reactive oxygen; detection by 1,10-phenanthroline CL; enhanced by surfactant and dye-sensitizer	coal fly ash	e.g. 2.0 x 10 ⁻⁸ M europium(III)	[62]
HYDROGEN PEROXIDE				
H ₂ O ₂	peroxyoxalate - sulphorhodamine 101	synthetic	3.0 x 10 ⁻⁹ M	[63]
H ₂ O ₂	luminol immobilization on solid supports	synthetic	0.15 μM Ambersorb	[64]
H ₂ O ₂	luminol enhanced with mixed dye sensitizer (eosin Y/uranine)	tap water	1 x 10 ⁻¹¹ M	[65]
H ₂ O ₂	catalytic effect of iron(II)-oxime complexes on oxidation of luminol by hydrogen peroxide	synthetic	1.3 x 10 ⁻⁸ M	[66]
H ₂ O ₂	peroxidases covalently immobilized on affinity membranes; catalytic luminol oxidation; use of fibre bundle	synthetic	1 x 10 ⁻⁸ M	[67]
H ₂ O ₂	1,1'-oxalyldiimidazole - hydrogen peroxide; use of immobilized fluorophore	water	1 x 10 ⁻⁸ M	[68]
H ₂ O ₂	oxidation of alkaline luminol in presence of copper(II) catalyst	sea water	5 nM	[69]
H ₂ O ₂	luminol oxidation; use of sequential injection analysis and novel fountain cell	synthetic	not reported	[70]
OTHER SPECIES				
ammonium ions	ammonia - hypobromite system in alkaline solution	rainwater, fogwater	6.1 x 10 ⁻⁶ M	[71]
singlet oxygen quenching efficiencies	reaction with 1,2-diethoxyethene; thermal decomposition in presence of fluorophore	synthetic	not reported	[72]

Analyte	CL reaction	Sample matrix	LOD (as specified in original paper)	Reference
ozone O ₃	ozonated water sample mixed with indigotrisulfonate (ITS) dye reagent	potable water	2 µg l ⁻¹	[73]
NaCl, NaNO ₃ , KCl, HCl, HNO ₃ , MgCl ₂ , MgSO ₄ , CaCl ₂ , CdCl ₂ , CoCl ₂ , AlCl ₃ , Al(NO) ₃ , FeCl ₃ , tartaric / succinic acids	displacement of copper(II) ions from ion-exchange column	synthetic	e.g. 3.2 x 10 ⁻⁷ M NaCl 1.2 x 10 ⁻⁷ M FeCl ₃	[74]
sodium nitroprusside (SNP)	luminol oxidation by H ₂ O ₂ in alkaline medium	pharmaceutical preparations	0.05 µg ml ⁻¹	[75]
water in non-aqueous solutions	quenching of CL between cyclohexane and methylsilicone	coolants, hydraulic fluids	0.1% (v/v) (10µl injection)	[76]
CN ⁻	CL sensor using luminol immobilized on anion-exchange resin and copper ion immobilized on cation-exchange resin	tap, industrial waste water	2 x 10 ⁻⁹ g ml ⁻¹	[77]
[NO ₂] ⁻	reduction of nitrite; detection of liberated NO using thermal energy analyser	foods, human biological materials	5 µg kg ⁻¹	[78]
[NO ₂] ⁻	reduction to NO by aqueous iodide in acid; gas-phase CL emission on reaction with ozone	human saliva, food extracts	0.04 ppb	[79]
[NO ₃] ⁻	photochemical activation in a flow-through reactor; luminol - nitrate reaction after irradiation with mercury lamp	natural water	7 x 10 ⁻⁸ M	[80]
[NO ₃] ⁻ , [NO ₂] ⁻	reduction to NO, followed by membrane separation and gas-phase CL	river water, sewage treatment samples	5 µg l ⁻¹ [NO ₃] ⁻ 3 µg l ⁻¹ [NO ₂] ⁻	[81]
[SiO ₃] ²⁻	ion-exclusion chromatography; detection by acidified silicate - luminol system	synthetic	0.1 ng ml ⁻¹ Si(IV)	[82]
[SO ₃] ²⁻	suppression of luminol CL; EDTA amplifies suppression	wine	ca. 10 µM	[83]
[SO ₃] ²⁻	acidic oxidation of sulphite by cerium(IV); sensitized by cyclooctylamine	synthetic	5.4 x 10 ⁻⁷ M	[84]

Metal ions: Several metal ions catalyse the luminol reaction; e.g., Cr(III) has been determined at sub-nM levels using the luminol - hydrogen peroxide system [48]. However, as other ions such as Co(II), Cu(II), Fe(II), Ti(III) also catalyse the reaction, an inherent problem in most applications is lack of selectivity. The CL spectra from interfering species are generally too similar, weak or lacking in fine structure to be distinguished from the spectrum of the analyte by wavelength discrimination. Sample pretreatment or analyte separation is therefore necessary and the use of selective solid phase chelating resins is becoming increasingly popular [47, 55, 56].

Furthermore, there is a noticeable trend towards the development of novel CL systems, primarily based on the oxidation of organic compounds, that are more selective towards the analyte in question, despite often possessing lower CL quantum yields in comparison to the luminol system. The utilization of reversed micelles and surfactant assemblies as CL reaction media has also been of increasing interest for improving the characteristics of the luminol [52-54, 59] and other [44, 47, 57, 58] reactions. Weak CL emissions have also been enhanced by the use of sensitizers in indirect reactions [44, 55, 57, 58]. This involves a non-radiative transfer of energy from a weak or non-fluorescent excited product of the CL reaction, to a sensitizer, which becomes the emitting species. An interesting application was reported where ion-exchange resins were used for the simultaneous determination of several species of a particular metal [50, 51], with post column CL detection.

Matrices in which trace metals have been determined include foods, vitamins, pharmaceutical preparations and industrial alloys, although the most commonly analysed matrix is water. One recent development has been the shipboard use of FI-CL [46, 47, 55-57], because it is robust, simple, portable, inexpensive and requires little sample handling, which reduces the likelihood of contamination. The combination of a sensitive CL reaction with selective preconcentration on an immobilized cation ion-exchange resin (e.g. 8-hydroxyquinoline) has proved a successful method of attaining the detection limits necessary for trace metal seawater analyses (often sub-nM).

Hydrogen peroxide: The luminol system has frequently been used to determine H_2O_2 and variations include enhancement of the emission using sensitizers [65] and catalysts [66, 69]. Of particular note is the immobilization of luminol on a solid support packed within a column [64]. Luminol is then released by injection of, e.g., an alkaline sample and the

resulting CL monitored as with conventional FI methods. Chemiluminescence sensors based on immobilized luminol have also been developed [77].

H₂O₂ has also been determined by peroxyoxalate chemiluminescence (POCL), which involves oxidation, usually with hydrogen peroxide, of an aryl oxalate in the presence of a fluorescent sensitizer [63]. POCL reactions are the most efficient non-enzymatic CL reactions known, having quantum yields as high as 50%, although aryl oxalate esters are often insoluble in aqueous solutions. A novel system for H₂O₂ determination involves using the reagent 1,1'-oxalyldiimidazole (ODI) combined with an immobilized fluorophore on an acrylate polymer, and a detection limit of 10nM has been reported [68]. An H₂O₂ chemiluminometric sensor has also been developed using immobilized peroxidases in a catalytic oxidation of luminol [67]. Optical fibres carried the light from the flow cell to the PMT, and the reported range of determination was 10⁻³ - 10⁻⁸M.

Other species: A variety of non-metals and other species have been determined using CL reactions, e.g., nitrate and nitrite have been determined by a reduction step followed by the detection of liberated NO using a thermal energy analyser [78] or by the reaction of NO with ozone [81]. Nitrate has also been determined by its reaction with luminol after irradiation in a photochemical reactor [80]. Ammonium ion concentrations in rain and fogwater have been determined at the μM level using the reaction between ammonia and hypobromite, where potential interferences were removed by inserting a glass filter between the CL cell and the PMT [71].

An interesting modification to the luminol - peroxidase system has been used to determine free and total sulphite in wines [83]. The method was based upon the suppression of luminol CL which was linearly proportional to [SO₃]²⁻; EDTA greatly amplified this suppression and a detection limit of 10μM was reported. Water in non-aqueous solutions such as coolants and hydraulic fluids has been selectively measured by utilizing the quenching of chemiluminescence between cyclohexane and methylsilicone [76], achieving a detection limit of 0.1% (v/v).

A universal application utilizing the catalytic effect of Cu(II) on luminol - hydrogen peroxide CL has been used to determine mono-, di- and trivalent cations, counter anions and weak acids [74]. These species displaced Cu(II) ions from a strongly acidic ion-exchange column, before the metal ions participated in the CL reaction; limits of detection were in the sub-μM range.

1.3.6. Applications of FI-CL to Organic Species

Applications of organic species [85-137] using FI-CL can be classified according to the nature of the analyte into eight categories: alcohols, amines, amino acids, carbohydrates, drugs, enzymes and substrates, vitamins and miscellaneous, as listed in Table 1.7. These methods show considerable variation and ingenuity but, as with inorganic applications, there are four main reaction types. The first involves reaction of the analyte with a synthetic organic CL reagent (e.g. luminol, lucigenin, peroxyoxalate), in which the analyte is the oxidant, catalyst or sensitizer. In the second type of reaction, determination of the analyte is based on its direct or sequential derivatisation to form a molecule that is subsequently used in a CL reaction (e.g. production of hydrogen peroxide in an immobilized enzyme system). In the third type, the analyte reacts directly with an oxidant or reductant, under a particular set of reaction conditions. The fourth and least common type of reaction differs from the others in that the quantitative inhibitory effect of the analyte on the CL reaction is monitored.

Alcohols: Ethanol and methanol have been determined at the sub- μM level [85, 86, 88] by the enzymatic production of hydrogen peroxide which then acted as the oxidant in the luminol system (type two reaction above). An interesting modification to conventional CL methods was the use of an optical fibre to transport the luminescence from the flow cell to the detector [85]. A new chemiluminometric method for determining glycerol in wines has been reported [87], based on the combination of immobilized glycerol dehydrogenase and NADH oxidase. Results were in good agreement with official reference methods; the technique was specific and was not affected by self-fluorescence. Recently, volatile phenols have been monitored in polluted waters by their ability to quench the chemiluminescence of p-chlorobenzenediazonium fluoroborate in alkaline hydrogen peroxide [89], with a detection limit of $0.015 \mu\text{g ml}^{-1}$ for phenol being reported.

Amines: A method for primary amines has been described, in which Schiff bases derived from phenylacetaldehyde in methanol produced strong chemiluminescence when oxidised with iron(II) and hydrogen peroxide (Fenton's reaction) [92]. The suppressive effect of alkanolamines on the Cu(II)- or Co(II)-catalysed luminol reaction has also been applied to their determination, after ion-pair separation on an ODS column [90]. The negative signal from eluting amines was due to complexation with the metal ion, which destroyed its ability to catalyse the luminol reaction.

Table 1.7. Flow injection chemiluminescence applications for the determination of organic species.

Analyte	CL reaction	Sample matrix	LOD (as specified in original paper)	Reference
ALCOHOLS				
ethanol	enzymatic production of H ₂ O ₂ ; luminol - potassium hexacyanoferrate (III) reaction	wines	3 x 10 ⁻⁶ M	[85]
ethanol	enzymatic production of H ₂ O ₂ luminol - 4-iodophenol with immobilized horseradish peroxidase flow cell	synthetic	1 x 10 ⁻⁸ M	[86]
glycerol	combination of immobilized glycerol dehydrogenase and NADH oxidase	wines	0.1 mM	[87]
methanol	H ₂ O ₂ production in immobilized enzyme system; luminol CL detection	synthetic	0.1 mg l ⁻¹	[88]
phenols	quenching of p-chlorobenzenediazonium fluoroborate in alkaline hydrogen peroxide	polluted water	e.g. 0.015 µg ml ⁻¹ phenol 0.030 µg ml ⁻¹ 2,4-xyleneol	[89]
AMINES				
alkanolamines	separation by ion-pair chromatography; suppressive effect on Cu(II) or Co(II) - luminol reaction	synthetic	0.8 nmol ethanolamine 1.2 nmol diethanolamine 0.2 nmol triethanolamine (20µl injection)	[90]
amines	aryl oxalate - sulphorhodamine 101	fish	e.g. 7 x 10 ⁻¹⁰ M cadaverine 1.2 x 10 ⁻⁸ M hexylamine 1.4 x 10 ⁻⁸ M diethylamine	[91]
primary amines, amino acids	derivatised to Schiff bases; oxidation of iron(II) and H ₂ O ₂ (Fenton's reaction)	synthetic	1.5 x 10 ⁻⁸ M n-hexylamine 1.4 x 10 ⁻⁷ M alanine	[92]
epinephrine norepinephrine dopamine L-dopa	action of analyte on CL oxidation with potassium permanganate in acidic medium; enhanced with formaldehyde	synthetic	0.05 µg ml ⁻¹ epinephrine, L-dopa 0.1 µg ml ⁻¹ dopamine, norepinephrine	[93]

Analyte	CL reaction	Sample matrix	LOD (as specified in original paper)	Reference
AMINO ACIDS				
primary amino acids	based on Schiff base formation in reversed micelles	synthetic	1.4×10^{-6} M alanine	[94]
amino acids	inhibition of mimetic peroxidase catalysis of luminol - H_2O_2 reaction	synthetic	6.8×10^{-8} M L-cysteine 1.3×10^{-7} M L-tyrosine 8.5×10^{-6} M L-tryptophan 2.2×10^{-5} M L-cystine	[95]
L-lysine	enzymatic production of H_2O_2 in lysine oxidase reactor; fibre-optic detection via peroxidase-catalysed luminol reaction	synthetic	10 μ M	[96]
CARBOHYDRATES				
glucose, uric acid	H_2O_2 with peroxyoxalate and 2,4,6,8-tetrathiomorpholinopyrimido [5,4-d] pyrimidine using immobilized enzyme reactor	serum	5×10^{-7} M glucose 5×10^{-7} M uric acid	[97]
glucose	peroxidase-catalysed luminol	microdialysis samples	0.008 μ M	[98]
glucose	H_2O_2 production in immobilized glucose oxidase - luminol - ferricyanide system; fibre optic chemiluminescence transport	fruit juices	0.20 mM	[99]
glucose	luminol oxidation; use of sequential injection analysis and novel fountain cell	synthetic	not reported	[70]
glucose	catalytic effect of iron(II) - dimethylglyoxime complex on oxidation of luminol using hydrogen peroxide	synthetic	0.79 μ g ml ⁻¹	[66]
glucose	H_2O_2 determination in luminol system; glucose oxidase and HRP covalently co-immobilized on nylon membrane	synthetic	24 μ M	[64]

Analyte	CL reaction	Sample matrix	LOD (as specified in original paper)	Reference
DRUGS				
morphine	morphine with acidic potassium permanganate in tetraphosphoric acid	process streams	$5 \times 10^{-8} \text{M}$	[100]
tetracyclines	oxidation with H_2O_2 , catalysed by copper ion in ammonia medium; persulfate co-oxidising agent	pharmaceutical preparations	10 pmol chlortetracycline 0.1 nmol tetracycline 0.1 nmol oxytetracycline	[101]
ENZYMES and SUBSTRATES				
albumin	enhancement of metalloporphyrin catalysed luminol - H_2O_2 system	serum	$2.5 \mu\text{g ml}^{-1}$	[102]
albumin, immunoglobulin-G	enhanced reaction between METQ, H_2O_2 and 8-anilino-1-naphthalene sulphonic acid	serum	1.05 μg albumin 0.156 ng IgG (100 μl sample injection)	[103]
1,5-anhydroglucitol	H_2O_2 production; luminol - hexacyanoferrate(III) reaction; anion-exchange column and immobilized pyranose oxidase reactor	serum	$2 \times 10^{-7} \text{M}$	[104]
creatinine	H_2O_2 production; consecutive reaction of three immobilized enzymes	serum	not reported	[105]
L-glutamate, L-glutamine	luminol catalysed by peroxidase; immobilized L-glutamate and glutaminase coupled with peroxidase	synthetic	$1 \times 10^{-7} \text{M}$ L-glutamate $1 \times 10^{-6} \text{M}$ L-glutamine	[106]
3-hydroxybutyrate	H_2O_2 production; luminol - hexacyanoferrate(III) reaction; immobilized enzyme reactor	serum	0.1 μM	[107]
proteases	oxidation of tripeptide-isoluminol derivative immobilized on affinity support; released isoluminol detected by its copper-catalysed oxidation	synthetic	$2.7 \times 10^{-4} \text{mg l}^{-1}$ alpha-chymotrypsin $4 \times 10^{-2} \text{mg l}^{-1}$ trypsin $2 \times 10^{-3} \text{mg l}^{-1}$ commercial protease	[108]

Analyte	CL reaction	Sample matrix	LOD (as specified in original paper)	Reference
VITAMINS				
ascorbic acid	Fe(III) reduction; Fe(II) detection in luminol - hydrogen peroxide system	pharmaceutical preparations, fruit juices	$1 \times 10^{-12} \text{M}$	[109]
ascorbic acid	photooxidation of analyte; reaction with alkaline lucigenin sensitized by toluidine blue	pharmaceuticals, fruit juices, soft drinks, blood serum	$1 \times 10^{-9} \text{M}$	[110]
L-ascorbic acid	reaction of L-ascorbic acid with ascorbate oxidase; lucigenin chemiluminescence	drugs, health drinks	$0.1 \mu\text{g ml}^{-1}$	[111]
folic acid	action of cerium(IV) on analyte in acidic medium; emission enhanced by rhodamine-B	pharmaceutical formulations	$1 \times 10^{-8} \text{M}$	[112]
riboflavin, riboflavin 5'-phosphate	photo-reduction of analyte by EDTA; reduction of hydrogen peroxide monitored via luminol system; hematin catalyst	pharmaceutical preparations, foods, animal tissues	$1 \times 10^{-7} \text{M}$	[113]
vitamin B ₁₂	vitamin B ₁₂ acidified to release Co(II); luminol - hydrogen peroxide system	pharmaceutical products	1 ng (50 μl injection)	[114]
MISCELLANEOUS				
adenosine-5'-triphosphate (ATP)	hydrogen peroxide - sodium hydroxide - brilliant sulfoflavine system	human urine	$1.0 \times 10^{-5} \text{M}$	[115]
ATP, glucose, bile acid	1-methoxy-5-methylphenazinium methyl sulphate / isoluminol / microperoxidase system; immobilized enzyme reactors	human serum samples	2.5 pmol bile acid 0.5 nmol glucose $5 \times 10^{-7} \text{M}$ ATP	[116]
adrenaline	aerobic oxidation of adrenaline using ordered surfactant assemblies and manganese(II) catalyst	drug samples	$3 \times 10^{-6} \text{M}$	[117]
aromatic ketone hydrazones	KMnO ₄ oxidation with formic acid carrier; rhodamine B sensitizer	synthetic	e.g. $3 \times 10^{-6} \text{M}$ benzophenone hydrazone	[118]
bile acids	oxidation of sulphite by cerium(IV) sensitized by bile acids	synthetic	e.g. $2.0 \mu\text{g ml}^{-1}$ ursodeoxycholic acid	[119]

Analyte	CL reaction	Sample matrix	LOD (as specified in original paper)	Reference
citrate	photochemical decomposition of iron(III)-citrate complex; detection by iron(II)-catalysis of luminol reaction	pharmaceutical preparations, soft drinks	$2.0 \times 10^{-7} \text{M}$	[120]
cyclamate, sodium	sensitizing effect on oxidation of sulphite by cerium(IV) in sulfuric acid	synthetic	$1.0 \mu\text{g ml}^{-1}$	[121]
DNA	interaction of porphyrin mesotetrakis (4-N-methylpyridinyl)porphyrin (TMPyP) manganese derivatives with DNA; catalytic effect on luminol - H_2O_2 system	synthetic	0.20 ng ml^{-1}	[122]
fluorescent organic compounds (e.g. rhodamine B, pyranine)	ketone catalysed decompositions of peroxymonosulfate ion / acetone system	synthetic	not reported	[45]
humic acid	reaction between humic acid and hypobromite in alkaline solution; on-line anion exchange column	natural water	0.01 ppm	[123]
isoprenaline	isoprenaline with lucigenin in aqueous potassium hydroxide carrier stream	synthetic	$1 \times 10^{-7} \text{M}$	[124]
lactate, pyruvate	reactor column containing co-immobilized oxidoreductases; enzyme amplification followed by H_2O_2 generation	synthetic	48 nM lactate 103 nM pyruvate	[125]
lactate, lactate-dehydrogenase nucleosides	luminol in reversed micelles; immobilized enzyme column; ferricyanide reactor production of OH radicals in reaction of H_2O_2 with Co(II) - 1,10-phenanthroline complex in alkaline solution; CL emission on analyte reaction with OH radicals	serum synthetic	$10 \text{ pmol } \mu\text{l}^{-1}$ lactate e.g. $68 \text{ pmol uridine-5'-diphosphogucose (UDP-Glu)}$ ($10 \mu\text{l}$ injection)	[126] [127]
oxalate	photochemical decomposition of iron(III)-oxalate complex; iron(II) detection via luminol system	urine	$1.0 \times 10^{-7} \text{M}$	[128]

Analyte	CL reaction	Sample matrix	LOD (as specified in original paper)	Reference
organotin compounds: di-n-butyltin dichloride diphenyltin dichloride tri-n-butyltin chloride triphenyltin chloride oxalate	reaction of bis(2,4,6-trichlorophenyl) oxalate (TCPO) with H ₂ O ₂	synthetic	0.5 μM DBTC 1.25 μM DPTC 25 μM TBTC 100 μM TPTC	[129]
	H ₂ O ₂ production detected via luminol - hexacyanoferrate(III) system; immobilized oxalate oxidase column reactor	urine	34 μM	[130]
phenylpyruvic acid (PPA)	aerobic oxidation of PPA in alkaline solution; surfactant molecular assemblies and cobalt(II) catalyst	urine	1 x 10 ⁻⁷ M	[131]
promethazine	inhibition of luminol - hydrogen peroxide - chromium(III) system	pharmaceutical preparations	3 x 10 ⁻⁹ M	[132]
steroids	sensitizing effect of analyte on cerium(IV) - sulphite reaction	commercial formulations	e.g. 0.02 μg ml ⁻¹ cortisone	[133]
tetrahydrofuran (THF)	THF - methylsilicone solid polymer reaction; enhanced with dye-sensitizer, surfactant and visible light	synthetic	1 x 10 ⁻³ M	[134]
thiazide compounds	reaction of thiazide diuretic compounds with tris(2,2'-bipyridine) ruthenium(III)	pharmaceutical capsules	e.g. 1 ng ml ⁻¹ hydroflumethiazide	[135]
triphosphonucleotide	loading triphosphonucleotide chemically to copper(II)-modified clinoptilolite (zeolite); copper(II) - 1,10-phenanthroline system after material exchange column	human urine	e.g. 50 fmol adenosine triphosphate (ATP) (100μl injection)	[136]
urea	urea and hypobromite in alkaline solution; on-line cation exchange column	human urine, natural aqueous samples	9.0 x 10 ⁻⁸ M	[137]

Another application for 55 aliphatic, aromatic and heterocyclic amines involved the aryl oxalate - sulphorhodamine 101 chemiluminescence reaction [91], without the need for a derivatisation step. The detection limits for the amines studied ranged from sub-nM to μM ; the proposed method was applied to the determination of histamine in fish and compared favourably with an LC system using post column derivatisation and fluorescence detection. Epinephrine, norepinephrine, dopamine and L-dopa have been determined by their chemiluminogenic oxidation with permanganate in an acidic medium, enhanced by the presence of formaldehyde [93]. Detection limits were in the $0.05 - 0.1 \mu\text{g ml}^{-1}$ range.

Amino Acids: Three FI-CL techniques for amino acids have been published recently. The first approach involved Schiff base formation with phenylacetaldehyde and α -amino acids [94]. Sodium bis(2-ethylhexyl)sulphosuccinate reversed micelles were found to be an effective medium for the reaction. Another approach exploited the quenching of the peroxidase catalysed luminol reaction, using H_2O_2 as the added oxidant [95]. A typical detection limit for this method was $6.8 \times 10^{-8}\text{M}$ for L-cysteine. Once the system was effective for detecting a chosen analyte, a silica-based LC separation of the amino acids was incorporated, using phosphate buffer (pH 7.3) as mobile phase. L-lysine has been determined at micromolar levels by coupling a lysine oxidase reactor with a fibre-optic hydrogen peroxide detector [96].

Carbohydrates: Sugars have most commonly been analysed by oxidase-catalysed reactions that convert glucose to hydrogen peroxide, which is subsequently determined by luminol CL [64, 66, 99]. The peroxyoxalate system has also been exploited to determine glucose and uric acid in serum [97] at sub-micromolar levels, and results correlated well with conventional colorimetric methods. A novel system for the determination of glucose used sequential injection analysis (SIA) and a fountain cell, a device with radial flow properties that enabled quantitative analyses and a study of the reaction kinetics [70].

Drugs: A limited number of FI applications for analysing drugs have been reported. Problems of specificity have usually been overcome by combining CL detection with LC separation (*see Table 1.12*). Morphine has been determined in process streams using the CL emission from the reaction of the analyte with potassium permanganate in the presence of tetraphosphoric acid [100]. Interferences from other structurally related alkaloids were negligible which provided favourable results when compared with a validated LC method. Tetracyclines have been determined by their reaction with H_2O_2 and persulfate, catalysed by copper ions in an ammonia medium [101].

Enzymes and Substrates: Numerous methods have been reported for the determination of enzymes and substrates, most commonly in serum. The catalysed-oxidation of luminol was the system used for several analyses, often measuring the enzymatic production of hydrogen peroxide [104, 105, 107]. Immunoglobulin-G and albumin have been determined using an enhanced peroxyoxalate CL system [103]. An interesting adaptation to determine proteases exploited the oxidation of a tripeptide-isoluminol derivative immobilized on an affinity support incorporated into a flow system [108]. Injected enzyme sample solutions catalysed the hydrolysis of the derivatives at pH 8.47, and the released isoluminol was detected by the CL produced by its copper-catalysed oxidation with hydrogen peroxide, with detection limits at the parts per billion level.

Vitamins: Pharmaceutical preparations, fruit juices, foods, blood serum and animal tissues are all sample matrices in which vitamins have been determined. The oxidation of lucigenin (bis-N-methylacridinium nitrate, 10,10'-dimethyl-9,9'-bi-sacridinium dinitrate) in basic solution produces light emission which can last for several minutes, and this was exploited to monitor ascorbic acid (vitamin C) [110, 111]. The luminol - hydrogen peroxide system has been used for the determination of vitamin B₁₂ after release of Co(II) [114], and for the analysis of ascorbic acid after reduction of Fe(III) [109]. Riboflavin and riboflavin 5'-phosphate were photo-reduced by ethylenediaminetetraacetic acid, and determined by measuring the H₂O₂ reduced in a luminol reaction by the 1,5-dihydro forms of these flavins generated during the photochemical process [113]. The method was successfully applied in analysing B₂ vitamers at sub- μ M levels. The oxidation of folic acid (vitamin B₉) by cerium(IV) in an acidic medium was enhanced by rhodamine B and enabled its determination in pharmaceutical formulations at the 10nM level [112].

CL, when coupled with FI technologies, can provide analytical procedures with extremely low detection limits and the number of reported applications of FI with CL detection has increased considerably in recent years. For the analyses of real samples the limited selectivity of CL reactions can be overcome by incorporating physical or chemical separation techniques into an FI manifold to remove the matrix and/or to modify the analyte. This is generally achieved using solid phase reagents, immobilized on a column upstream of the detector or within the flow cell itself. For most applications however, the FI-CL combination is still not selective enough and so a means of physical separation, e.g. liquid chromatography, may be required.

1.4. CHROMATOGRAPHY

1.4.1. Basic Principles

Chromatography describes analytical methods that are used for the separation, identification, and determination of the chemical components in complex mixtures, many of which could not otherwise be resolved. Several excellent reviews and book chapters have been written on this subject [138-142].

Chromatographic separations are achieved by exploiting the differences between species of a variety of properties including; volatility, polarity, charge size and mass. Components of a mixture are carried through a stationary phase by the flow of a gaseous or liquid mobile phase, separations being based on the differences in migration rates among the sample components. Chromatographic methods have been classified according to the type of mobile and stationary phase as well as the kind of equilibria involved in the transfer of solutes between phases (Table 1.8.).

Classification	Specific method	Stationary phase	Equilibrium type
Gas chromatography (GC) (gas mobile phase)	Gas-liquid	Liquid adsorbed on a solid	Partition between gas and liquid
	Gas-solid	Solid	Adsorption
	Gas-bonded phase	Organic molecules bound to surface	Partition/adsorption
Liquid chromatography (LC) (liquid mobile phase)	Liquid-liquid	Liquid adsorbed on solid	Partition between two liquids
	Liquid-solid	Solid	Adsorption
	Liquid-bonded phase	Organic molecules bound to solid support	Partition/adsorption
	Ion-exchange	Ion-exchange resin	Ion-exchange
	Gel-permeation	Liquid within the interstices of a polymeric solid	Partition sieving

1.4.2. High performance liquid chromatography

In high performance liquid chromatography (HPLC) the mobile phase is a liquid and is commonly referred to as the eluent. HPLC instrumentation includes a pump, injector, column, detector and recorder or data system (Figure 1.13).

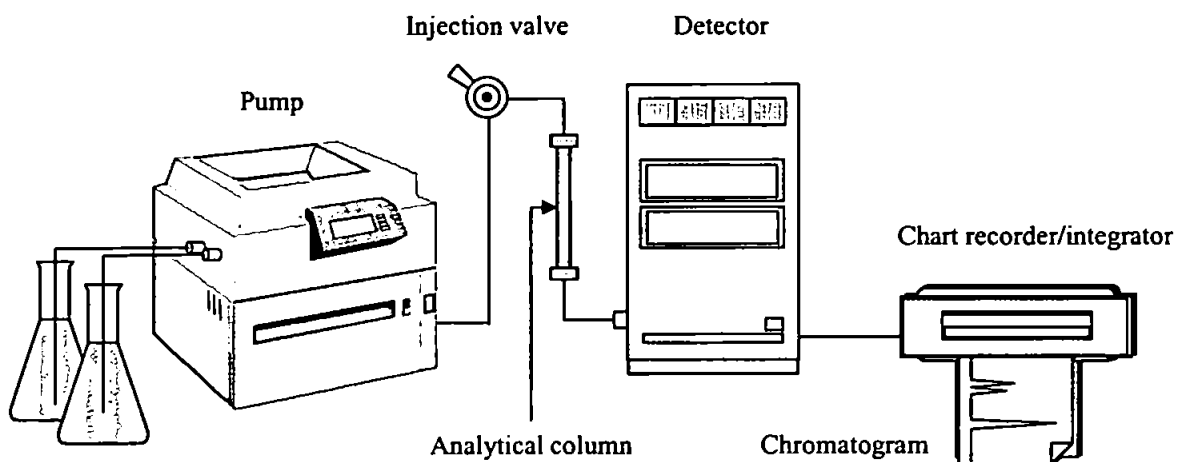


Figure 1.13. Typical layout of major components for HPLC.

The heart of the system is the column where separation occurs. Since the stationary phase is usually composed of micrometer size porous particles, a high-pressure pump is required to move the mobile phase through the column. The chromatographic process begins by injecting the solute onto the top of the column. Separation of components occurs as the analytes and mobile phase are pumped through the column interacting with the stationary phase. Each component elutes from the column as a narrow band (or peak) on the recorder. Detection of the eluting components is important, and this can be either selective or universal, depending upon the detector used. The response of the detector to each component is displayed on a chart recorder or computer screen and is known as a chromatogram. To collect, store and analyse the chromatographic data, computers, integrators, and other data processing equipment are frequently used.

Adsorption chromatography: All of the pioneering work in chromatography was based upon liquid-solid adsorption, in which the stationary phase was the surface of a finely divided polar solid. With such a packing the analyte competes with the mobile phase for sites on the surface of the packing, and retention is the result of adsorption forces.

The mobile phase systems used in adsorption chromatography are based on non-polar solvents, commonly hexane, containing a small amount of polar modifier, such as dichloromethane or methyl-*t*-butyl ether. When the sample is applied to the column, sample molecules with polar functional groups are attracted to the active sites on the column packing. These are subsequently displaced by the polar modifier molecules of the mobile phase, as the chromatogram develops, and will pass down the column to be re-adsorbed on fresh sites. The retention behaviour of individual sample solutes is governed by the polarity of functional groups, more polar molecules will be adsorbed more strongly and hence will elute more slowly from the column.

High performance partition chromatography: Partition chromatography has become the most widely used of all LC procedures and is divided into liquid-liquid (LLC) and bonded-phase chromatography (BPC). In liquid-liquid partition packings retention is governed by physical adsorption, while in bonded-phase packings covalent bonds are involved [143]. LLC is limited by the choice of truly immiscible solvent pairs and has almost entirely been superseded by BPC, with LLC being relegated to certain special applications.

The most common solid support for bonded phase systems is prepared by reaction of an organochlorosilane with the $-OH$ groups formed on the surface of silica particles by hydrolysis in hot dilute hydrochloric acid, to form an organosiloxane.

BPC can be divided into two further categories, normal phase and reversed phase. For reversed-phase applications R is based on a hydrocarbon, e.g. octadecyl ($-C_{18}H_{37}$), octyl ($-C_8H_{17}$), phenyl, while for normal-phase, amino, diamino and nitrile groups are examples of functional groups that have been bonded to the silica surfaces.

In normal-phase LC the stationary phase is polar and the mobile phase is non-polar, the least polar components are eluted first and increasing the polarity of the mobile phase leads to a decrease in retention time. Mobile phases used are similar to those used in adsorption LC, the separations obtained are similar as well although there are selectivity differences. The main advantage of these systems compared to the adsorption systems described previously is the facility to undertake gradient elution.

In reversed-phase LC the stationary phase is non-polar and the mobile phase is relatively polar, and in contrast to normal-phase systems, the most polar component elutes first and

increasing the polarity of the mobile phase leads to an increase in retention time. The most common mobile phases consist of water with water miscible organic solvents e.g. acetonitrile, methanol and tetrahydrofuran, added to modify the elution characteristics of the samples. Gradient elution techniques are used in order to change the organic composition of the mobile phase with time. It has been estimated that over 70% of all HPLC separations are carried out using reversed-phase systems and that it has been applied to the separation of virtually all molecules of relative molecular masses below 2000 daltons [144].

In general, although not fully understood, the predominant factor for retention in reversed-phase LC is the non-specific hydrophobic interactions of the solute molecules with the stationary phase. This explains the wide applicability of the mode, as practically all organic molecules possess a structural region of hydrophobic nature. Assuming all other factors remain constant, bonded reversed-phase packings with the longest hydrocarbon chain are more retentive for non-polar compounds [145].

1.4.3. Chromatographic Parameters

A number of parameters can be derived from a chromatogram to describe the component peaks individually and relative to one another, these are summarised in Table 1.9.

Retention: Retention is the term used to describe the interaction of sample components with stationary phase. For a particular component the degree of retention is characteristic of the component, and is described by the retention volume, v_r . Components that do not interact with the stationary phase are eluted in the dead volume of the column, also called the column void volume, v_o . Unretained material appears as a small peak at the beginning of a chromatogram with a time of t_o , using this and the flow rate we can calculate v_o . Sometimes the first peak of the chromatogram does not appear at the void volume if, for example, the detector is not sensitive to the unretained material or if all the components of a sample interact with the stationary phase.

Retention volumes of components derived from a particular chromatogram are absolute values and as such they will vary with flow rate. A relative term for retention which does not vary with flow rate is the capacity factor, k' , which is calculated for each peak using the derivation described in Table 1.9. Useful separations typically involve capacity factors

in the range 1-10, capacity factors greater than 10 can lead to excessive analysis times [146].

Table 1.9. Chromatographic parameters.	
Measured parameters	Symbol
Column void volume (time)	$v_0 (t_0)$
Retention volume (time)	$v_r (t_r)$
Peak base width	W
Peak width at half peak height	$W_{1/2}$
Peak height	h
Derived parameters	Symbol and derivation
Retention/capacity factor	$k' = \frac{v_r - v_0}{v_0} = \frac{t_r - t_0}{t_0}$
Selectivity factor (for two peaks, <i>a</i> and <i>b</i>)	$\alpha = \frac{k'_b}{k'_a} = \frac{(t_{rb} - t_0)}{(t_{ra} - t_0)}$
Column efficiency; number of theoretical plates (calculated from a peak, <i>a</i>)	$N = 16(t_{ra}/W_a)^2$
Height equivalent to a theoretical plate (for a column length <i>L</i>)	$H = L/N$
Resolution; resolution factor (for two peaks, <i>a</i> and <i>b</i>)	$R = 2(t_{rb} - t_{ra})/(W_b - W_a)$

Selectivity: The various components of a mixture will have different values of k' . The selectivity factor α is a function of the relative retention of each component by a stationary phase. For separation to occur α should be greater than unity, however in HPLC α is almost unity for closely eluting components having 'narrow' peaks and typically falls in the range 1.1-2.0 [147]. If the value is unity the components undergo the same interactions with the stationary phase and cannot be separated by that particular set of chromatographic conditions.

Efficiency: Samples can be thought of as being injected on to a column as a band, which moves through the column under the influence of the mobile phase. If the

chromatography were ideal little or no dispersion would occur, the components separating and eluting as discrete bands whose total volume will be equal to the original sample volume with rectangular peak profiles [148]. In practice, as the sample passes through the column, its components diffuse to form peaks that approximate to Gaussian distributions.

The width of the bands will greatly effect the separation of a mixture on a column. The mixing and diffusion phenomena that lead to band broadening (Table 1.10.) must therefore be kept to a minimum, to enable good separations in short times. The ability of a column to minimise band broadening is termed the column efficiency and can be expressed as the number of theoretical plates, N of a column. Several methods have been used for the calculation of column efficiencies, which vary with point where the peak width is measured. If a chromatographic peak is not symmetrical the base width is not a true reflection of the dispersion of the peak. The width at half the peak height, $W_{1/2}$, can be used to calculate column efficiency [149].

Table 1.10. Sources of band broadening in LC.	
Process	Cause
Eddy diffusion (A term)	Differing flow path lengths present in a column due to lack of uniformity of packing material
Longitudinal diffusion (B term)	Tendency of molecules to migrate from the concentrated centre of a band towards more dilute outer regions.
Mass transfer (C term)	Speed of diffusion between mobile and stationary phases and diffusion between mobile phase and mobile phase trapped within pores in the solid support particles.
Extra-column diffusion	Dead volumes associated with the detector flow cell and fittings connecting it to the column.

The number of theoretical plates contains no information about the dimensions of a column. Efficiency may also be determined as length of column per unit number of theoretical plates. The term used is height equivalent to a theoretical plate, H , the lower its value the more efficient the column.

Band broadening in LC is considered as arising from four sources, of which three forces can be related to H by the van Deemter equation [150];

$$H = A + B/u + Cu$$

where A, B and C are constants determined by the physical properties of the stationary and mobile phases and u is the mobile phase velocity (cm s⁻¹). Therefore, increasing the velocity of the mobile phase reduces longitudinal diffusion. Eddy diffusion can be reduced by using smaller diameter particulate packing material consistent with producing uniform packing. Mass transfer effects are made worse at higher mobile phase velocities, they can be minimised by reducing the diameter of the support particles, eliminating long narrow pores that trap mobile phase and by using thin coatings of stationary phase upon the solid support. Keeping the dead volume of all fittings to a minimum can help reduce extra-column band broadening effects.

Resolution: With the width of the peak defined, a real measure of the resolution of the two peaks is possible using the resolution factor, R. When this equals unity there is still approximately 3% overlap of two peaks, however as R increases to 1.5 the overlap is reduced to approximately 0.3%. The resolution for a given stationary phase can be improved by lengthening the column and hence increasing the number of plates. An adverse consequence of the added plates, however, is an increase in analysis time.

General resolution equation: The expressions for resolution, column efficiency, selectivity and capacity factors can be combined in one equation to describe resolution. This is termed the general resolution equation [147, 151];

$$R = \sqrt{N}[(\alpha - 1)/\alpha][k'_a/(k'_b + 1)]/4$$

On inspection it is observed that R is directly related to selectivity (nature of interactions) and capacity (the extent of phase interaction). Altering these by manipulation of the mobile and stationary phases will therefore be the most effective way of improving resolution between two peaks, very large changes in efficiency are required to achieve the same result.

1.4.4. Detectors for HPLC

Regardless of the principle of operation, an ideal LC detector should have the following properties; Low drift and noise level (particularly crucial in trace analysis), high sensitivity, fast response, wide linear dynamic range (this simplifies quantitation), low

dead volume (minimal peak broadening), insensitivity to changes in type of solvent, flow rate, and temperature, operational simplicity and reliability, and it should be non-destructive to the sample. Unfortunately no truly universal detector which satisfies these criteria has yet been developed for HPLC [152]. Thus the system used is generally dependent on the nature of the sample.

The detectors for HPLC can be split into three categories;

1. Detectors that monitor a bulk property of the mobile phase, e.g. refractive index, dielectric constant and density, are called general detectors. In this instance the solute modifies the base value of the property associated with the solvent.
2. Detectors that monitor a specific property of the solute that is not shared with the solvent, e.g. UV absorbance and fluorescence. Possession of such a property by the solute in the mobile phase affords its detection in the column effluent.
3. Detectors that function by desolvation from the mobile phase, e.g. mass spectrometry.

The most common methods of detection are summarised in Table 1.11. Many other methods of detection have also been applied to HPLC and new detection systems continue to be developed and reported in the literature [153, 154].

The detection methods described in the table each have their drawbacks. Refractive index detectors have the advantage of responding to all solutes, although in complex samples components may cover a wide range of index values and some may be too close to that of the mobile phase to allow detection. They are also very temperature dependent and are unsuitable for solvent gradient programming. Similarly electrochemical detection is extremely solvent dependent and thus gradient programming is not compatible. Mass spectrometric detectors are finding increasing use for HPLC although the technology is still relatively expensive and extremely specialised. UV absorbance has found the widest application, although detectability and sensitivity can be greatly effected by the nature of the sample matrix and its inherent absorbance characteristics.

Table 1.11. Characteristics of common detectors for HPLC.

Mode of detection	General description
Absorbance	Absorbance of ultraviolet (UV), infrared (IR) and visible radiation, UV absorbance is the most common. Species with one or more double bonds, unshared lone bonding electrons absorb UV e.g. olefins, aromatics, compounds containing $>C=O$, $>C=S$, $-N=O$, $-N=N-$, therefore of wide applicability. Detector consists of a flow cell, a beam of UV light is focused through the cell on to a photodiode. Can sometimes be programmable.
Refractive index	The first on line LC detector, they are bulk property detectors. Pure mobile phase is passed through half of the cell while column eluent passes through the other. The incident beam of light source shining through the cell is bent by the difference in the refractive indices of the two solvent streams, due to the presence of solutes in the mobile phase. Refractive index detectors have found application for sugar analysis in the food industry and as a detector in size exclusion chromatography in the polymer industry.
Electrochemical	Conductivity, polarographic, amperometric and coulometric detectors have been described. Conductivity is applicable to ionic compounds, while the other electrochemical methods are applied to compounds that can be electrolytically oxidised or reduced e.g. phenols, mercaptans, catecholamines aldehydes and ketones. Mobile phases are selected so as to be electrically conducting.
Mass spectrometric	Successful interfacing of HPLC with vacuum requirements of mass spectrometry by a variety of methods e.g. molecular jet, vacuum nebulising and thermospray systems. May well prove to be the most informative of all detectors for HPLC as not only does it afford quantitative analysis, but single ion monitoring (SIM) procedures offer high sensitivity and selectivity.

Luminescence detectors: Fewer species possess inherent luminescence and so luminescence detection for HPLC provides simpler chromatograms with less matrix effects that are very selective. Fluorescence detectors represent one of the most commonly used detector-types in modern HPLC and are the most specific and selective of all optical detectors.

For those compounds having natural fluorescing capability, or which can be made to fluoresce through derivatization, this type of detection is extremely sensitive. The fundamental properties of fluorescence and other luminescence techniques have been discussed above (*section 1.2*).

Two kinds of fluorescence instruments have commonly been used for HPLC;

1. Filter fluorimeters using filters to select broad bands of radiation thereby providing high sensitivity but lacking specificity.
2. Spectrofluorimeters which use monochromators that allow both the excitation and emission wavelengths to be scanned, greatly increasing the selectivity and sensitivity [155, 156].

More recently there has been increased interest in the application of CL reactions to LC detection. One advantage of using CL rather than fluorescence detectors is the absence of an excitation source. This is useful because the background due to the excitation light is one of the main obstacles in obtaining sensitivity with fluorescence monitors. For CL detection in HPLC however the compatibility between the CL reaction and the solvent and pH requirements of the separation needs careful consideration.

1.4.5. Analytical applications of LC with CL detection.

In recent years, liquid chromatography (LC) has become a preferred technique for the analysis of a wide range of pharmaceutical and environmental samples. The goal of CL based reaction schemes is to enhance the detectability of a class of compounds or of a particular target analyte, shown by an increase in sensitivity and/or selectivity towards the analyte relative to more conventional detection methods. A typical system used for post-column CL detection in LC is shown in Figure 1.14.

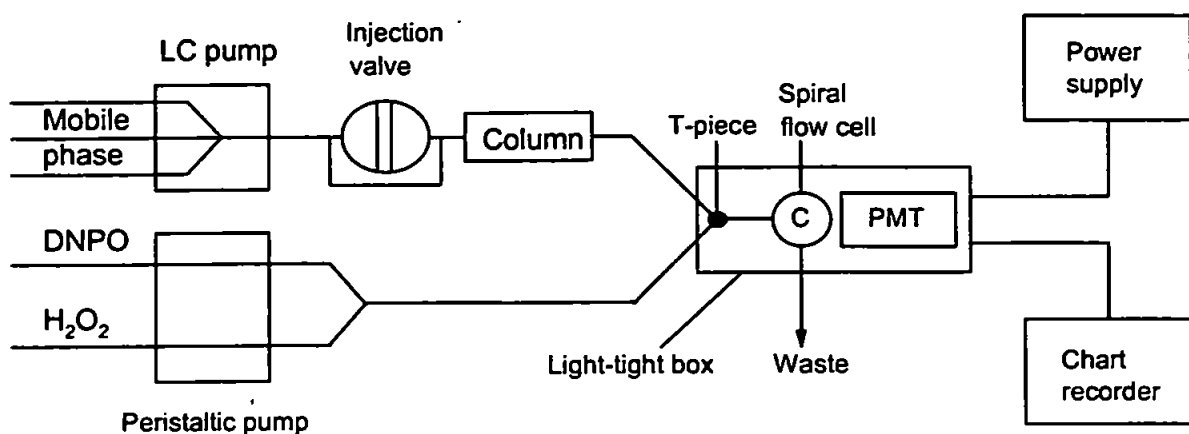


Figure 1.14. Typical liquid chromatography manifold for POCL applications.

Although a number of CL systems have been used for LC detection, the peroxyoxalate system (POCL) is the most commonly used. Applications of LC-CL, have been the subject of some recent reviews [157, 158] and are shown in Table 1.12. [159-200].

Amines: The analysis of primary and secondary amines, using LC with CL detection, has been extensively reported [159-165]. One method [160] described the synthesis and use of Luminarins 1 and 2, which are labelling agents having a quinolizinocoumarin, structure and an N-hydroxysuccinimide ester reactive function. These reacted with amines, under relatively mild conditions, to produce highly fluorescent / chemiluminescent derivatives. Another method [159] described pre-column derivatization of amines using 6-isothiocyanatobenzo[g]phthalazine-1,4(2H,3H)-dione in the presence of triethylamine to yield highly chemiluminescent derivatives. Such derivatives then reacted with H_2O_2 in the presence of potassium hexacyanoferrate (III) to produce CL emission. Ethylenediamine (ED) [162] and 1,2-diphenylethylenediamine [161] have both been used as fluorogenic derivatization reagents for the detection of catecholamines using post-column POCL.

Nitrosamines have been fluorogenically derivatized and detected using CL after denitrosation with hydrobromic acid-acetic anhydride to their corresponding secondary amines. Derivatization was then performed using sodium hydrogencarbonate and dansyl chloride to form dansyl derivatives that were detected using POCL [163]. The only method not to involve derivatization is the determination of polyamines [165] with aryl oxalate-sulphorhodamine 101, which was reported to be 5-1000 times more sensitive than GC and LC methods incorporating derivatization.

Table 1.12. Liquid chromatography chemiluminescence applications.

Analyte	CL reaction	Sample matrix	LOD (as specified in original paper)	Reference
AMINES				
amines (primary/secondary)	(IPO) derivatization; post column H ₂ O ₂ hexacyanoferrate (III)	synthetic	30-120 fmol (primary amines) 0.8-3 fmol (secondary amines)	[159]
amines (primary/secondary)	pre-column Luminarin 1 and 2 derivatization; post-column PO-CL	synthetic	low femtomole range	[160]
catecholamines	1,2-diphenylethylenediamine derivatization; post-column PO-CL (TDPO)	blood-plasma, urine	150-450 amol	[161]
catecholamines	on-column fluorogenic derivatization; post- column PO-CL (TDPO)	rat plasma	1.0 fmol	[162]
nitrosamines	denitrosation; dansyl chloride derivatization; post-column PO-CL (2-NPO)	synthetic	6.9 fmol NDMA 6.5 fmol NPy 8.6 fmol NDEA 8.0 fmol NPip 7.4 fmol NDPA 9.4 fmol NDBA	[163]
N-nitrosamines	fluorogenic derivatization;	groundwater	4.3-8.3 fmol (N-nitrosamines)	[164]
secondary amines	PO-CL (2-NPO)		4.6-7.3 fmol (secondary amines)	
polyamines	aryl oxalate (TDPO) sulphorhodamine 101	tomatoes	1.0-7.0×10 ⁻⁹ M	[165]
AMINO ACIDS				
amino acids	Dns-Cl derivatization; electro-generated CL; post-column (Ru[bpy] ₃ ³⁺)	synthetic	dansyl-derivatized glutamate 0.1 μM	[166]
amino acids (dansyl derivatives)	PO-CL (TCPO)	synthetic	2-4 fmol	[167]

Analyte	CL reaction	Sample matrix	LOD (as specified in original paper)	Reference
CARBOXYLIC ACIDS				
carboxylic acids	quinoxalinone derivatization; post-column PO-CL	plasma-sample extract	500attomole/injection	[168]
carboxylic acids	9-anthracene-methanol derivatization; post- column PO-CL (DNPO)	oxidised engine oils	130 pmol on- column	[169]
carboxylic acids (aliphatic)	9-anthracene-methanol derivatization; post- column PO-CL (DNPO)	non aqueous	1.8-4.5 pmol (C-6 - C-20 aliphatic acids)	[170]
carboxylic acids	(dansyl-BAP) derivatization; post-column PO-CL (2-NPO)	synthetic	25 fmol (retinoic acid)	[171]
carboxylic acids (enantiomers)	derivatization; PO-CL (TDPO and TCPO)	synthetic	0.49-15 fmol (TDPO) 0.74-29 fmol (TCPO)	[172]
carboxylic acids and prostaglandin E2	Luminarin 4 derivatization; post-column PO-CL	synthetic	50 fmol injected 32 fmol inj. (prostaglandin E2)	[173]
DRUGS				
anticholinergics	post-column (Ru[bpy] ₃ ³⁺)	commercial tablets	0.1-1.0 µgml ⁻¹	[174]
antihistamines	post column,(Ru[bpy] ₃ ³⁺)	tablets, urine samples	5-10 pmol	[175]
benzylamine	post-column PO-CL (TDPO)	rat plasma	147 nM	[176]
cyclosporin A	PO-CL (TDPO); sulphorhodamine 101	blood samples	6.0 ngml ⁻¹	[177]
dipyridamole	post-column PO-CL (TDPO)	rat plasma	345 pM	[176]
dipyridamole	post-column PO-CL (TDPO)	synthetic	10 amol	[178]
ibuprofen/naproxen	on-line generation of electrochemical reagent; porous graphite electrode; isoluminol derivatization	synthetic	0.15 pmol (ibuprofen) 0.45 pmol (naproxen)	[179]

Analyte	CL reaction	Sample matrix	LOD (as specified in original paper)	Reference
local-anaesthetics	acidic permanganate treatment	synthetic	benzocaine 30 ngml ⁻¹ butacaine 20 ngml ⁻¹ butoform 30 ngml ⁻¹ procaine 40 ngml ⁻¹ tetracaine 3 ngml ⁻¹	[180]
metoprolol	post-column PO-CL (TDPO)	serum	0.8 ngml ⁻¹	[181]
PEROXIDES				
hydrogen peroxide	post-column PO-CL (TDPO/TCPO)	cola drinks	188 fmol	[182]
hydrogen peroxide	PO-CL (TCPO)	synthetic	10nm	[183]
phosphoglyceride	luminol;	rat plasma	N/A	[184]
hydroperoxides	cytochrome c			
PHENOLS				
alkyl, nitro and chlorophenols	organically labelled derivatization; post-column photolysis PO-CL (2-NPO)	surface waters	0.01-0.1 ng ml ⁻¹	[185]
p-cyanophenol	PO-CL	soils	1×10 ⁻¹² M	[186]
phenolic herbicides	PO-CL	soils	10ppm	[186]
PCBs	photoinduced O production; dioxetane CL	fish oil sample	3.2×10 ⁻⁸ -1.7×10 ⁻⁴ mol l ⁻¹	[187]
POLYCYCLIC AROMATIC HYDROCARBONS				
aminopyrenes, diaminopyrenes	sodium hydrosulphide reduction; PO-CL (TCPO)	diesel/gasoline emission particulates	sub-fmol range	[188]
dinitropyrenes	off-line reduction; post-column PO-CL (TCPO)	synthetic	0.025 pg 1,8- and 1,6-DNP 0.050 pg 1,3-DNP	[189]
nitropyrenes	on-line electrochemical reduction; post-column PO-CL (TCPO)	urban air	2.19 ⁺ /-0.81 fmol m ⁻³ 1,3-DNP 4.03 ⁺ /-1.52 fmol m ⁻³ 1,6-DNP 3.63 ⁺ /-1.40 fmol m ⁻³ 1,4-DNP 0.70 ⁺ /-0.28 pmol m ⁻³ 1-DNP	[190]

Analyte	CL reaction	Sample matrix	LOD (as specified in original paper)	Reference
PAH, nitro-PAH	sodium hydrosulphide reduction; PO-CL (TCPO)	airborne particulates	N/A	[191]
SULFUR				
thiocarbamate pesticides	H ₂ /air reducing flame, reaction between SO and O ₃	apples	600 fg	[192]
pesticides, proteins and blood thiols	reduction, post-column reaction between SO and O ₃	aqueous	10 ppb S in aqueous samples	[193]
thiocarbamate pesticides	H ₂ /air reducing flame, reaction between SO and O ₃	synthetic	4 pg/s	[194]
MISCELLANEOUS				
adenine	reaction with phenylglyoxal	synthetic	1.9 × 10 ⁻⁷ M	[195]
ammonium nitrogen	high temperature oxidation; O ₃	waste waters	5 ng	[196]
bile-acids (conjugated)	NADH generation	human urine	8-250 pmol	[197]
guanine nucleos(t)ides	reaction with phenylglyoxal	synthetic	4-19 pmol ml ⁻¹	[198]
oxalate	(Ru[bpy] ₃ ²⁺); platinum electrode	urine and plasma	< 1 nmol ml ⁻¹	[199]
3-alpha, 5-beta-terahydroaldosterone	H ₂ O ₂ , potassium hexacyanoferrate (III)	human urine	0.6 pmol in urine	[200]

Carboxylic acids: The methods reported for the determination of carboxylic acids by LC generally use derivatization techniques, reversed-phase separation and POCL detection. Fluorescent labels have included 9-anthracene-methanol [169, 170], quinoxalinone [168], N-(bromoacetyl)-N'-[5-(dimethylamino)naphthalene-1-sulphonyl]piperazine (dansyl-BAP) [171] and Luminarin 4 [173]. A detection limit of 500 attomole/injection for the POCL determination of carboxylic acids after derivatization with quinoxalinone has been reported, which was 10 times more sensitive than the corresponding fluorescence detection method.

Drugs: A growing area for LC-CL applications is drug analysis. A ruthenium tris-bipyridine system has been used for the CL detection of antihistamines [175] and anticholinergics [174] in commercially available pharmaceuticals. This CL system was noteworthy because of its compatibility with reverse-phase LC solvent systems. Another system used the direct oxidation of drugs with an oxidising compound (acidic permanganate) [180], which was used to determine five local anaesthetics. An on-line method for the generation of electrochemical reagents for LC has been reported [179] for the determination of the drug ibuprofen after being labelled with an isoluminol derivative. The method involved the use of a porous graphite working electrode which was inserted post-column to produce an oxidative reagent for the luminol-based reaction. The use of LC with POCL detection has also been reported for a variety of drugs, including benzydamine [176], cyclosporin A [177], dipyrindamole [176, 178] and metoprolol [181]. The reported method of assay for metoprolol, after derivatization with a fluorogenic reagent, using POCL detection was 50 times more sensitive than conventional methods. Interferences from the plasma matrix in the POCL reaction were lower than those in fluorescence analysis which negated the need for tedious clean-up procedures.

Polycyclic aromatic hydrocarbons: Polycyclic aromatic hydrocarbons (PAHs), e.g., benzo[a]pyrene and chrysene, and substituted derivatives, e.g., diaminopyrenes and nitropyrenes have been detected at fg-pg levels using peroxyoxalate CL [188-191]. Methods for their determination involved reversed-phase separation with an acetonitrile mobile phase prior to CL detection. Nitro-PAHs have been determined by LC-CL using a variety of reduction techniques to convert the nitro compounds into the corresponding amines. Both on-line [190] and off-line [188, 189, 191], pre-column reduction techniques have been reported. Methods of pre-treatment have included on-line electrochemical reduction [190] and reduction by refluxing in the presence of sodium hydrosulfide [188, 191].

Sulfur compounds: Many environmentally interesting sulfur-containing compounds cannot be separated by gas chromatography (GC) and so a need has arisen to develop a sulfur-selective detector for use in LC. All three methods [192-194] reporting such a development were based on the CL reaction of ozone (O₃) with sulfur monoxide (SO), a technique referred to as ozone-induced sulfur chemiluminescence detection (SCD). The difference between the methods was the nature of SO production. Two methods reported the use of a flame-based ozone-induced SCD interfaced directly to LC [192, 194], in which a gas chromatographic FID was used for SO production. A non-flame method has also been reported [193] in which SO was formed from dissolved sulfur-compounds at elevated temperature and pressure. After permeation across a membrane to the gas phase, the CL reaction was used to selectively detect the analyte. This method was used in the detection of a number of sulfur-containing species, including blood thiols, peptides, and proteins, with detection limits in the order of 10 ppb S in aqueous solutions.

Other analytes: A novel CL method has been described for the determination of guanine and its nucleosides and nucleotides [198]. The fluorescent species produced as a result of the reaction between guanine, its nucleos(t)ides and phenylglyoxal (PGO) have been shown to exhibit CL in an alkaline medium in the presence of an aprotic polar solvent, N,N-dimethylformamide (DMF). The structure of the chemiluminescing species was not reported although the proposed method was simple, and the mild reaction conditions make it a potential detection method for LC. When compared with fluorescence methods the sensitivity of the proposed CL method produced a twenty-fold improvement in sensitivity for the nucleos(t)ides. PGO also reacted with adenine and adenosine [195] in acidic propan-2-ol solution and showed good CL response, with LODs of 1.9×10^{-7} M and 1.8×10^{-7} M respectively. The proposed CL method for the determination of adenine was selective and should therefore be applicable to the detection of adenine or adenine derivatives in biological materials by combination with LC.

It is therefore evident that there are an abundance of situations where the selectivity of LC separations has been coupled with the high sensitivity of CL detection methods. Because of the attractive characteristics of the method, the number of applications is expected to increase further as new CL reactions are discovered that are compatible with the conditions of LC separations.

1.5. RESEARCH OBJECTIVES

The primary aim of this research was to investigate the potential of the peroxyoxalate CL reaction for the quantitative determination of target analytes in non-aqueous matrices. This was carried out with the view to developing sensitive and selective assays that could be used in field deployable instrumentation.

The specific objectives of this research were;

1. To design and optimise an FI-CL manifold for the determination of PAHs in non-aqueous matrices and to compare the results with FL detection.
2. To couple the optimised manifold with LC in order to separate and quantify PAHs in non-aqueous matrices.
3. To investigate the relative performances of multivariate calibration routines for the quantification of individual PAHs in simple mixtures using FL and CL detection without prior separation.
4. To design and optimise a FI manifold for the aryl oxalate-sulphorhodamine 101 CL detection of amines in non-aqueous matrices as a precursor to the design of a portable test kit to analyse fuel additives in the field, e.g. at the point of distribution.

CHAPTER 2

*Determination of PAHs using flow injection
with fluorescence and peroxyoxalate
chemiluminescence detection*

2. DETERMINATION OF PAHs USING FLOW INJECTION WITH FLUORESCENCE AND PEROXYOXALATE CHEMILUMINESCENCE DETECTION

2.1 INTRODUCTION

The most frequently applied laboratory methods for PAH determinations use either capillary gas chromatography with flame ionisation or mass spectrometric detection or HPLC with ultraviolet or fluorescence (FL) detection [201] due to their high resolution and sensitivity. Recent reviews on the analytical applications of liquid phase chemiluminescence (CL) [14, 157], and more specifically on peroxyoxalate chemiluminescence (POCL) [202], suggest that the POCL system is also well suited to the detection of PAHs in environmental matrices, *e.g.* diesel exhaust particulates and shale oils, following separation by LC [203]. This chapter describes the development and optimisation of a FI method for the determination of PAHs in non-aqueous matrices and compares POCL detection with fluorescence detection.

2.2 EXPERIMENTAL

2.2.1 Reagents

High quality de-ionised water from a Milli-Q system (Millipore) and analytical grade reagents were used throughout. Acetonitrile (ACN), dichloromethane (DCM), cyclohexane and hexane were of HPLC grade (Rathburn, Walkerburn, UK).

Stock PAH solutions were initially prepared in the range 100-200 mg l⁻¹ [204], using acetonitrile solvent, for anthracene, benz[*a*]anthracene, benzo[*b*]fluoranthene, benzo[*k*]fluoranthene, benzo[*g,h,i*]perylene, benzo[*a*]pyrene, chrysene, dibenz[*a,h*]anthracene, fluoranthene, indeno[*1,2,3-c,d*]pyrene, naphthalene and perylene (Qm_x Laboratories Ltd., Halstead, UK). Working solutions in the range 0-20 mg l⁻¹ were prepared in acetonitrile by serial dilution of the appropriate stock solutions.

Chemiluminescence reagents

Solutions of bis(2,4-dinitrophenyl)oxalate (DNPO; Fluka Chemika-BioChemika, Gillingham, Dorset, UK) and bis(2,4,6-trichlorophenyl)oxalate (TCPO; Fluka Chemika-BioChemika, Gillingham, Dorset, UK) were prepared in ACN. Hydrogen peroxide solutions were prepared by dilution of 30 % v/v stock solution (AnalR; Merck, Darmstadt, Germany) with ACN. Mobile phase was prepared on a volume/volume basis and was degassed by sonication for 1 minute. The aryl oxalate, hydrogen peroxide and mobile phase were prepared freshly each day, and all reagents were degassed by sonication for two minutes.

Stock imidazole solution (2.0 mol l^{-1}) was prepared by dissolving imidazole (Fluka) in water. Imidazole buffer was prepared by dilution of the stock with water and adjusting the pH with nitric acid (1.0 mol l^{-1}). Citrate buffer ($5.0 \times 10^{-2} \text{ mol l}^{-1}$) was prepared from citric acid (Merck) and the pH adjusted with sodium hydroxide (Merck, 0.1 mol l^{-1}).

Standard conditions for POCL optimisation study

The following reaction conditions were used unless otherwise stated;

1. aryl oxalate solution, $3.0 \times 10^{-3} \text{ mol l}^{-1}$
2. hydrogen peroxide solution, 1.0 mol l^{-1}
3. mobile phase, neat ACN
4. analyte, 0.04 (for DNPO reaction) and 0.20 (for TCPO reaction) mg l^{-1} perylene

2.2.2 Instrumentation and Procedures

Determination of optimum excitation and emission wavelengths

Excitation and emission spectra were obtained for 12 PAHs using a Hitachi F-4500 fluorescence spectrophotometer (Hitachi Ltd., Tokyo, Japan) fitted with a 1 cm pathlength quartz cuvette. The parameter settings for the instrument are shown in Table 2.1. In all cases spectra were acquired with a resolution of 0.2 nm.

Table 2.1. Instrument parameter settings for F-4500.		
Scan Mode	Excitation	Emission
Scan Speed (nm min⁻¹)	1200	1200
EX Start WL (nm)	200	-
EX End WL (nm)	500	-
EM Start WL (nm)	-	350
EM End WL (nm)	-	550
EX Slit (nm)	5	
EM Slit (nm)	5	
PMT Voltage (V)	700	
Shutter Control	ON	

FL data acquisition was achieved using Hitachi F-4500 control and data acquisition software (Hitachi Ltd., Tokyo, Japan). Both the excitation and emission spectra were obtained in the four solvents; ACN, DCM, cyclohexane and hexane. Each PAH was subjected to an Auto Pre-Scan, a function of the F-4500, to find out the optimum excitation wavelength. The emission spectrum was then obtained using the optimum excitation wavelength.

FI with fluorescence detection

A flow injection manifold (Figure 2.1) was constructed using black poly(tetrafluoroethylene) (PTFE) tubing of 0.75 mm i.d. (Jaytee Biosciences, Whitstable, UK).

A peristaltic pump (Mini-S 820; Ismatec, Carshalton, UK) with 1.02 mm i.d. Ismaprene pump tubing was used to transport the sample stream at 1.25 ml min⁻¹ to a Perkin Elmer LS-4 spectrofluorimeter. Standards (50 µl) were injected using a solenoid-operated, Rheodyne 5041 PTFE rotary valve (Rheodyne Inc., Cotati, CA, USA). FL emission was recorded using a Chessel BD 4004 chart recorder (Chessel Ltd., Worthing, UK).

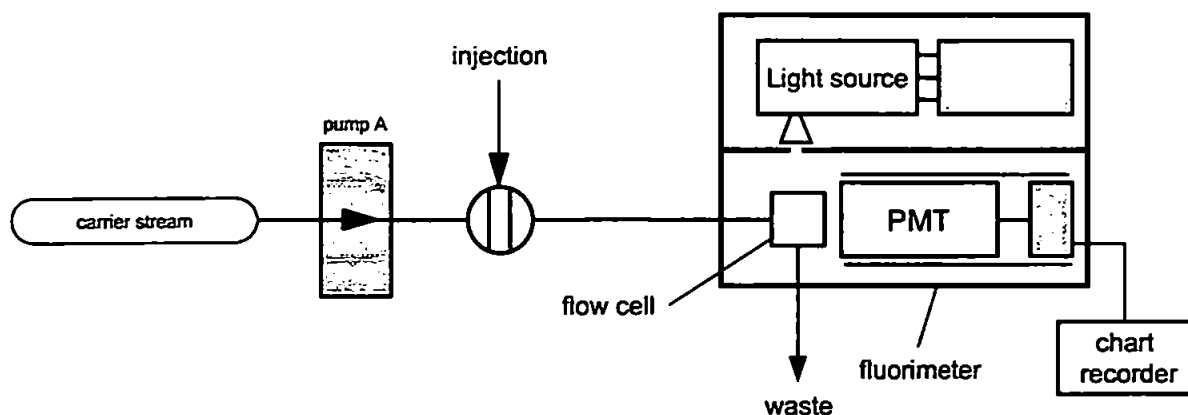


Figure 2.1. FI manifold with FL detection for the determination of PAHs.

FI with POCL detection

A FI manifold (Figure 2.2) was constructed using black poly(tetrafluoroethylene) (PTFE) tubing of 0.75 mm i.d. (Jaytee Biosciences, Whitstable, UK), and was used to facilitate sample and reagent mixing and delivery to either a photodiode based detector (Camspec CL-1, Camspec Scientific Instruments, Cambridge, UK) or a low power (12 V) PMT based detector (Camspec CL-2, Camspec Scientific Instruments, Cambridge, UK), fitted with a 120 μ l quartz flow cell. A Minipuls 2 peristaltic pump (Gilson, Villiers-le-Bel, France) with 1.02 mm i.d. Ismaprene (PharMed 65) pump tubing (Ismatec UK Ltd, Weston-Super-Mare, UK) was used to propel the DNPO and H₂O₂ reagent streams to a polyetherether ketone (PEEK) T-piece (Phenomenex UK Ltd, Macclesfield, UK). A second peristaltic pump (Mini-S 820; Ismatec, Carshalton, UK) with 1.02 mm i.d. Ismaprene pump tubing was used to transport the sample stream to a second PEEK T-piece, where it mixed with the combined DNPO/H₂O₂ reagent stream, before passing into the flow cell. Standards (50 μ l) were injected using a solenoid-operated, Rheodyne 5041 PTFE rotary valve (Rheodyne Inc., Cotati, CA, USA).

CL emission was recorded (mV) using a Chessel BD 4004 chart recorder (Chessel Ltd., Worthing, UK). In all cases, the background level was measured as the response above recorder zero and noise was measured as the peak-to peak noise of this background (determined when only the carrier stream and CL reagents were mixed). Analyte response was recorded as the peak height (signal) above the background. Signal-to-noise was calculated as the peak height above the background divided by the peak-to-peak noise of the background.

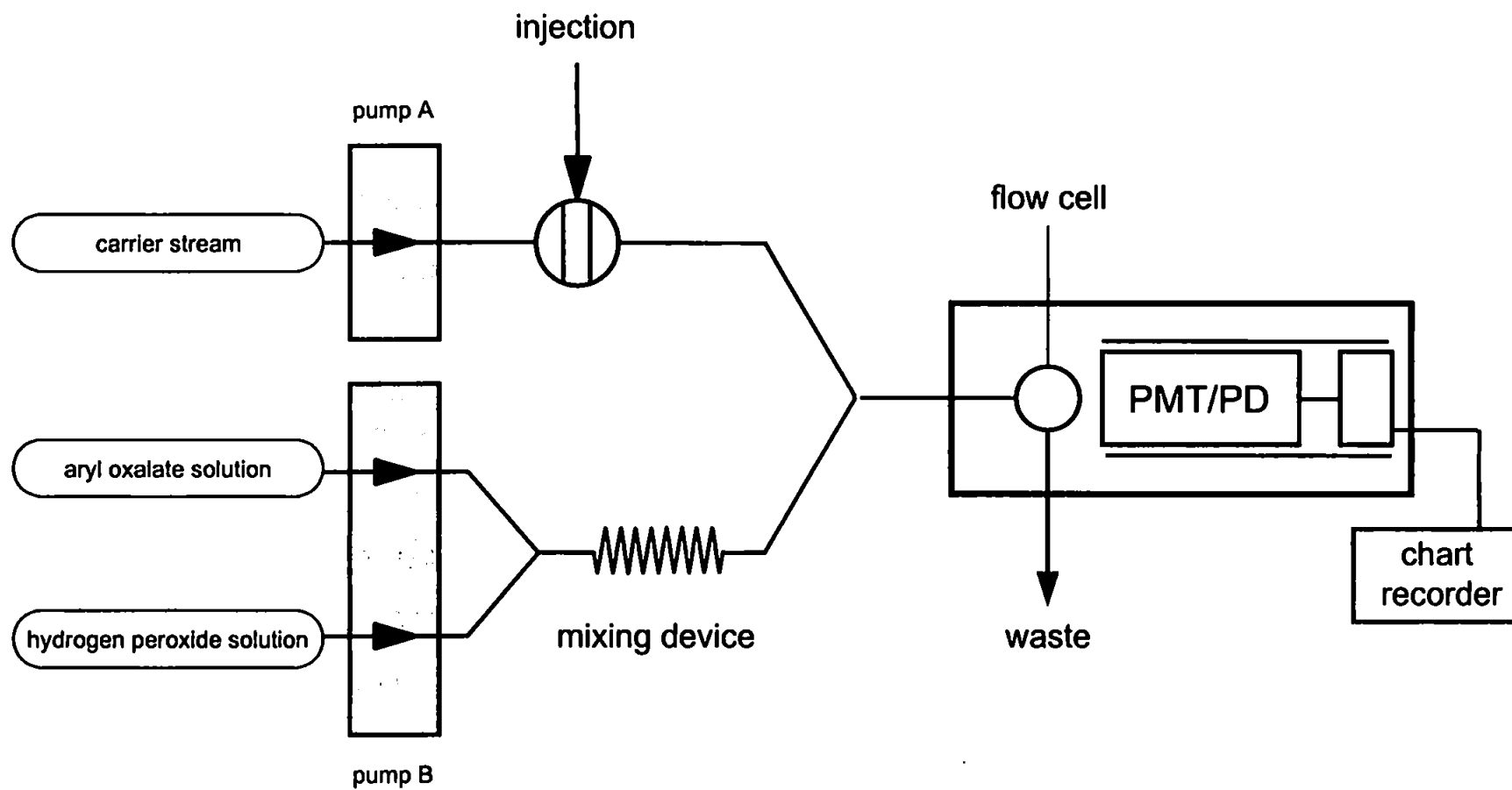


Fig. 2.2. FI manifold for the investigation of the POCL reaction.

2.3 RESULTS AND DISCUSSION

2.3.1. Fluorescence properties of PAHs obtained using a batch fluorimeter

The physical and spectroscopic properties of PAHs are dominated by their conjugated π -electron systems, which also account for their chemical stability. The availability of high-energy π -bonding orbitals and of relatively low energy π^* -antibonding orbitals in PAHs leads to the absorption of visible or ultraviolet radiation by the transition of an electron from the π - to π^* -orbital. The energy required for this is typically in the range 400-600 kJ mol⁻¹ and this gives characteristic UV absorption and fluorescence spectra.

Figures 2.3.(a,b,c) show the excitation and emission spectra of the twelve PAHs investigated and Figure 2.4 shows the structures of these PAHs. From the spectra obtained the optimum wavelengths for excitation and emission in ACN have been determined and are summarised in Table 2.2 together with previously reported values from the literature [205].

PAH	Experimental values			Literature values	
	λ_{Ex} (nm)	λ_{Em} (nm)	Intensity (arbitrary units)	λ_{Ex} (nm)	λ_{Em} (nm)
Anthracene	250	400	7132	249	405
Benzo[<i>k</i>]fluoranthene	247	408	3824	296	404
Benzo[<i>a</i>]pyrene	264	404	2311	258	380
Chrysene	267	381	1201	268	375
Dibenz[<i>a,h</i>]anthracene	287	394	1061	287	390
Benz[<i>a</i>]anthracene	277	387	978	277	382
Benzo[<i>b</i>]fluoranthene	256	444	775	286	433
Perylene	252	437	479	n/a	n/a
Fluoranthene	286	461	409	279	455
Indeno[<i>1,2,3-c,d</i>]pyrene	250	474	309	258	473
Benzo[<i>g,h,i</i>]perylene	289	407	306	287	405
Naphthalene	221	333	301	219	327

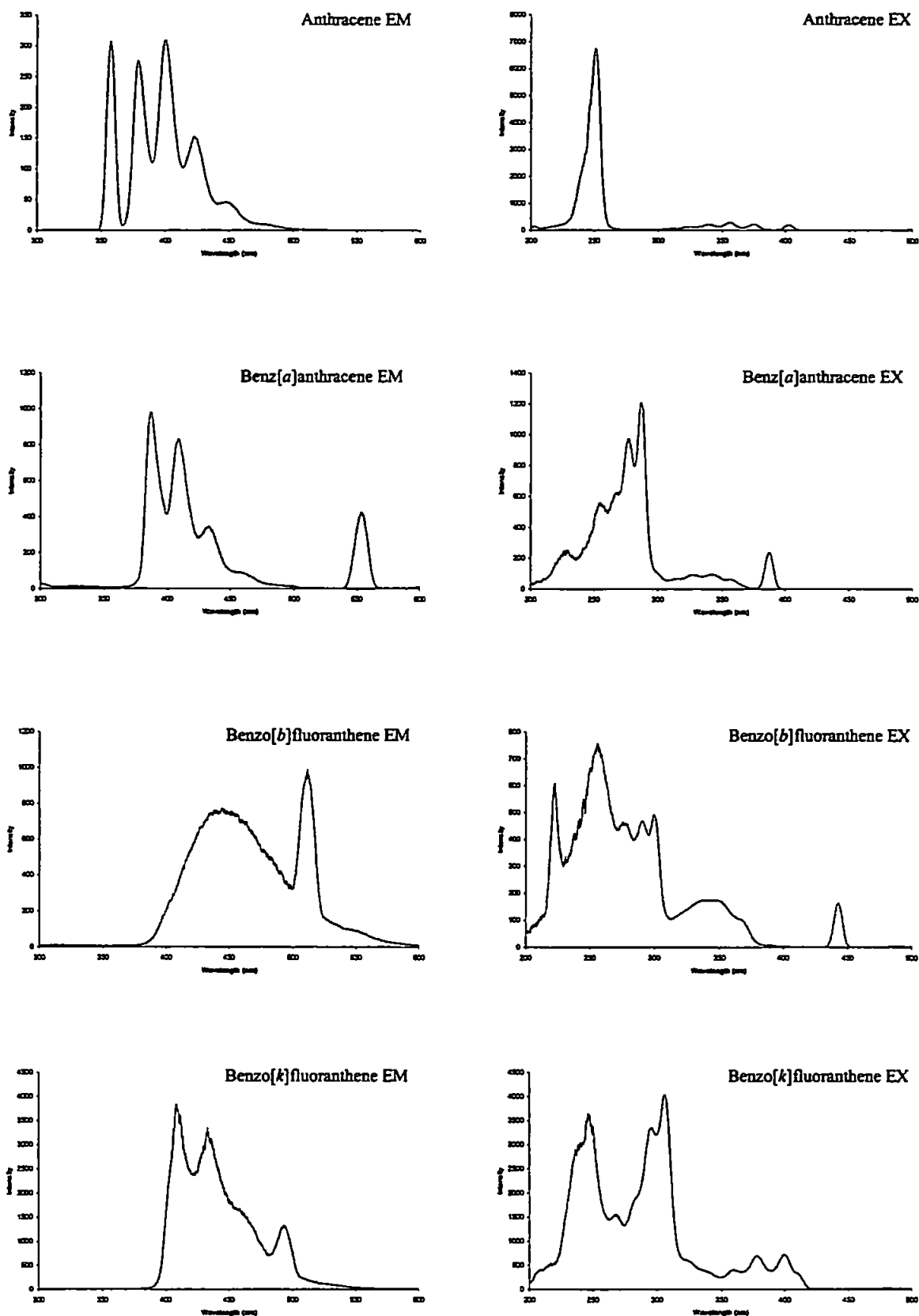


Figure 2.3.(a). Experimentally acquired emission and excitation fluorescence spectra of PAHs dissolved in ACN solvent at a concentration of 100ppb (Intensity = arbitrary units).

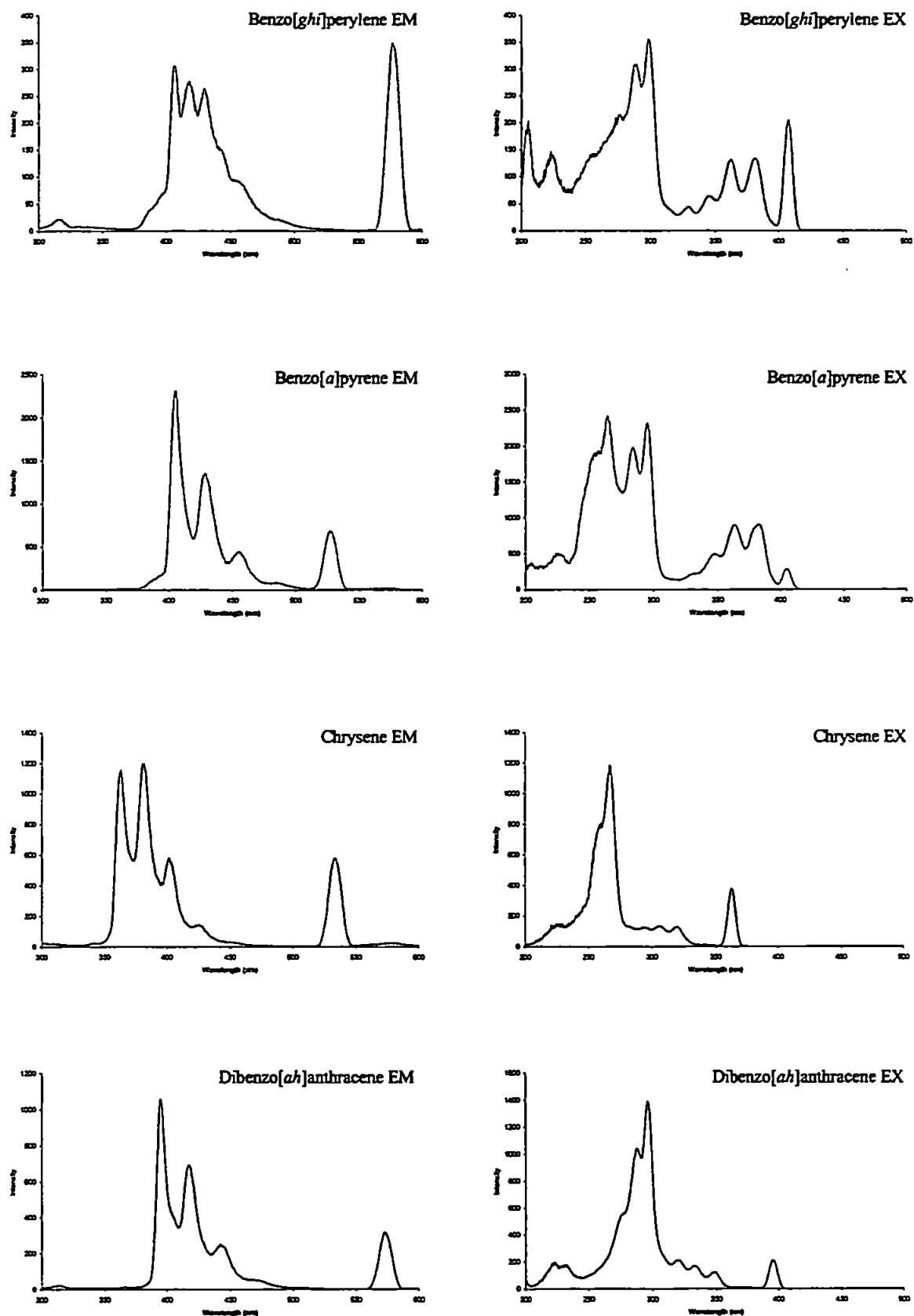


Figure 2.3.(b). Experimentally acquired emission and excitation fluorescence spectra of PAHs dissolved in ACN solvent at a concentration of 100ppb (Intensity = arbitrary units).

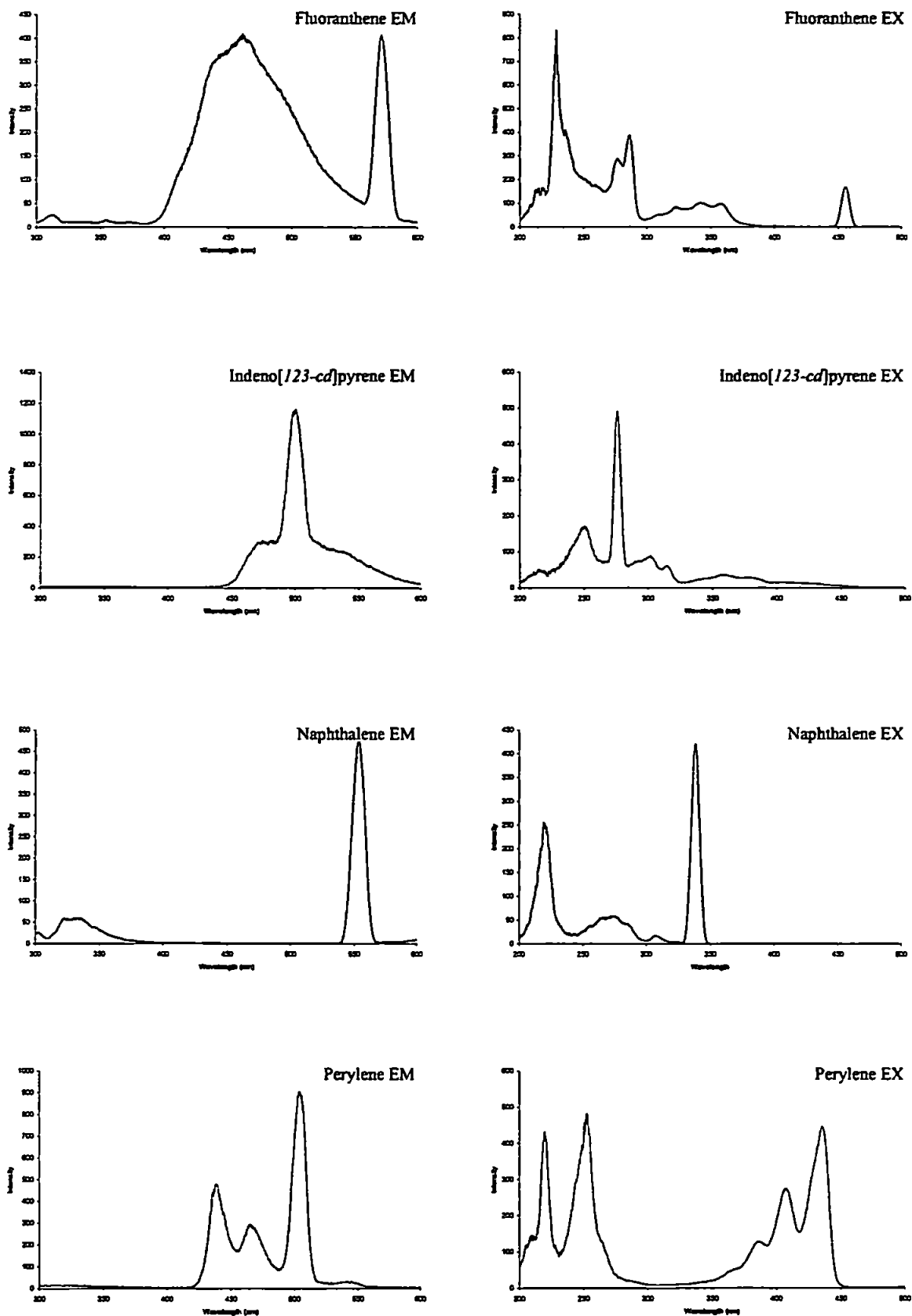


Figure 2.3.(c). Experimentally acquired emission and excitation fluorescence spectra of PAHs dissolved in ACN solvent at a concentration of 100ppb. (Intensity = arbitrary units).

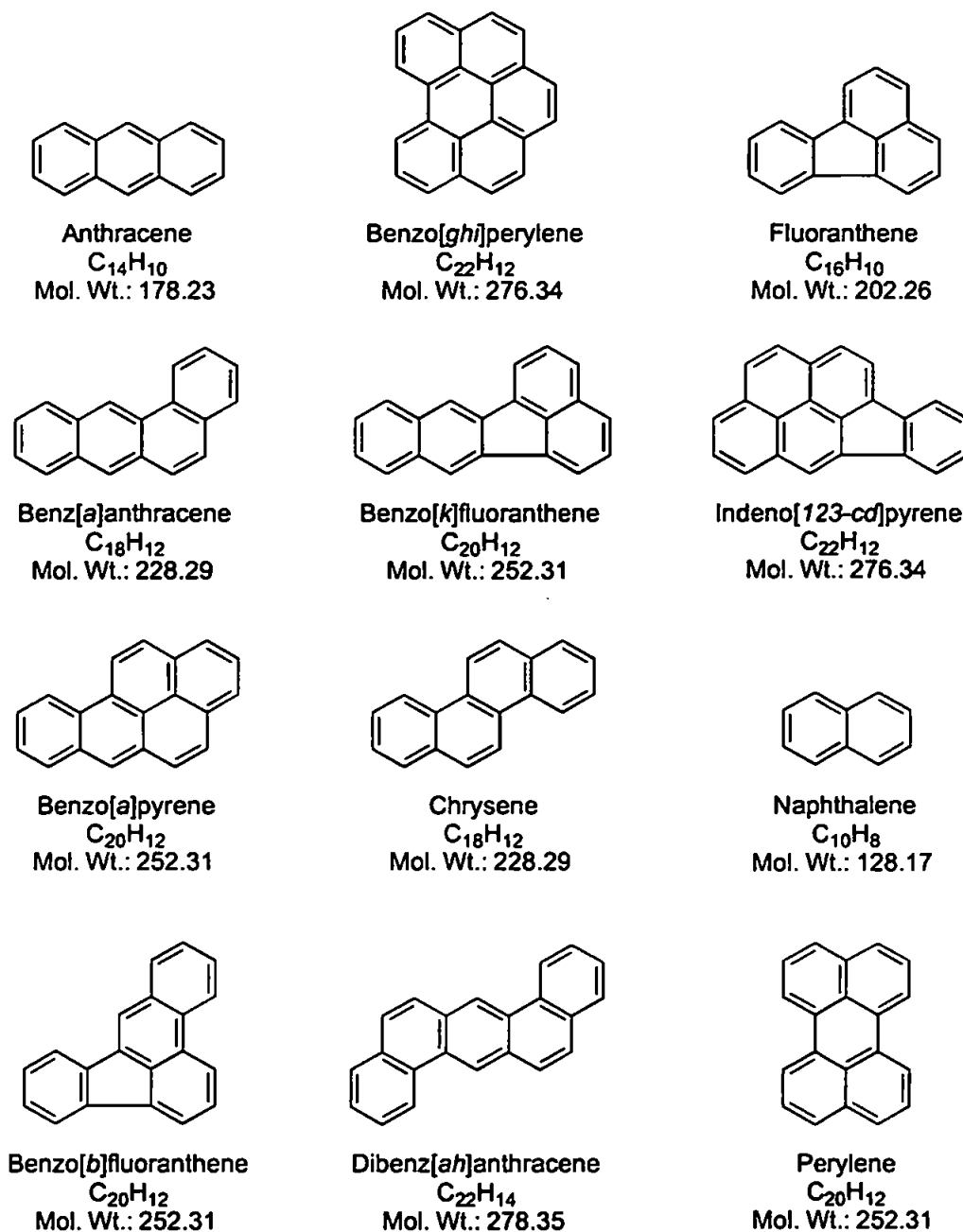


Figure 2.4. Structures of the 12 PAHs used for the FL investigation.

As shown in the figures, each PAH had characteristic excitation and emission spectra, which means that λ_{ex} and λ_{em} need to be individually optimised for each PAH to obtain maximum sensitivity. The solvent in which fluorescence spectra are measured also plays a major role in determining the spectral positions and intensities with which fluorescence bands occur. Solvent interactions with solute molecules are electrostatic in nature. Because the electronic transition accompanying excitation necessarily entails a change in electronic dipole moment, an excited molecule in a polar solvent may find itself more or less stabilised with respect to its ground electronic state by going from a less to a more

polar solvent. If the excited state is more polar than the ground state, a more polar solvent will stabilise the excited state more than the ground state and cause the fluorescence to shift to longer wavelengths relative to those observed in a less polar solvent. If, however, the ground state is more polar than the excited state, which is rarely the case, the former will be the more stabilised by a more polar solvent and the fluorescence will shift to shorter wavelengths.

Benzo[*k*]fluoranthene (Figure 2.5) showed an obvious shift when comparing the emission spectra in the four solvents, with longer emission wavelengths in ACN and DCM than in hexane and cyclohexane. The strength of these solvents (ϵ°) are 0.52, 0.30, 0.00 and 0.03 respectively [206].

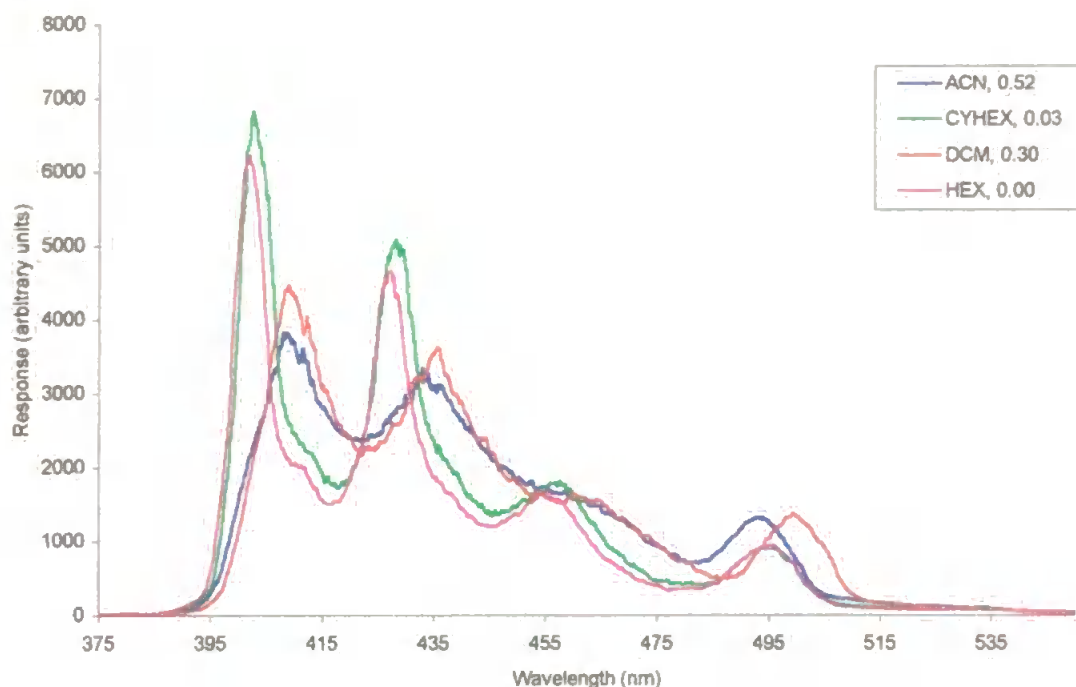


Figure 2.5. Spectra observed for benzo[*k*]fluoranthene in four different solvents.

Not all the PAHs exhibited spectral shifts in different solvents. Benzo[*a*]pyrene, benz[*a*]anthracene (shown in Figure 2.6) and dibenz[*a,h*]anthracene were examples in which emission wavelength maxima were independent of solvent, although the emission intensity was greatest in the most polar solvent.

Solvents also affected the fluorescence intensity of the 12 PAHs. Anthracene, benzo[*k*]fluoranthene and benzo[*b*]fluoranthene had higher fluorescence intensities in

hexane than in ACN. However, benz[*a*]anthracene, benzo[*a*]pyrene, dibenz[*a,h*]anthracene and naphthalene had higher fluorescence intensities in ACN than in hexane.

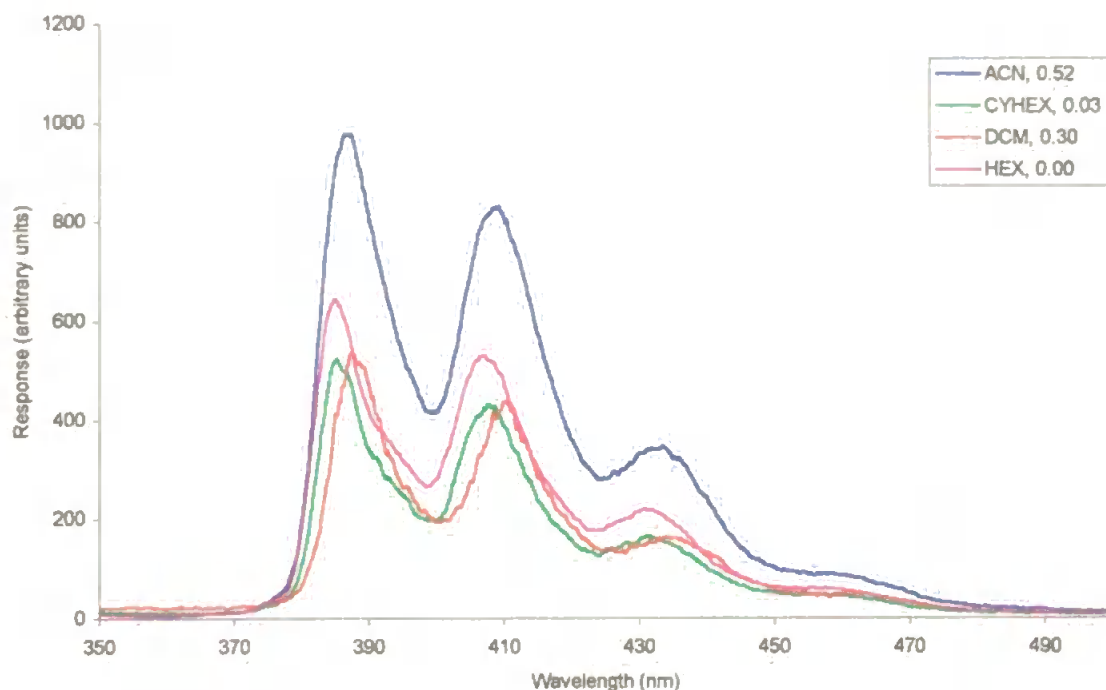


Figure 2.6. Spectra observed for benz[*a*]anthracene in four different solvents.

Experimental results (optimum excitation wavelength, emission wavelength and strongest fluorescence intensity) for each PAH in the four solvents investigated are summarised in Table 2.3.

The results reported above are in good agreement with those reported elsewhere [207] and provide a sound experimental basis for the quantitative experiments described below with both FI and LC.

Table 2.3. Excitation wavelengths, emission wavelengths and intensities for 11 PAHs in four different solvents.

	<u>ACETONITRILE</u>			<u>CYCLOHEXANE</u>			<u>HEXANE</u>			<u>DICHLOROMETHANE</u>		
	λ_{Ex} (nm)	λ_{Em} (nm)	Intensity (arbitrary units)	λ_{Ex} (nm)	λ_{Em} (nm)	Intensity (arbitrary units)	λ_{Ex} (nm)	λ_{Em} (nm)	Intensity (arbitrary units)	λ_{Ex} (nm)	λ_{Em} (nm)	Intensity (arbitrary units)
Anthracene	250	400	7132	308	402	932	252	397	8940	359	403	176
Benz[<i>a</i>]anthracene	277	387	978	268	385	524	288	385	645	258	388	536
Benzo[<i>a</i>]pyrene	264	404	2311	265	403	2507	263	403	1233	386	406	1333
Benzo[<i>b</i>]fluoranthene	256	444	775	259	449	1001	255	428	1242	259	429	974
Benzo[<i>g,h,i</i>]perylene	289	407	306	280	419	218	289	418	184	385	408	220
Benzo[<i>k</i>]fluoranthene	247	408	3824	248	402	6824	248	402	6228	250	409	4467
Chrysene	267	381	1201	268	382	1162	267	381	766	269	383	1020
Dibenz[<i>a,h</i>]anthracene	287	394	1061	298	394	1491	288	394	621	322	396	193
Fluoranthene	286	461	409	287	462	437	236	451	323	239	457	245
Indene[<i>1,2,3-c,d</i>]pyrene	250	474	309	252	472	317	247	464	305	251	478	293
Naphthalene	221	333	301	275	324	83	246	436	120	275	336	55
Perylene	252	437	479	436	438	1264	362	438	107	254	441	1309

2.3.2. FI determination of PAHs using FL detection

In order that high sensitivity could be achieved each PAH standard was detected using optimum excitation and emission wavelengths as summarised in Table 2.4.

PAH	excitation wavelength (nm)	emission wavelength (nm)
Benz[<i>a</i>]anthracene	277	387
Perylene	252	438
Benzo[<i>a</i>]pyrene	264	405
Benzo[<i>g,h,i</i>]perylene	289	407
Benzo[<i>k</i>]fluoranthene	247	409
Benzo[<i>b</i>]fluoranthene	256	444

Table 2.5 shows the detection limits for six PAHs in acetonitrile obtained by FI using FL detection. These were calculated as $\bar{y}_b + 3s_{y/x}$ where \bar{y}_b is the mean response ($\eta = 5$) of the blank and $s_{y/x}$ is the standard error of the y estimate [208].

PAH	LOD ng ml ⁻¹	LOD ng
Benz[<i>a</i>]anthracene	5.0 ± 0.3	0.25
Perylene	1.2 ± 0.1	0.06
Benzo[<i>a</i>]pyrene	2.8 ± 0.2	0.14
Benzo[<i>g,h,i</i>]perylene	9.7 ± 0.5	0.19
Benzo[<i>k</i>]fluoranthene	1.8 ± 0.1	0.09
Benzo[<i>b</i>]fluoranthene	7.3 ± 0.4	0.37

As one might expect, the order of sensitivity follows the order of FL emission response as obtained when investigating the spectra of the individual PAHs (*section 2.3.1.*) using a batch fluorimeter. The detection limits are also in broad agreement with those reported elsewhere [209] although the exact values will be a function of the quality of the

instrumentation used, e.g. the intensity of the xenon lamp used as the source and the efficiency of the optical compartment (grating or filter).

2.3.3. FI determination of PAHs using POCL detection

The first example of POCL was reported in 1963 by Chandross [210] who studied the reaction of oxalylchloride with hydrogen peroxide in the presence of a fluorescent compound, such as 9,10-diphenylanthracene. Rauhut and co-workers further investigated the reaction by synthesising and testing several substituted aryl oxalates, which eventually resulted in the development of long-lived light sources for military and civilian use [211, 212].

A wide range of fluorophores were found to act as sensitisers for the reaction. Lechtken and Turro [213] studied several fluorophores and concluded that it was possible to generate electronically excited states with an energy of up to 430 kJ/mole.

Reaction mechanism

The mechanism for the POCL reaction is the subject of continuing debate [214]. In their initial work Rauhut and co-workers proposed the formation of an energy rich intermediate, 1,2-dioxetanedione, as a possible chemical excitation source for the fluorophore, producing its excited singlet state and leading to a typical fluorescence emission process (Figure 2.7).

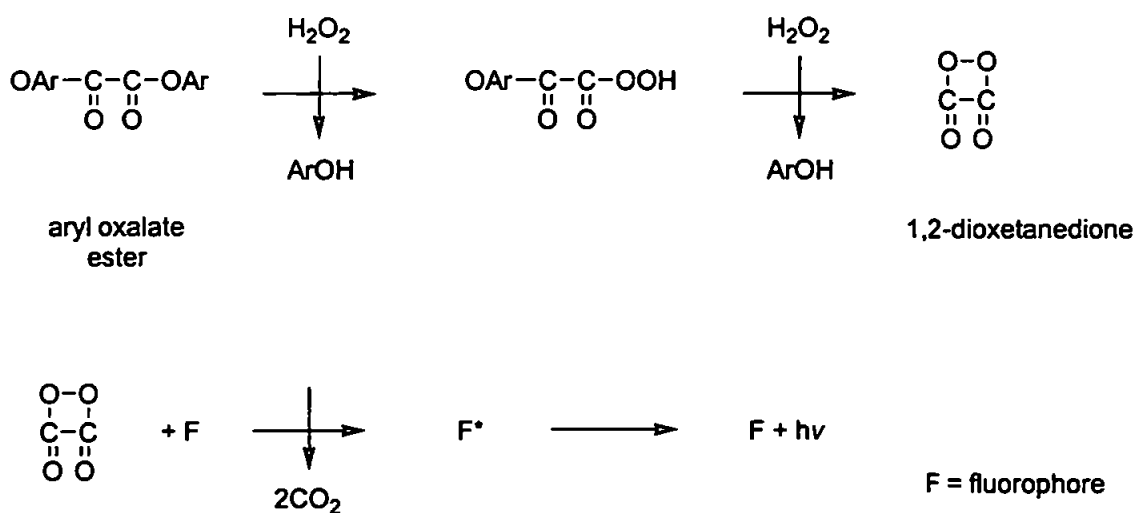


Figure 2.7. POCL mechanism as originally proposed by Rauhut *et al* [211].

Schuster and co-workers [215, 216] later introduced the chemically initiated electron exchange luminescence (CIEEL) concept by studying the CL decomposition of dioxetanes. The chemi-excitation step is the electron transfer from the intermediate back to the fluorophore resulting in its excited state. POCL is also thought to follow a CIEEL-type mechanism as proposed by McCapra [217] and is shown in Figure 2.8. This mechanism suggests that molecules with good fluorescence quantum yields and low oxidation potentials would give high CL efficiencies with the POCL reaction, which has been shown to be true for polycyclic aromatic hydrocarbons [218].

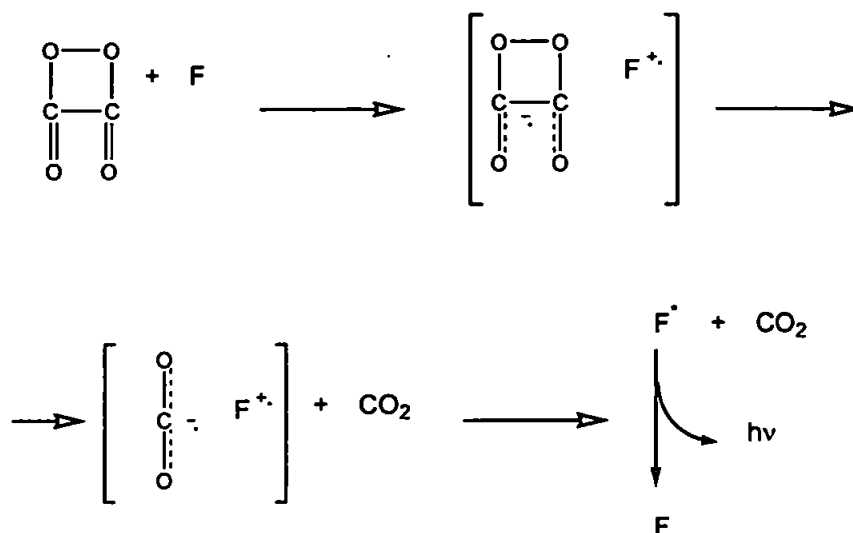


Figure 2.8. The proposed CIEEL mechanism for energy transfer [18,19].

The Rauhut mechanism, with or without the McCapra modification, has been used as the basic model for the POCL reaction by most authors although the key 1,2-dioxetanedione intermediate has not been isolated, despite a number of attempts [219, 220]. Recent work has led to new proposals for the reaction mechanism and alternative structures of the high-energy intermediates involved [221].

Optimisation of POCL reaction conditions

Optimisation of the POCL reaction for FI or LC requires the ‘fine-tuning’ of reaction conditions to capture the maximum intensity of emission in the flow cell with minimum light loss before and after the cell. Five factors have been established as having the greatest influence upon emission intensity and the speed of the reaction [222], and therefore should be investigated for optimisation of the reaction conditions for POCL detection in flowing streams;

1. Nature and composition of the aryl oxalate,
2. Presence and concentration of base catalyst,
3. pH,
4. Concentration of the hydrogen peroxide,
5. Nature of the mobile phase.

Although alternative oxalate esters have been the subject of a number of publications [e.g. 223-225], DNPO and TCPO remain the most widely used oxalate esters for POCL detection. A discussion of the synthesis of these oxalate esters can be found in the literature [226] but they are now both commercially available. The structures of analytically useful aryl oxalates are shown in Table 2.6.

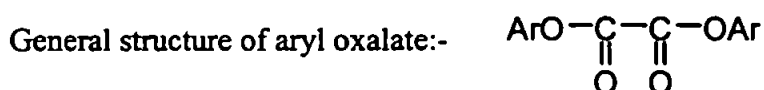
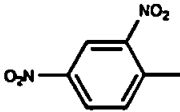
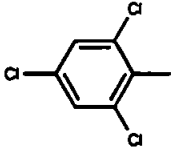
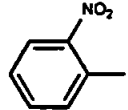
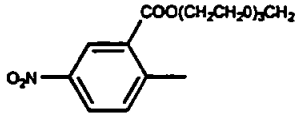


Table 2.6. Structures of analytically useful aryl oxalates.	
oxalate ester	Ar =
bis(2,4-dinitrophenyl)oxalate (DNPO)	
bis(2,4,6-trichlorophenyl)oxalate (TCPO)	
bis(2-nitrophenyl)oxalate (2-NPO)	
bis[4-nitro-2-(3,6,9-trioxadecyloxy-carbonyl)phenyl]oxalate (TDPO)	

The choice of oxalate ester depends on the application and results desired. For example the DNPO-CL reaction has been shown to be superior to TCPO-CL in terms of sensitivity in FI [227]. This is explained by the faster reaction kinetics caused by the more

electronegative nitro-aryl substituents which provide better leaving groups, resulting in a faster rate of intermediate formation. However, DNPO is less stable in solution and has a higher background signal than TCPO. A comparison of the two reagents is given in Table 2.7.

Table 2.7. Comparison of DNPO and TCPO reagents.	
DNPO	TCPO
unstable in solution due to hydrolysis	more stable in solution than DNPO when mixed with H ₂ O ₂
intense emission compared with TCPO	lower background CL emission compared with DNPO
working pH range 2-7	working pH range 5-9
soluble in solvents commonly used with reversed-phase HPLC	less soluble than DNPO in reversed-phase HPLC solvents
expensive	relatively inexpensive
fast reaction kinetics which results in increased sensitivity	relatively slow reaction kinetics, but can be catalysed by imidazole and other bases

Effect of water

To investigate the effect of the water on the POCL emission intensity the water content of the ACN mobile phase was gradually increased from 0 - 50%. All other reaction conditions were as described in *section 2.2.1*. The results obtained are shown in Figures 2.9.(a). and 2.9.(b). for the DNPO and TCPO systems respectively.

Increasing the ratio of water in the solvent increased peak-to-peak noise and also lead to a decrease in CL yield above 10% water for the DNPO reagent, as shown by Figure 2.9.(a) The results for the TCPO system showed that increasing the ratio of water in the solvent increased peak-to-peak noise and also lead to a dramatic increase in the background emission, leading to a decrease in the CL yield, as shown by Figure 2.9.(b).

Figure 2.10 shows the results obtained during the investigation calculated as the signal-to-noise ratio, which illustrates more clearly the relative sensitivities of each reaction for POCL detection in the presence of water.

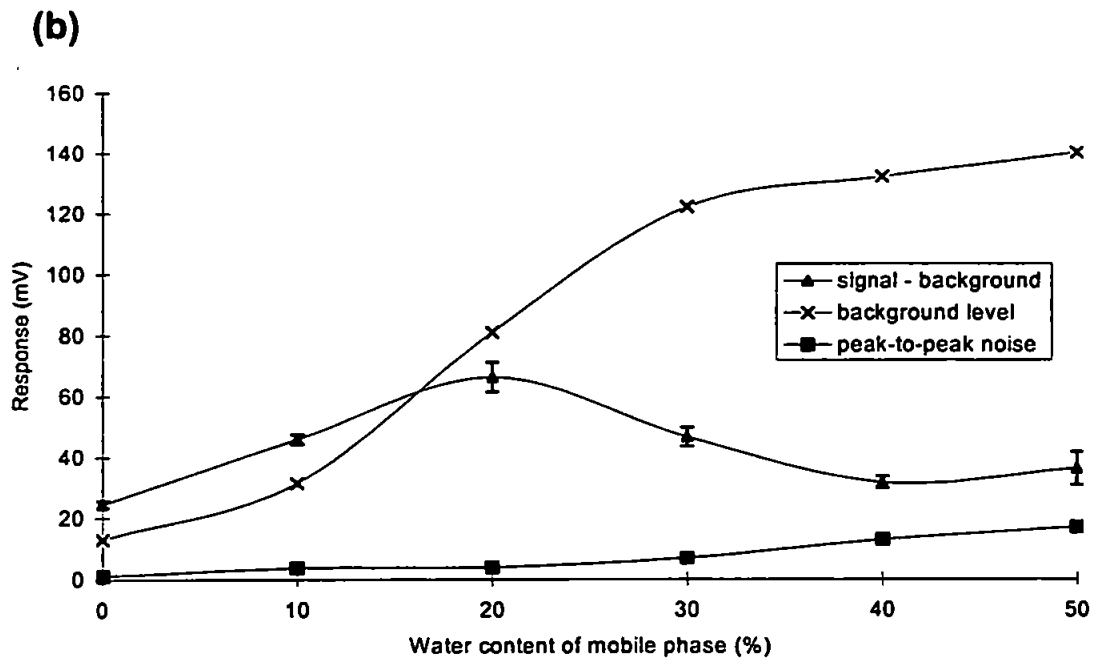
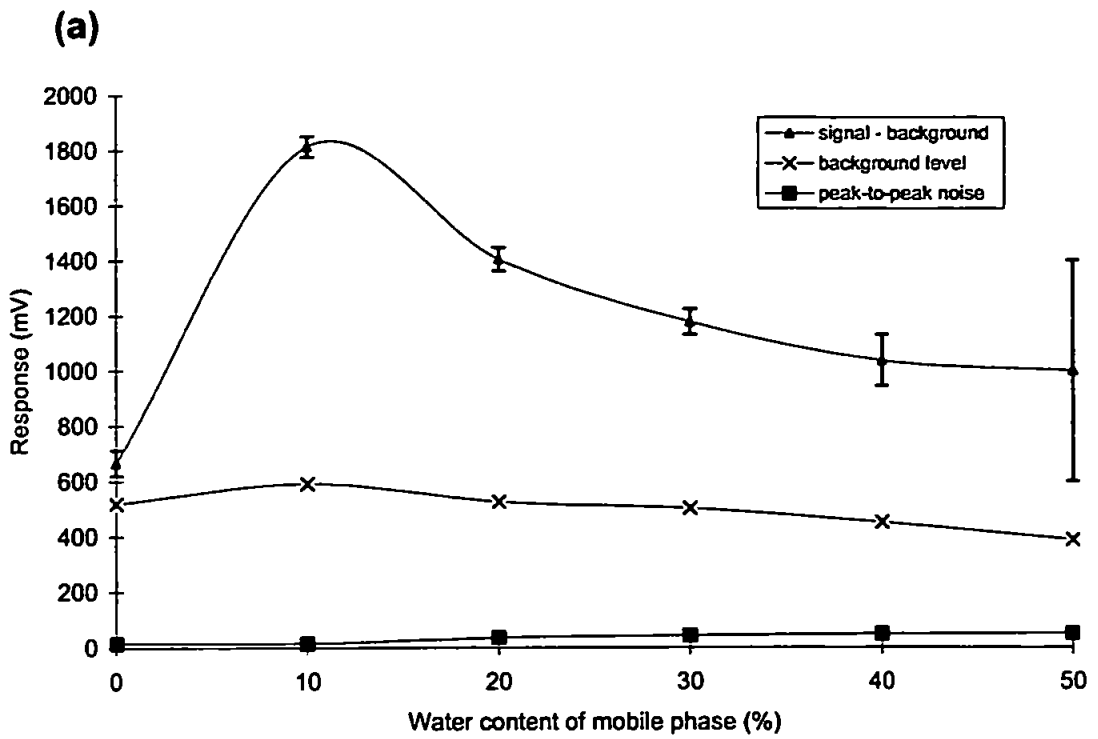


Figure 2.9. Effect of water on the CL emission intensity for the two reagents (a) DNPO and (b) TCPO (error bars = 3σ).

Figure 2.10. shows that increasing the water content to 10% led to an increase in the signal-to-noise for DNPO and, when increased further, the signal-to-noise decreased significantly. No such enhancement was observed for TCPO, where the increase in water content led to a gradual decrease in the signal-to-noise.

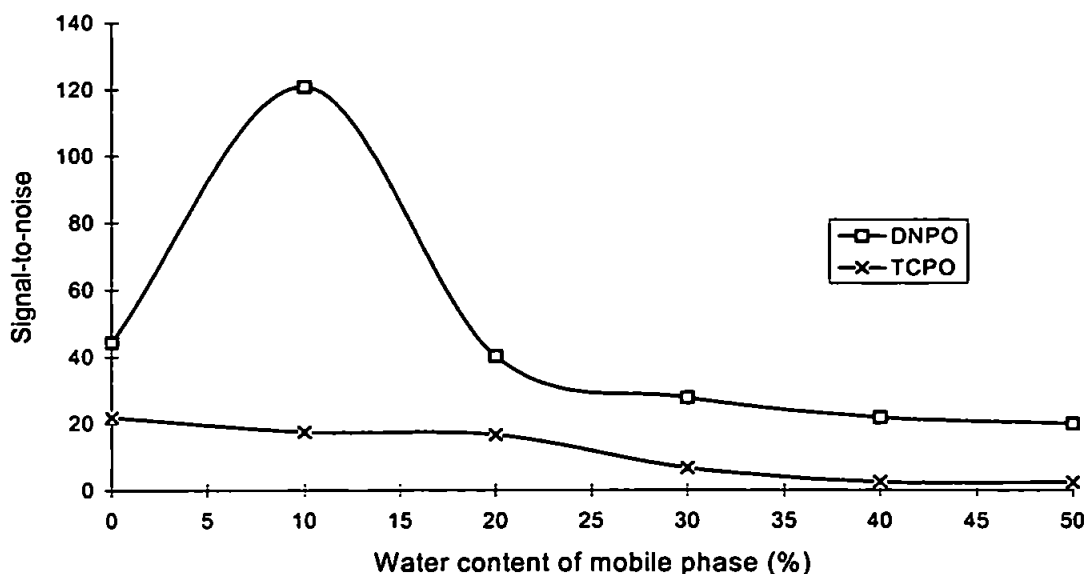


Figure 2.10. Effect of water on the CL emission intensity for DNPO and TCPO.

These results are observed because the water has a strong influence on the rate of formation and lifetime of the various POCL intermediates and also causes the premature hydrolysis of the reagent, which severely degrades its analytical utility [228-230]. The results using DNPO can be explained by the fact that the reaction rate increases with increasing the concentration of water and that when 10% water is present, maximum CL emission is coincident with the passage of the sample through the flow cell. At lower concentrations of water the reaction proceeds more slowly and the maximum CL emission occurs after the sample zone has passed through the detector. At high concentrations of water the reaction rate has been accelerated sufficiently enough such that maximum CL emission occurs prior to entering the detector. With TCPO the absolute intensities are much lower due to the slower reaction kinetics. As the concentration of water increases the CL emission increases for the reason discussed for DNPO, however the background emission is also seen to increase and so the overall signal-to-noise decreases. These results emphasise the importance of optimisation of the system for each application, particularly for post column detection after LC separations where, more often than not, a reversed phase system, incorporating acetonitrile/water gradients is used.

Recent work reported by Barnett *et al* [230] indicates that this problem can be addressed by synthesis of novel oxamide reagents that are resistant to hydrolysis in aqueous solutions. The structures of the two disulfonated oxamides reported are shown in Figure 2.11.

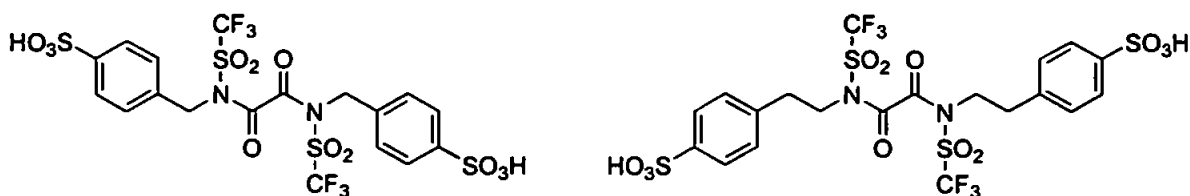


Figure 2.11. Reported structures of disulfide oxamides [230].

Effect of imidazole

Weak bases such as triethylamine, tris(hydroxymethyl)aminomethane and imidazole have been used to catalyse the peroxyoxalate reaction. Imidazole is thought to play a key role in the reaction mechanism for the hydrolysis of the aryl oxalate esters to peroxyoxalate intermediates [222]. The precise method by which the base-catalyst acts upon the aryl-oxalate has been the subject of a number of papers and is thought to operate via a nucleophilic substitution reaction [229, 231-234]. This may be expressed schematically as shown in Figure 2.12.

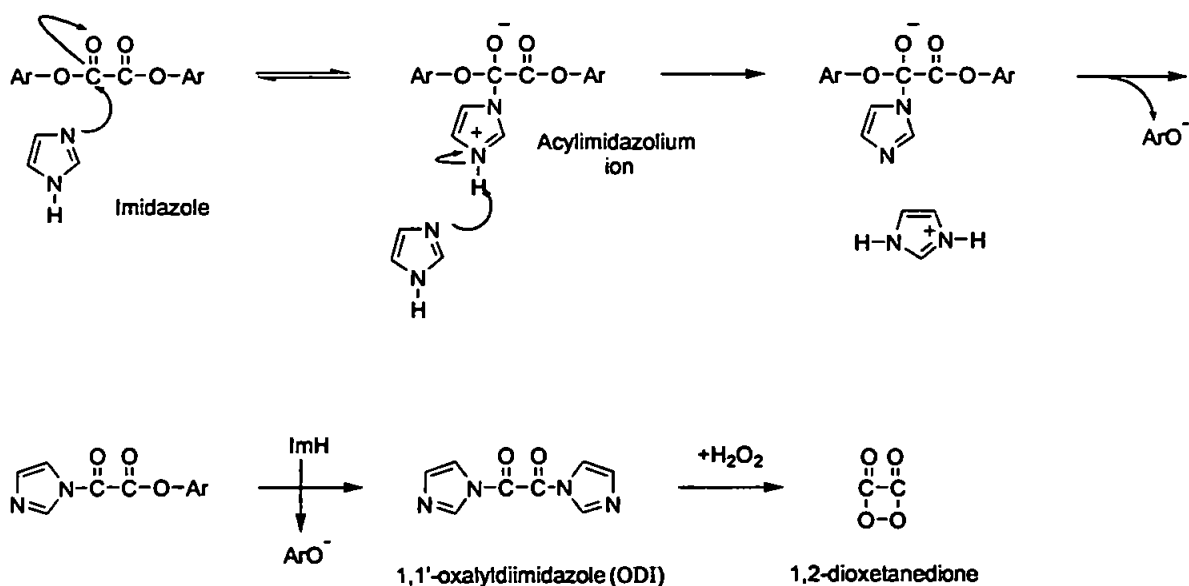


Figure 2.12. Scheme of the proposed reaction between imidazole and an aryl oxalate ester to form the intermediate 1,2-dioxetanedione (ImH = imidazole).

The mechanism begins with a pre-equilibrium step in which imidazole adds to one of the carbonyls to form a zwitterionic, tetrahedral intermediate. Another molecule of imidazole acts as a base catalyst and accepts a proton from the acylimidazolium ion. The intermediate releases the phenoxide ion, and the same process is repeated at the other

carbonyl of the oxalate to form 1,1'-oxalyldiimidazole (ODI). On addition of H_2O_2 to ODI a cyclisation reaction occurs to produce the proposed intermediate 1,2-dioxetanedione which undergoes the CIEEL sequence as discussed above (section 2.3.3).

To investigate the effect of imidazole on the DNPO and TCPO reactions, the water content of the mobile phase was replaced by imidazole solutions (0-0.20 mol l^{-1} imidazole in the water fraction). The results obtained are shown in Figures 2.13. and 2.14. for the DNPO and TCPO systems respectively.

In the case of DNPO (Figure 2.13.) each of the measured signals undergoes a significant decrease as the concentration of imidazole is increased. In contrast, a considerable increase in CL yield is seen for the TCPO system when up to 0.03 mol l^{-1} imidazole is added (Figure 2.14.) although after this point a marked decrease in CL yield was the result. It should however be noted that the peak-to-peak noise also decreased which will affect the signal-to-noise ratio. Therefore, these results become more meaningful when expressed as the signal-to-noise ratio (Figure 2.15.) where the overall effect of imidazole on the sensitivity of the two systems can be observed.

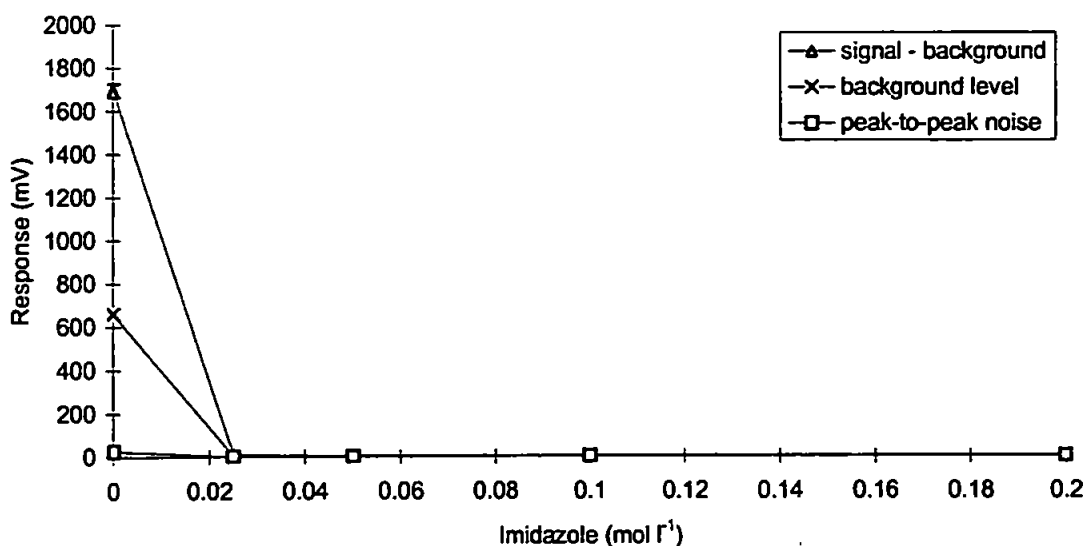


Figure 2.13. Effect of imidazole on the CL emission intensity for DNPO (error bars = 3σ).

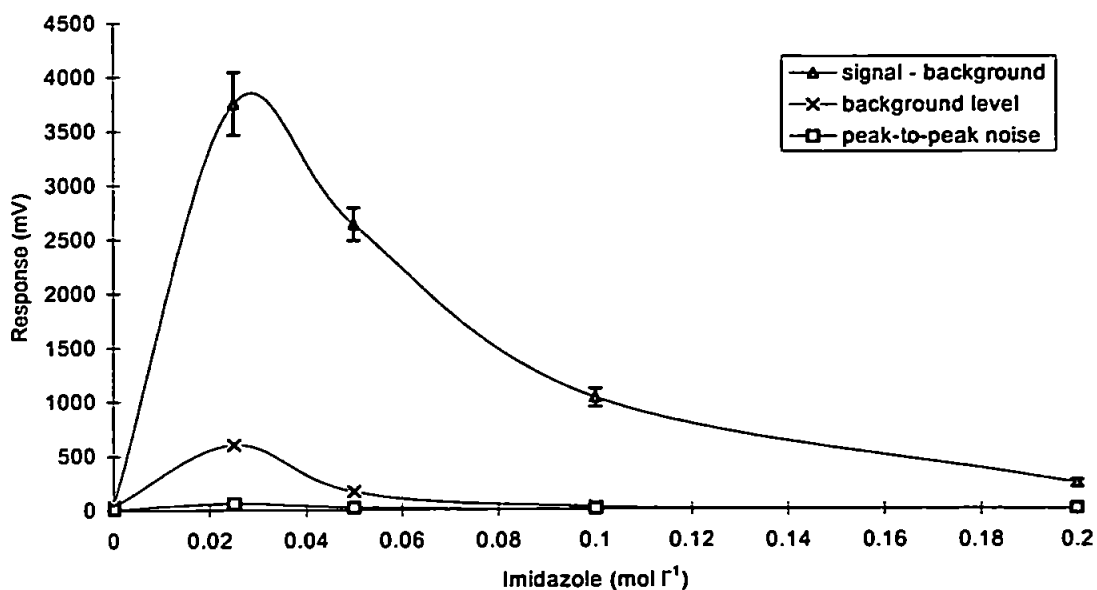


Figure 2.14. Effect of imidazole on the CL emission intensity for TCPO (error bars = 3σ).

From Figure 2.15, it was observed that the signal-to-noise ratio of the TCPO reaction increased with the increase in imidazole concentration. This is in agreement with the suggestion that the formation of the intermediate from TCPO is base catalysed and therefore accelerated by the addition of imidazole.

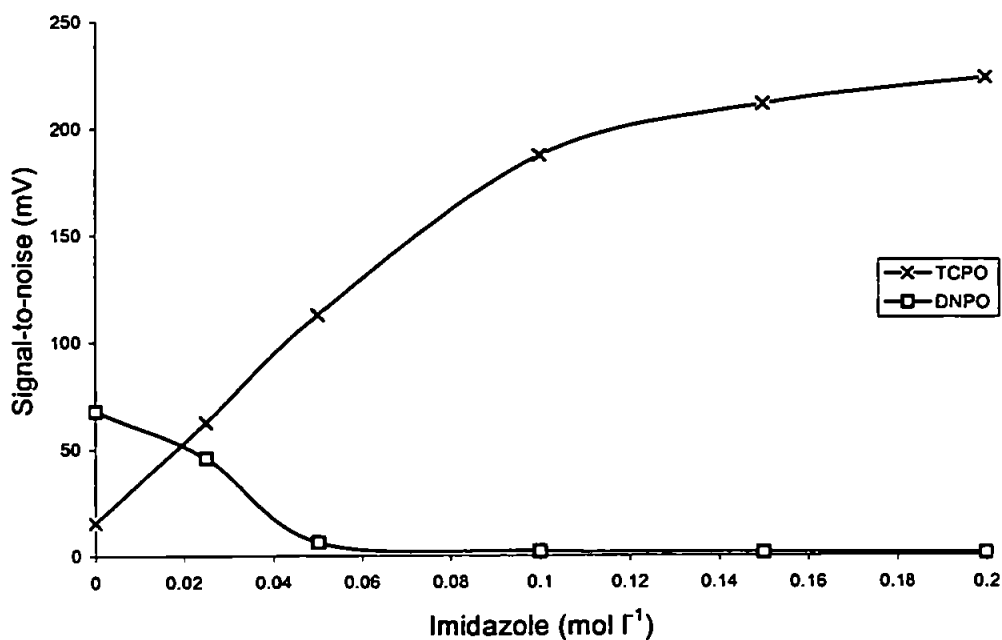


Figure 2.15. Effect of imidazole on the CL emission intensity for DNPO and TCPO plotted as imidazole concentration against signal-to-noise.

An imidazole concentration of 0.15 mol l^{-1} was recommended as the optimum. Above this value the response curve began to 'plateau', showing no significant improvement in the signal-to-noise ratio. This would indicate that the imidazole is in sufficient excess not to affect the reaction rate and further addition of imidazole will not improve reaction conditions. The optimum values are similar to those reported elsewhere for POCL detection with FIA and HPLC [235].

The signal-to-noise response from the DNPO system showed no such enhancement on the addition of imidazole; indeed a dramatic decrease in the signal-to-noise was observed when only 0.05 mol l^{-1} of imidazole had been added. In the case of DNPO it is thought that the kinetics of the reaction have been accelerated sufficiently such that the emission of light occurs outside of the flow cell as explained by the 'time-window concept' [236]. An additional factor contributing to the difference in response to imidazole of the DNPO and TCPO is that the nature of the leaving group has an influence on the susceptibility of the oxalate ester to undergo nucleophilic substitution [233].

Effect of H_2O_2 concentration

The effect of hydrogen peroxide over the range of $0.25\text{-}1.5 \text{ mol l}^{-1}$ was investigated and the results obtained are shown in Figure 2.16.

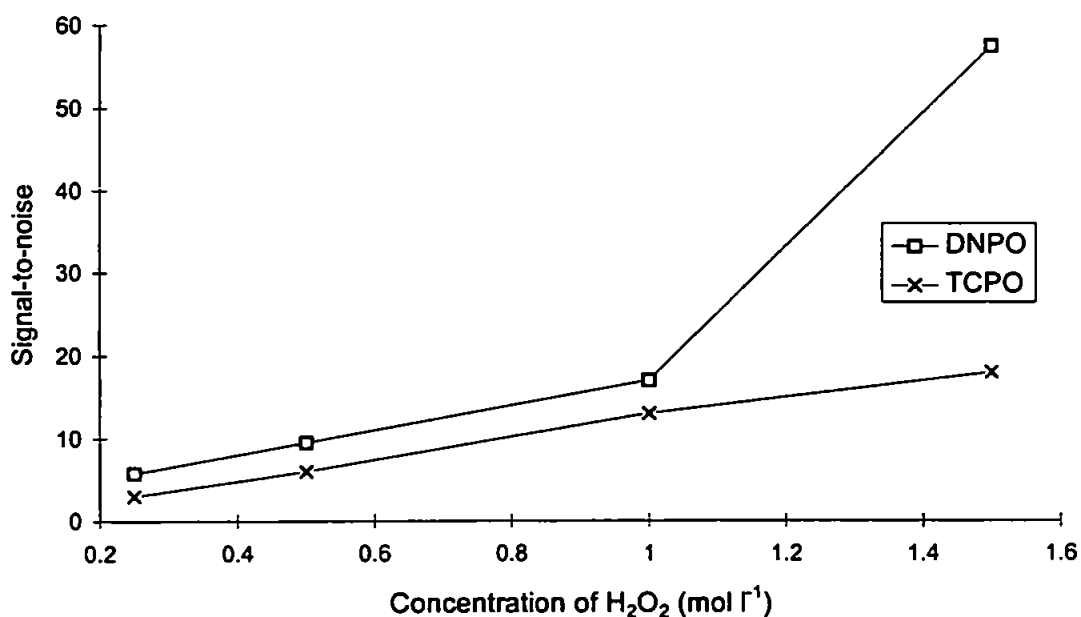


Figure 2.16. Effect of H_2O_2 on the CL emission intensity for DNPO and TCPO plotted as H_2O_2 concentration against signal-to-noise.

The results show that there was an increase in the signal-to-noise when the concentration of hydrogen peroxide was increased. The concentration range was not extended further however, because the reproducibility was poor due to the formation of bubbles within the system, which led to poor reproduction of peak profiles from one injection to the next. Furthermore, concentrated solutions of H₂O₂ are less stable with time and are therefore unsuitable for long term use.

Effect of pH

An investigation of the effect of pH on the CL emission intensity for the POCL reaction gave the results shown in Figures 2.17. and 2.18. for the DNPO and TCPO systems respectively. Signal-to-noise ratios were also calculated and are shown graphically in Figure 2.18.

DNPO has previously been reported as having a more acidic optimum than TCPO [237]. Using a citrate buffer ($5.0 \times 10^{-2} \text{ mol l}^{-1}$) the pH of the carrier stream was adjusted between 2.2 and 6.9 using sodium hydroxide. The results show that the signal-to-noise ratio was improved when a relatively low pH was used. The effect of pH on TCPO was investigated over the range 1.9-9.5 by adjusting the pH of the imidazole with nitric acid. From the signal-to-noise results (Figure 2.19.) it can be seen that the TCPO reaction is more effective in slightly alkaline conditions than in acidic conditions.

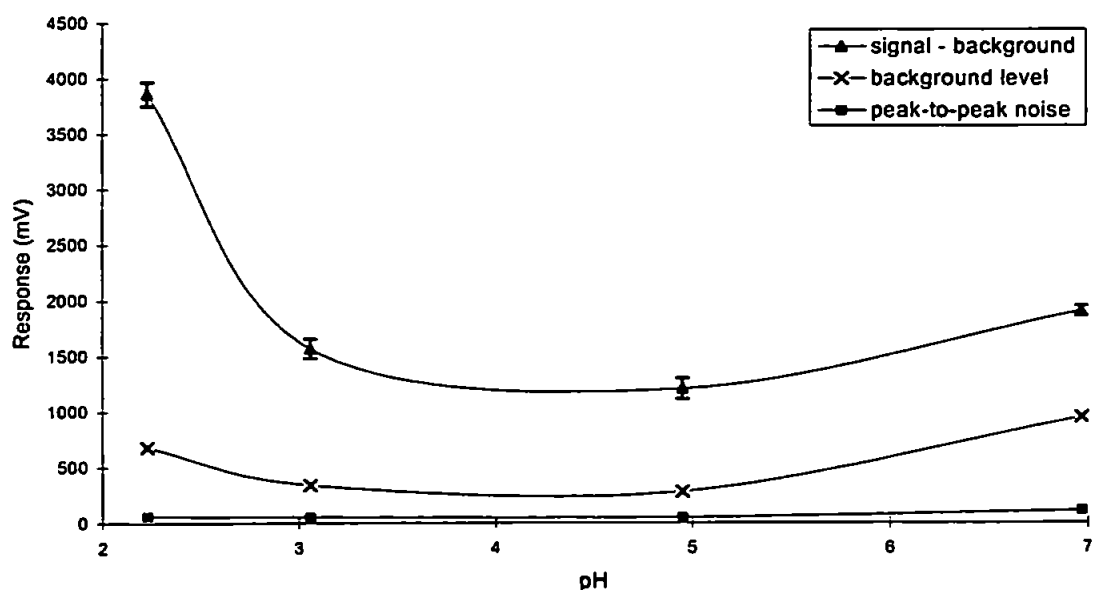


Figure 2.17. Effect of pH on the CL emission intensity for DNPO
(error bars = 3σ).

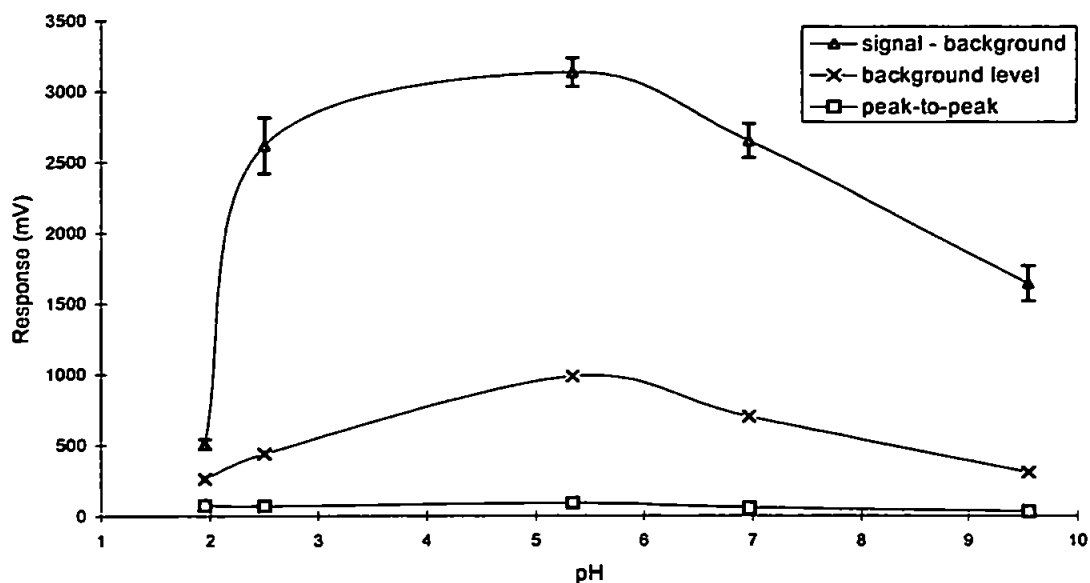


Figure 2.18. Effect of pH on the CL emission intensity for TCPO (error bars = 3σ).

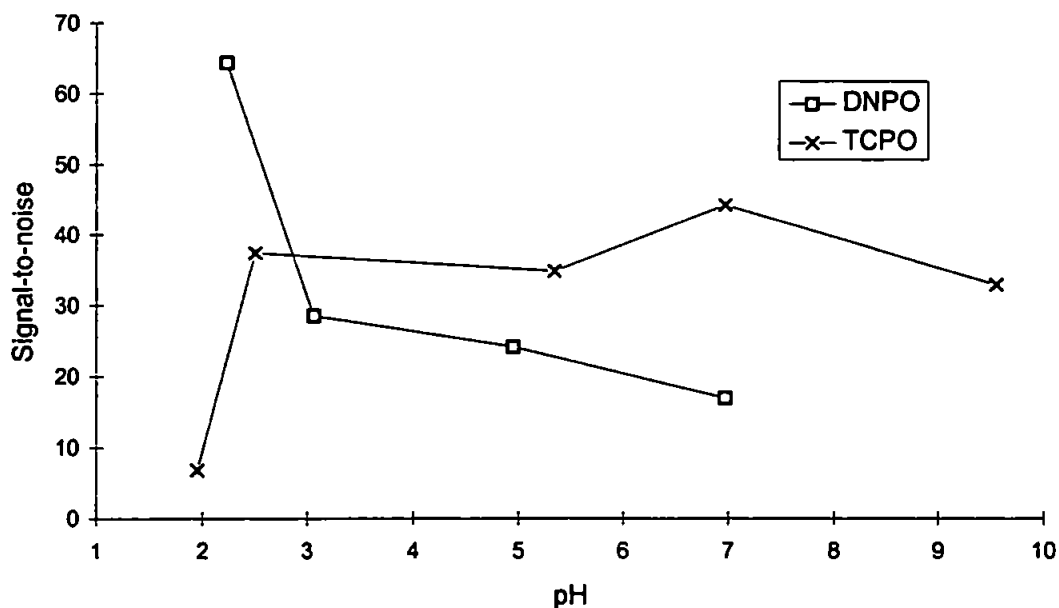


Figure 2.19. Effect of pH on the CL emission intensity for DNPO and TCPO plotted as pH against signal-to-noise.

The observed results can be explained as being related to the relative stability of the oxalate esters at different pHs. Therefore at low pHs the leaving group of the TCPO is unable to be cleaved by base, whereas the leaving group for DNPO undergoes cleavage. At higher than optimum pH the response levels deteriorate as a result of two factors. The first is that simple hydrolysis of the oxalate ester occurs at a faster rate than peroxide

attack. The second is more rapid formation of the chemical excitor than can effectively form the donor-acceptor complex with the fluorophore, thereby leading to decomposition of the excitor through solvent collisions.

Table 2.8 summarises the optimum conditions that have been chosen as a result of the discussions in the previous paragraphs.

Aryl oxalate	DNPO	TCPO
Mobile phase composition	90:10 ACN:water	Neat ACN
Imidazole	0 mol l ⁻¹	1.5 mol l ⁻¹
Hydrogen peroxide	1.0 mol l ⁻¹	1.0 mol l ⁻¹
pH	2.5	7.0

Limits of detection

The optimum conditions were used for the determination of the limits of detection of six selected PAHs. DNPO was chosen as the aryl oxalate to use for the quantitative investigations because it had generally been shown to be more sensitive than TCPO when performing the optimisation investigations.

Table 2.9 shows the detection limits for six PAHs in acetonitrile, obtained by FI with the PD and PMT based detectors. These were calculated as for FL detection (*section 2.3.2*) and compared with results reported in previous literature [238-239].

Perylene gave the most sensitive CL response and the lowest detection limit (0.58 ng ml⁻¹). The results also show that detection with the low power (12 V) PMT based detector is more sensitive than when using the PD based detector. The difference in sensitivity between the two CL detection systems can partly be explained from the spectral response curves of the detectors [240], shown in Figure 2.20. The radiant sensitivity of the PD used for detection is highest between 600 and 800 nm while for the low power PMT, radiant sensitivity is highest at shorter wavelengths (350-550 nm). The wavelengths of maximum emission intensity for some CL reactions have already been given in Table 1.4 and for the POCL detection of PAHs lies between 380 and 480 nm. Therefore, the low power PMT,

in comparison with the PD, will be operating in the region of highest sensitivity when used for the POCL detection of PAHs.

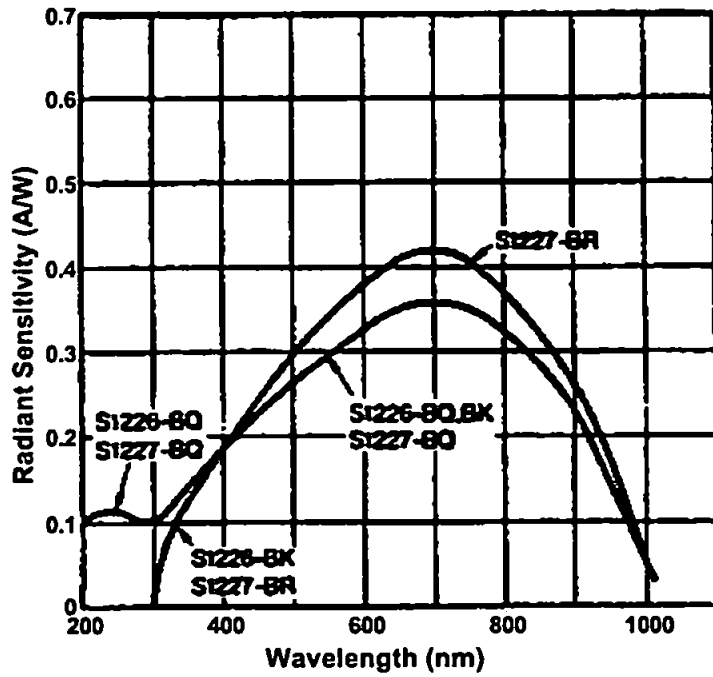
PAH	LOD ng ml ⁻¹ (PD detection)	LOD ng ml ⁻¹ (PMT detection)	LOD ng ml ⁻¹ [238]
Benz[<i>a</i>]anthracene	108 ± 5	22.5 ± 0.9	
Perylene	0.58 ± 0.02	0.12 ± 0.02	0.12
Benzo[<i>a</i>]pyrene	17.2 ± 0.8	4.53 ± 0.3	2.00
Benzo[<i>g,h,i</i>]perylene	37.5 ± 1.2	10.3 ± 0.6	
Benzo[<i>k</i>]fluoranthene	55.5 ± 2	25.3 ± 0.8	2.27
Benzo[<i>b</i>]fluoranthene	119 ± 6	29.2 ± 0.7	71.9

The use of PD detection should not be discounted altogether, however, because it still offers certain advantages over PMTs, which include;

1. PDs are generally cheaper than PMTs.
2. PDs are more robust than PMTs and will withstand more vibration and shock.
3. PDs have a potentially longer lifetime than PMTs.
4. PDs offer easy inspection of the light chamber since they are not affected by normal light when the power supply is turned off, unlike PMTs which can only be inspected in the dark.

Detection limits for the PAHs investigated in this work using the low power (12 V) PMT based detector were in the pg range and broadly comparable with those reported elsewhere [238-239] for CL detection using high power (1 kV) PMTs. The results were in agreement with previously reported data [239] in terms of relative CL efficiency (perylene > benzo[*a*]pyrene > benzo[*g,h,i*]perylene > benzo[*k*]fluoranthene > benzo[*b*]fluoranthene).

(a)



(b)

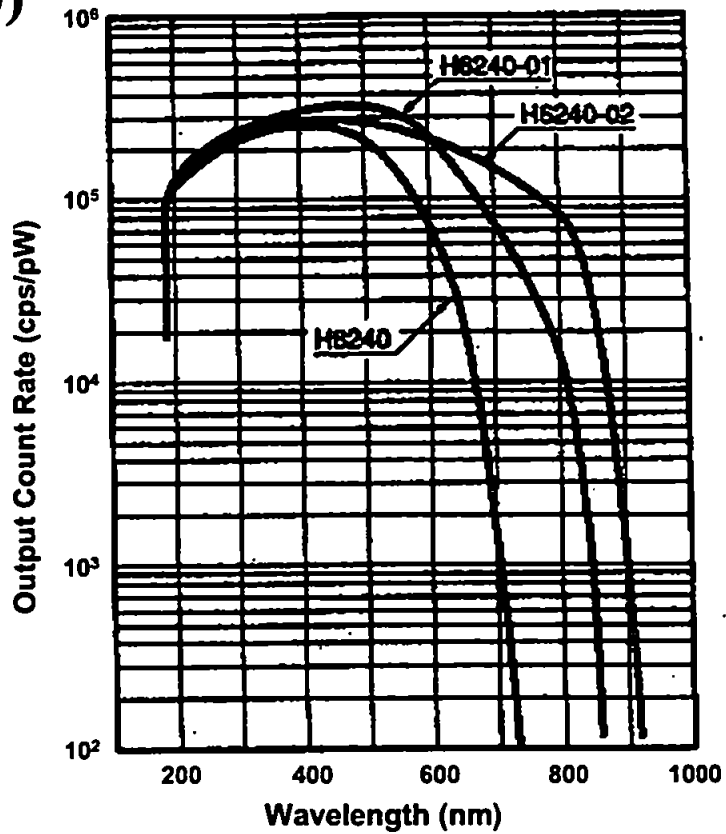


Figure 2.20. Typical spectral response of (a) photodiodes and (b) low power PMT that are commercially available [239].

2.3.4. A comparison of FL and POCL detection methods

In summary it can be seen (Table 2.10) that for most of the PAHs investigated FL detection methods provided better detection limits but for perylene, POCL gave a significantly lower detection limit. The two detection systems can therefore be seen as complementary and could be used in series to improve the characterisation and quantification of PAHs in complex matrices such as oils and fuels.

PAH	FL detection		CL detection	
	ng ml ⁻¹	ng	ng ml ⁻¹	ng
Perylene	1.2	0.06	0.12	0.006
Benzo[<i>k</i>]fluoranthene	1.8	0.09	25.3	1.27
Benzo[<i>a</i>]pyrene	2.8	0.14	4.53	0.22
Benz[<i>a</i>]anthracene	5.0	0.25	22.5	1.13
Benzo[<i>b</i>]fluoranthene	7.3	0.37	29.2	1.46
Benzo[<i>g,h,i</i>]perylene	9.7	0.49	10.3	0.51

The FL data has been listed such that the order of sensitivity decreases from perylene through to benzo[*g,h,i*]perylene, which is in agreement with the batch derived data given in section 2.3.1. As previously mentioned this order holds true relative to the response observed on measurement of the FL emission spectra of these PAH compounds. However, for the CL data it can be observed that no such correlation of detection limits can be drawn relative to the FL emission efficiencies, as previously described during earlier work by Rauhut [241].

2.4 CONCLUSIONS

1. FL generally gave lower limits of detection than POCL, with perylene being a notable exception.
2. The presence of water in the mobile phase/carrier of a flowing stream had an adverse effect on the CL emission intensity for the TCPO reaction, but enhanced the signal-to-

noise ratio for the DNPO reaction, at low levels ($\leq 10\%$), before causing a markedly diminished response on further increase.

3. The presence of imidazole in the mobile phase greatly enhanced the CL emission intensity for the TCPO reaction up to a level of 1.0 mM, but significantly reduced the CL emission intensity for the DNPO reaction.
4. Hydrogen peroxide had a significant influence on the CL emission intensities of both reagents with an increase in concentration leading to an increase in the overall signal-to-noise ratio.
5. The optimum pH for the TCPO reaction was 7 and for the DNPO reaction ≤ 2 .
6. The DNPO reaction was more sensitive than the TCPO reaction.
7. The low power PMT based CL detector gave lower limits of detection than the PD based CL detector for the DNPO reaction.

CHAPTER 3

*Determination of PAHs using
liquid chromatography with fluorescence
and chemiluminescence detection*

3. DETERMINATION OF PAHs USING LIQUID CHROMATOGRAPHY WITH FLUORESCENCE AND PEROXYOXALATE CHEMILUMINESCENCE DETECTION

3.1 INTRODUCTION

Depending on the source of pollution, environmental samples of PAHs can be extremely complex and difficult to analyse. Even after comprehensive separation and isolation of a PAH fraction from an environmental sample there is still likely to be a complex mixture containing many hundreds of compounds of varying volatility and concentration. In these circumstances FI is therefore not the ideal technique for their analysis.

Gas and liquid chromatographic techniques are complementary in the characterisation of PAHs in environmental samples. The larger, less volatile PAHs cannot be analysed by GC because they will either not elute or, if they do, the peaks will be unacceptably broad. Reversed phase HPLC is therefore the preferred method for the analysis of PAHs in complex matrices. The popularity of RP-LC for PAH analysis is due to the excellent selectivity encountered when using this technique for the separation of PAH isomers.

This chapter describes the development of a LC method for the determination of PAHs in non-aqueous matrices and compares post column POCL detection with fluorescence and UV detection methods.

3.2 EXPERIMENTAL

3.2.1 Reagents

High quality de-ionised water from a Milli-Q system (Millipore) and analytical grade reagents were used throughout. All solvents used were of HPLC grade (Rathburn, Walkerburn, UK).

Stock PAH solutions were prepared as described previously in *section 2.2.1*. A commercially available PAH mixture containing 16 EPA priority pollutant PAHs, all at a concentration of 2000 mg l⁻¹ in ACN, was also used (Supelco cat. No. 4-8905).

Two standard reference materials (SRMs) were also investigated using RP-LC methods. The SRMs investigated were SRM 1650 (Diesel Particulate Matter) and SRM 1649 (Urban Dust/Organics) (NIST, Gaithersburg, USA). The details of the certified values for PAHs within these SRMs are given in Table 3.1. Further discussion concerning the SRMs can be found in *section 3.3.3*.

Table 3.1. Certified values for PAHs in SRM 1649 and SRM 1650.		
Compound	Concentration (mg kg ⁻¹)	
	SRM 1649 (urban dust)	SRM 1650 (diesel soot)
Benz[<i>a</i>]anthracene	2.6	6.5
Benzo[<i>a</i>]pyrene	2.9	1.2
Benzo[<i>g,h,i</i>]perylene	4.5	2.4
Fluoranthene	7.1	51
Indeno[<i>1,2,3-cd</i>]pyrene	3.3	N/C*
Pyrene	N/C*	48

*N/C means that the compound has not been certified on this reference material

3.2.2 Instrumentation and procedures

Sample preparation

Working solutions of individual PAHs in the range 0-20 mg l⁻¹ were prepared in ACN by serial dilution of the appropriate stock solutions. The 16 PAH mixture was diluted in ACN 1 ml to 100 ml and designated STOCK. The STOCK was then diluted 5 ml to 100 ml to produce a working standard of 1000 µg l⁻¹ in ACN which was designated STANDARD1. The STOCK was also diluted 2 ml to 100 ml to produce a second working standard of 400 µg l⁻¹ in ACN which was further diluted 5 ml to 50 ml to produce a working standard of 40 µg l⁻¹ in ACN which was designated STANDARD2.

The SRM 1649 (1025 mg) and SRM 1650 (50.7 mg) were extracted by Soxhlet extraction. This was performed using propan-2-ol (IPA) in a round-bottomed flask for 12 h at approximately 8 cycles h⁻¹. The Soxhlet extracts were dissolved into 10 ml (SRM 1649) and 5 ml (SRM 1650) propan-2-ol. Any subsequent dilution required for analysis by LC was done using ACN.

LC with fluorescence detection

Two chromatographic systems were used throughout this investigation. The first system (System I) consisted of a high pressure gradient Varian 9012 single piston pump, a Rheodyne 7010 injection valve (Rheodyne Inc., Cotati, CA, USA) with 20 µl sample loop and a Perkin Elmer LS-4 spectrofluorimeter (Perkin-Elmer Ltd., Beaconsfield, UK) or Hitachi Merck F1050 spectrofluorimeter (Hitachi Ltd., Tokyo, Japan). FL emission was recorded using a Chessel BD 4004 chart recorder (Chessel Ltd., Worthing, UK).

The second system (System II) consisted of a HP 1090 Series II liquid chromatograph, with HP 1040 diode array UV detector and HP1046A fluorescence detector (Hewlett Packard, Surrey, UK). Automated sample introduction was via a Rheodyne 7012 injection valve (Rheodyne Inc., Cotati, CA, USA) with 15 µl sample loop. Instrument control and data acquisition was achieved using a PC running HP Chemstation software (Hewlett Packard, Surrey, UK).

LC with chemiluminescence detection

Chemiluminescence detection was performed by post-column addition of the chemiluminescence reagents using the manifold shown in Figure 3.1. A Minipuls 2 peristaltic pump (Gilson, Villiers-le-Bel, France) with 1.02 mm i.d. Ismaprene (PharMed 65) pump tubing (Ismatec UK Ltd, Weston-Super-Mare, UK) was used to propel the DNPO and H₂O₂ reagent streams to a polyetherether ketone (PEEK) T-piece (Phenomenex UK Ltd, Macclesfield, UK). The waste stream from the fluorescence detector was connected to a second PEEK T-piece, where it mixed with the combined DNPO/H₂O₂ reagent stream, before passing into the flow cell. CL detection was performed using a low power (12 V) PMT based detector (Camspec CL-2, Camspec Scientific Instruments, Cambridge, UK). The conditions used for the post-column detection of PAHs were those suggested as a conclusion to the optimisations by FI in *section 2.4*.

RP-LC columns and chromatographic parameters

Three different reversed phase analytical columns were investigated using the two chromatographic systems (System I and System II). The details of each column are given in Table 3.2 and further discussion of the performance of individual columns is given in *section 3.3.2*.

Name	Dimensions (mm)	Particle size (μm)	Supplier
Spherisorb S5 PAH	150 \times 4.6	5	Phase Separations Ltd, Deeside, UK
LiChrospher PAH	250 \times 3.0	5	Merck, Darmstadt, Germany
Envirosep-PP	125 \times 4.6	5	Phenomenex UK Ltd, Macclesfield, UK

In order that optimum separation of the 16 PAH mixture was achieved in reasonable time a gradient of water and ACN was used throughout. The mobile phase gradient that was selected for use is shown in Table 3.3. All solvents used were degassed by helium sparging for 30 minutes and to ensure that the mobile phase was free from dissolved air at all times, helium was bubbled through the solvent throughout.

Time (min)	Water (%)	ACN (%)
0.0	50	50
3.0	50	50
15.0	40	60
25.0	10	90
40.0	10	90
40.1	50	50
50.0	50	50

Mobile phase was delivered at 1.0 ml min^{-1} and, when CL detection was used, mixed with a pre-mixed CL reagent stream at 0.5 ml min^{-1} (Figure 3.1).

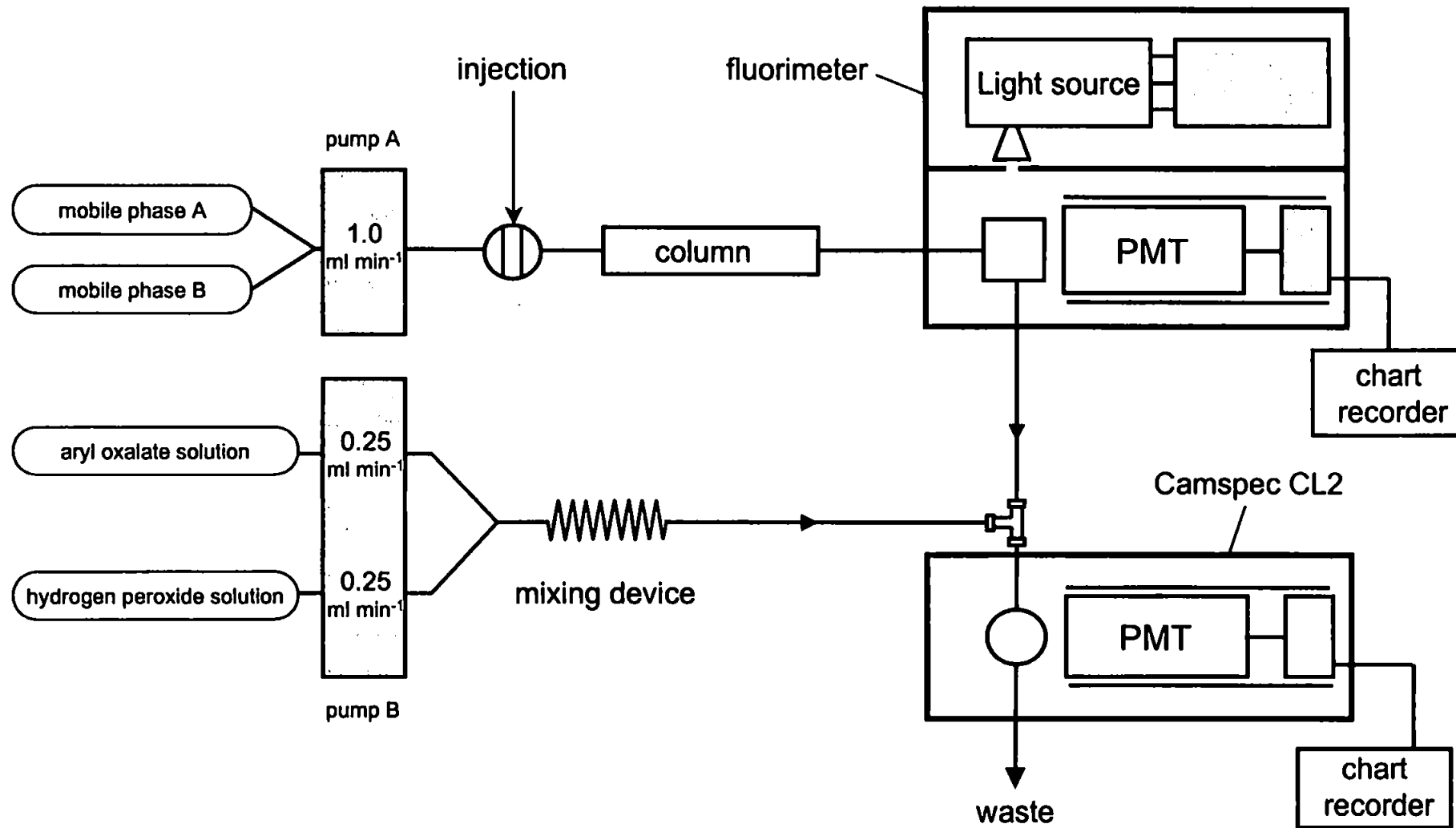


Figure 3.1. LC manifold for the detection of PAHs with FL and POCL detection.

Both fixed wavelength FL detection (System I) and wavelength programmed FL detection (System II) were investigated. An excitation wavelength of 270 nm and emission wavelength of 395 nm were chosen as compromise wavelengths during fixed wavelength detection for the best overall response for all 16 PAHs in the separated mixture. For optimisation of response to any given PAH, programmed wavelength FL detection is recommended and the programme used, unless otherwise stated, is shown in Table 3.4.

Table 3.4. Wavelength programme used for programmed FL detection.		
Time (min)	Excitation (nm)	Emission (nm)
0.0	230	330
7.0	210	314
10.0	250	368
13.0	237	440
17.0	277	376
21.0	255	420
26.0	230	453

NP-LC columns and chromatographic parameters

An investigation into the use of a normal phase LC separation coupled to the CL detection system was investigated. This work used the chromatographic System II but used a normal phase column in place of the reversed phase column. The NP-LC column used during this investigation contained a Hypersil Green PAH-2 stationary phase (Hypersil, Runcorn, UK). The column dimensions were 150 × 4.6 mm with a particle size of 5 µm. Further discussion of the performance of the Hypersil Green PAH-2 column together with the mobile phase gradient used is given in *section 3.3.5*.

3.3 RESULTS AND DISCUSSION

3.3.1. Occurrence and properties of polycyclic aromatic hydrocarbons

Polycyclic aromatic hydrocarbons (PAHs) are a complex class of condensed, multinumbered benzoid-ring compounds (three or more fused benzene rings in linear, angular or cluster arrangement) containing only carbon and hydrogen atoms.

PAHs are environmental pollutants that are found in air, water and soil, and are formed during both natural and anthropogenic processes. The natural sources include grassland/forest fires and volcanoes. Emissions containing PAHs from anthropogenic sources account for the largest percentage in terms of annual global production, and are either stationary or mobile processes (see Table 3.5) involving combustion of organic materials.

Mobile sources	Stationary sources
Gasoline and diesel engine automobiles.	Industrial sources e.g. coke production.
Aeroplanes.	Power and heat generation.
Sea transport.	Residential heating and cooking.
	Refuse incineration, agricultural burning.

PAHs are widespread throughout the environment and determination of these pollutants in complex environmental samples is, therefore, of paramount importance due to their toxicity. Major efforts have therefore been made to develop sensitive analytical methods for the determination of PAHs in matrices such as exhaust emissions, smokes, airborne particulates, surface and drinking waters, foodstuffs, soils, sediments and lubricating oils.

PAHs are formed from reactions at high temperatures and under pyrolytic conditions during the combustion of organic matter. The radicals formed from organic molecules at high temperatures recombine to form larger, thermodynamically favoured and relatively stable aromatic ring hydrocarbons. The type of PAH formed depends on the temperature of combustion. Lower temperatures (400-800°C) produce mainly alkyl-substituted PAHs

whereas higher temperatures (2000°C) are responsible for the production of unsubstituted PAHs. The proposed stepwise synthesis of benzo[*a*]pyrene from Badger and co-workers [243] is outlined in Figure 3.2.

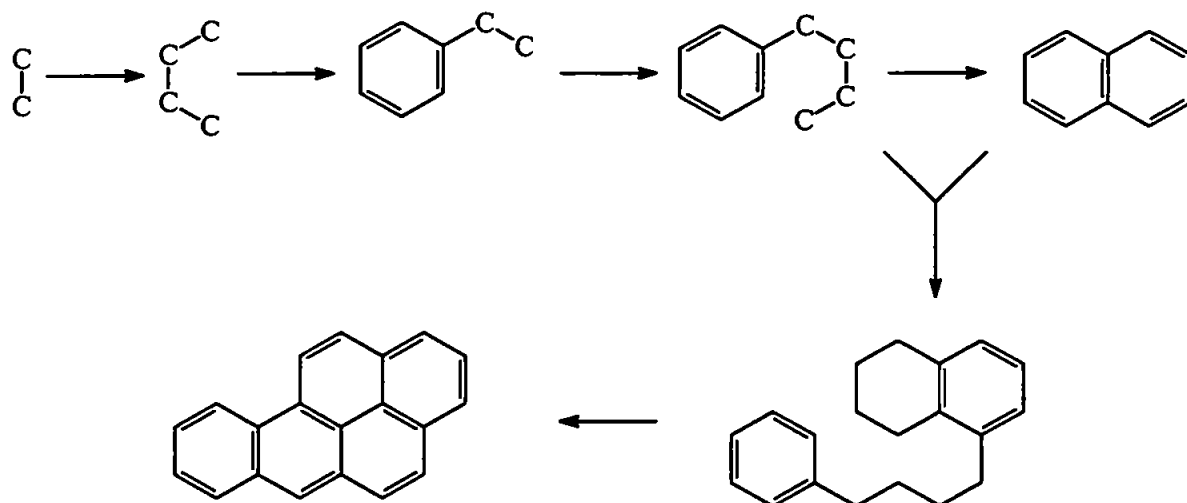


Figure 3.2. Pyrosynthesis of benzo[*a*]pyrene.

Toxicity of PAH

As with most pollutants there are health risks associated with PAHs; they can be carcinogenic and/or mutagenic, that is they can cause cancer and/or cause cells within the body to mutate, thus causing cancer. The carcinogenic property of PAHs was first demonstrated by Cook, in 1933, by applying benzo[*a*]pyrene isolated from coal tar on the skin of mice [244].

It is well known that PAHs are metabolised by enzymatic oxygenation to epoxides, phenols, dihydrodiols, quinones and water-soluble conjugates in an attempt to make them more soluble and thus facilitate their excretion from the organism [245]. Unlike the detoxification of other xenobiotics, for benzo[*a*]pyrene and other PAHs that possess a bay region, one of the intermediate products in this multi-step process can be diverted instead into the formation of a very stable cation that induces cancer.

The first chemical transformation in this metabolic activation, catalysed by the cytochrome P₄₅₀ system, is the formation of an epoxide ring across one C=C bond in the PAH (Figure 3.3). A second microsomal enzyme, epoxide hydrolase (EH), causes a fraction of these epoxide molecules to add H₂O, to yield two –OH groups on adjacent carbons. The double

bond that remains in the ring attached to the two –OH groups subsequently undergoes epoxidation, thereby yielding the molecule that is the active carcinogen. By the addition of H^+ this molecule can form a particularly stable cation that can bind to molecules such as DNA, thereby inducing mutations and cancer.

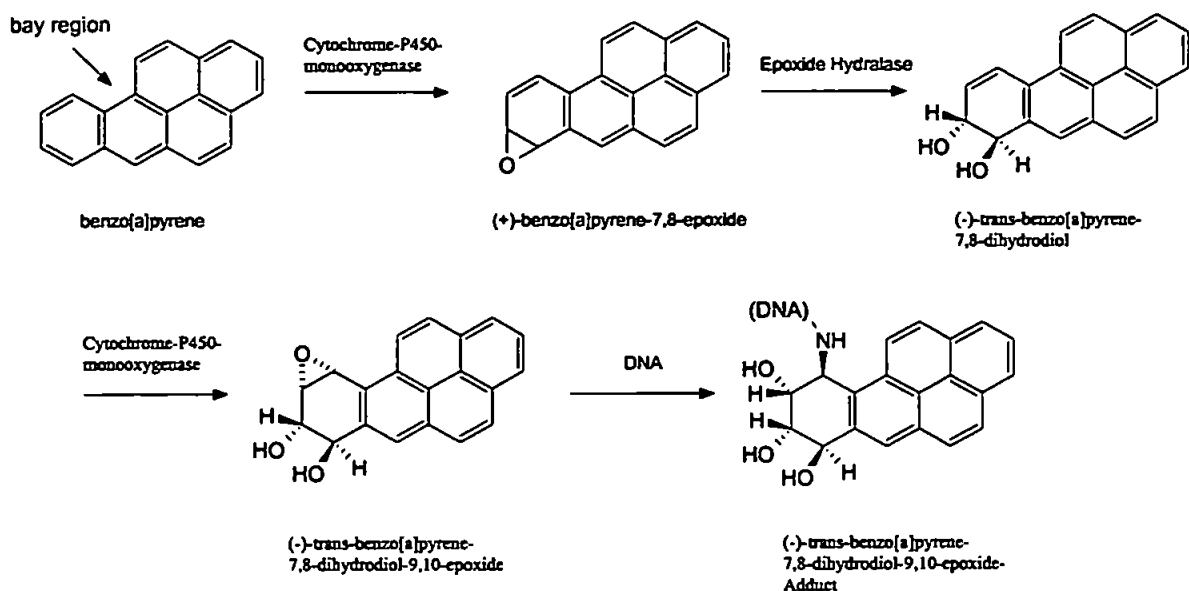


Figure 3.3. Enzymatic activation of benzo[a]pyrene [246].

The carcinogenic activities of PAHs are dependent on their structure, shape, size and steric effects. Furthermore the addition of substituent groups in favourable positions in certain PAHs has an activating influence, as can be seen from the data in Table 3.6.

PAH	Activity	PAH	Activity
Pyrene	0	Indeno[1,2,3- <i>cd</i>]pyrene	+
Benz[<i>a</i>]anthracene	+	Fluoranthene	0
Perylene	0	Chrysene	+
Benzo[<i>e</i>]pyrene	0	Benzo[<i>b</i>]fluoranthene	++
Benzo[<i>a</i>]pyrene	++++	3-Methylcholanthene	++++
Benzo[<i>g,h,i</i>]perylene	+	Benzo[<i>c</i>]phenanthrene	+++

0, inactive; +, weakly active; ++, moderately active; +++, very active; +++++, extremely active.

The PAHs that are the most potent carcinogens each possess a bay region formed by the branching of the benzene ring sequence. The organisation of the carbon atoms as a bay region imparts a high degree of biochemical reactivity to the PAH. Figure 3.4 illustrates some 'bay region' containing PAHs and their related dihydrodiol epoxides that are considered as the carcinogenic precursors produced during metabolism [248].

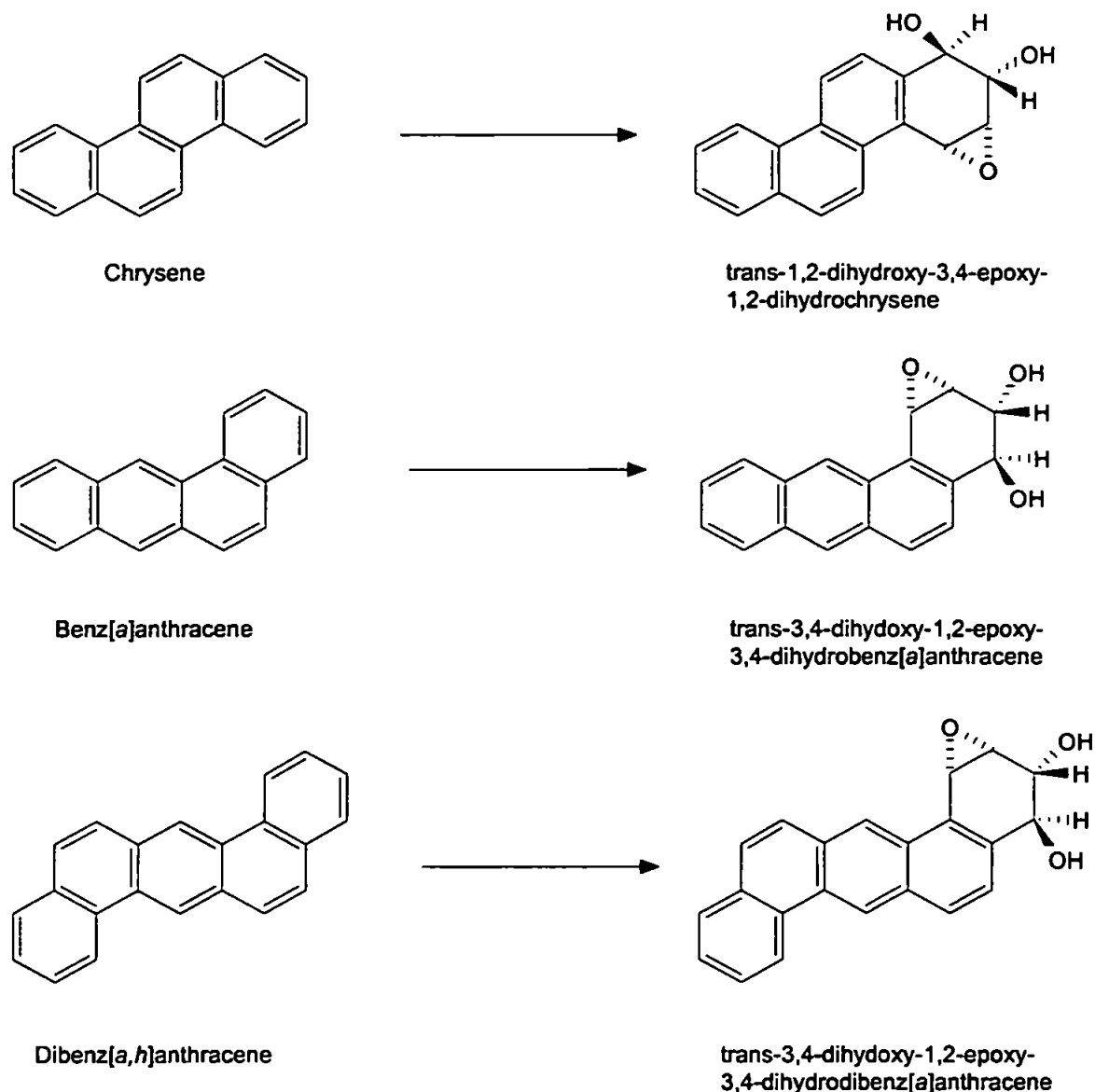


Figure 3.4. Bay region containing PAHs and related dihydrodiol epoxides.

Because of the mutagenic and carcinogenic effects of PAHs, in 1971 the World Health Organisation (WHO) placed an upper limit of 200 ng l⁻¹ for the total concentration of six priority PAHs (fluoranthene, benzo[b]fluoranthene, benzo[k]fluoranthene, benzo[a]pyrene, benzo[g,h,i]perylene and indeno[1,2,3-*cd*]pyrene) in potable water. This regulatory standard has also been adopted by the European Community (EC Directive 80/778/EEC) [249]. Soon after this, in 1976, the U.S. Environmental Protection Agency (EPA) drew up

a list of 16 PAHs that are believed to cause skin cancer and sarcomas. These 16 PAHs are known as priority pollutants and are representative of different ring sizes and toxicities of PAH compounds. Another series that has been suggested is the Grimmer series [250] which contains 31 PAH compounds, including a number of alkyl substituted PAHs. Throughout the remainder of the work discussed in this thesis the EPA 16 priority pollutant PAHs have been used because they are generally accepted as the standard suite of PAH compounds to investigate.

3.3.2 RP-LC determination of PAH with FL detection.

When PAHs are associated with polar media, such as water, the typical mode of analysis is reversed phase liquid chromatography (RP-LC) with FL detection [203, 251-252], usually using a bonded stationary phase. There are however problems associated with the use of standard bonded phases due to the structural similarities of certain PAHs and hence complete resolution of the 16 priority pollutants is difficult to attain. The results obtained from preliminary investigations (Figure 3.5) clearly illustrate that co-elution is observed between acenaphthene and fluorene (peaks 3 and 4) and benzo[*g,h,i*]perylene and indeno[1,2,3-*cd*]pyrene (peaks 15 and 16). Peak numbers corresponding to the 16 EPA PAH structures illustrated in Figure 3.6.

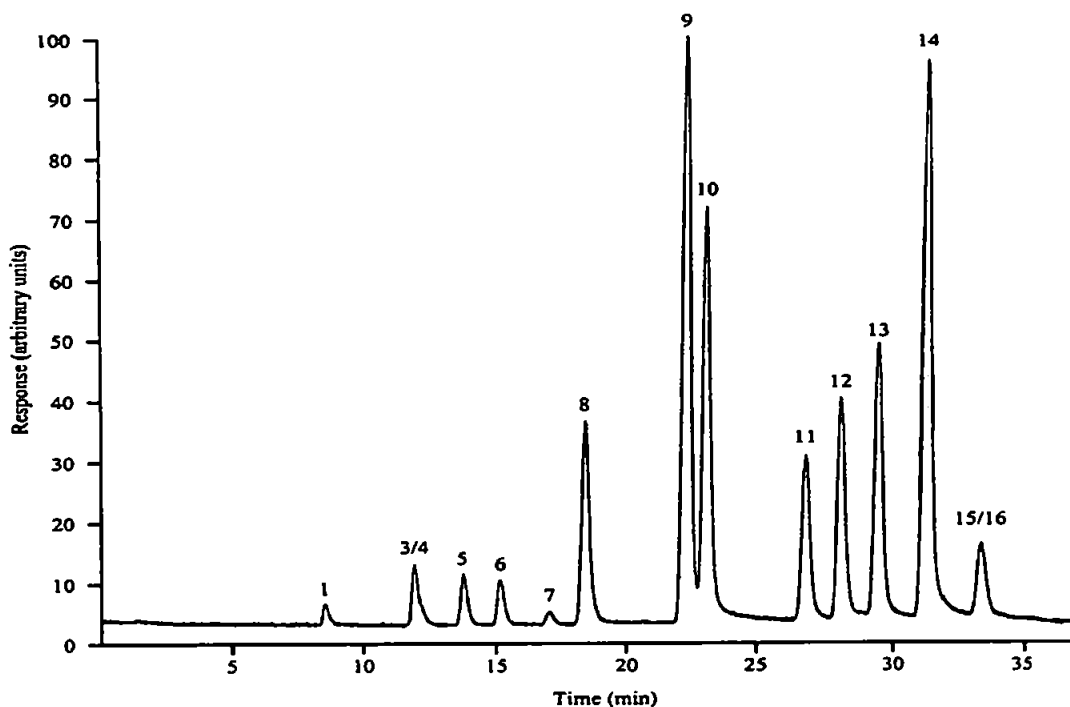


Figure 3.5. Separation of 16 PAH test mixture using Spherisorb S5 PAH column using System I.

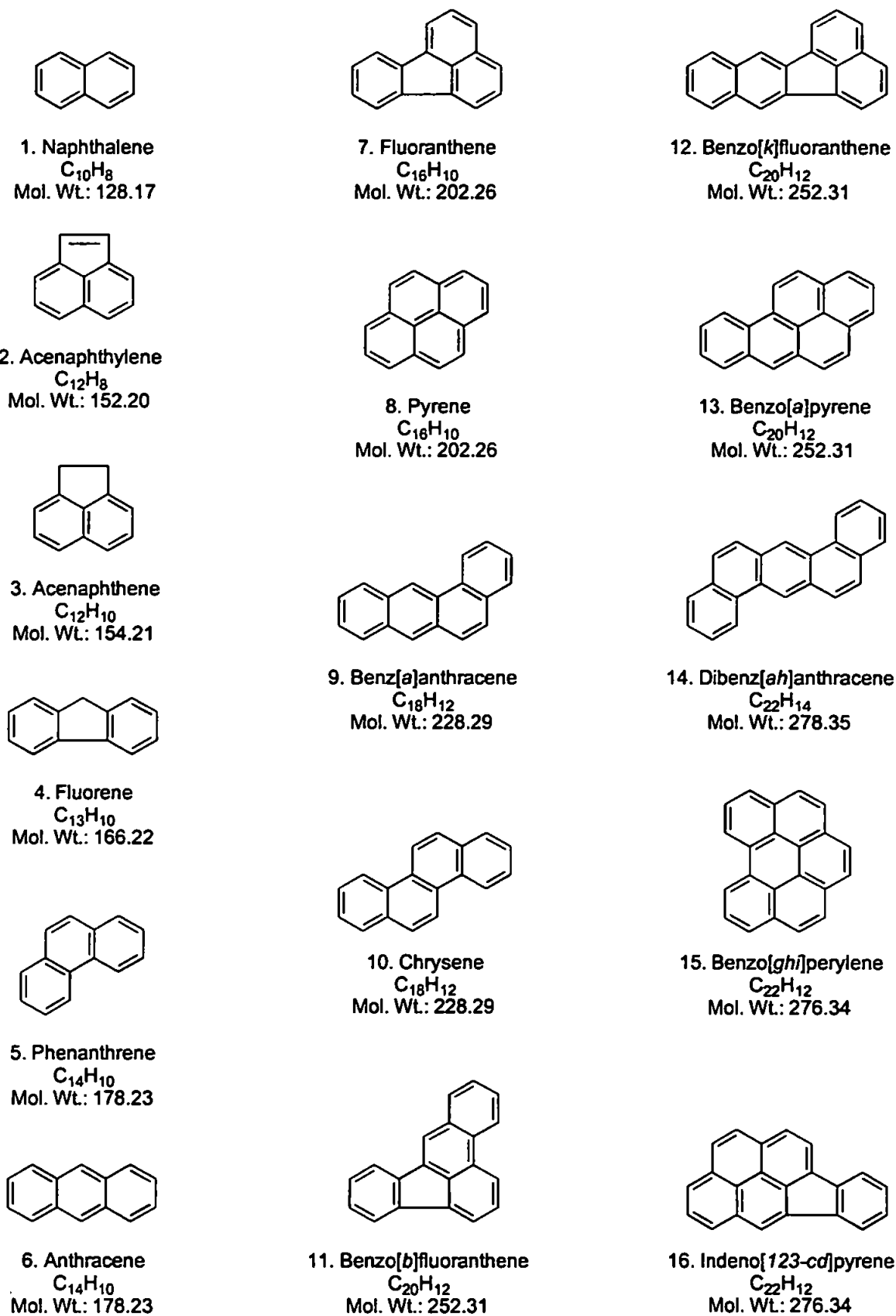


Figure 3.6. Structures of the 16 PAHs identified as priority pollutants by the EPA.

These problems can be overcome by the use of a LiChrospher PAH column, a specially tailored alkyl bonded phase with a high carbon loading designed specifically for complete resolution of the 16 priority pollutants. Figure 3.7 shows complete resolution of 15 PAHs from the 16 EPA priority pollutants using the LiChrospher PAH column (peak number related to PAH structures in Figure 3.6.).

To increase the sensitivity of detection for all 15 PAHs that fluoresce, a programmable fluorescence detector is recommended. This wavelength tuning is only possible when using a column that offers good resolution between peaks. It is also important that the system remains stable with respect to retention times so that the wavelength programme remains constant during any subsequent analysis.

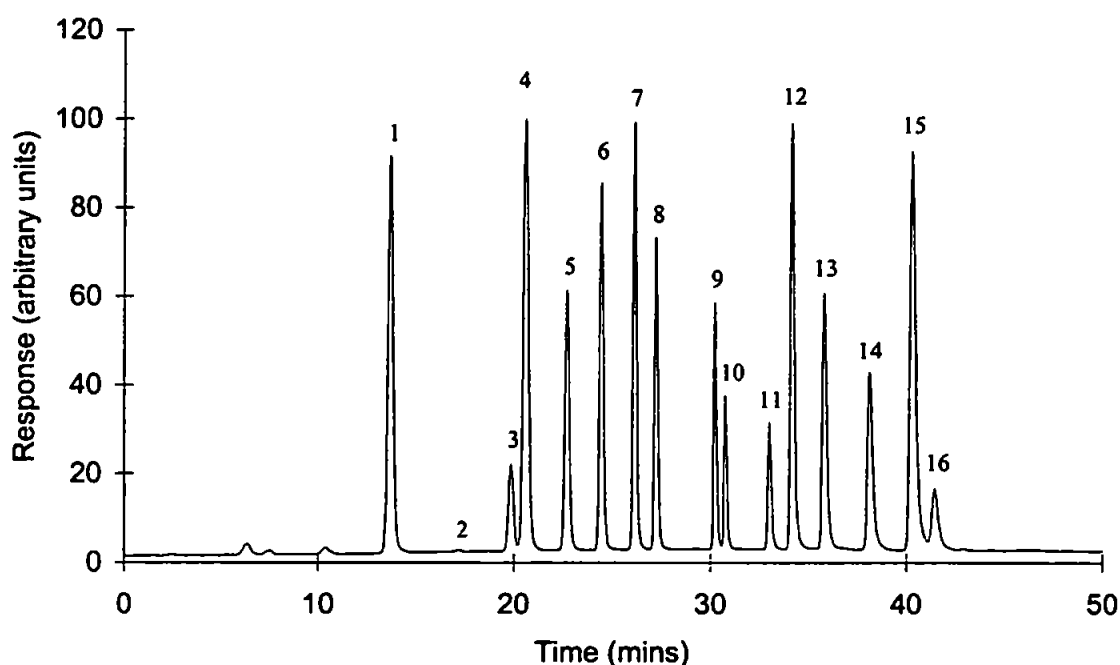


Figure 3.7. Chromatogram of 16 PAH test mixture using programmed FL detection.

The only PAH on the priority pollutant list that is not included on any of the FL chromatograms is acenaphthylene, which elutes between naphthalene and acenaphthene. Unlike the majority of PAHs acenaphthylene does not display native fluorescence. In order that detection of all 16 priority pollutant PAHs can be performed a fluorescence detector and diode-array UV detector were used in series (System II). Figure 3.8 shows the chromatogram obtained for the separation of the 16 PAH test mixture using UV detection ($\lambda=230\text{nm}$).

Diode-array detection of PAHs after separation by LC allows acquisition and storage of the UV spectrum of each eluting peak. The chromatogram can then be reconstructed at any defined wavelength after the analysis. The spectral output of the diode array is not only used for qualitative and quantitative analysis but also to augment the resolution of chromatographic separation, since poorly resolved peaks can be identified by deconvolution of the eluent spectra [253].

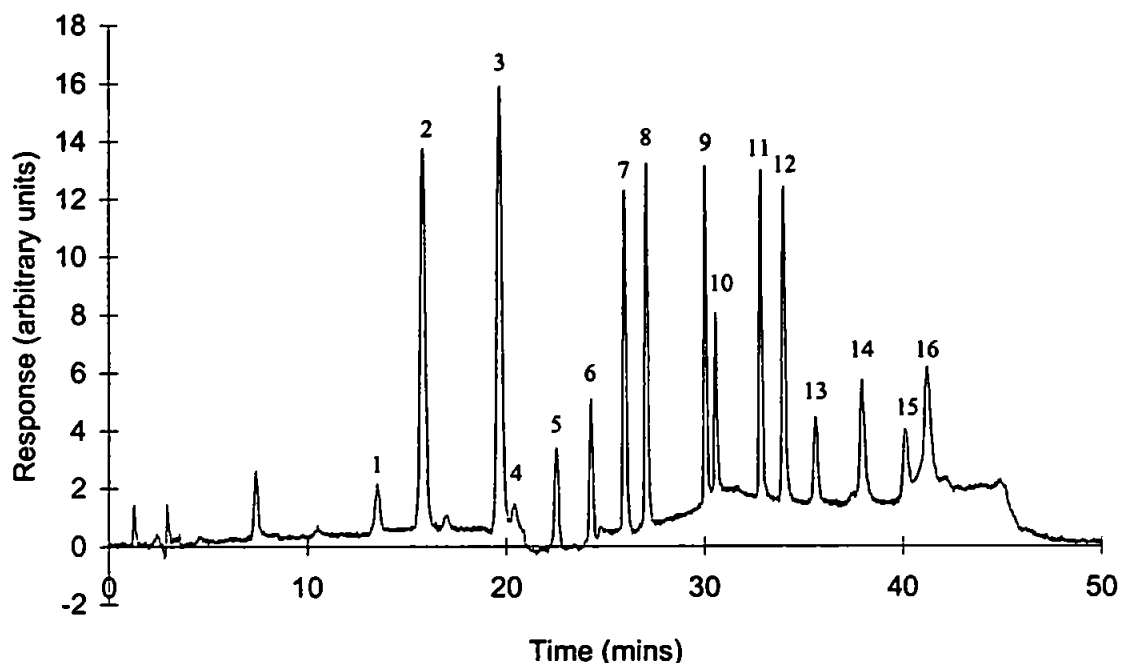


Figure 3.8. Chromatogram of 16 PAH test mixture using UV ($\lambda=230\text{nm}$) detection.

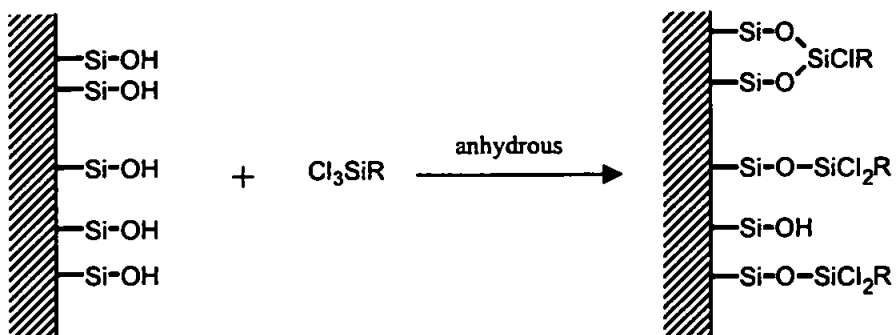
Table 3.7 shows the retention data obtained for the separation of a 16 PAH test mixture using three different commercially available columns. From this table it can be seen that the three columns showed differences in selectivity towards the PAHs in the test mixture. Both the Envirosep-PP and LiChrospher PAH showed good resolution for the separation of all 16 PAHs within the test mixture but the Spherisorb S5 PAH showed a lack of resolution between acenaphthene and fluorene and benzo[*g,h,i*]perylene and indeno[*1,2,3-cd*]pyrene. The improved separation with the Envirosep-PP and LiChrospher PAH columns can be explained by the nature of the bonded phase used for the separation and how it was manufactured.

An investigation of several chemically bonded reversed phase stationary supports (e.g. C_2 , C_6 , C_8 , C_{18} , C_{22} and phenyl) showed that C_{18} phases generally provided the best separations of PAHs [254]. The reversed phase separations of PAHs can be further split into two distinct types. Those using either a monomeric phase or a polymeric phase [255].

3.7. Retention times of PAHs using three different columns.				
PAH		Retention time (min)		
Peak	Name	Spherisorb S5	Envirosep-PP	LiChrospher PAH
1	Naphthalene	8.4	8.5	13.7
2	Acenaphthylene	N/A	10.2	15.8
3	Acenaphthene	11.8	12.9	19.9
4	Fluorene	11.8	13.4	20.6
5	Phenanthrene	13.6	15.1	22.7
6	Anthracene	15.0	16.7	24.5
7	Fluoranthene	17.0	18.5	26.2
8	Pyrene	18.4	19.8	27.2
9	Benz[<i>a</i>]anthracene	22.2	23.9	30.2
10	Chrysene	22.9	24.6	30.8
11	Benzo[<i>b</i>]fluoranthene	26.6	28.1	33.0
12	Benzo[<i>k</i>]fluoranthene	28.0	29.4	34.2
13	Benzo[<i>a</i>]pyrene	29.2	30.9	35.8
14	Dibenz[<i>a,h</i>]anthracene	31.2	32.9	38.1
15	Benzo[<i>g,h,i</i>]perylene	33.4	34.5	40.3
16	Indeno[<i>1,2,3-cd</i>]pyrene	33.4	35.1	41.4

Monomeric phases are prepared by derivatizing silica with monochlorotrialkylsilane, resulting in only a single moiety on each derivatized silanol. Polymeric phases are prepared by the reaction of a dichlorodialkyl- or trichlorotrialkyl silane with the silanols in the presence of water which results in cross linking to form silane polymers on the silica surface. Repetition of the process yields a bonded alkyl-substituted polysiloxane. The most widely used polymeric reversed phases are generated with an octadecylsilane, in which a dichloro- or trichlorosilane is used. Figure 3.9 illustrates how monomeric and polymeric phases are produced [256].

a.



b.

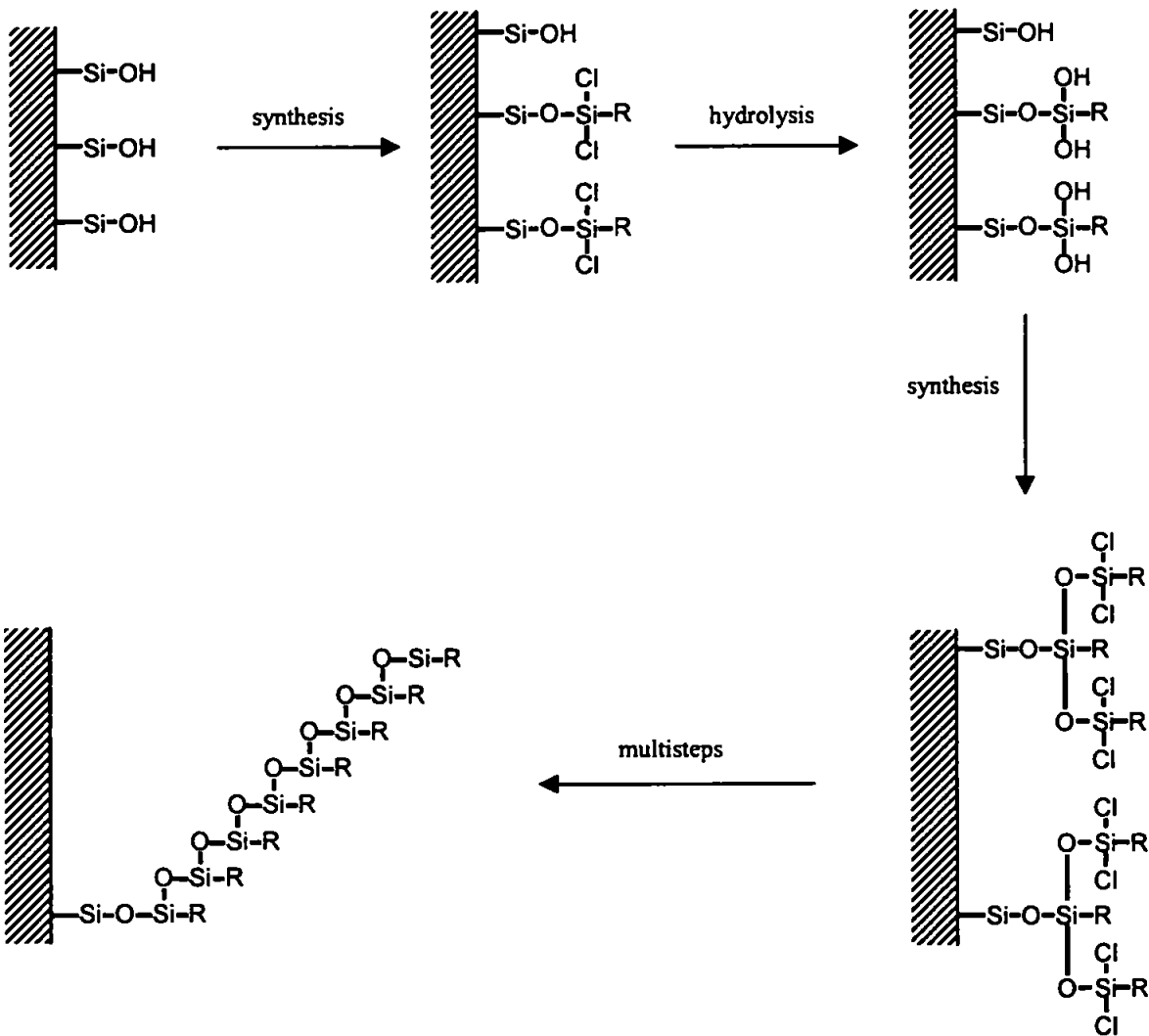


Figure 3.9. Synthesis of a) monomeric and b) polymeric type bonded phases.

In monomeric phases, PAH are basically separated according to the number of aromatic rings, whereas a polymeric phase separates PAHs according to their three dimensional shapes, resulting in very effective isomeric separations. To account for the selective retention of PAH isomers on polymeric phases, the 'slot model' which represents the bonded phase onto which solutes penetrate is used. Long narrow solutes that have a large length-to-breadth (L/B) ratio penetrate a larger number of available slots than square solutes causing them to be retained longer than square solutes. Planar solutes are able to penetrate deeper into the slots than non-planar solutes of similar molecular weight and L/B ratio. Thus planar PAH isomers with large L/B ratio are retained longest in polymeric phases [257]. The more 'polymeric like' that the bonded stationary phase becomes then the better the isomeric separation of the PAHs becomes.

A selectivity assessment test has been reported to assess the selectivity of C18 stationary phases for the separation of PAHs [258-259]. The test is based on the shape selectivity of benzo[*a*]pyrene relative to 1,2:3,4:5,6:7,8-tetrabenzonaphthalene (TBN). The shape selectivity factor $\alpha_{\text{TBN/BaP}}$ has been shown to correlate with the retention behaviour of PAHs and the bonded phase type. Values of $\alpha_{\text{TBN/BaP}} \leq 1$ indicate polymeric C18 phases, and values of $\alpha_{\text{TBN/BaP}} \geq 1.7$ indicate monomeric phases. Among the polymeric C18 phases, selectivity varies with density or coverage of the polymeric layer. A listing for over 40 commercial C18 columns has been published and the relative merits of some of these columns is discussed. Included in the list were two of the columns used in this investigation, Spherisorb PAH and Envirosep-PP. The $\alpha_{\text{TBN/BaP}}$ values for these two columns were 0.82 and 0.58 respectively, indicating that the Envirosep-PP column showed a higher polymeric-like selectivity than the Spherisorb PAH column. This would explain why the separation of the 16 PAH test mixture was not performed as successfully using the Spherisorb column.

3.3.3 RP-LC determination of PAHs in SRMs with FL detection.

To accurately identify and quantify individual PAHs in complex environmental samples, it is necessary to use analytical procedures that have been validated as to their accuracy. SRM 1649 is an air particulate sample that was collected in the mid-1970's in Washington DC. USA and the PAH mixtures on this material are representative of pyrolytic sources. SRM 1650 is a diesel particulate sample and is representative of heavy-duty, diesel emissions in the early 1980's.

SRM 1649 was prepared from atmospheric particulate matter collected in Washington DC area using a baghouse specially designed for the purpose. The material was collected over a period in excess of twelve months and therefore represents a time integrated sample. The sample is not meant to be representative of the area in which it was collected but should generally typify atmospheric particulate matter obtained in an urban area.

Table 3.8 shows a summary of the results as supplied on the certificate of analysis for SRM 1649. Certified values are based on the results obtained by two different analytical methods utilising 1g sample sizes. Non-certified values are provided for information only.

Compound	Concentration (mg kg ⁻¹)		
	GC	LC-1	LC-2
*Benz[<i>a</i>]anthracene	2.4 ± 0.1 (4)	2.8 ± 0.3 (18)	2.4 ± 0.1 (3)
*Benzo[<i>a</i>]pyrene	3.0 ± 0.3 (4)	2.6 ± 0.4 (18)	2.6 ± 0.1 (9)
Benzo[<i>b</i>]fluoranthene		6.2 ± 0.3 (18)	
Benzo[<i>e</i>]pyrene	3.3 ± 0.2 (4)		
*Benzo[<i>g,h,i</i>]perylene	4.7 ± 0.2 (4)	3.9 ± 0.8 (12)	5.2 ± 0.6 (9)
Benzo[<i>k</i>]fluoranthene		2.0 ± 0.1 (18)	2.1 ± 0.1 (9)
Chrysene		3.5 ± 0.1 (5)	3.7 ± 0.2 (9)
Dibenz[<i>a,h</i>]anthracene			0.41 ± 0.07 (9)
*Fluoranthene	7.3 ± 0.2 (4)	7.0 ± 0.5 (24)	6.8 ± 0.4 (9)
*Indeno[<i>1,2,3-cd</i>]pyrene	3.3 ± 0.3 (4)	3.4 ± 0.4 (16)	3.6 ± 0.2 (4)
Perylene	0.84 ± 0.09 (4)	0.80 ± 0.04 (17)	0.65 ± 0.02 (9)
Phenanthrene			4.5 ± 0.3 (9)
Pyrene	7.2 ± 0.2 (4)	6.3 ± 0.4 (17)	6.2 ± 0.2 (9)
Triphenylene			1.7 ± 0.1 (3)

* indicates the compounds listed as certified values.

SRM 1649 (1025 mg) was extracted by Soxhlet extraction and the extract dissolved in 10 ml propan-2-ol. Using the conditions described previously for the separation of a mixture containing 16 EPA priority pollutant PAHs, the SRM1649 sample extract was investigated

using RP-LC with programmed FL detection. The chromatogram obtained from this separation (Figure 3.10) shows that 14 of the 16 EPA priority pollutant PAHs were quantified in the extract.

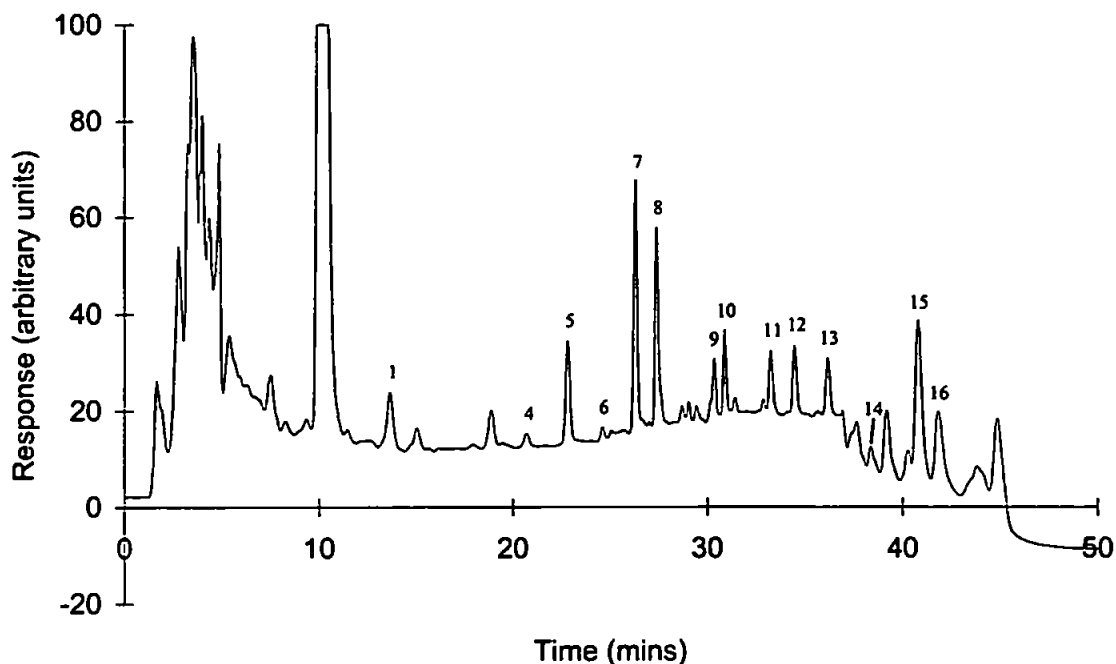


Figure 3.10. LC chromatogram of SRM 1649 using programmed FL detection.

Other prominent peaks are observed in the chromatogram and are due to uncharacterised hydrocarbons and other PAH isomers within the sample. One previous investigation reported in the literature [260] describes the characterisation of polycyclic aromatic hydrocarbons from SRM 1648 and SRM 1649. In this report thirteen major PAH were quantified in each SRM using RP-LC with wavelength programmed FL detection and capillary column GC after isolation of the PAH fraction by normal-phase LC. Quantification of the minor PAH components was also achieved by separation of the total extracted PAH mixture into 10 subfractions using normal-phase LC. The PAH subfractions were then analysed using RP-LC, GC and GC-MS. Using such a multidimensional chromatographic approach over 180 PAHs are reported in the two SRMs.

The concentrations of the PAHs observed in SRM 1649 have been calculated by three different approaches. The first of these utilises the instrument control and data acquisition software which automatically calculates the PAH concentrations in the sample using previously obtained calibration data stored within the PC. The second and third methods are based on a ratio technique where the peak areas or peak heights were used to calculate

the concentrations of PAHs in SRM 1649 using the chromatographic data collected from the analysis of the EPA 16 priority pollutant mixture. The results of using each of these approaches are listed in Table 3.9 and are compared with concentration data supplied with the SRM 1649 certificate of analysis.

PAH	Concentration (mg kg ⁻¹)			
	1090 data	Peak areas	Peak height	SRM ^a
Naphthalene	1.5 ± 0.1	1.6 ± 0.1	1.2 ± 0.2	n/d
Fluorene	0.3 ± 0.1	0.3 ± 0.1	0.3 ± 0.1	n/d
Phenanthrene	3.4 ± 0.2	4.2 ± 0.2	3.2 ± 0.4	4.5 ± 0.3
Anthracene	n/d	n/d	n/d	n/d
Fluoranthene	5.1 ± 0.3	8.0 ± 0.4	5.1 ± 0.4	6.8 ± 0.4
Pyrene	6.0 ± 0.3	8.6 ± 0.2	5.3 ± 0.3	6.2 ± 0.2
Benzo[<i>a</i>]anthracene	2.9 ± 0.1	4.2 ± 0.2	2.2 ± 0.2	2.4 ± 0.1
Chrysene	5.7 ± 0.3	9.4 ± 0.4	5.2 ± 0.4	3.7 ± 0.2
Benzo[<i>b</i>]fluoranthene	4.7 ± 0.4	8.1 ± 0.4	4.8 ± 0.4	6.2 ± 0.3 ^b
Benzo[<i>k</i>]fluoranthene	1.4 ± 0.1	2.1 ± 0.2	1.5 ± 0.2	2.1 ± 0.1
Benzo[<i>a</i>]pyrene	3.1 ± 0.2	3.9 ± 0.2	2.6 ± 0.2	2.6 ± 0.1
Dibenz[<i>a,h</i>]anthracene	1.1 ± 0.1	1.4 ± 0.1	1.2 ± 0.2	0.41 ± 0.07
Indeno[<i>1,2,3-cd</i>]pyrene	0.8 ± 0.2	0.9 ± 0.2	0.9 ± 0.3	3.6 ± 0.2
Benzo[<i>g,h,i</i>]perylene	22.7 ± 0.8	17.9 ± 0.6	13.5 ± 0.9	5.2 ± 0.6

^a Results listed for analysis on SRM1649 using method LC-II

^b Results listed for analysis on SRM1649 using method LC-I

n/d PAH not detected or not listed as detected.

It can be seen from Table 3.9 that the values of the PAH concentrations observed in the extracted SRM 1649 sample were slightly different dependent on the method of calculation used. In most cases however the levels of PAHs calculated were relatively close to one another. In general the levels of PAHs observed within the extract were found to be similar to those reported on the certificate of analysis for SRM 1649. Significant exceptions to this were the three PAHs dibenz[*a,h*]anthracene, indeno[*1,2,3-cd*]pyrene and benzo[*g,h,i*]perylene. These three PAHs were the last to be eluted from the LC column in an area of the chromatogram where resolution between peaks was seen to diminish. The baseline observed during this stage of the chromatogram was also dropping off quite

rapidly which would also effect the quality of data collected. Table 3.8 shows that although the concentrations of certain PAHs within SRM 1649 are certified the reported PAH concentrations are clearly method dependent. The concentration differences reported for the different methods of analysis show no apparent trend. There may however be up to 10% difference for some of the more concentrated PAHs e.g. fluoranthene and greater still (>40%) for the less concentrated PAHs e.g. benzo[*a*]pyrene. The results reported throughout this chapter should therefore be considered in the light of these differences between reference methods as recorded on the certificates of analysis.

SRM 1650 (Diesel Particulate Matter)

Table 3.10 shows a summary of the results as supplied on the certificate of analysis for SRM1650. Certified values are based on the results obtained by two different analytical methods utilising 1g sample sizes. Non-certified values are provided for information only.

Compound	Concentration (mg kg ⁻¹)			
	GC-MS (EI)	GC-MS (NICI)	LC-FL	LC-EC
9-Fluorenone	33 ± 1			
Phenanthrene	79 ± 1		63 ± 2	
*Fluoranthene	48.5 ± 1	54.5 ± 1	49.8 ± 0.3	48.5 ± 1
*Pyrene	49.0 ± 0.7	49.0 ± 0.7	45.5 ± 1.7	49.0 ± 0.7
*Benz[<i>a</i>]anthracene	6.0 ± 0.1		7.1 ± 0.3	6.0 ± 0.1
Chrysene			22 ± 1	
Benzo[<i>e</i>]pyrene	9.6 ± 0.3			
*Benzo[<i>a</i>]pyrene	1.3 ± 0.1	0.9 ± 0.1	1.4 ± 0.1	1.3 ± 0.1
Indeno[<i>1,2,3-cd</i>]pyrene	1.8 ± 0.1	2.1 ± 0.1	3.2 ± 0.3	1.8 ± 0.1
*Benzo[<i>g,h,i</i>]perylene	2.3 ± 0.1	2.6 ± 0.1	2.4 ± 0.4	2.3 ± 0.1
Perylene			0.13 ± 0.02	
Benzo[<i>k</i>]fluoranthene			2.1 ± 0.2	
*1-Nitropyrene	19.9 ± 0.5	19.3 ± 0.6	19.9 ± 0.4	16.8 ± 0.6
6-Nitrobenzo[<i>a</i>]pyrene			1.6	

* indicates the compounds listed as certified values.

SRM 1650 was prepared from particulate matter collected from the heat exchangers of a dilution tube facility, following 200 engine hours of particle accumulation. The material was collected from more than one direct injection four-cycle diesel engine, operating under a variety of conditions. The sample is not meant to be representative of any particular diesel engine under any specific operating conditions, but should generally typify particulate matter emissions obtained from a heavy-duty diesel engine.

SRM 1650 (50.7 mg) was extracted by Soxhlet extraction and the extract dissolved in 5 ml propan-2-ol, then using the conditions described previously for the separation of a mixture containing 16 EPA priority pollutant PAHs, the SRM1650 sample extract was investigated using RP-LC with programmed FL detection. The chromatogram (Figure 3.11) and concentration data (Table 3.11) obtained from this separation shows that 7 of the 16 EPA priority pollutant PAHs were quantified in the extract.

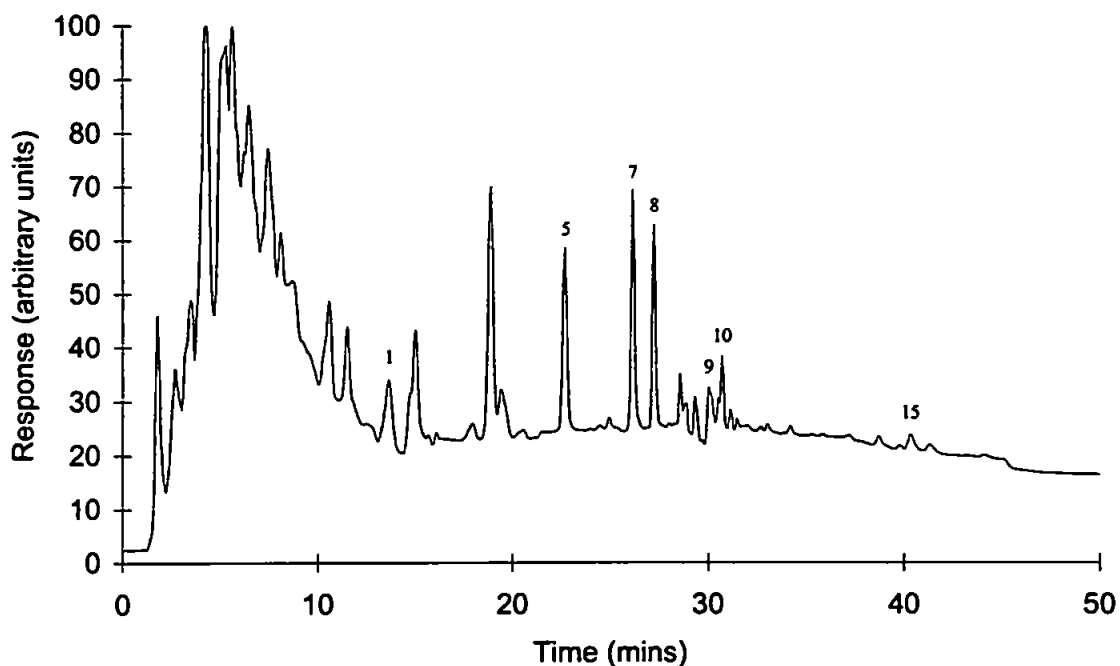


Figure 3.11. Chromatogram of SRM 1650 (Diesel Particulate Matter) using programmed FL detection.

It can be seen from Table 3.11 that the values of the PAH concentrations observed in the extracted SRM 1650 sample were slightly different dependent on the method of calculation used. In most cases however the levels of PAHs calculated were relatively close to one another. In general the levels of PAHs observed within the extract were found to be similar to those reported on the certificate of analysis for SRM 1650. Significant exceptions to this were the two PAHs benz[*a*]anthracene and chrysene. Both of these

peaks occur around about 30 minutes on the chromatogram in an area where several other unquantified PAHs elute. This has resulted in shoulders on the peaks that will effect the concentration calculations performed by the software and will also have influenced the peak areas/heights. Once again the data supplied with the certificate of analysis for SRM 1650 indicates that the concentrations of PAHs detected in an extract of SRM 1650 differ slightly dependent on the nature of the analytical procedure used to obtain the data. Small differences between experimental and reported figures would therefore be anticipated.

Table 3.11. Concentrations of PAHs found for SRM 1650 using LC-FL.				
PAH	Concentration (mg kg ⁻¹)			
	1090 data	Peak areas	Peak height	SRM ^a
Naphthalene	19.6 ± 2	18.9 ± 2	12.8 ± 3	n/d
Acenaphthalene	n/d	n/d	n/d	n/d
Fluorene	n/d	n/d	n/d	n/d
Phenanthrene	55.4 ± 3	52.4 ± 2	52.0 ± 4	63 ± 2
Anthracene	n/d	n/d	n/d	n/d
Fluoranthene	47.3 ± 2	47.8 ± 2	44.6 ± 3	49.8 ± 0.3
Pyrene	52.3 ± 1	50.7 ± 2	49.8 ± 2	45.5 ± 1.7
Benz[<i>a</i>]anthracene	33.2 ± 4	33.9 ± 2	17.9 ± 5	7.1 ± 0.3
Chrysene	48.5 ± 3	50.3 ± 2	43.3 ± 3	22 ± 1.0
Benzo[<i>b</i>]fluoranthene	n/d	n/d	n/d	n/d
Benzo[<i>k</i>]fluoranthene	n/d	n/d	n/d	2.1 ± 0.2
Benzo[<i>a</i>]pyrene	n/d	n/d	n/d	n/d
Dibenz[<i>a,h</i>]anthracene	n/d	n/d	n/d	n/d
Indeno[<i>1,2,3-cd</i>]pyrene	3.2 ± 1	3.2 ± 1	3.3 ± 1	3.2 ± 0.3
Benzo[<i>g,h,i</i>]perylene	n/d	n/d	n/d	2.4 ± 0.3

^a Results listed for analysis on SRM1650 using HPLC with FL detection
n/d PAH not detected or not listed as detected.

3.3.4. RP-LC analysis of PAH using POCL detection.

It has already been discussed how the presence of water in the mobile phase of flow systems effects the signal obtained during POCL detection. When the POCL system was used post-column for the analysis of PAHs by LC the baseline was observed to change as the water content of the gradient profile changed. Figure 3.12 shows the baseline obtained when the acetonitrile-water gradient was applied. As the percentage of water in the mobile phase dropped so the baseline level increased and the noise associated with the baseline decreased. Figure 3.12 shows that a direct correlation between the water content of the mobile phase and the baseline level/noise exists.

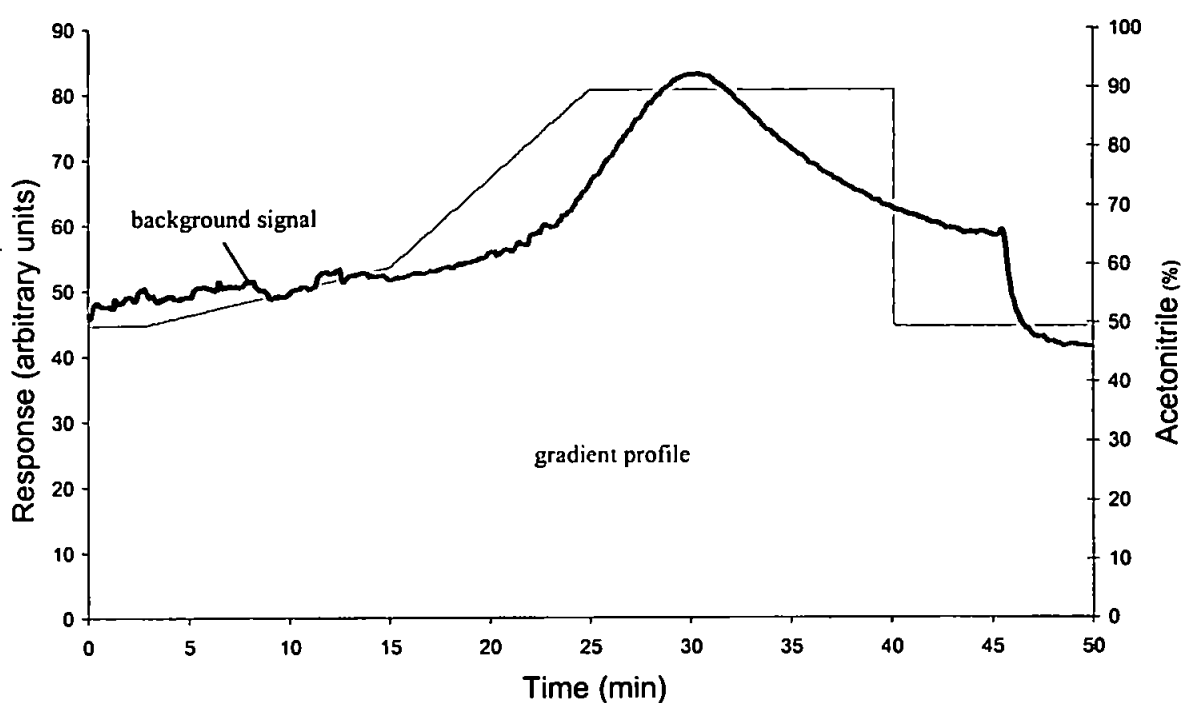


Figure 3.12. Chromatogram of background signal (blank) using RP-LC with post column POCL detection.

The analysis of a 16 PAH mixture showed that the POCL detection method was unable to detect all of the PAHs on the EPA priority pollutant list when applied post-column. Figure 3.13 shows the chromatogram obtained when 10 μl of a 1000 $\mu\text{g l}^{-1}$ solution containing 16 PAHs in ACN was injected into a RP-LC system. Table 3.12 shows the data associated with this chromatogram. From the chromatographic data it was seen that although the baseline was seen to shift it was still possible to observe peaks for some of the PAH compounds. Many of the earlier eluting PAHs have not been detected and this could be

due to the fact that a sufficiently large volume of water was present in the mobile phase that the POCL reaction was ineffective for PAH detection.

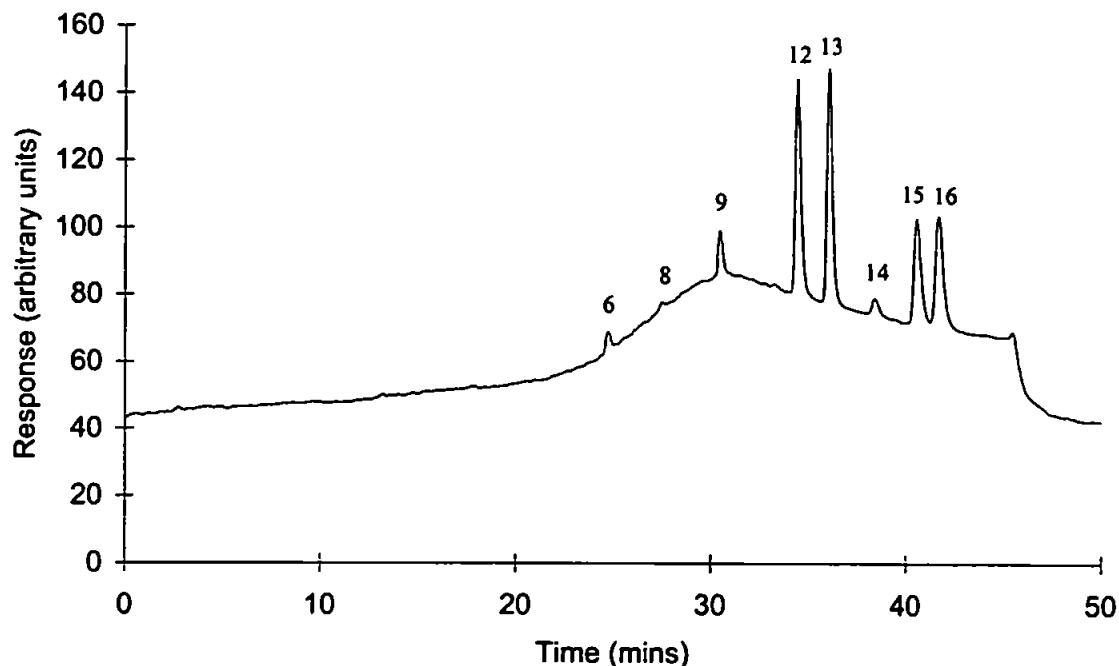


Figure 3.13. Chromatogram of 16 PAH test mixture using post column POCL detection.

PAH		Response		
Peak No.	Name	Ret. Time (min)	Peak Area (arbitrary units)	Peak Height (arbitrary units)
6	Anthracene	24.7	110	6
9	Benz[<i>a</i>]anthracene	30.4	246	14
12	Benzo[<i>k</i>]fluoranthene	34.4	1306	65
13	Benzo[<i>a</i>]pyrene	36.0	1344	70
14	Dibenz[<i>a,h</i>]anthracene	38.3	113	5
15	Indeno[<i>1,2,3-cd</i>]pyrene	40.5	827	32
16	Benzo[<i>g,h,i</i>]perylene	41.7	942	33

The chromatogram produced by the analysis of an extract of SRM 1649 can be seen in Figure 3.14. From this chromatogram it can be seen that only 4 of the 16 EPA priority pollutant PAHs were detected by the POCL system. This is compared with 14 of the 16 PAHs that were detected using the wavelength programmed FL method.

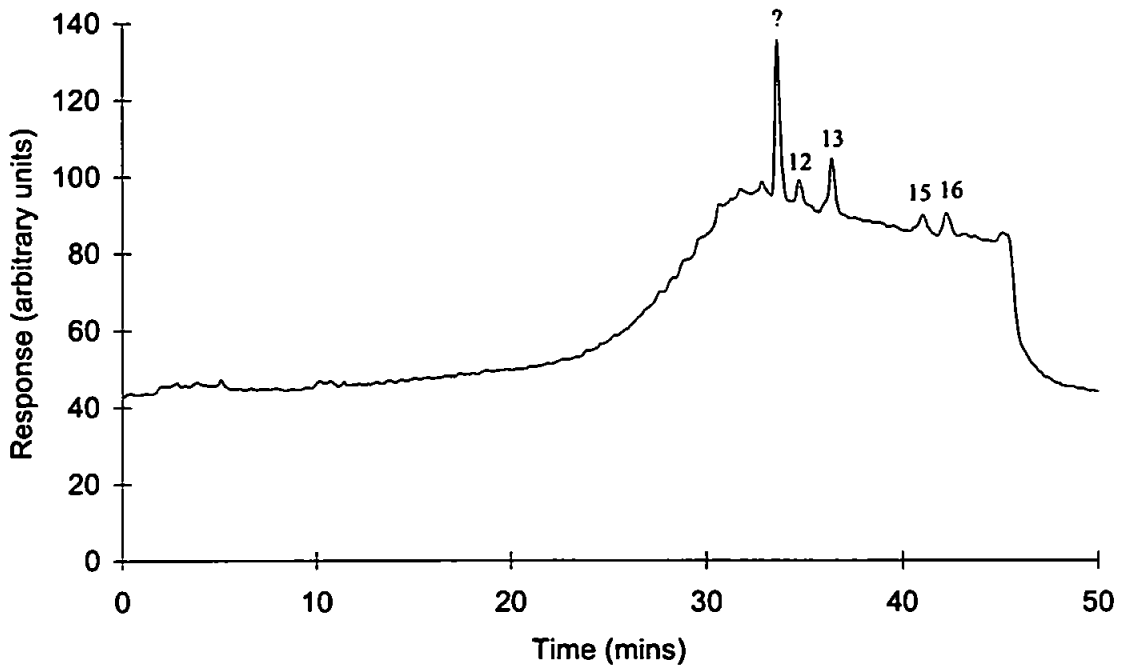


Figure 3.14. Chromatogram of SRM 1649 (Urban Dust Organic Extract) using post column POCL detection.

Table 3.13. Response data for the five PAHs detected in SRM 1649 using post column POCL detection.				
PAH		Response		
Peak No.	Name	Ret. Time (min)	Peak Area (arbitrary units)	Peak Height (arbitrary units)
?	Unknown	33.6	760	42
12	Benzo[<i>k</i>]fluoranthene	34.7	169	7
13	Benzo[<i>a</i>]pyrene	36.4	378	15
15	Indeno[<i>1,2,3-cd</i>]pyrene	41.0	95	4
16	Benzo[<i>g,h,i</i>]perylene	42.3	148	6

Table 3.13 shows the retention data together with the peak areas and peak heights for the POCL chromatogram. From this data and the chromatogram (Figure 3.14) it was observed that an unknown compound showing good CL response was eluted after 33.6 minutes. It is thought that this peak was most probably due to the presence of perylene, which is found in the SRM but was not present in the 16 PAH mixture analysed previously. Perylene has already been shown to be very sensitive to POCL detection and has been reported as having a retention time between that of benzo[*b*]fluoranthene and benzo[*k*]fluoranthene [261]. During this investigation benzo[*b*]fluoranthene and benzo[*k*]fluoranthene had retention times of 33.0 and 34.2 minutes respectively, and so the peak at retention time 33.6 minutes would fit the theory that perylene was responsible. In order to confirm this a standard would be required containing perylene so that unambiguous identification could be obtained.

Using a ratio technique the concentrations of the PAHs responsible for producing the peaks in the chromatogram were calculated and are listed in Table 3.14. It can be seen from this table that the results are of a similar value whether peak area or peak height is used to calculate the concentration. Two of the PAHs are in good agreement with the values expected from the SRM, but the PAHs indeno[*1,2,3-cd*]pyrene and benzo[*g,h,i*]perylene were not so accurate. As described previously this can be attributed to the differences between analysis routines used for the experimentally and literature derived data.

Table 3.14. Concentrations of PAHs found for SRM 1649 using LC-CL.			
PAH	concentration (mg kg ⁻¹)		
	Peak areas	Peak height	SRM ^a
Benzo[<i>k</i>]fluoranthene	1.4 ± 0.1	1.2 ± 0.2	2.1 ± 0.1
Benzo[<i>a</i>]pyrene	2.3 ± 0.1	1.9 ± 0.2	2.6 ± 0.1
Indeno[<i>1,2,3-cd</i>]pyrene	1.1 ± 0.1	1.4 ± 0.1	3.6 ± 0.2
Benzo[<i>g,h,i</i>]perylene	1.8 ± 0.1	1.8 ± 0.2	5.2 ± 0.6

^a Results listed for analysis on SRM1649 using method LC-II

The chromatogram produced by the analysis of an extract of SRM 1650 showed no apparent peaks. The data produced by the acquisition software indicates that only very small responses were recorded for 4 of the PAHs previously analysed in the 16 PAH mixture. The data produced by the instrument software has been summarised in Table 3.15.

PAH		Response		
Peak No.	Name	Ret. Time (min)	Peak Area (arbitrary units)	Peak Height (arbitrary units)
12	Benzo[<i>k</i>]fluoranthene	34.7	21.2	1.3
13	Benzo[<i>a</i>]pyrene	38.8	10.5	0.9
15	Indeno[<i>1,2,3-cd</i>]pyrene	41.0	25.8	0.8
16	Benzo[<i>g,h,i</i>]perylene	42.3	31.3	1.1

This data was subjected to a ratio calculation in order to obtain the concentrations of PAHs in the SRM 1650 extract analysed using RP-LC coupled with POCL detection (Table 3.16.). The data shows that only small amounts of PAHs were detected in the SRM 1650 extract but the figures obtained were in good agreement to those reported on the certificate of analysis.

PAH	concentration (mg kg ⁻¹)		
	Peak areas	Peak height	SRM
Benzo[<i>k</i>]fluoranthene	1.8 ± 0.1	2.3 ± 0.2	2.1 ± 0.2
Dibenz[<i>a,h</i>]anthracene	5.8 ± 0.2	9.9 ± 0.3	-
Indeno[<i>1,2,3-cd</i>]pyrene	3.0 ± 0.2	2.8 ± 0.2	3.2 ± 0.3
Benzo[<i>g,h,i</i>]perylene	3.8 ± 0.2	3.5 ± 0.3	2.4 ± 0.4

3.3.5. NP-LC analysis of PAH using POCL detection.

An investigation using a normal phase column was performed in order to ascertain whether more PAH compounds could be detected post-column if the problems associated with the ACN/water gradient were eliminated. In order to achieve this a normal phase column (Hypersil Green PAH-2) was substituted for the reversed phase LiChrospher PAH column.

Separations on Hypersil Green PAH-2 stationary phase are based upon the highly specific electron transfer properties of the bonded phase. The mechanism is based on the strong delocalisation of electrons between the stationary phase and the PAH analyte. As PAHs are electron donors, an electron donor-acceptor complex can be formed with a chemically bonded electron-acceptor stationary phase. The stationary phase used in such PAH columns is a tetrachlorophthalimidopropyl bonded silica (Figure 3.15), which is suitable for both analytical and preparative purposes.

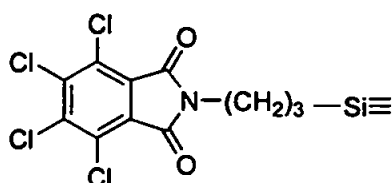


Figure 3.15. Structure of the tetrachlorophthalimidopropyl bonded silica support.

Table 3.17. shows the gradient elution programme that was set up with heptane and 1,2-dichloroethane using the Hypersil PAH-2 column. This was then used to analyse the 16 PAH mixture previously described during the RP-LC investigations.

Time (min)	Heptane (%)	1,2-Dichloroethane (%)
0.0	100	0
5.0	100	0
15.0	85	15
25.0	85	15
25.1	100	0
30.0	100	0

Figure 3.16 shows the chromatogram obtained from the normal phase separation of the 16 PAH mixture using POCL detection. The peaks have been identified by the use of a UV diode array detector, which was connected in series with the CL detection system.

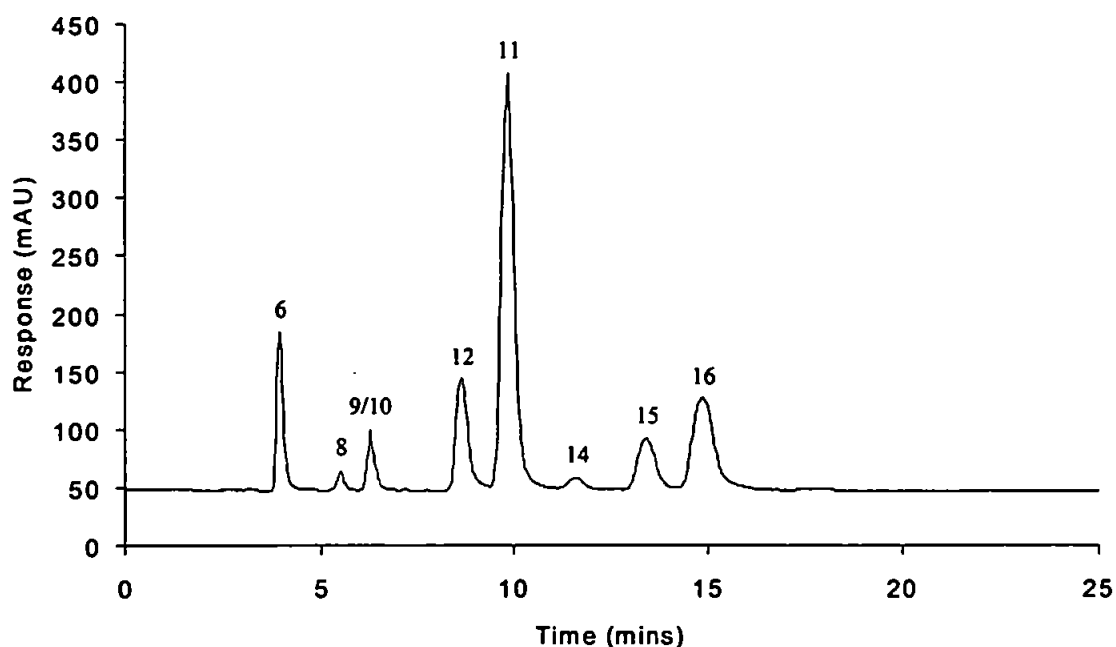


Figure 3.16. Chromatogram of 16 PAH test mixture using NP-LC and CL detection.

PAH		Response		
Peak No.	Name	Ret. Time (min)	Peak Area (arbitrary units)	Peak Height (arbitrary units)
6	Anthracene	3.9	1659	137
8	Pyrene	5.5	158	10
9	Benz[<i>a</i>]anthracene	6.3	570	31
10	Chrysene	6.3	570	31
12	Benzo[<i>k</i>]fluoranthene	8.6	2124	82
11	Benzo[<i>b</i>]fluoranthene	9.8	7381	252
14	Dibenz[<i>a,h</i>]anthracene	11.6	326	8
15	Indeno[<i>1,2,3-cd</i>]pyrene	13.4	1451	36
16	Benzo[<i>g,h,i</i>]perylene	14.9	3158	63

Table 3.18 lists the retention and response data for the NP-LC system. The NP-LC approach does not produce the shift in baseline that was observed for the RP-LC method because the chromatographic system is free of the aqueous phase that caused the baseline problems. It was therefore possible to detect a greater number of the PAHs from the 16 PAH mixture. The CL responses for the PAHs detected were also observed as being greater than in the RP-LC system. The sensitivity increase observed for the NP system was due in part to the reduced baseline effects but also because of the change in solvent characteristics of the mobile phase being used. The greater sensitivities recorded for the PAHs in the normal phase system are due to the lower polarity of the mobile phase (1,2-dichloroethane and heptane), compared with that of the RP gradient (ACN and water), which resulted in reduced radiationless losses from the excited state PAH species. The batch results for the fluorescence investigations showed a similar response change in *section 2.3.1*.

3.3.5. Comparison of the detection systems.

A comparison between the different approaches to PAH separation addressed during this investigation has revealed that FL methods are more suited to PAH detection after RP-LC separations. Unlike FL detection, the CL method was subjected to interference problems associated with the acetonitrile/water gradient. Quantification of all but one of the 16 PAHs was possible with the RP-LC FL system compared with only 7 PAHs using CL detection. The analysis of SRMs showed good agreement with reported values for both FL and CL methods.

The use of NP-LC increased the number of PAHs that were quantified in the 16 PAH mixture but still only 9 PAHs could be detected. As a laboratory based procedure RP-LC with FL detection is therefore recommended as the best technique for the quantification of PAHs in the matrices investigated.

Despite these findings the use of a CL detection system should not be discounted, particularly for a field deployable unit that could be used for rapid screening purposes in order to make quick assessments of selected PAH concentrations. Among the attractions of the CL detection system one has to consider the simplicity and low cost technologies involved compared with a programmable FL detector. However, in real matrices PAHs do not exist as single entities and therefore some form of characterisation between isomers would still be a requirement of any method developed.

3.4 CONCLUSIONS

1. Reversed phase LC has been shown to provide a suitable method for the separation of PAH mixtures. From the three columns investigated (Spherisorb S5 PAH, LiChrospher PAH, and Envirosep-PP) it was shown that the LiChrospher PAH column provided the best separations of the 16 PAH test mixture.
2. Wavelength programmed fluorescence detection has been shown to provide an excellent technique for the sensitive detection of PAHs after chromatographic separation and has shown good agreement with SRM1649 and SRM1650 certified values.
3. Post column POCL detection has been applied to the analysis of PAHs after reversed phase and normal phase LC separations. It was observed that problems due to the water content of the mobile phase gradient for the reversed phase system severely hampered the detection of PAHs at environmentally significant levels.
4. Normal phase chromatography (Hypersil Green PAH-2) was shown to offer some improvement for the analysis of PAHs by LC using POCL detection because the absence of water from the mobile phase gradient provided a more stable baseline.

CHAPTER 4

*Determination of PAHs using
multivariate calibration with fluorescence
and chemiluminescence detection*

4. DETERMINATION OF PAHs USING MULTIVARIATE CALIBRATION WITH FL AND CL DETECTION

4.1 INTRODUCTION

The development of computer-controlled laboratory instrumentation and array detectors has provided the analytical chemist with ever larger and more complex data sets. As a result of this, increasingly sophisticated mathematical and statistical methods have been required to derive useful information from such data. This trend first became apparent in the early 1970s with the introduction of techniques such as pattern recognition and multivariate statistics [262]. In 1972 the term 'chemometrics' was proposed by the Swedish physical organic chemist, Svante Wold, as a generic name for the discipline of chemistry in which mathematical and statistical techniques are used for the purposes of optimising experimental design procedures and maximising the information obtainable from analytical data [263-264]. Since that time, chemometrics has expanded into a very prominent area of chemical research, and a growing number of textbooks [263, 265-269] and two specialist journals (*Journal of Chemometrics*, Elsevier, *Chemometrics and Intelligent Laboratory Systems*, Wiley) are now available.

One of the most important applications of chemometrics in the field of analytical chemistry is multivariate calibration [270-271], which can be applied to the quantification of single or multiple analytes when more than one data points are acquired for each sample (*i.e.* multivariate data). This is particularly appropriate in the case of multiwavelength spectroscopic techniques.

Fluorescence spectroscopy is one of a number of analytical techniques to which multivariate calibration routines can be applied. Results from a previous chapter (*section 2.3.2.*) showed that each PAH investigated had characteristic excitation and emission spectra. The spectrum for each PAH was studied and in each case, only a single value for the maximum response was used to build a univariate calibration model. This approach is subject to interference problems with real samples and so separation of individual PAH components is required (*section 3.3.3.*). The remainder of the spectrum however is rich in information that can be used if the data is examined using a multivariate approach. This potentially allows the quantification of simple mixtures of PAHs without the need for prior physical separation if suitable calibration models can be constructed.

Two-dimensional charge coupled devices (CCDs) are particularly suitable as CL detectors because they are capable of high spatial resolution and sensitivity across the UV, visible and near-IR spectral range. They also have a low dark current and provide a wide linear response range [272], while the signal-to-noise ratio can be further improved by integrating the response over time. The FI-CL-CCD combination therefore offers the advantage of a robust yet sensitive analytical system, thus increasing the possibility of being utilised as a field technique. The enhanced information content from the CCD detector allows the possibility of using multivariate calibration routines to provide selectivity without the need for separation.

This chapter describes an investigation of the application of multivariate calibration routines to FL and CL emission data sets of selected PAH compounds. The accuracy in determining the concentration of PAHs in simple multicomponent systems is discussed.

4.2 EXPERIMENTAL

4.2.1 Reagents

Working PAH solutions and the chemiluminescence reagents (*section 2.2.1*) were prepared as previously described. All solutions were degassed by sonication for two minutes prior to use.

4.2.2 Instrumentation and procedures

FL instrumentation and software

All FL spectra were obtained using a fluorescence spectrophotometer (Hitachi F-4500, Hitachi Ltd., Tokyo, Japan) fitted with a 1 cm pathlength quartz cuvette. The settings used are shown in Table 4.1.

FL data acquisition was achieved using Hitachi F-4500 control and data acquisition software (Hitachi Ltd., Tokyo, Japan). Multivariate calibration routines were performed using The Unscrambler version 6.1 multivariate analysis software package (Camo AS, Trondheim, Norway).

Scan speed	1,200 nm min ⁻¹
Em start/Em end	360 nm/500 nm
Slit (Ex/Em)	5.0 nm/5.0 nm
Sampling interval	0.2 nm
PMT Voltage	700 V

FL Procedures

A 5² factorial design was used to produce a 25-sample calibration set in acetonitrile for a 2-component system, comprising anthracene and benzo[*k*]fluoranthene in the range 0-4.0 mg l⁻¹. A separate test set of 10 samples was produced using randomised combinations within the same concentration range.

Similarly a 3³ factorial design was used to produce a 27-sample calibration set in acetonitrile for a 3-component system, comprising anthracene, benzo[*k*]fluoranthene and benzo[*a*]pyrene in the range 0-4.0 mg l⁻¹. A 2⁴ factorial design was used to produce 16-sample calibration and test sets in acetonitrile for a 4-component system comprising anthracene, benzo[*k*]fluoranthene, benzo[*a*]pyrene and fluoranthene, in the range 0-4.0 mg l⁻¹. A 2⁵ factorial design was used to produce 32-sample calibration and test sets for a 5-component system comprising anthracene, benzo[*k*]fluoranthene, benzo[*a*]pyrene, fluoranthene and chrysene, in the range 0-4.0 mg l⁻¹. Test sets were then produced as detailed in Table 4.2. using randomised combinations within the same concentration range (concentration data tables shown in Appendices 1-5).

PAH mixture	Factorial design	No. of calibration samples	No. of test set samples
2 PAHs	5 ²	25	10
3 PAHs	3 ³	27	15
4 PAHs	2 ⁴	16	16
5PAHs	2 ⁵	32	32

In all cases, spectra were measured at 0.2 nm intervals over the range 360-500 nm. Each solution was measured in triplicate and the triplicate sets were averaged to produce a mean spectrum. Multiple spectra were obtained for each solution by measuring at the optimum excitation wavelength, as experimentally determined previously (*section 2.3.1*), for each individual PAH in the sample solution (*e.g.* 3 spectra per sample for each 3-component sample). The multiple spectra were then joined end-to-end in continuous series to produce a single 'spectrum' for each sample solution, ensuring that each spectral set was joined together in the same order. This process of spectral 'gluing' is illustrated in Figure 4.1.

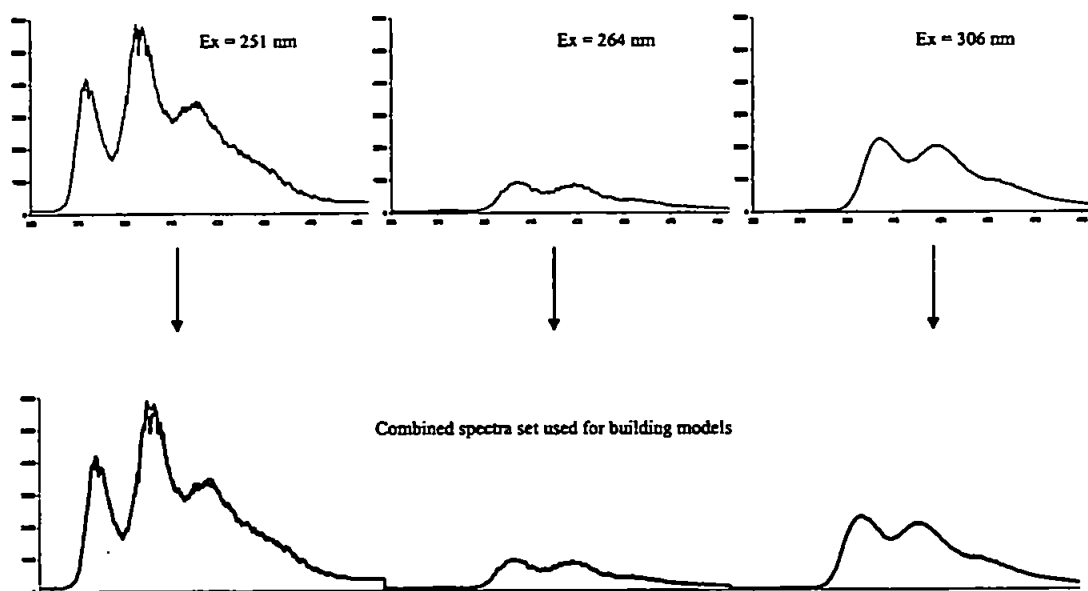


Figure 4.1. Schematic to show the process of joining spectra together in series.

The combined spectra were then imported into Unscrambler, in ASCII format, where multivariate calibration models were constructed and then used to predict PAH concentrations in the corresponding test set samples.

CCD based continuous flow manifold for CL detection

A Spex Spectrum One charge coupled device detection system (256 × 1024 pixel array cooled to 140 K by liquid nitrogen) with Spex 270M imaging spectrograph (600 g mm⁻¹ grating; Instruments S.A., Edison, New Jersey, USA) was used to obtain CL spectra in the range 380-500 nm for all samples. A continuous flow manifold (Figure 4.2) was constructed by modification of the FI manifold described previously (*section 2.2.2*).

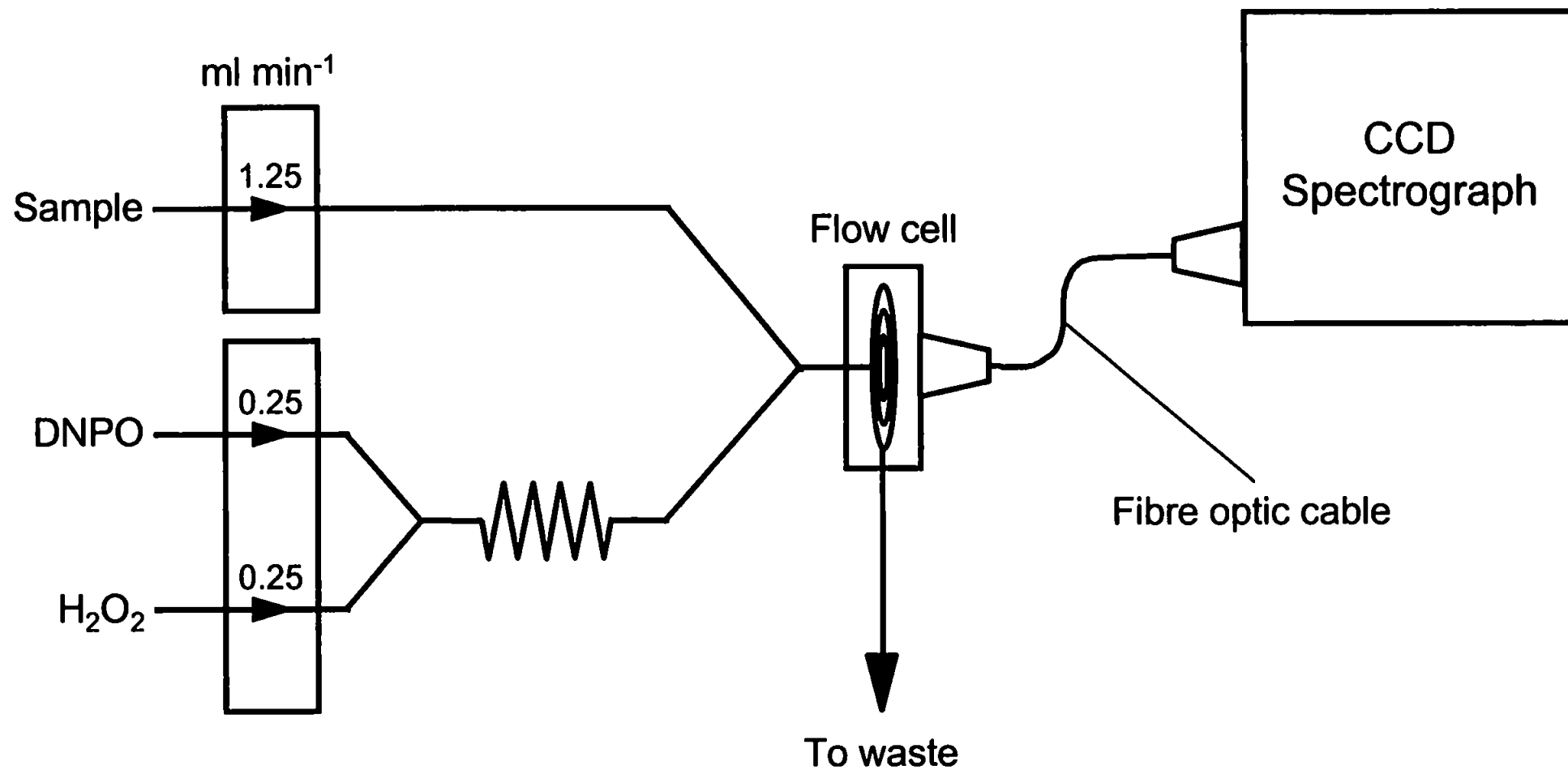


Figure 4.2. Schematic diagram of the continuous flow manifold used for CL-CCD determination of PAHs.

In this case, the flow cell was a quartz-glass coil (240 μ l) housed within a light-tight aluminium case (in-house design and construction). Emitted light was focused onto a 1 m quartz fibre optic cable (18 fibre bundle; 1.0 mm i.d.; Instruments S.A.) leading to the CCD spectrograph.

CCD data acquisition was achieved using Jobin-Yvon/Spex Spectramax version 1.1d spectroscopic acquisition and analysis software (Instruments S.A.). Multivariate calibration routines were performed using The Unscrambler version 6.1 multivariate analysis software package (Camo AS, Trondheim, Norway).

CL Procedures

The CCD system was used to obtain chemiluminescence spectra for pure solutions of all five PAH compounds in both acetonitrile and hexane in order to examine the effect of solvent on the spectral response. Spectra were acquired at 0.15 nm intervals to produce 801 data points per spectrum. Each solution was measured in triplicate against a solvent blank, using an integration time of 50 s, and the triplicate sets were averaged to produce a mean spectrum.

A calibration set was designed for a two-component system in hexane, comprising benzo[*k*]fluoranthene and benzo[*a*]pyrene in the range 0-2.0 mg l⁻¹. A five-level factorial design (5²) was used to produce a full set of 25 samples, with the order of measurement randomised to reduce the risk of obtaining biased results. A set of 10 test solutions was produced using a randomised combination of concentrations in the same range as the calibration set (Appendix 6). Multivariate calibration models were constructed using the spectral data obtained for the two-component calibration set. These were then used to predict PAH concentrations in the test set samples. Mean centring was applied to all variables used for calibration.

Detection limits were determined for benzo[*k*]fluoranthene, benzo[*a*]pyrene and perylene in hexane solution, using the CCD based continuous flow system.

4.3 RESULTS AND DISCUSSION

4.3.1 Data pre-processing techniques

Raw experimental data may have a distribution that is not suitable for mathematical analysis, i.e. the variance in the raw experimental data does not adequately describe the variance in the system under observation. Background effects, different units of measurement and poor resolution are all examples of limitations to the quality of meaningful information acquired from an experiment. Manipulation of the original data using data pre-processing techniques reduces the noise (not analytically useful information) from such effects to provide enhanced information recovery. The main types of pre-processing applied to spectral data in this investigation are described below.

Mean Centring

The most common form of data pre-processing is mean centring. This involves the subtraction of the mean spectrum for the data set from each individual spectrum [273]. The main reason for centring the data is to prevent data points that are farther from the origin from exerting any undue leverage over points in close proximity to the origin. Thus mean centring ensures that the mean is placed at the origin and that principal components can therefore pass through and describe the total variance in the response variables. Origin centring, another alternative, is only used where a linear relationship that is known to pass through the origin exists between the variables.

Smoothing

Smoothing is beneficial where response variables are subject to underlying noise. Two smoothing algorithms are commonly applied.

- **Moving average:** is a classical smoothing method in which each observation is replaced with an average of the adjacent observations (including itself). The number of observations on which to average is a user-defined parameter.
- **Savitsky-Golay:** equivalent to a zero order derivative in which a polynomial line is fitted to each successive curve segment of n response variables within a user-defined window,

thus replacing the original values with more regular variations.. The advantage of Savitsky-Golay smoothing over the moving average filter is that the amount of signal distortion that results from use of the latter is reduced.

Derivatisation

Derivatisation techniques are commonly used for the resolution of partially overlapping peaks in spectroscopy and can therefore be thought of as a form of resolution enhancement. The process of derivatisation sharpens the spectral peaks, but unfortunately this is offset by the amplification of noise. In order to overcome this increase in noise a smoothing method is often used simultaneously with derivatisation producing a combined technique.

4.3.2 Multivariate calibration routines

Multivariate and univariate calibration are similar insofar as they both involve the construction of a calibration model relating instrumental response to analyte level for a set of known standards, and use this model to predict analyte levels in new samples. As the name implies however, multivariate calibration incorporates multiple instrumental measurements of each sample (*e.g.* the spectral data obtained by multiwavelength spectrometers) into the calibration model.

Multivariate calibration has two significant advantages over a univariate approach. Firstly, multivariate instrumental response can be related to the levels of more than one analyte in a sample, thereby enabling simultaneous determination of multiple sample components. Secondly, it follows that instrumental response does not have to be selective for only one analyte, and complete separation of the analyte(s) of interest is therefore unnecessary. In addition, errors produced in the instrumental response of new samples by interferences not present in the calibration standards can be detected, and the sample rejected as an 'outlier' [274].

The mathematical tools for modelling can be divided into two types of approach: inverse least squares and factor analysis. The main difference between the traditional inverse least squares approach and factor analysis methods is that no data reduction occurs for inverse least squares, unlike the procedure by which the factor analysis methods extract factors, which are often fewer in number for suitable model development than the original

dimension of the data set. The extraction of descriptive factors is often more beneficial than the use of the data in its entirety, since this may prevent overfitting of the data, which is often seen with the use of inverse least square methods. In this work two factor analysis approaches have been investigated and are discussed below.

Principal components regression

Principal components regression (PCR) is a method of calibration derived from factor analysis, which describes patterns in large data sets in terms of a much smaller number of underlying factors (*i.e.* reduces the dimensionality of the data set) [275]. Factors are linear combinations of the original variables that describe correlations within the data set. The method of factor analysis most frequently used in chemistry is principal components analysis (PCA) [276-277].

When spectroscopic data is used there can be hundreds or thousands of measured variables for each sample, with many responses being interrelated, *i.e.* many of the variables are correlated, such that the analysis of the variables individually often yields incoherent and impractical results. PCA assumes that concentration is a function of instrumental response, although in this case the problem of colinearity is overcome by decomposing the response matrix *A* into its most dominant factors, or 'principal components' (PCs), as they are also termed. The first PC is that which best describes the variability within the matrix, while the second and subsequent PCs successively describe the remaining variance, with the proviso that each PC is orthogonal (*i.e.* perpendicular) to the previous one. Projection of the original data onto each PC produces a matrix of PC scores, which are then regressed using a multiple linear regression procedure.

Partial least squares regression

Partial least squares (PLS) regression is a similar technique to PCR, and is based upon a decomposition of original, full-spectrum data into dominant factors. Unlike PCR however, PLS involves simultaneous analyses of both the response and the concentration matrices to calculate scores and loading vectors for each. In this way, it is able to determine which factors in the response matrix are most relevant to variance in the concentration matrix, thereby reducing the influence of irrelevant factors upon the calibration model [278-280].

The technique of PLS was first introduced in 1977 and, in analytical chemistry, it is increasingly being applied to the calibration of multicomponent spectroscopic data, particularly UV-visible [281-282], NIR [283-284] and FT-IR [285].

Two forms of the PLS algorithm are commonly applied in chemometrics [286]. The first is PLS 1, which performs calibration and prediction with respect to one analyte only (i.e. a separate calibration model is required for each analyte in the sample set). An alternative method is PLS2, in which modifications to the algorithm used for PLS 1 permit two or more analytes to be modelled simultaneously. In practice, PLS2 can represent the most convenient and rapid method of calibration and prediction in cases where the sample matrix is complex and the calibration set is large. However, PLS 1 tends to provide more accurate predictions for multicomponent samples, since PLS2 is restricted to a single optimal number of factors to represent all the components, and in many cases the optimal number is found to be different for each individual component.

The precision of each multivariate calibration technique is expressed here in terms of the relative root-mean-square error of prediction (RRMSEP), as shown in equation 1:

$$\text{RRMSEP (\%)} = \frac{100}{\bar{y}_j} \sqrt{\sum_{i=1}^I \frac{(y_{ij} - \hat{y}_{ij})^2}{I}} \quad (1)$$

$$\text{PRESS (\%)} = \sum_{i=1}^I (y_i - \hat{y}_i)^2 \quad (2)$$

where \bar{y}_j = the true concentration mean of component j in the test set, I = the number of samples in the set, y_{ij} = the true concentration of component j in sample i , and \hat{y}_{ij} = the predicted concentration of component j in sample i .

The optimal dimensionality of the calibration models is defined either as that corresponding with the first local minimum in the value of the prediction error sum of squares (PRESS), which is defined in equation 2, or as the fewest number of principal components (PCs) yielding a value of PRESS not significantly greater, by using an F -statistic comparison ($\alpha = 0.05$), than the minimum PRESS [278].

Interpretation of Results

Throughout the modelling process it is extremely important to examine the results at each stage. This allows for the early detection of outliers and for the development of a more robust model, which in turn leads directly to more confident predictions. The output from most multivariate calibrations can be summarised as: -

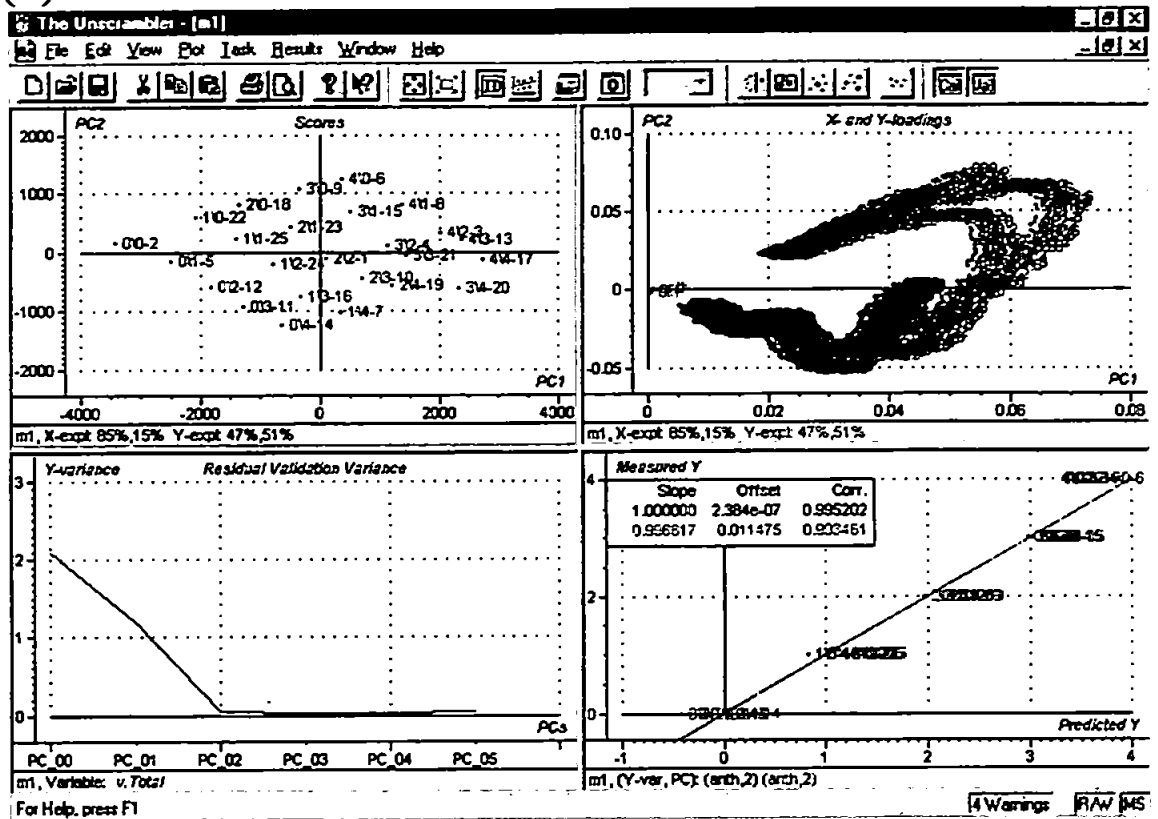
1. **Scores:** show the locations of the samples along each model component, and can be used to detect sample patterns, groupings, similarities or differences.
2. **Loadings:** show how well a variable is taken into account by the model components. These can be used to understand how much each variable contributes to the meaningful variation in the data, and to interpret variable relationships.
3. **Loading Weights:** show how much each predictor contributes to explaining response variation along each model component.
4. **Regression coefficients:** are the numerical coefficients that express the link between variation in the predictors and variation in the response (i.e. which variables are important to the model).

The above criteria provide graphical and numerical outputs from which the raw analytical data can be converted into useful information by selection of suitable approaches.

When Unscrambler completes the calculation of a PLS or PCR the user is presented with four graphs as shown in Figure 4.3.a. They are a scores plot (factor 1 or PC1 versus factor 2 or PC2), a loadings plot (PC1 versus PC2), an actual versus predicted plot (for calibration and validation data) and a residual standard deviation versus PCs in the calibration.

In this thesis however two different plots have been used in place of the loadings and actual versus predicted plots (see Figure 4.3.b.). The new plots are those suggested by Davies [287-288] and are plots of loading weights for each PC used in the optimum regression and an influence plot. An influence plot is a measure of residual y variance versus leverage, which is a statistic measuring the relative importance of each sample to the calibration.

(a)



(b)

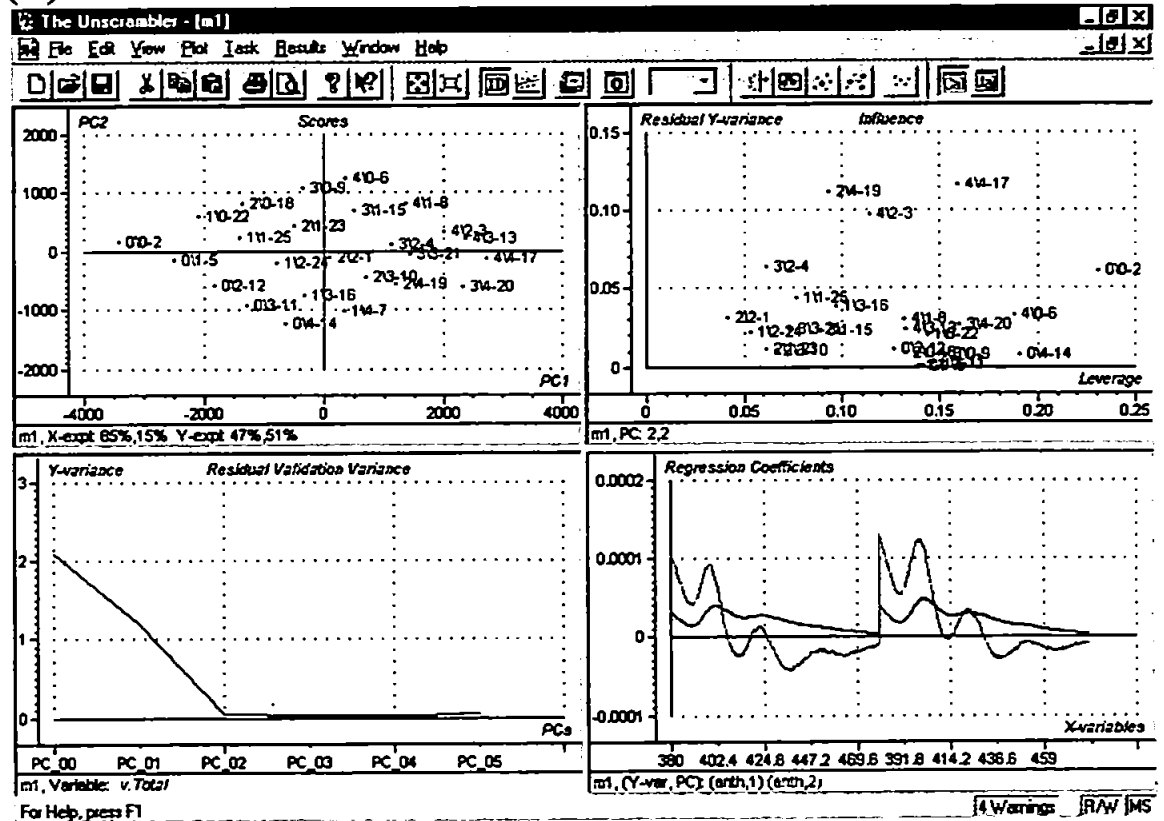


Figure 4.3. Display of regression overview
(a) standard Unscrambler overview (b) preferred overview used

From the scores and influence plots one can determine whether there are any outliers in the model. For a factorial design a good data set will lead to formation of a square shaped distribution on the scores plot. Outliers may be detected by spotting any marked deviations from the square shaped distribution. A true outlier will also be shown to exhibit either high variance or high leverage, indicated by the influence plot. The residual standard deviation (residual variance) versus PCs plot indicates how much variation in the data remains to be explained once the current PC has been taken into account and therefore defines the importance of each principal component. Finally, the loading weights plot shows the relationship between the specified component and the different X-variables. If a variable has a large positive or negative loading, this means that the variable is important for the component. This plot can be used to examine whether the number of PCs used in the model is necessary or if some overfitting and therefore modelling of noise is being performed.

These plots were used to evaluate the models produced using the experimental data obtained and will be referred to as and when required throughout the remainder of this discussion.

4.3.3 FL Investigation

The PAHs used for the FL investigations were selected because they had been shown to possess sufficiently different excitation and emission profiles (*section 2.3.1.*) to provide a reasonable, but not impossible, test for the approach. A summary of the λ_{Ex} and λ_{Em} wavelengths used to obtain data for the multivariate calibration modelling routines (unless otherwise stated) are given in Table 4.3.

PAH	λ_{Ex} (nm)	λ_{Em} (nm)	I_F (arbitrary units)
Anthracene	250	400	7132
Benzo[<i>k</i>]fluoranthene	306	408	3824
Benzo[<i>a</i>]pyrene	264	404	2311
Fluoranthene	286	461	409
Chrysene	267	381	1201

The excitation values used for the acquisition of emission spectra for the PAH mixtures were those identified as optimal in a previous chapter (*section 2.3.1.*), with the exception of benzo[*k*]fluoranthene for which 306 nm was used in place of 247 nm. This was because the optimum excitation wavelength (247 nm) overlapped with that of anthracene (250 nm). From earlier data (*section 2.3.1.*) it can be seen that 306 nm was the second most efficient wavelength for excitation as shown in Figure 2.3.(a).

Two-component system

RRMSEPs for the two-component FL system are represented as bar charts in Figure 4.4. and Figure 4.5. From these bar charts it can be seen that there are no significant differences observed between the overall precisions when determined using the PCR, PLS1 and PLS2 calibration routines. Figure 4.4. illustrates the degree of predictive accuracy that was obtained when only one wavelength (250 nm) was used for excitation of the two component PAH mixture.

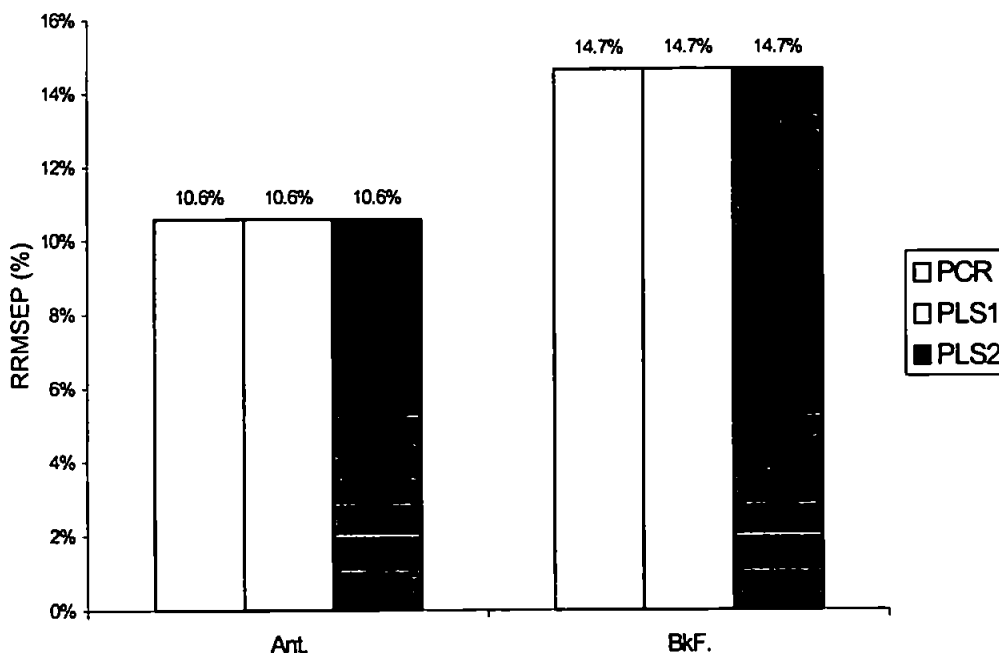


Figure 4.4. Prediction errors for the two-component system using single wavelength (250 nm) excitation method.

As a comparison, Figure 4.5 shows that a slightly better degree of predictive accuracy was obtained if the two component mixture was measured at two independent excitation wavelengths and the spectra thus obtained were ‘glued’ in series before undergoing any

statistical analysis. It should be noted in this case however that the differences in the degree of predictive precision were minimal between the two approaches because the optimum wavelengths for excitation of the two PAHs in the mixture were very similar.

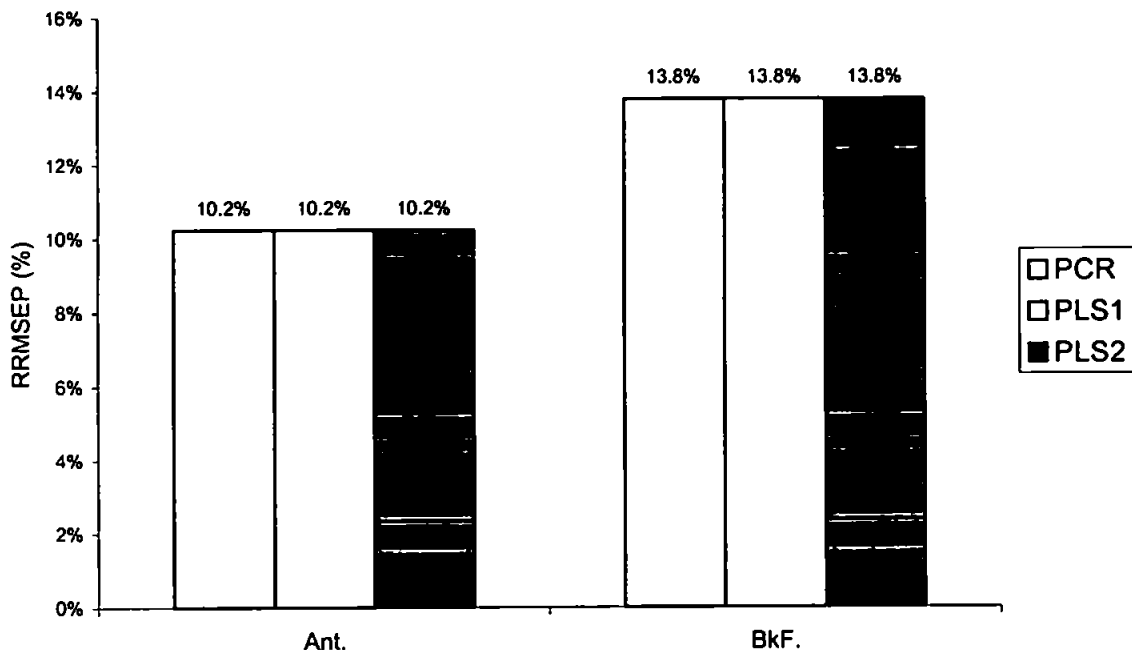


Figure 4.5. Prediction errors for the two-component system using dual wavelength (250 nm and 306 nm) excitation method with spectral gluing.

From a qualitative inspection of the excitation and emission spectra shown in Figure 2.3.(a)-2.3.(c) one would have expected a better level of predictive accuracy than that determined. The poor results of this two component system, however, can be attributed to the similarity between the emission profiles of the two components (Figure 2.3.(a)). All of the results shown in the above figures were obtained using 2 PCs, which was the number recommended by the Unscrambler software as determined using the PRESS function described earlier (section 4.3.2.). The use of additional PCs would lead to modelling of noise and this would be detrimental to the overall model.

Three-component system

RRMSEPs for the three-component FL system are represented as bar charts in Figure 4.6. and Figure 4.7. The recommended number of PCs to be used was 3 and so all the results shown for the three component system have been predicted using 3 PCs. Figure 4.6. illustrates the degree of predictive precision that was obtained when only one wavelength

(250 nm) was used for excitation of the three component PAH mixture. The degree of predictive accuracy obtained for the anthracene (< 6%) and benzo[*k*]fluoranthene (< 12%) is acceptable but for benzo[*a*]pyrene (< 18%) is rather poor. Previously (*section 2.3.1.*) it was shown that benzo[*a*]pyrene exhibits a weaker relative emission intensity than both anthracene and benzo[*k*]fluoranthene in acetonitrile. As a result, the predictive accuracy for benzo[*a*]pyrene relative to anthracene and benzo[*k*]fluoranthene was adversely effected. Another observation was that anthracene ($\lambda_{\text{Ex}} = 250 \text{ nm}$) and benzo[*k*]fluoranthene ($\lambda_{\text{Ex}} = 247 \text{ nm}$) were better suited to the compromise λ_{Ex} (250nm), while benzo[*a*]pyrene ($\lambda_{\text{Ex}} = 264 \text{ nm}$) would have benefited had it been a little higher.

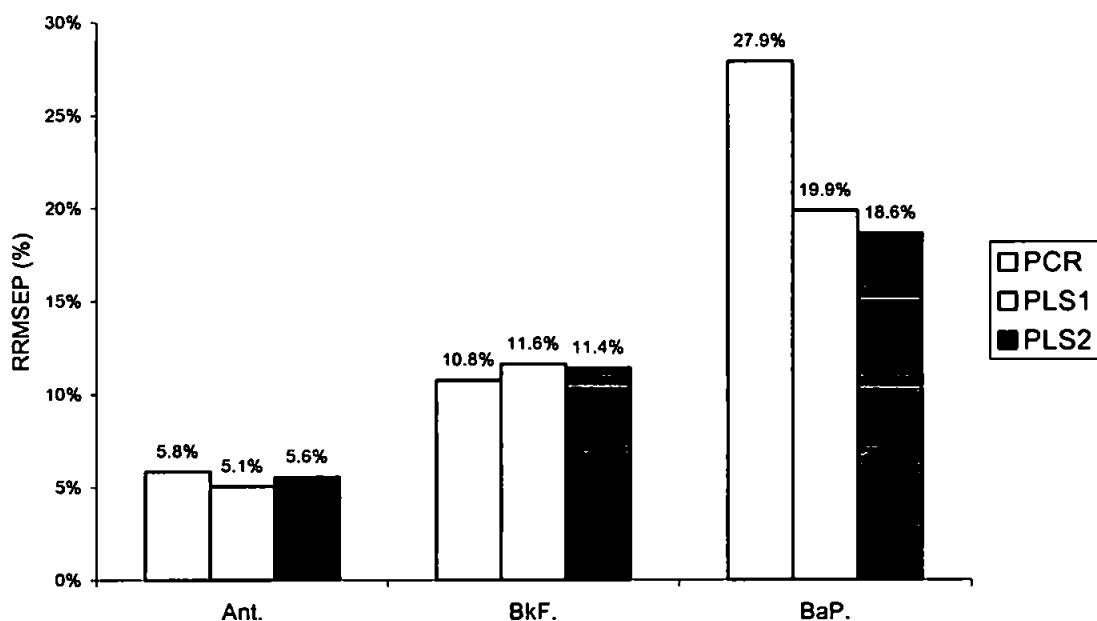


Figure 4.6. Prediction errors for the three-component system using single compromise wavelength (250 nm) excitation method.

Figure 4.7. illustrates that a better degree of predictive accuracy was obtained if the three component mixture was measured at three independent excitation wavelengths (247 nm, 306 nm and 264 nm) and the spectra thus obtained were joined in series before undergoing any statistical analysis. From this bar chart it can be seen that there are no significant differences observed between the overall precision's when determined using the PCR, PLS1 and PLS2 calibration routines. The chart also demonstrates that a high degree of predictive accuracy is obtained for all three PAH components, with prediction errors < 7% for anthracene, < 11% for benzo[*k*]fluoranthene and < 8% for benzo[*a*]pyrene. The relative

accuracies observed for each of the three PAHs can be related to the relative FL emission intensity exhibited by the individual PAH compounds.

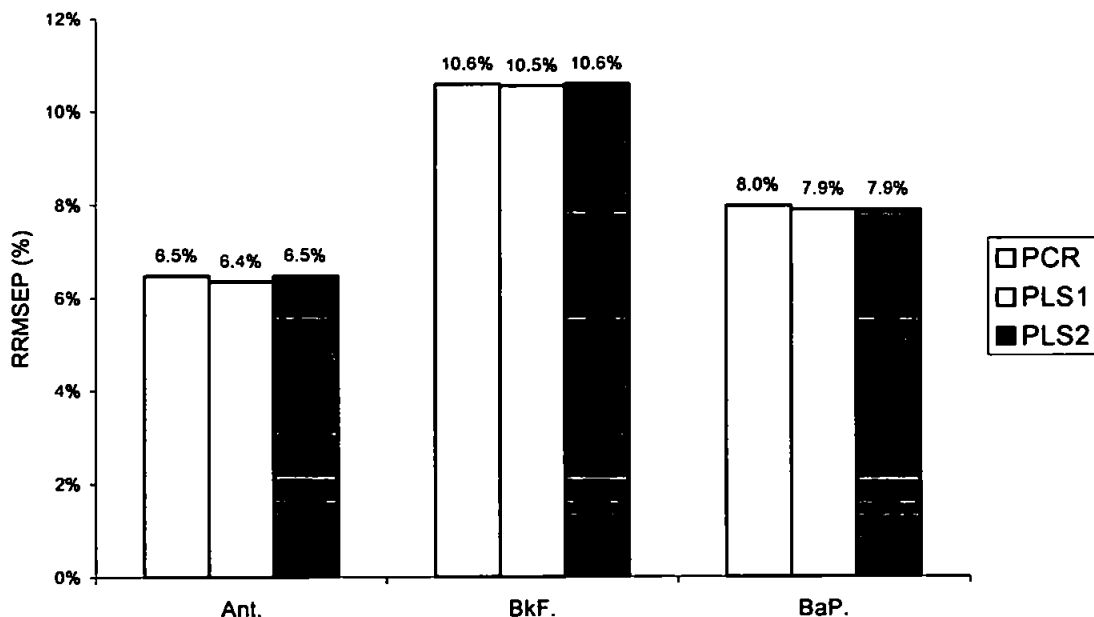


Figure 4.7. Prediction errors for the three-component system using multiple wavelength (247 nm, 306 nm and 264 nm) excitation method with spectral gluing.

The most important observation from these results is the significant improvement in the predictive accuracy for the PAH with the weakest emission (benzo[*a*]pyrene) that results from spectral ‘gluing’. This requires very little additional analysis and data processing time to accomplish the improved accuracies. It was therefore decided that any further investigations would use only the ‘gluing’ method in order to produce the calibration models and subsequent predictions. A further improvement to the method would be to use synchronous scanning [289-290]. This method would allow both excitation and emission to be scanned synchronously, producing a spectrum with a more resolved structure and more readily identified peaks. Such a method has been applied by Horning *et al.* [291] for the monitoring of aromatic compounds in environmental matrices. Further scanning at different $\Delta\lambda$ intervals would allow a 3D contour plot to be obtained. Whilst this could potentially provide an even better model (i.e. better predictive accuracies) one would need to be careful about the size of the data files and associated time needed for processing and model construction.

Four-component system

Figure 4.8 summarises the prediction accuracies for the four-component FL system. As in the three-component system, no significant differences between the overall accuracies obtained using the PCR, PLS1 and PLS2 calibration routines were observed.

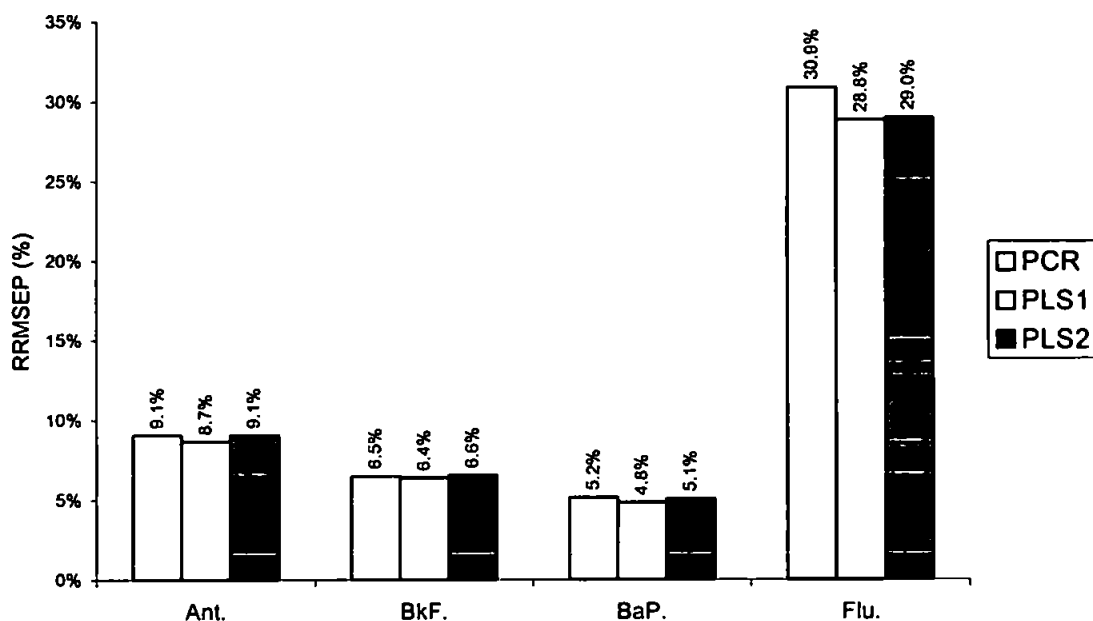


Figure 4.8. Prediction errors for the four-component system.

Once again low RRMSEP values ($< 10\%$) were obtained for anthracene, benzo[k]fluoranthene and benzo[a]pyrene but higher RRMSEP values ($> 25\%$) were observed for fluoranthene. In order to explain this result the emission data for the PAHs in the four component mixture have to be considered. From Table 4.3 it can be observed that fluoranthene has a significantly weaker FL emission profile than the other three PAHs. Indeed the emission intensity for fluoranthene is only 6% that of anthracene and, as a result, the spectrum was masked by the spectra of the other PAHs in the multicomponent mixture. The number of PCs used for these predictions was 4 in each case.

Five-component system

Figure 4.9 shows the overlay of the 'glued' spectra obtained for the 32-sample calibration set for a 5-component system comprising anthracene, benzo[k]fluoranthene, benzo[a]pyrene, fluoranthene and chrysene, in the range 0-4.0 mg l⁻¹. The figure clearly illustrates the complex nature of the analytical signal that is obtained when undertaking the construction of multivariate calibration routines.

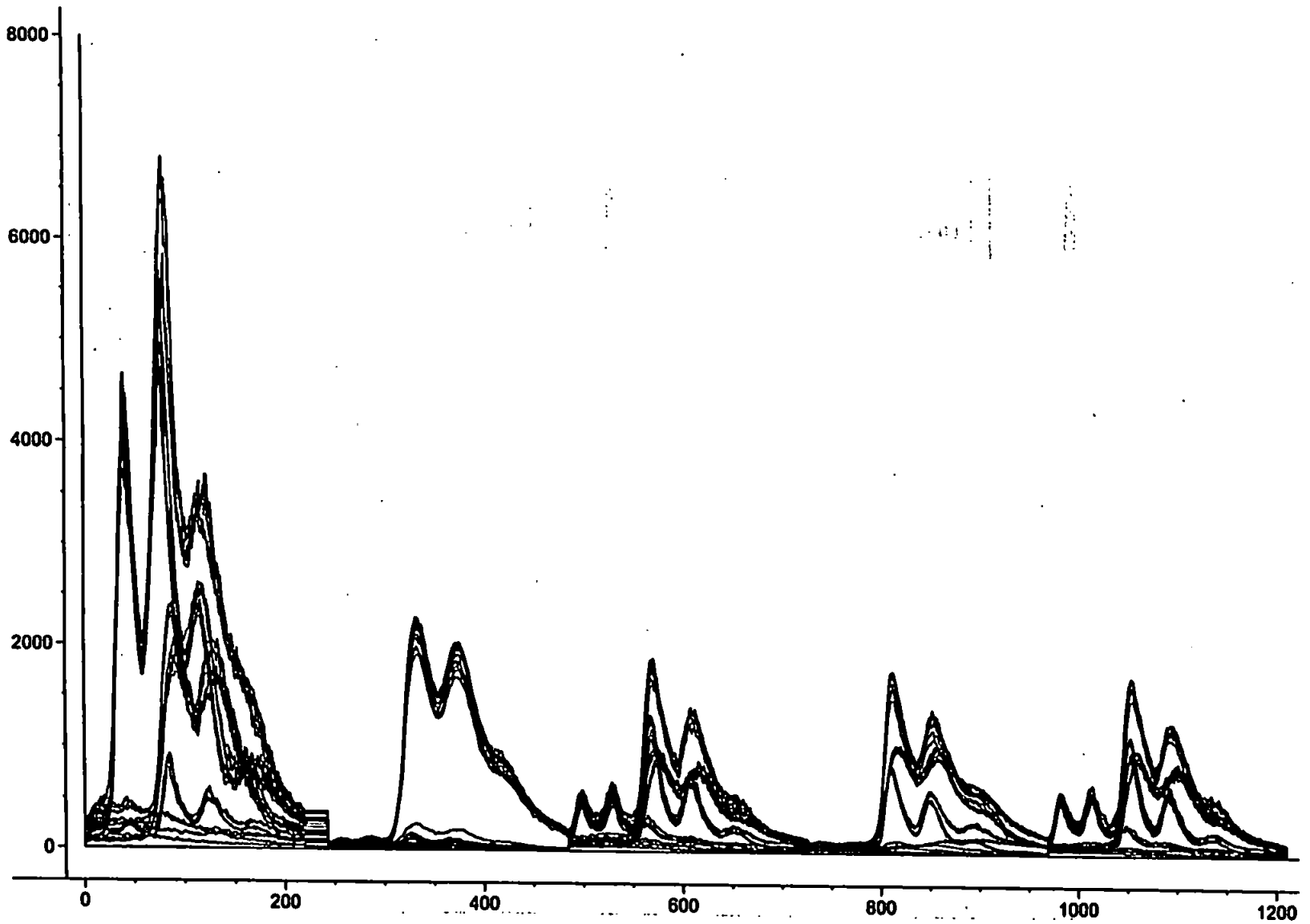


Figure 4.9. Overlay of 'glued' emission spectra for the 2^5 factorial 5-component calibration samples.

Figure 4.10 presents the prediction errors calculated for the five-component FL system using the PCs as suggested by the Unscrambler software. As in the three and four-component systems the RRMSEP values obtained for anthracene, benzo[*k*]fluoranthene and benzo[*a*]pyrene remained low (< 12%) in spite of the increased complexity of the mixture. Interestingly the RRMSEP values for fluoranthene (<20%) improved as compared with the 4 component system. This could be due to the effect of another relatively weak emission (from chrysene) on the modelling process.

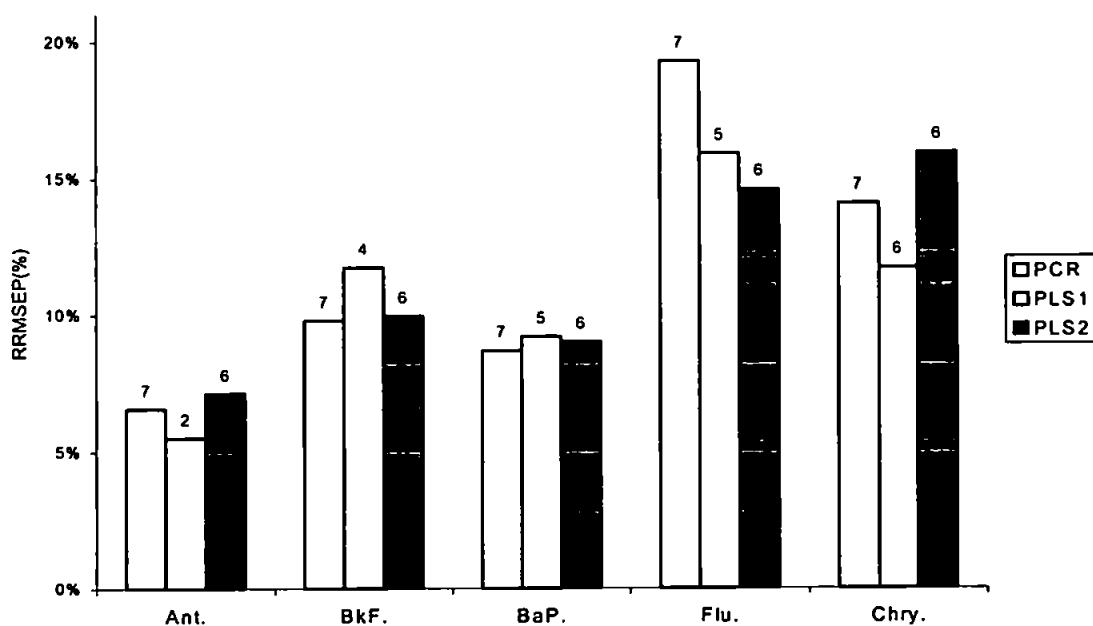


Figure 4.10. Prediction errors for the five-component system using PCs as recommended by the software (where the numbers represent the PCs used).

The RRMSEP values for the five components showed good agreement with the emission intensities (Table 4.3), suggesting (as one might expect) that this is the most important factor in determining the predictive accuracy of any model. It was also observed that for the five component system, the differences between the overall accuracies obtained using the three calibration routines were more significant. An added aspect of the five component system was that in order to obtain the prediction errors shown the number of PCs used for prediction changed for the different models used. In this case 7 PCs were necessary for the PCR model and 6 PCs were used for the PLS2 model (Figure 4.10). When using the PLS1 model the number of PCs used was dependent on the PAH that was being determined, thus only 2 PCs were used for anthracene, 4 PCs for benzo[*k*]fluoranthene, 5 PCs for benzo[*a*]pyrene and fluoranthene, and 6 PCs for chrysene.

From the results obtained for this system, PLS1 is recommended as the calibration method that should be used for the prediction of PAHs in the relatively simple multicomponent systems that have been investigated. This calibration routine was preferred over the others because it generally produced lower errors of prediction throughout the study undertaken. This does not, on first inspection, hold true for the five-component system discussed above. If however the number of PCs are chosen for each calibration method in order that the best RRMSEP is achieved (as opposed to the minimum PRESS) then PLS1 provided lower RRMSEP values for each of the components in the mixture (Figure 4.11.). Thus, from a visual inspection of the model statistics, PLS1 used 4 PCs for anthracene, 5 PCs for benzo[k] fluoranthene, 6 PCs for benzo[a]pyrene and 7 PCs for fluoranthene and chrysene. PLS2 used 4PCs for anthracene, 6 PCs for fluoranthene and 7 PCs for the other three components. PCR, which produced the highest RRMSEP values in each case used 4 PCs for anthracene, 5 PCs for fluoranthene and 7 PCs for the other three components.

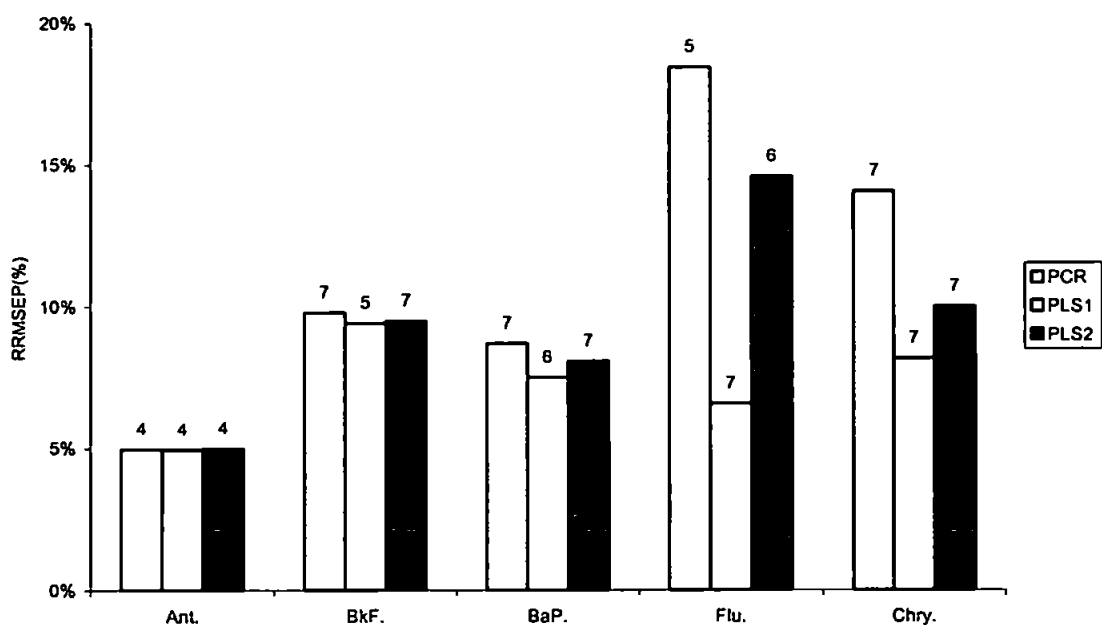


Figure 4.11. Prediction errors for the five-component system using PCs giving the lowest RRMSEP value (where the numbers represent the PCs used).

The reason why the PLS1 routine provided the best results (particularly for fluoranthene and chrysene) is related to the way in which the PLS1 algorithm works as discussed above (*section 4.3.2*). Due to the fact that each component is considered individually rather than as part of a mixture, one would intuitively expect the method to provide more accurate predictions. The main drawback of PLS1 is that as the number of individual components

in a mixture is increased, so the number of models that have to be constructed, and hence the analysis time, are also increased.

Applicability to a diesel particulate extract (SRM 1650).

All of the investigations above have been performed on mixtures of PAHs containing similar concentration levels of the individual components (0-4.0 mg l⁻¹). In a real sample this would be very unlikely to be encountered and the PAHs would normally be present in markedly differing concentrations, e.g. the individual PAH concentrations in the SRM 1650 (section 3.3.3.) range from 1.2 ± 0.3 µg g⁻¹ for benzo[*a*]pyrene to 49.8 ± 0.3 µg g⁻¹ for fluoranthene.

Therefore a set of calibration and test solutions was produced to simulate typical concentration ranges that would be expected on extraction of PAHs from such a reference material. The details of this set of solutions are shown in Table 4.4.

Table 4.4. Calibration and test set design for solutions used to simulate a real sample (SRM 1650 values shown for reference).			
PAH	Calibration (µg l⁻¹)	Test set (µg l⁻¹)	SRM 1650 (µg g⁻¹)
Anthracene	0, 3	1, 2	N/A
Benzo[<i>k</i>]fluoranthene	0, 3	1, 2	2.1 ± 0.2
Benzo[<i>a</i>]pyrene	0, 3	1, 2	1.2 ± 0.3
Fluoranthene	0, 50	20, 40	49.8 ± 0.3
Chrysene	0, 20	10, 15	22 ± 1.0

Using a 2⁵ level factorial design as previously described (section 4.2.2.), the accuracies of prediction for these solutions was calculated and the results obtained are shown in Figure 4.12. As in previous systems, the RRMSEP values that were obtained for anthracene were low (< 8%), but were somewhat higher (8-26%) for the other four components. The desired level of predictive accuracy in a laboratory situation is typically ≤5% but for use as a rapid screening method, that could be performed in the field, poorer relative accuracy, e.g. 10-15%, would normally be acceptable [292]. The predictive errors for each of the five component systems (Figures 4.10 - 4.12.) would nonetheless be perfectly adequate for

screening purposes in the field and this is the most realistic possibility for the FI-CL multivariate calibration approach.

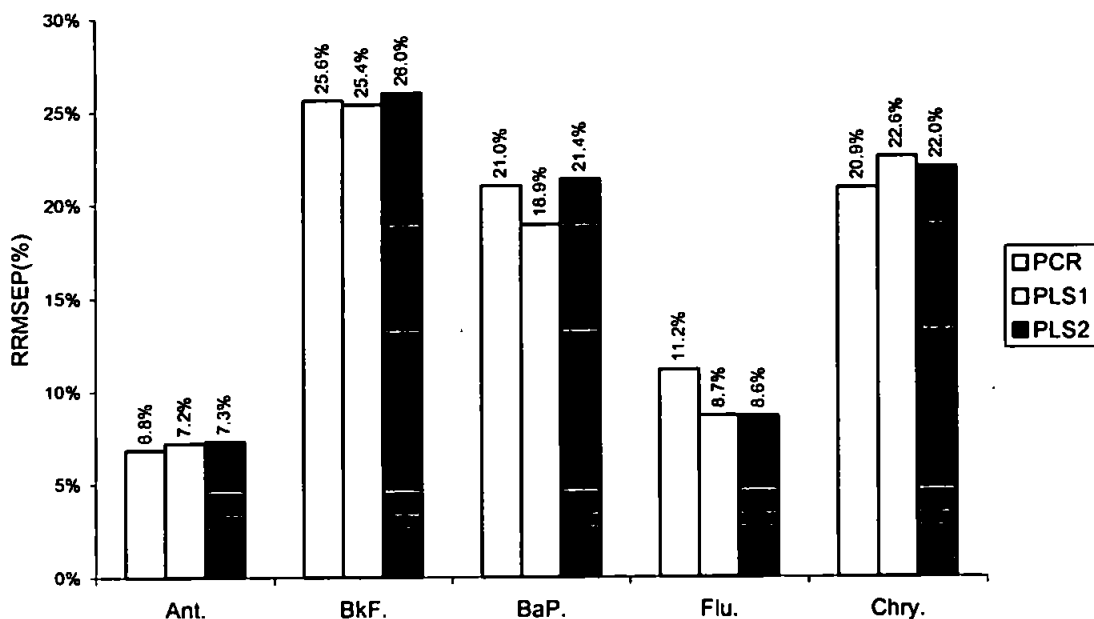


Figure 4.12. Prediction errors for the five-component system based on concentrations expected in a real sample.

For the SRM the relative accuracies were poorer than for the synthetic mixtures. This was because the extraction of SRM 1650 by the procedure outlined previously (*section 3.2.2.*) does not provide unique selectivity for PAH compounds. The chromatogram obtained for the RPLC analysis of the SRM 1650 extract has already been shown (Figure 3.11). It was evident from this chromatogram that the sample extract contains a whole host of uncharacterised hydrocarbons that exhibit inherent fluorescence. These compounds would therefore interfere with the multivariate routine if allowed to remain in the sample during FL analysis. A further clean-up protocol would have to be established to reduce these effects, which would probably centre around the use of a solid phase extraction (SPE) procedure. One available option would be to use silica gel cartridges in order to fractionate the aliphatics, monoaromatics, diaromatics and polyaromatics from one another [293] before analysis by FL spectroscopy.

It must therefore be stated that the method devised would be suitable for the quantification of simple mixtures of PAHs after considerable clean up techniques had been employed. This being said, however, the method after further investigation may provide a suitable means for a rapid screening technique for PAHs without the prior need for physical separation using conventional chromatographic methods.

4.3.4 CL Investigation

It has already been shown that PAHs possess unique excitation and emission fluorescence spectra (*section 2.3.1*) and how multivariate calibration routines such as PCR, PLS1 and PLS2 [271, 278] can be used for simultaneous quantification of PAHs from multi-analyte fluorescence spectra (*section 4.3.3*). This approach should also be suitable for the quantification of PAHs on the basis of their CL emission spectra. One potential advantage of CL is that a low cost CCD based instrument could be deployed in the field for rapid screening of samples.

Investigation of CL spectra

The structural formulae of benzo[*b*]fluoranthene, benzo[*k*]fluoranthene, benzo[*a*]pyrene, benzo[*g,h,i*]perylene and perylene are shown in Figure 4.13. CL spectra for these five compounds, measured using the continuous flow CCD system, are shown in Figures 4.14 (a) and 4.14 (b) for acetonitrile and hexane solutions respectively.

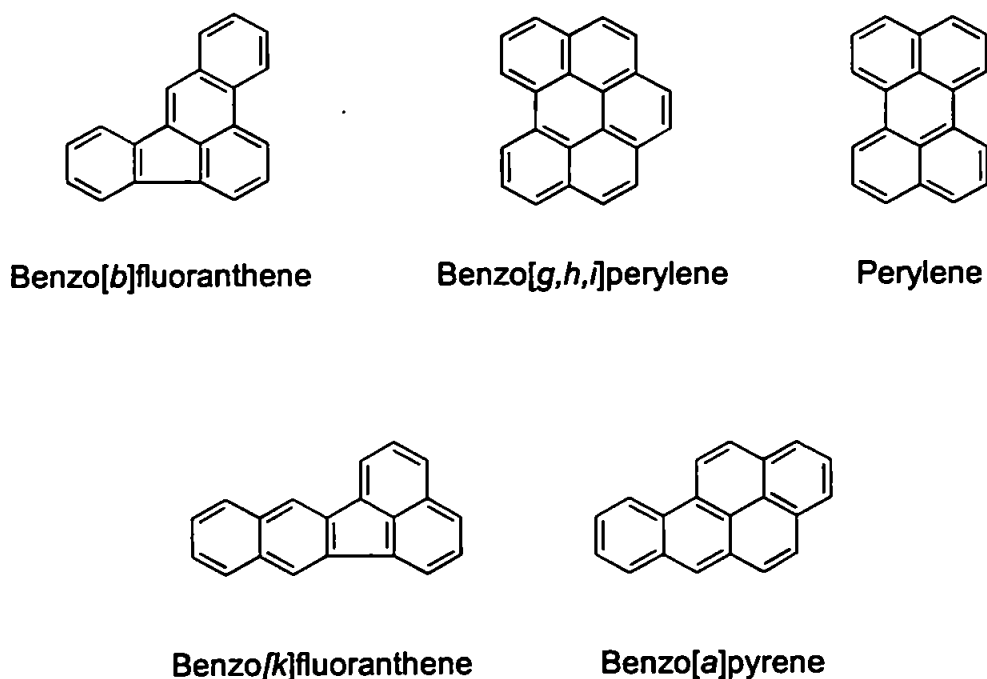


Figure 4.13. Structural formulae of benzo[*b*]fluoranthene, benzo[*k*]fluoranthene, benzo[*a*]pyrene, benzo[*g,h,i*]perylene and perylene.

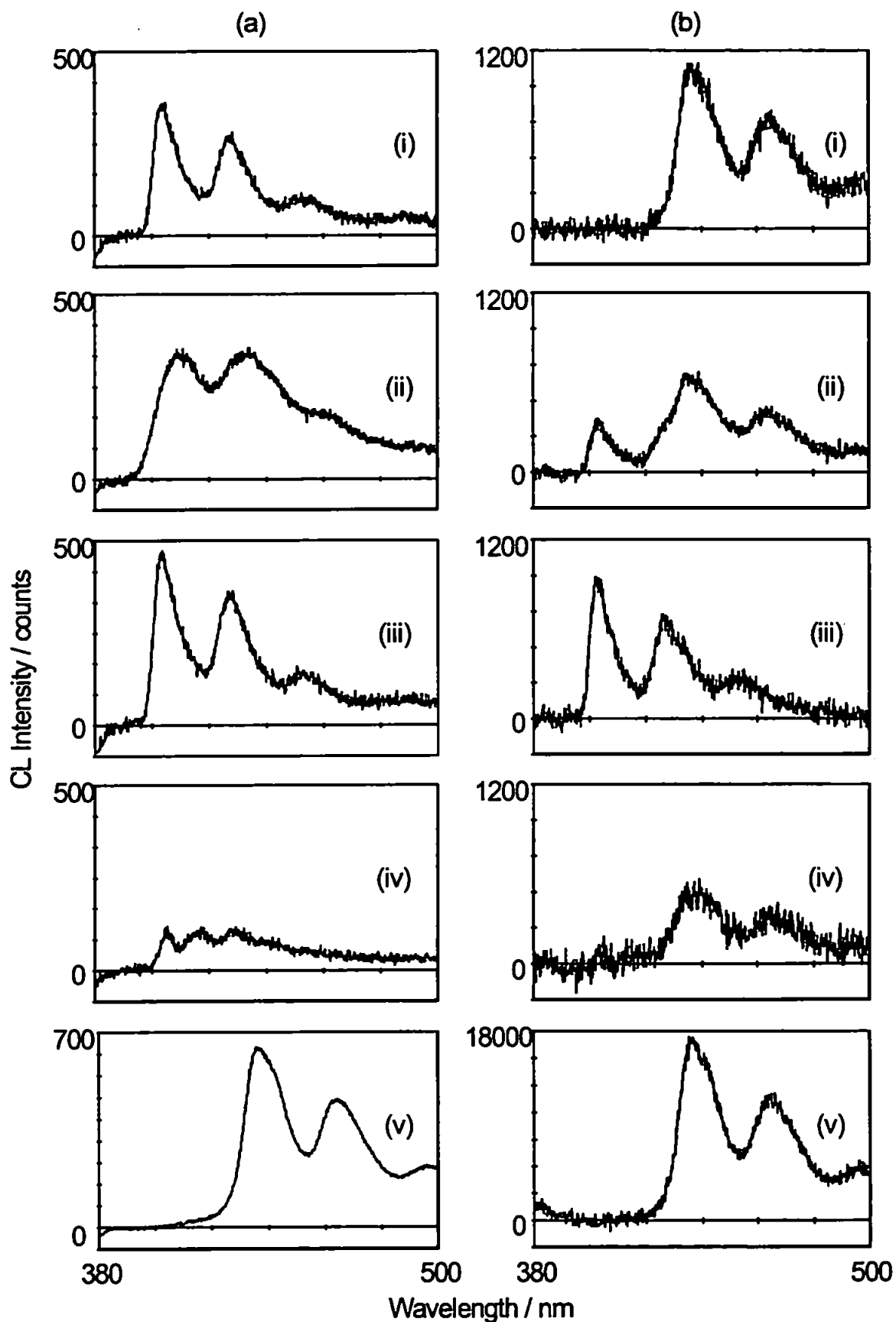


Figure 4.14 Chemiluminescence spectra for benzo[*b*]fluoranthene (i), benzo[*k*]fluoranthene (ii), benzo[*a*]pyrene (iii), benzo[*g,h,i*]perylene (iv) and perylene (v): (a) 20 mg Γ^{-1} solutions in acetonitrile; (b) 1 mg Γ^{-1} solutions (0.1 mg Γ^{-1} for perylene) in hexane.

Acetonitrile and hexane were chosen as the solvents because they had already been successfully used during the chromatographic separation of PAHs in previous investigations (*chapter 3*). This would make the method compatible with post-column LC detection so that it could also be used to quantify unresolved or partially resolved PAHs using LC-CL. The greater sensitivity in hexane is due to its lower polarity (*cf.* acetonitrile) that resulted in reduced radiationless losses from the excited state PAH species. Table 4.5. lists the λ_{maximum} values for the two lowest wavelength peaks for each spectrum, together with the ratio of peak heights. There was a significant degree of spectral shift between the two solvent systems, particularly in the case of benzo[*b*]fluoranthene, benzo[*k*]fluoranthene and benzo[*g,h,i*]perylene, and also between the peak intensity ratios. This means that the nature of the solvent system can be used to advantage in maximising the information content from CL spectra, thereby enhancing the predictive capability of the multivariate calibration models.

PAH	Acetonitrile solution			Hexane solution		
	Peak 1 λ_{max} (nm)	Peak 2 λ_{max} (nm)	P1:P2 height ratio	Peak 1 λ_{max} (nm)	Peak 2 λ_{max} (nm)	P1:P2 height ratio
B[<i>b</i>]F	405	428	1.27	438	465	1.46
B[<i>k</i>]F	410	433	0.98	405	437	0.44
B[<i>a</i>]P	405	428	1.22	404	428	1.28
B[<i>g,h,i</i>]P	407	416	0.59	437	465	1.50
Perylene	437	465	1.39	438	465	1.46

Detection Limits

Table 4.6 lists detection limits for benzo[*k*]fluoranthene, benzo[*a*]pyrene and perylene in hexane, determined using the CCD based continuous flow system. These were calculated as $\bar{y}_b + s_{yx}$ where \bar{y}_b is the mean response of the blank and s_{yx} is the standard error of the y estimate [208]. These detection limits were higher than those obtained using the PMT-FI system (*section 2.3.2*). This is partly attributable to the fact that the fibre optic bundle used to transmit the CL emission from the flow cell to the detector had a much smaller cross-sectional area than the photosensitive window of the PMT detector.

Table 4.6. Limits of detection for three PAHs in hexane solution, using the continuous flow system with CCD detection.					
PAH	LOD ($\mu\text{g l}^{-1}$)	Slope	Intercept	r^2	Range ($\mu\text{g l}^{-1}$)
Benzo[<i>k</i>]fluoranthene	79	68.0	9.14	0.994	0-1000
Benzo[<i>a</i>]pyrene	60	331	3.07	0.999	0-1000
Perylene	6.0	6260	36.6	0.999	0-100

Multivariate calibration of a two-component PAH system

A two-component system comprising mixtures of benzo[*k*]fluoranthene and benzo[*a*]pyrene in hexane was therefore designed in order to assess the feasibility of this approach. These two PAHs were chosen for the investigation because it was observed from the CL emission profiles that there were distinct differences between the two spectra. Also taken into consideration was the fact that the intensity of CL emission was in a similar range for both compounds. The importance of this was illustrated with the FL data (section 4.3.3.) where fluoranthene did not model very well due to its emission spectra being 'swamped' by the stronger emission spectra of the other PAHs in the mixture.

From Figure 4.14 it can be seen that the spectra obtained using the CL system were considerably more noisy than those obtained using the FL instrument. Data pre-processing was therefore required in order to eliminate the effects of some of this noise. The spectra were smoothed using a moving average filter (Unscrambler v. 6.1). Figure 4.15. shows the effect of increasing degrees of smoothing on the CL spectra on a two component mixture sample. As the level of smoothing increased the spectra became less noisy when the degree of smoothing reached 75 the λ_{max} value had shifted to a longer wavelength than for the raw data.

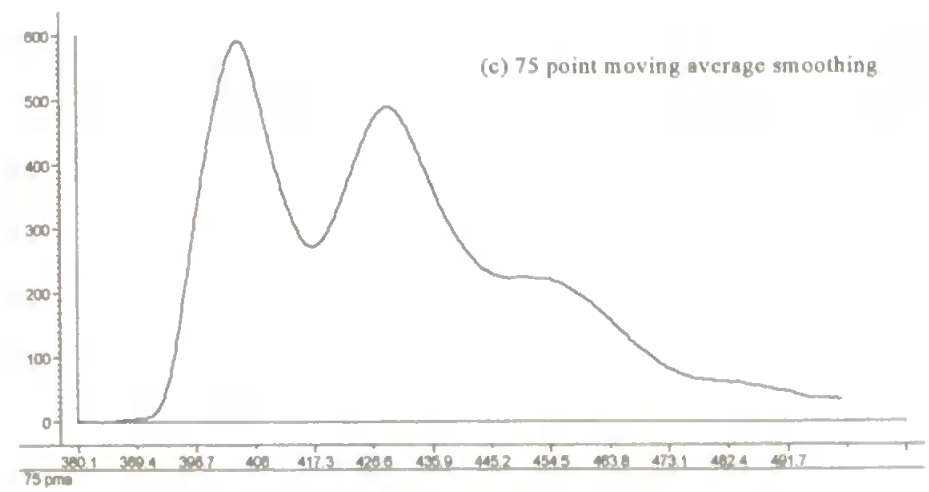
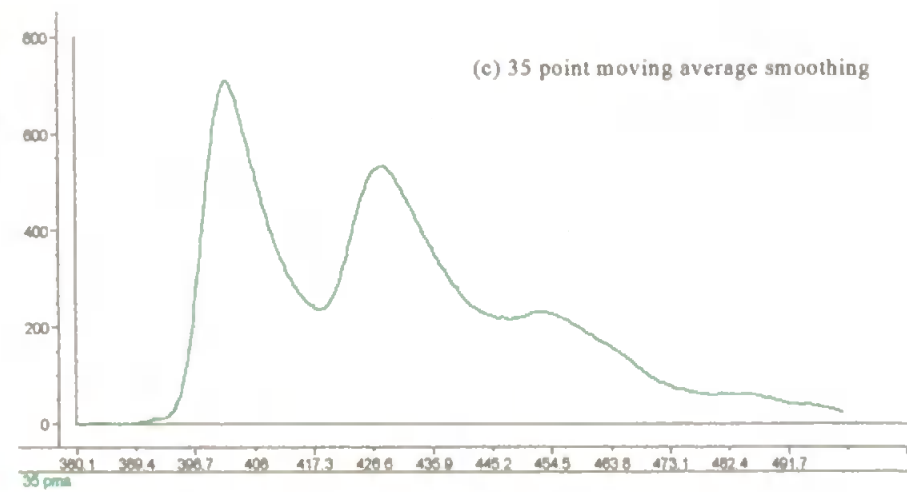
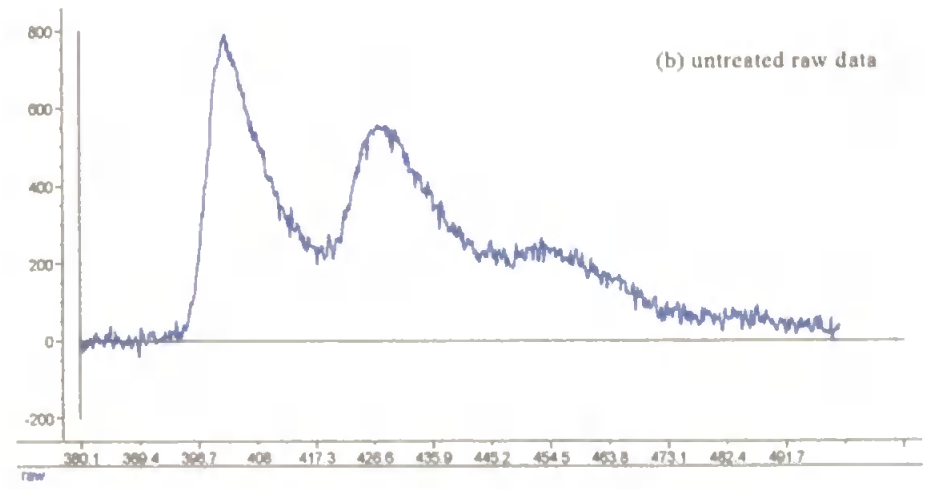
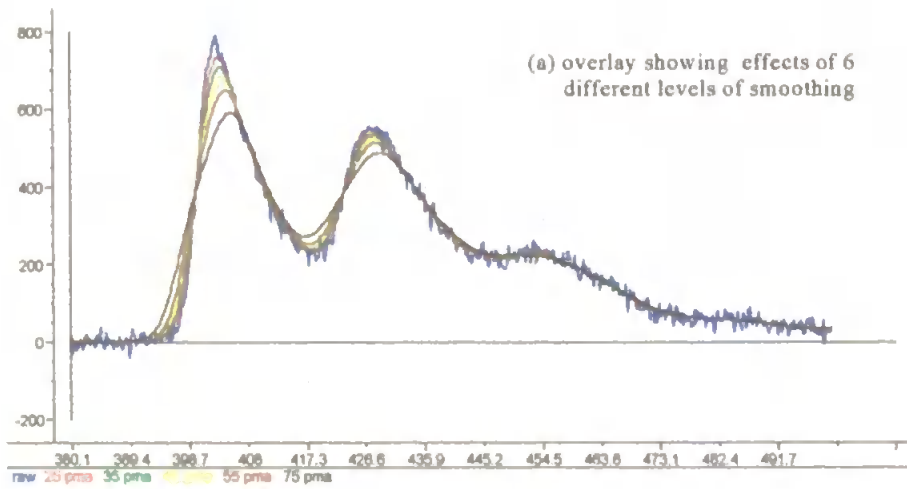


Figure 4.15. CL spectra of a 2 component mixture showing effect of different degrees of smoothing.

The relative intensity of the emission spectra also decreased as the degree of smoothing increased. It is therefore important to ascertain when enough data pre-processing has been carried out so as not to overfit the data and thereby lose some of the information that discriminates one set of data from the next.

In order to study this concept a PCR calibration model was built and used to predict the test set concentrations using both raw and smoothed data sets. The results are illustrated as a bar chart (Figure 4.16.). These results show that the highest degree of predictive precision was achieved using a model and test set that had undergone a 45 point moving average (pma) smoothing. This degree of smoothing was applied to all data sets investigated below.

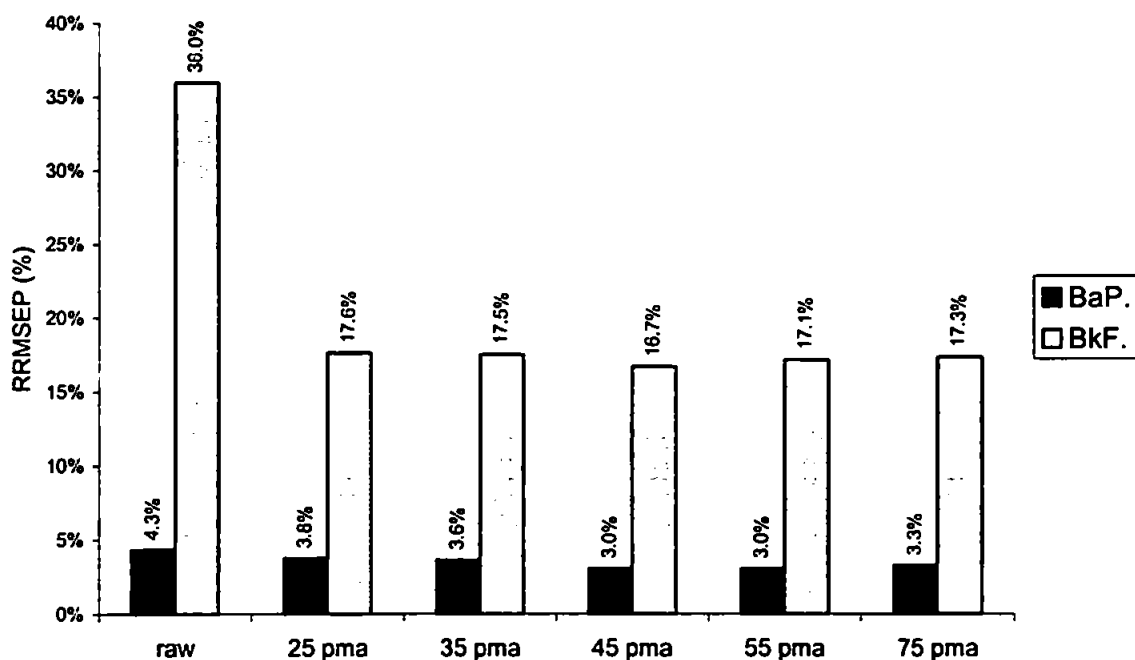


Figure 4.16. PCR prediction errors for a two-component system showing the effects of different degrees of smoothing.

The above investigation into smoothing was performed using a 3^2 factorial design. The overall degree of predictive precision, while good for benzo[a]pyrene, was poor for benzo[k]fluoranthene. In order to investigate the use of multivariate calibration routines on a two-component system further a 5^2 factorial design was produced. The spectra for a 25 sample calibration set and a 10 sample test set are shown in Figures 4.17.(a) and 4.17.(b) respectively. PCR, PLS1 and PLS2 calibration models were then constructed using the calibration sample spectra and used to predict the test set concentrations.

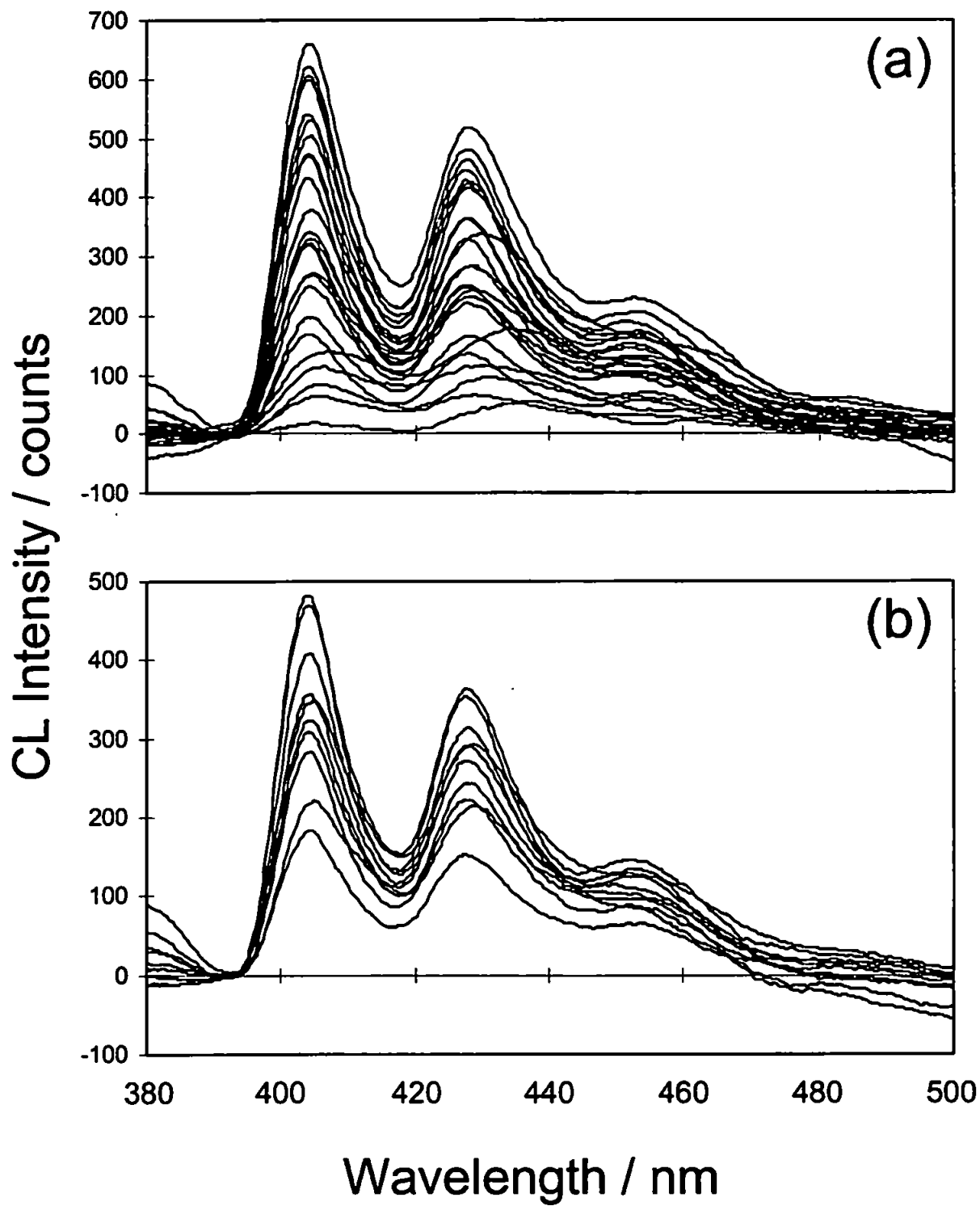


Figure 4.17. Chemiluminescence spectra for the benzo[*a*]pyrene/ benzo[*k*]fluoranthene two-component system: (a) calibration set; (b) test set.

The results (shown as a bar chart in Figure 4.18.) showed that a high degree of predictive accuracy was obtained for benzo[*a*]pyrene (< 4%) but for benzo[*k*]fluoranthene it was significantly worse (> 19%).

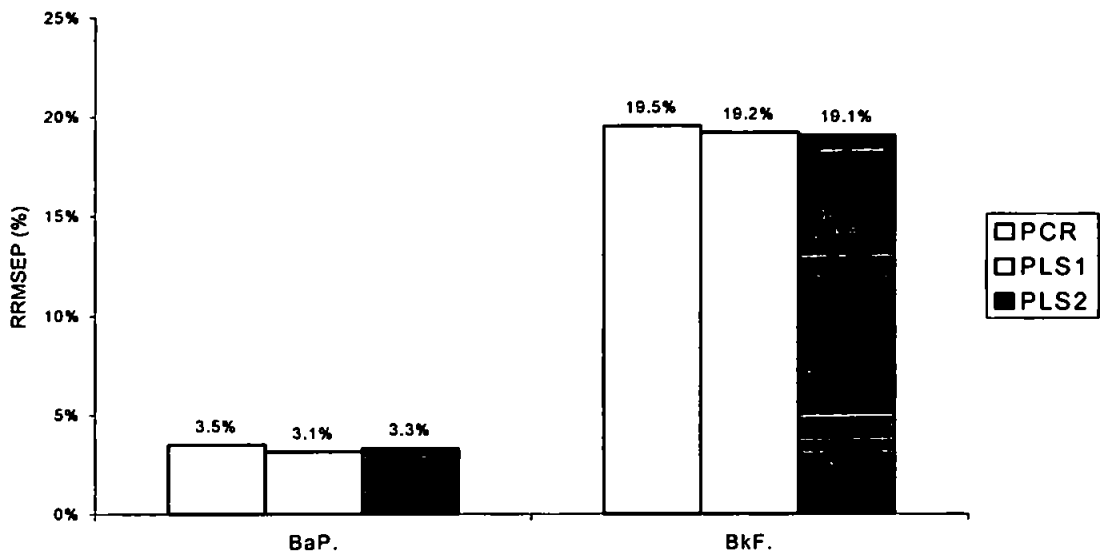


Figure 4.18. Prediction errors for the two-component system.

An investigation of the regression overview (displayed as a scores plot) showed that there were two possible outliers in the calibration series used to perform the above prediction (Figure 4.19.).

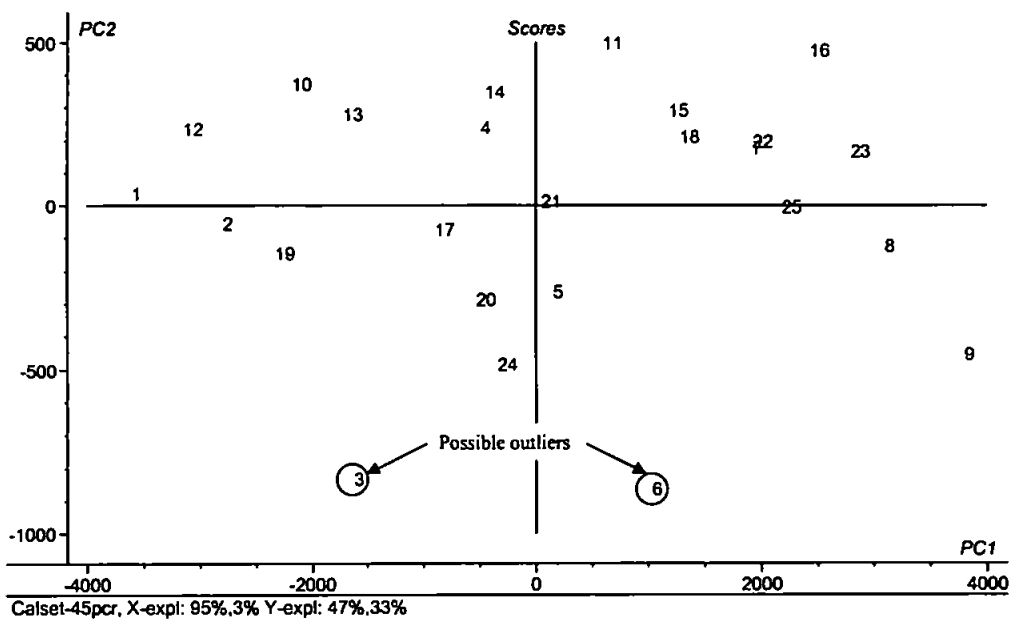


Figure 4.19. Scores plot for the PCR calibration model showing two possible outliers.

The calibration was therefore re-constructed with the omission of these outliers and the results for the prediction using the new calibration model gave much improved predictive accuracy. The results (Figure 4.20.) showed that a high degree of predictive accuracy was obtained for both PAH components, with prediction errors < 4% for benzo[*a*]pyrene and < 9% for benzo[*k*]fluoranthene for each of the three multivariate calibration techniques. It also emphasised the importance of evaluating the data, e.g. for outliers, prior to construction of the model.

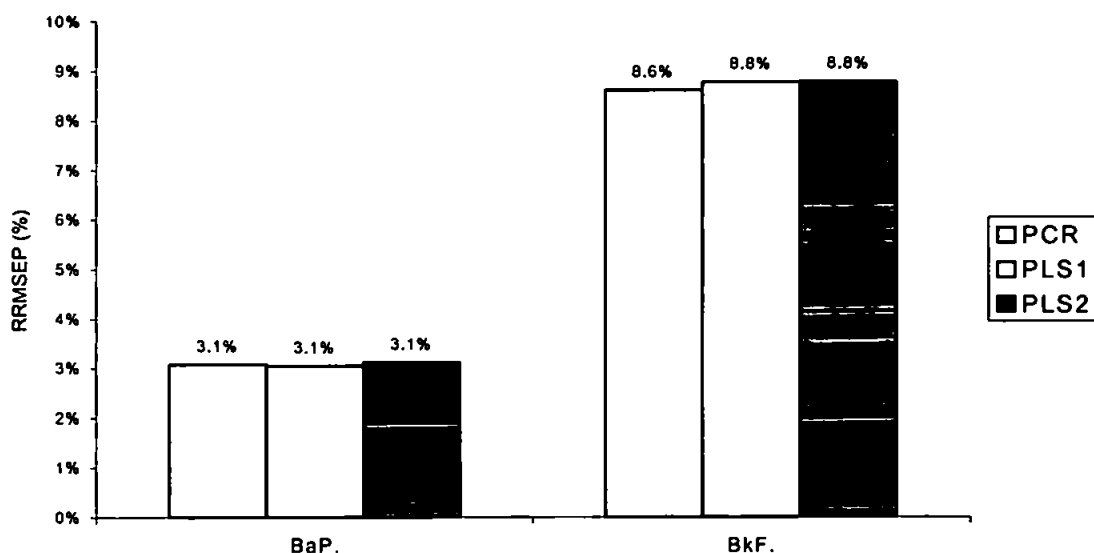


Figure 4.20. Prediction errors for the two-component system with ‘outliers’ removed from the calibration model.

The number of PCs used to obtain the above results were at the PRESS minimum. The prediction of benzo[*a*]pyrene used 3 PCs for PCR and PLS2 and only 2 PCs for PLS1, benzo[*k*]fluoranthene used 4 PCs for each of the calibration methods investigated.

The degree of similarity in predictive precision displayed here by the three calibration methods would be expected for a relatively simple multicomponent system such as this. Nonetheless these results clearly demonstrate that full-spectral CL acquisition, coupled with multivariate calibration, can be used to quantify individual PAHs in a mixture without the need for prior chromatographic separation. The greatest potential for this approach is likely to be as a field system for the rapid screening of environmental matrices, e.g. potable and waste waters, for the presence of PAHs. Whilst it is unlikely that multivariate calibration will be able to fully quantify individual PAHs, it is reasonable to expect that some classification based on molecular shape and ring size will be possible due to their effect on CL emission spectra.

4.4 CONCLUSIONS

1. When using FL detection the lowest prediction errors (4.8-10.6%) were achieved for anthracene, benzo[*k*]fluoranthene and benzo[*a*]pyrene, indicating that these PAHs could be accurately quantified in the 3-, 4- and 5-component systems. The predictive precisions for fluoranthene and chrysene in the 4- and 5-component systems were significantly poorer however, since their fluorescence intensities are significantly lower in acetonitrile than anthracene, benzo[*k*]fluoranthene or benzo[*a*]pyrene.
2. The method of 'spectral gluing' has enhanced the data set used for modelling. One possible problem with this 'spectral gluing' technique might arise from having introduced spectral artefacts as a result of the step caused where the individual spectra are joined to one another. Such artefacts could however be removed using a software 'fix' if indeed they were seen to cause significant effects to the modelling process.
3. The CCD based continuous flow system was able to acquire full spectrum CL emission profiles and, in conjunction with multivariate calibration, was capable of a high degree of predictive accuracy (< 9%) for a synthetic two-component mixture of benzo[*k*]fluoranthene and benzo[*a*]pyrene in hexane.
4. The combination of CL with CCD detection and multivariate calibration therefore has the potential to provide quantitative information in the field without the need for separation.

CHAPTER 5

Determination of amines using flow injection

with aryl oxalate sulphorhodamine-101

chemiluminescence detection

5. THE DETERMINATION OF AMINES USING FLOW INJECTION WITH ARYL OXALATE SULPHORHODAMINE-101 CHEMILUMINESCENCE DETECTION

5.1 INTRODUCTION

Gasoline and diesel fuels often contain additives in order to improve engine performance [294] and some examples of additive compounds and their functions are shown in Table 5.1. Detergents and dispersants are the most common class of these performance additives. Dodecylamine, for example, is a widely used detergent that is typically added to fuels in the 40-50 ppm concentration range.

Table 5.1. Common additive types and typical composition.		
Additive Type	Function	Composition (typical)
Antiknock	Boost octane value	Tetraalkyl lead, methyl cyclopentadienyl manganese tricarbonyl (MMT)
Antioxidant	Minimise residue	Aromatic diamines
Metal deactivator	Chelate trace metals	N,N'-Disalicylidene-1,2-propanediamine
Corrosion inhibitor	Prevent rust	Organic acids and salts
Detergent	Keep carburettor and injectors clean	Alkyl amines, amine phosphates
Dispersant	Keep entire intake system clean	Polymeric amines and succinimides
Dehazer	Coalesce suspended water droplets	Ethoxylated surfactants

In order that product quality is maintained throughout a distribution chain there is a need to check that such additives are present in the fuel at the correct concentrations. They can also be used as marker compounds in order to distinguish different manufacturers products and to identify the origin of the fuel in the event of accidental release into the environment.

At present this is achieved by collection of fuel samples from distribution terminals, garage forecourts etc. and returning them to the laboratory for analysis. There is however a growing need for portable systems which can be used *in situ* in order not to delay the identification of fuel which is not addivated correctly and, in regions of the world where fuel counterfeiting is commonplace, to help challenge fuel retailers about the authenticity of their product. It is therefore advantageous (both commercially and environmentally) to be able to detect such marker compounds rapidly and selectively.

In chapter 2 it was stated that peroxyoxalate chemiluminescence (POCL) involves the oxidation of an aryl oxalate in the presence of a fluorophore. This chapter discusses the determination of amines (including dodecylamine) by FI with POCL detection. The aryl oxalate used was bis(2,4-dinitrophenyl)oxalate (DNPO) and the fluorophore was sulphorhodamine 101. The objective of this investigation was to demonstrate that the FI-CL approach can be used to quantify dodecylamine in non-aqueous matrices with a view to the development of a field deployable instrument for the monitoring of fuels directly at the point of distribution.

5.2 EXPERIMENTAL

5.2.1 Reagents

High quality de-ionised water from a Milli-Q system (Millipore) and analytical grade reagents were used throughout. All solvents used were of HPLC grade (Rathburn, Walkerburn, UK).

Stock amine solutions were initially prepared in the range 100-200 mg l⁻¹, using acetonitrile solvent, for imidazole, ethylamine, diethylamine, triethylamine and dodecylamine (Fluka Chemika-BioChemika, Gillingham, Dorset, UK). Working solutions in the range 0-10 mg l⁻¹ were prepared in acetonitrile by serial dilution of the appropriate stock solutions.

Hydrogen peroxide solutions were prepared by dilution of 30 % v/v stock solution (AnalaR; Merck, Darmstadt, Germany) with deionised water. This was mixed with ACN on a volume/volume basis to produce the carrier stream (Reagent 1). Reagent 2, containing solutions of bis(2,4-dinitrophenyl)oxalate (DNPO; Fluka Chemika-

BioChemika, Gillingham, Dorset, UK) and sulphorhodamine 101 (Fluka Chemika-BioChemika, Gillingham, Dorset, UK) were prepared in ACN. All reagents were freshly prepared each day, and were degassed by sonication for two minutes.

Standard conditions for aryl oxalate-sulphorhodamine 101 optimisation

The following reaction conditions were used unless otherwise stated;

1. DNPO solution, $5.0 \times 10^{-4} \text{ mol l}^{-1}$
2. mobile phase, ACN/water [containing H_2O_2] (90/10)
3. sulphorhodamine 101, $1.0 \times 10^{-7} \text{ mol l}^{-1}$
4. hydrogen peroxide solution, $2.0 \times 10^{-2} \text{ mol l}^{-1}$ (in the water of the mobile phase)
5. analyte, imidazole $2.0 \times 10^{-2} \text{ mol l}^{-1}$ in ACN/water (90/10)

5.2.2 Instrumentation and Procedures

A Hitachi F-4500 fluorescence spectrophotometer (Hitachi Ltd., Tokyo, Japan) fitted with a 1 cm pathlength quartz cuvette was used to obtain excitation and emission spectra for sulphorhodamine 101 in ACN ($1.0 \times 10^{-6} \text{ M}$). Instrument parameter settings used are summarised in Table 5.2.

Table 5.2. Parameter settings for F-4500 fluorescence spectrophotometer.			
Scan Mode	Excitation	Emission	3D
Scan Speed (nm min⁻¹)	1200	1200	240
EX Start WL (nm)	200	-	500
EX End WL (nm)	500	-	600
EM Start WL (nm)	-	350	550
EM End WL (nm)	-	550	650
EX Slit (nm)	5		1
EM Slit (nm)	5		1
PMT Voltage (V)	950		400
Shutter Control	ON		ON

A FI manifold (Figure 5.1.) was constructed using black poly(tetrafluoroethylene) (PTFE)

tubing of 0.75 mm i.d. (Jaytee Biosciences, Whitstable, UK), and was used to facilitate sample and reagent mixing and delivery to a low power (12 V) PMT based detector (Camspec CL-2, Camspec Scientific Instruments, Cambridge, UK), fitted with a 120 μ l quartz flow cell.

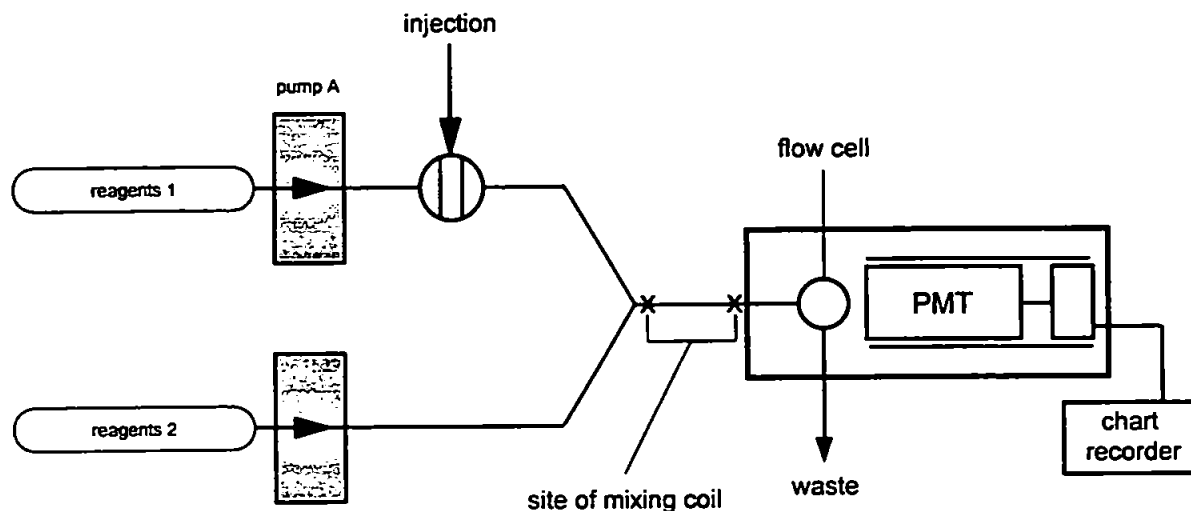


Fig. 5.1. FI manifold for the investigation of the sulphorhodamine 101-POCL reaction.

A Minipuls 2 peristaltic pump (Gilson, Villiers-le-Bel, France) with 1.02 mm i.d. Ismaprene (PharMed 65) pump tubing (Ismatec UK Ltd, Weston-Super-Mare, UK) was used to propel the two reagent streams to a polyetherether ketone (PEEK) T-piece (Phenomenex UK Ltd, Macclesfield, UK), where it mixed with the combined DNPO/H₂O₂ reagent stream, before passing into the flow cell. Standards (50 μ l) were injected using a solenoid-operated, Rheodyne 5041 PTFE rotary valve (Rheodyne Inc., Cotati, CA, USA). CL emission was recorded (mV) using a Chessel BD 4004 chart recorder (Chessel Ltd., Worthing, UK). In all cases, the background level was measured as the response above recorder zero and noise was measured as the peak-to-peak noise of this background (determined when only the carrier stream and CL reagents were mixed). Analyte response was recorded as the peak height (signal) above the background. Signal-to-noise was calculated as the peak height above the background divided by the peak-to-peak noise of the background.

5.3 RESULTS AND DISCUSSION

5.3.1 The aryl oxalate-sulphorhodamine 101 reaction

Figure 5.2 shows the structure of sulphorhodamine 101 and relevant physical data. This compound, on reaction with aryl-oxalate esters and hydrogen peroxide, has previously been shown to enable the chemiluminescence detection of amines [91].

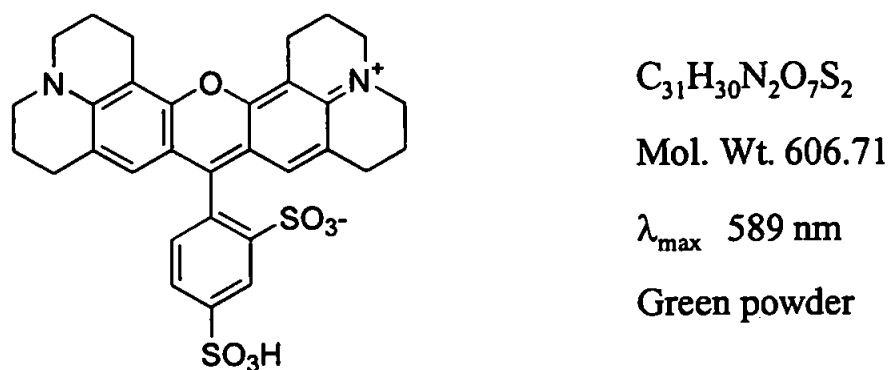


Figure 5.2. The structure and properties of sulphorhodamine 101.

The 3D scanning FL spectrum of sulphorhodamine 101 in ACN is shown in Figure 5.3.(a) together with the excitation (Figure 5.3.(b)) and emission (Figure 5.3.(c)) spectra. From the results obtained it was observed that the optimum wavelength of excitation was 573 nm and using this excitation value the emission spectrum was a single distinct peak with a λ_{max} at 589 nm. There is a small Stokes shift of 16 nm, which would make quantitative fluorescence measurements difficult in the presence of excess sulphorhodamine. Chemiluminescence detection however does not present such a problem in this regard due to the absence of a light source with the associated scatter and spectral overlap.

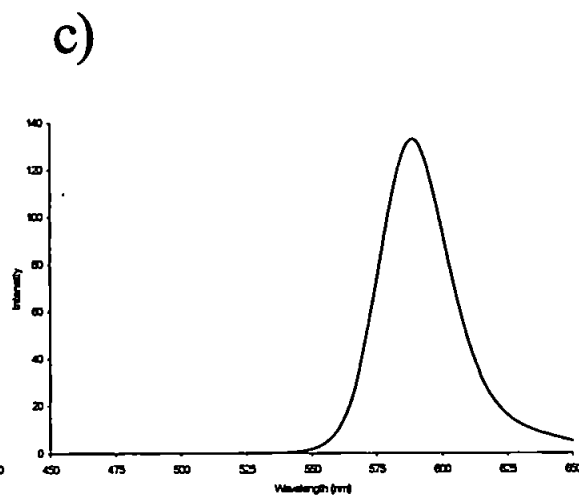
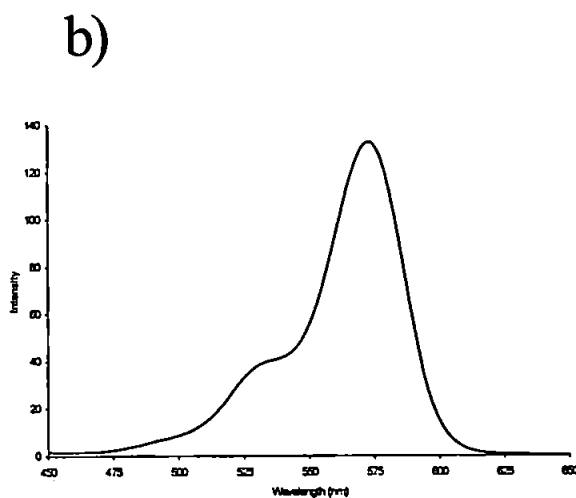
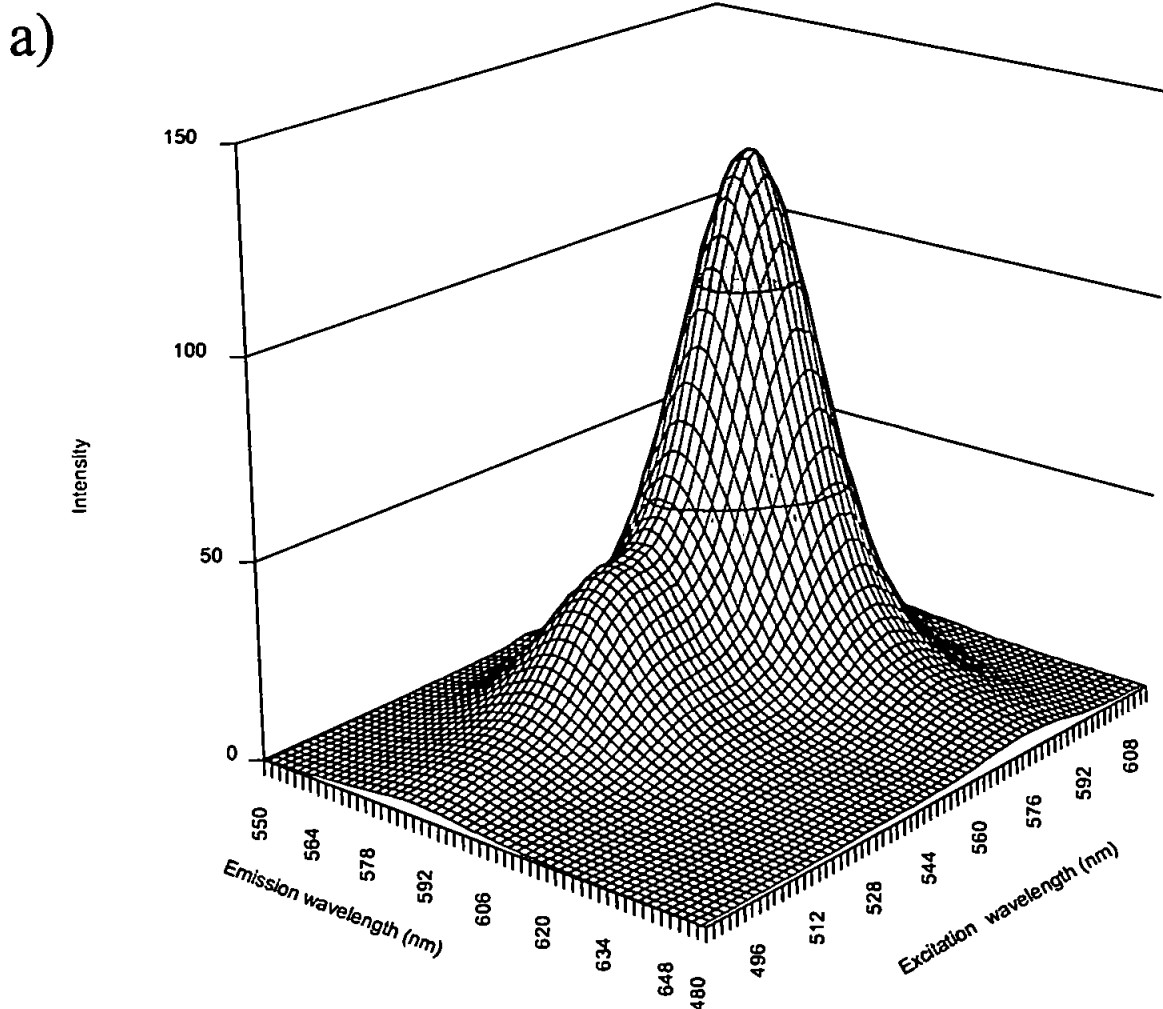


Figure 5.3. Spectra of sulphorhodamine 101 in ACN showing a) 3D scanning FL spectrum, b) FL excitation spectrum and c) FL emission spectrum.

5.3.2 Optimisation of reaction conditions for CL emission

In order that the maximum intensity of emission occurs in the flow cell, optimisation of the CL reaction for FI or LC detection requires “fine tuning” of the reaction conditions. Following the results obtained in a previous investigation (*section 2.3.3*) four factors were expected to have the greatest influence upon emission intensity and the speed of the reaction, and were therefore investigated for optimisation of the reaction conditions for aryl oxalate-sulphorhodamine 101 CL detection in flowing streams;

1. Nature of the mobile phase,
2. Presence and concentration of base catalyst,
3. Concentration of the aryl oxalate,
4. Concentration of the hydrogen peroxide,

Details of the optimisation of conditions for the aryl oxalate-sulphorhodamine 101 reaction are given below.

Effect of mixing coil length

Rapid, efficient mixing is essential for reproducible results and high sensitivity. Incomplete mixing can cause baseline noise and variance in the analytical signal. However, if the length of tubing from the point of mixing to the flow cell is too long, band broadening will occur which will lead to a diminished response. The distance between the sample injection point and the flow cell should be carefully optimised to suit the luminescence process being used. Changing the coil length and hence the mixing and reaction time, is a simple and effective way of maximising the CL emission intensity and reproducibility.

Figure 5.4 shows the effect of changing from having no mixing device present, other than the length of tubing (approximately 2 cm) joining the injection device to the flow cell, to having a coil length of 250 cm inserted between the point of reagent mixing and the flow cell (shown as X—X in Figure 5.1.). Figure 5.4 shows that the coil length giving the highest signal during the analysis using this system was 150 cm. Peak-to-peak noise did not change significantly when the length of mixing the coil was altered. A plot of signal-to-noise ratio and RSD (Figure 5.5) also showed that the optimum coil length using this system was 150 cm and this was used for all subsequent analyses.

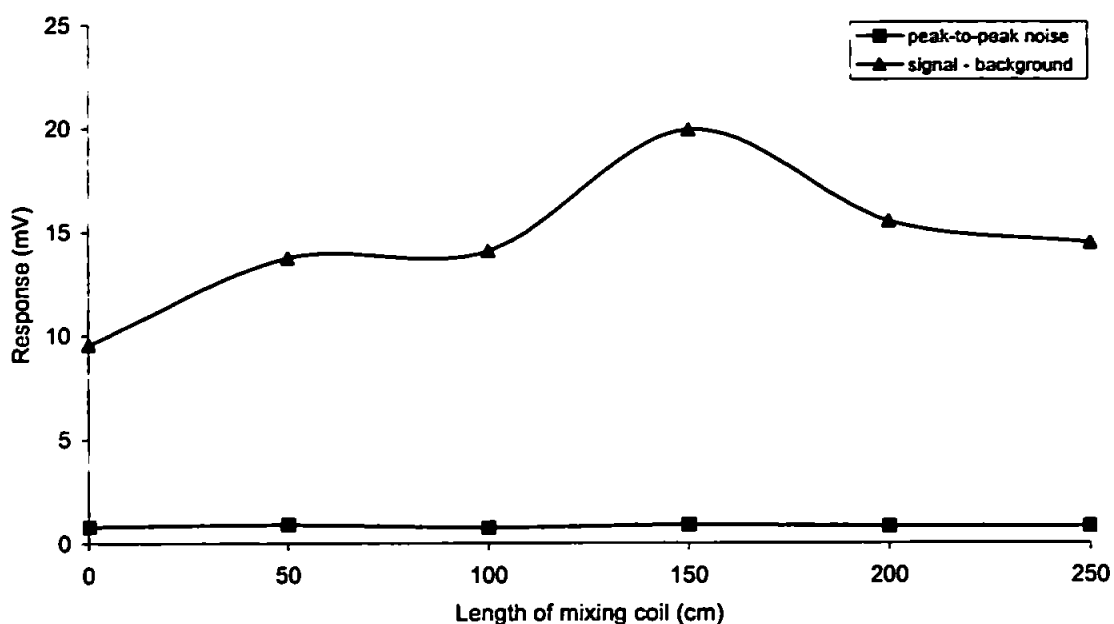


Figure 5.4. Effect of mixing coil length on the CL signal and peak-to-peak noise.

Either side of the optimum the signal-to-noise ratio and the overall reproducibility of the analysis diminished. This confirms the importance of optimising the mixing coil length for reaction rate based detection systems such as CL.

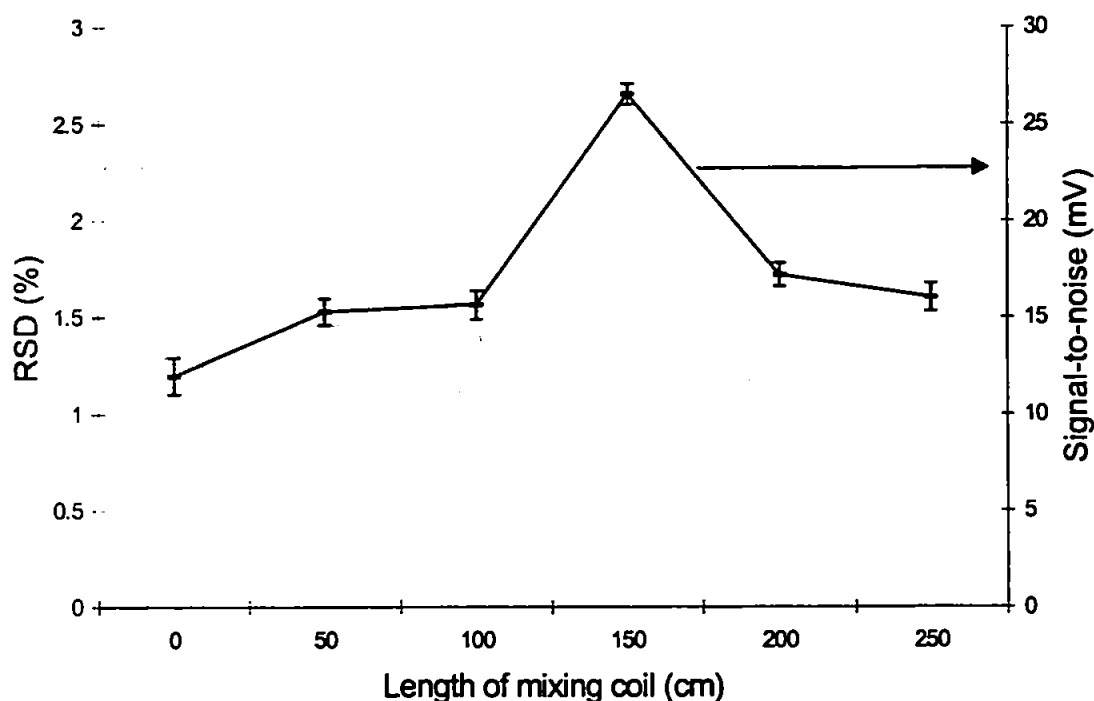


Figure 5.5. Effect of mixing coil length on the CL signal-to-noise (line chart, error bars = 3σ) and relative standard deviation (bar chart, $n = 5$).

With a change in coil length there is a change in the time taken for the analyte to reach the flow cell and therefore reaction kinetics significantly determine the final choice of coil length. Changes observed in signal-to-noise can be attributed to the increased or decreased light capture at the detector, as illustrated using the 'Time Window Concept' (Figure 5.6.) [236].

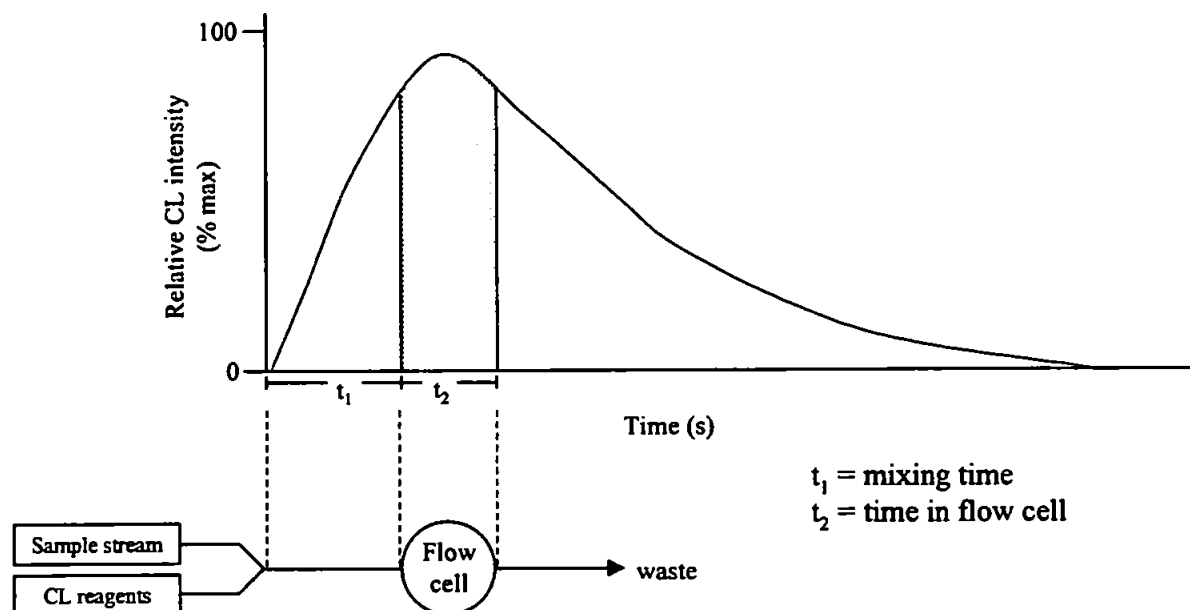


Figure 5.6. Time/intensity profile to illustrate the time window concept and how this is related to the length of the mixing coil.

With no reaction coil present the distance between the point of mixing and the flow cell was short ($\approx 2\text{cm}$) and therefore the point of maximum light emission occurred after passage through the flow cell, resulting in a low analyte signal being observed. As the distance between the point of mixing and the point of detection was increased (i.e. on addition of a mixing coil) the point of maximum light emission, and therefore detection occurred increasingly nearer to the flow cell. Further increases in the coil length increased the distance between mixing point and detection point and so the 'window' of maximum emission occurred before passage through the flow cell. Another way to optimise the CL emission intensity occurring in the detector window would be to alter the flow rates. However these were fixed in accordance with flow rates typically used in LC investigations, i.e. 0.1 to 10 ml min^{-1} [295-296]. Any changes in flow rate would lead to the requirement of existing chromatographic parameters having to be re-addressed if the aryl oxalate-sulphorhodamine 101 reaction was applied post-column.

Effect of water

To investigate the effect of water on the aryl oxalate-sulphorhodamine 101 reaction, the water content of the mobile phase was gradually increased (0 – 30%). This is an important parameter to investigate because it has already been shown that in aryl oxalate based CL systems containing water, hydrolysis diminishes the CL emission (*section 2.3.3*).

Figure 5.7 shows that an increase in water content to 10% led to an increase in the signal but, when increased further, the signal decreased dramatically. The figure also shows that the peak-to-peak noise decreased as the water content approached 10% before gradually increasing with a further increase in water content.

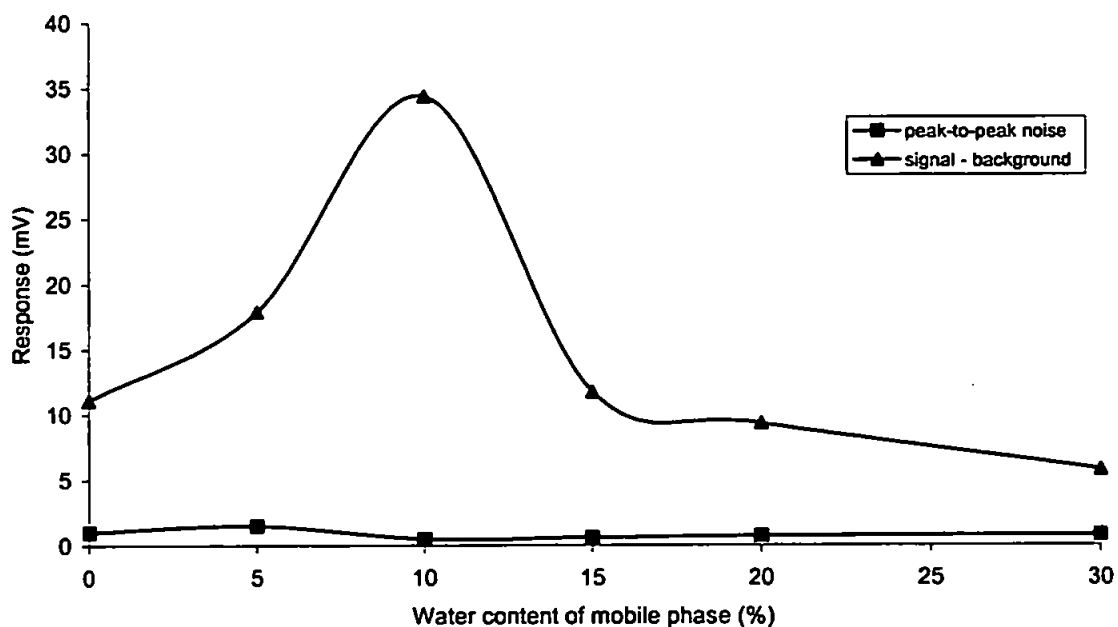


Figure 5.7. Effect of water content of mobile phase on the CL signal and peak-to-peak noise.

Figure 5.8 expresses the results as signal-to-noise ratio and clearly shows that an increase in water content up to 10% led to an increase in the signal-to-noise for the sulphorhodamine 101 system but, when increased further the signal-to-noise decreased. This was particularly severe at 30% water. The figure also shows that the RSD associated with the measurement of CL intensity increased as the water content of the mobile phase deviated in either direction from the 10% optimum.

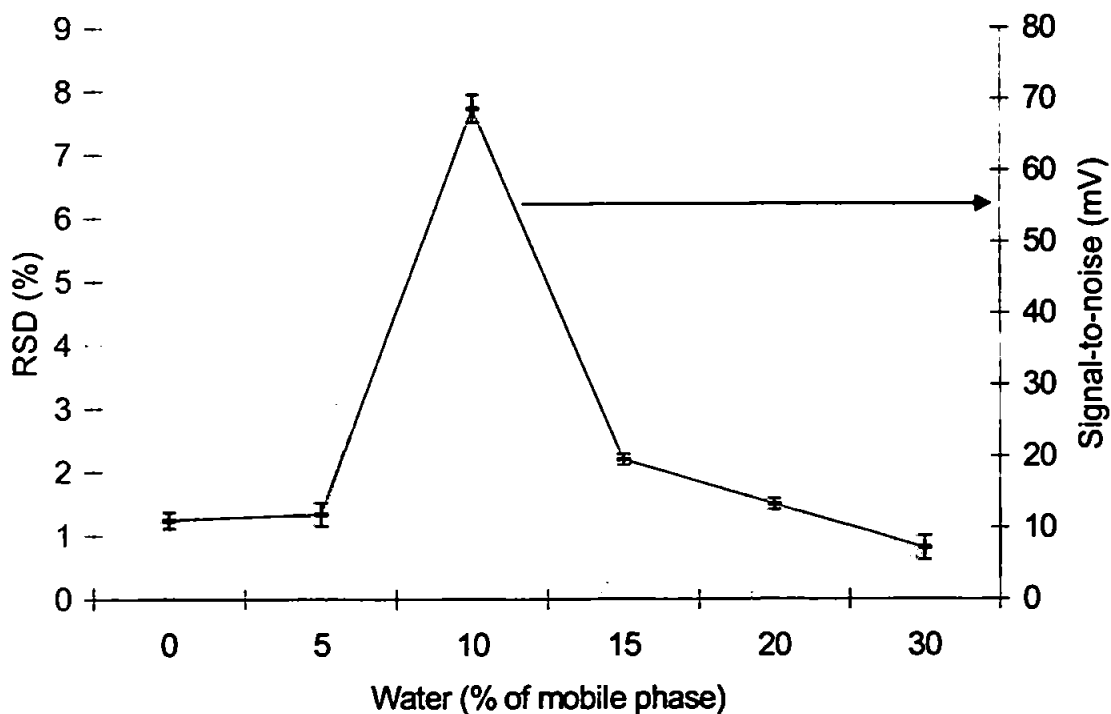
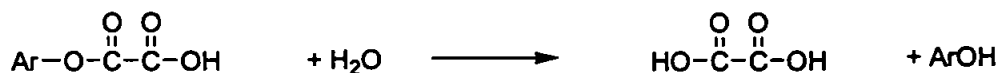
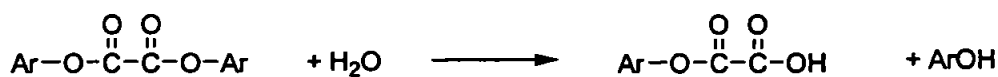
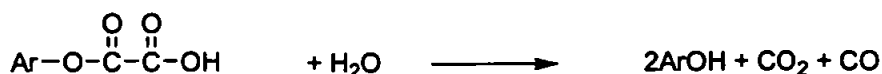


Figure 5.8. Effect of water content of mobile phase on the CL signal-to-noise (line chart, error bars = 3σ) and relative standard deviation (bar chart, $n = 5$).

The results observed are explained by the fact that water has a strong influence on the rate of formation and lifetime of the various POCL intermediates as described in the literature [228]. A 'concerted reaction mechanism' [297], 'an unexpected decomposition' [298] and a 'stepwise process' [228] are the three different mechanisms that have been postulated for the hydrolysis of aryl oxalates. The 'concerted reaction mechanism' involves the simultaneous hydrolysis of both ester functionalities of DNPO to liberate oxalic acid and two molecules of 2,4-dinitrophenol.



The 'unexpected decomposition' mechanism involves the hydrolysis coupled with decomposition of the DNPO to yield two molecules of 2,4-dinitrophenol and the gases carbon dioxide and carbon monoxide.



More recently it has been suggested that the hydrolysis takes the form of a stepwise process in which the hydrolysis of one of the ester groups is followed by rapid decomposition of the intermediate thus formed, through successive decarboxylation and decarbonylation processes rather than further hydrolysis [228].

The conclusion from each of these postulated mechanisms is that a species which is kinetically unfavourable for CL emission is produced and, in some cases, a species that will not participate in the formation of the CL intermediates required for POCL is formed. The 'Time Window Concept' has to be considered because as the kinetics of the reaction are altered then the point of maximum light emission will change. This helps to explain why a stronger signal was obtained when 10% water was included in the carrier stream than when no water was used at all. Indeed these results can be favourably compared with those observed during the optimisation of reaction conditions in *section 2.3.3*.

It is important at this stage to note that all mechanisms are postulated rather than proven because the intermediates required for unambiguous proof of a reaction mechanism have not been isolated.

Effect of H₂O₂ concentration

The effect of hydrogen peroxide over the range of 0.002-0.2 M was investigated and the results obtained are shown in Figure 5.9.

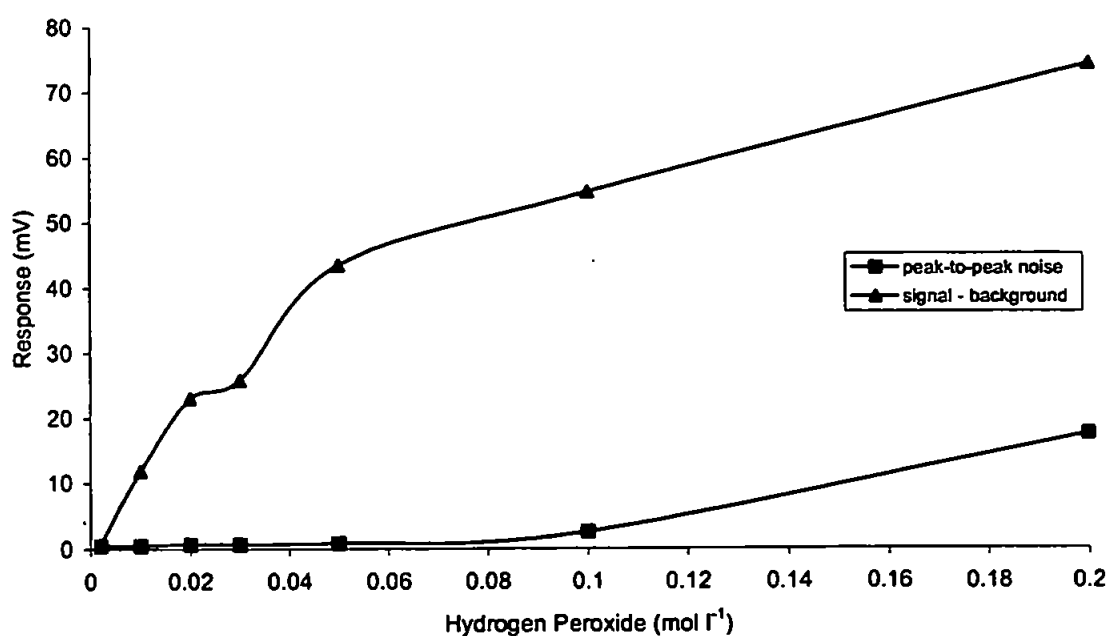


Figure 5.9. Effect of H₂O₂ on the CL signal and peak-to-peak noise.

Hydrogen peroxide was shown to have a major influence on the results obtained. The results show that there was an increase in both the observed signal and peak-to-peak noise as the concentration of hydrogen peroxide was increased. A plot of signal-to-noise ratio (Figure 5.10.) shows that there was an increase in the signal-to-noise as the concentration of hydrogen peroxide was increased up to 0.05 M, after which point a rapid decrease in signal-to-noise was observed.

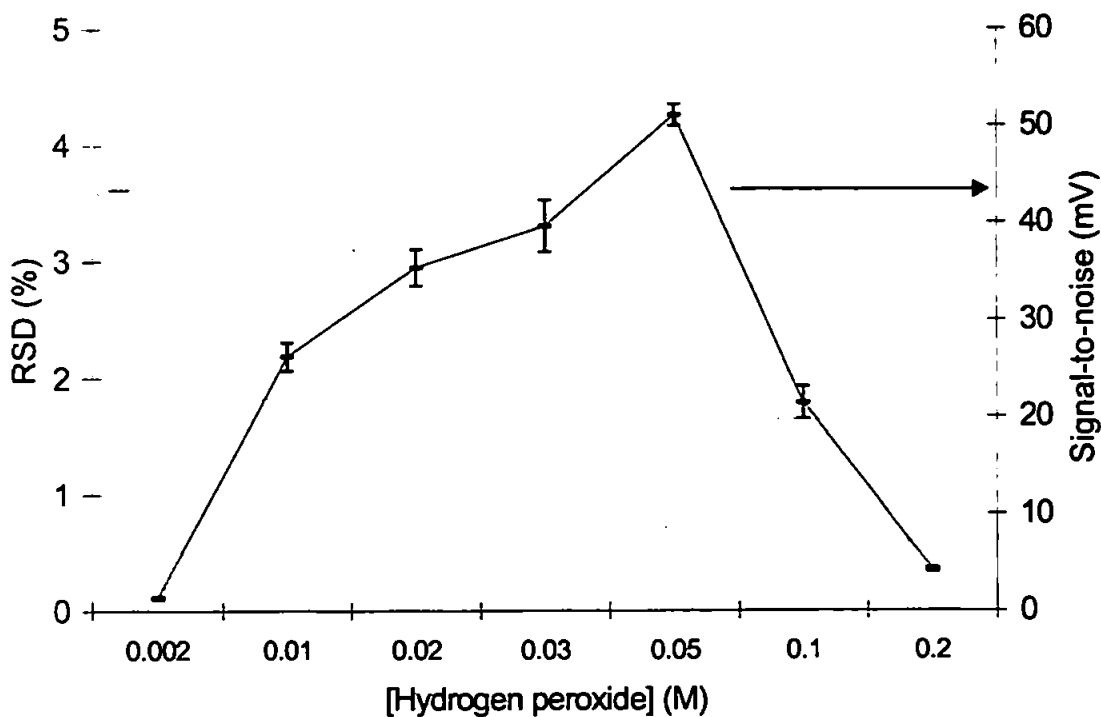


Figure 5.10. Effect of H_2O_2 on the CL signal-to-noise (line chart, error bars = 3σ) and relative standard deviation (bar chart, $n = 5$).

The concentration needs to be maintained between 0.04 M and 0.06 M in order to obtain greatest sensitivity. At lower than optimum concentrations the decrease in signal-to-noise can be explained by the lack of aryl oxalate oxidation. At higher than optimum concentrations the decrease in signal-to-noise can be explained by the formation of bubbles within the flowing stream which leads to increased peak-to-peak noise. At these levels the increase in peak-to-peak noise was more significant than the increase in observed signal and therefore a reduction in the overall signal-to-noise was obtained. A value of 0.05 M was recommended for future use, which falls within the typical range of 30 to 500 mM suggested for POCL detection systems in the literature [235].

Effect of DNPO concentration

The effect of DNPO concentration over the range of $5.0 \times 10^{-5} - 5.0 \times 10^{-3}$ M was investigated. The upper limit of this range was governed by solubility constraints and the results obtained are shown in Figure 5.11. The results show that the best signal was achieved using 5.0×10^{-4} M DNPO.

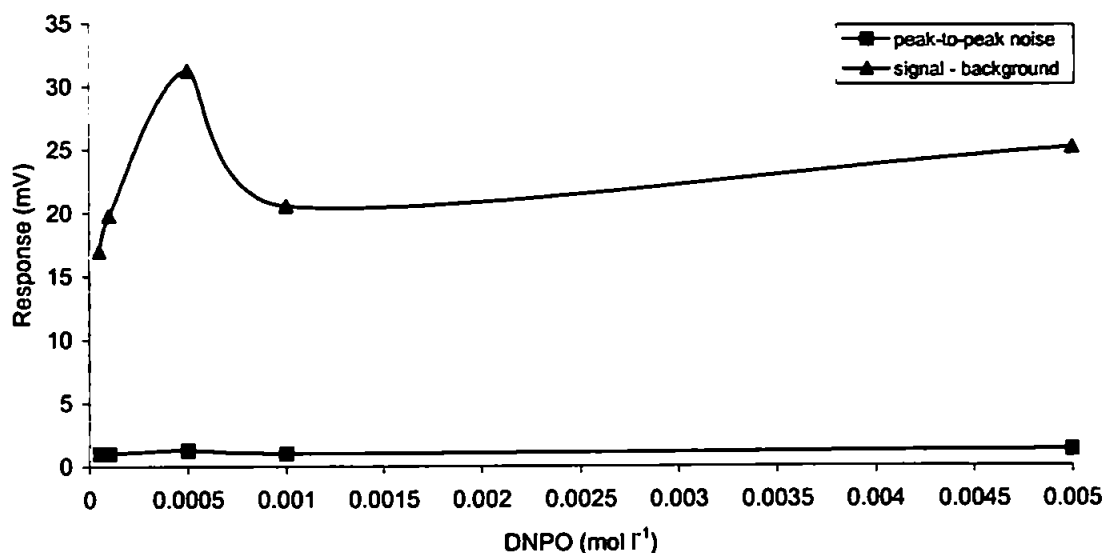


Figure 5.11. Effect of DNPO concentration on the CL signal and peak-to-peak noise.

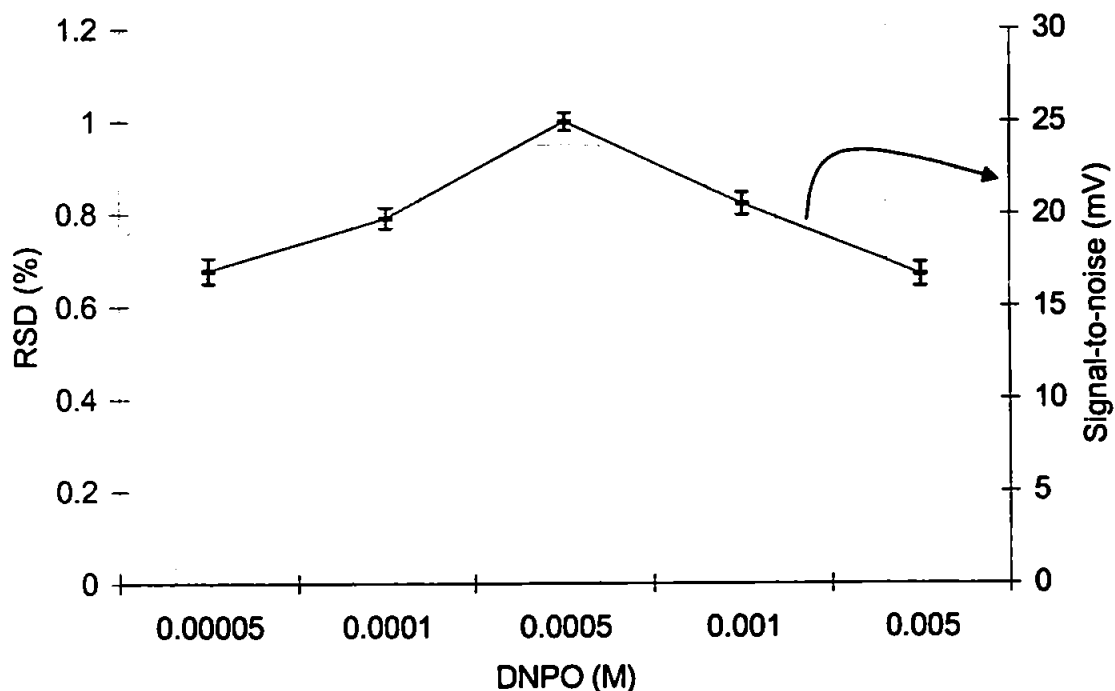


Figure 5.12. Effect of DNPO concentration on the CL signal-to-noise (line chart, error bars = 3σ) and relative standard deviation (bar chart, $n = 5$).

As the peak-to-peak noise did not change significantly, the best signal-to-noise was also achieved using 5.0×10^{-4} M DNPO (Figure 5.12.), which was recommended as the optimum value for DNPO for all further analyses. This value is slightly lower than the typical concentrations of oxalate ester used for the detection of fluorophores [235], which range from 1 to 10 mM. However the effect of DNPO concentration on response, signal-to-noise ratio and RSD is much less than the effect of the other parameters.

Effect of sulphorhodamine 101 concentration

The effect of sulphorhodamine 101 over the range of 1.0×10^{-8} – 1.0×10^{-5} M was investigated and the results obtained are shown in Figure 5.13. The observed signal increased over this range with sulphorhodamine concentration and the peak-to-peak noise also increased slightly.

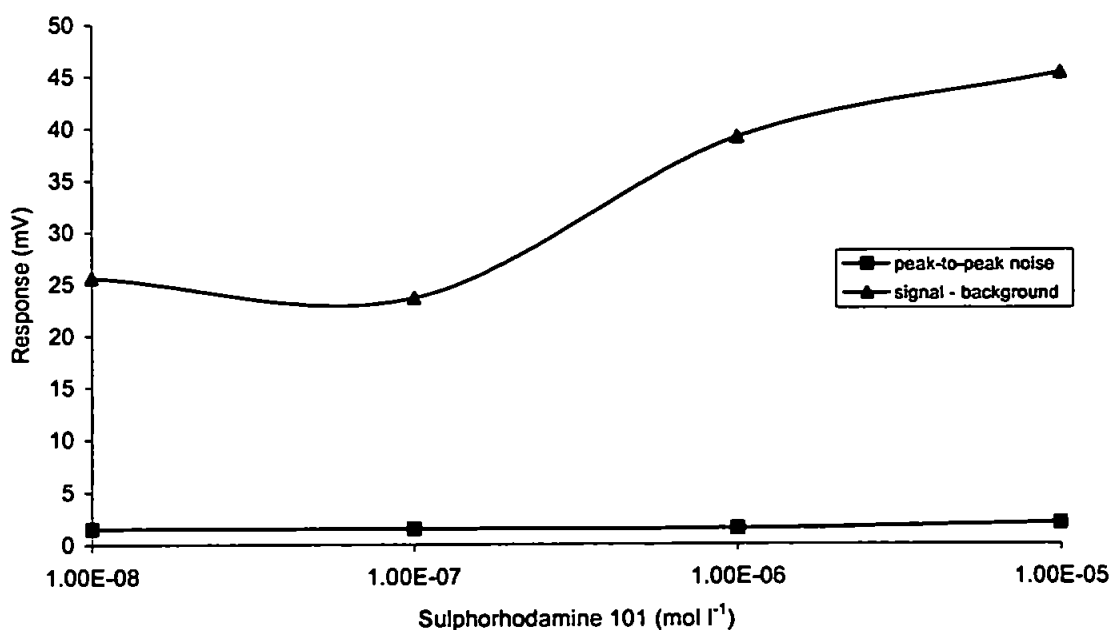


Figure 5.13. Effect of sulphorhodamine 101 concentration on the observed CL signal and peak-to-peak noise.

When plotted as a signal-to-noise ratio (Figure 5.14.) the results show that there was an increase in the signal-to-noise ratio as the concentration of sulphorhodamine 101 was increased. Although no optimum value was determined on the basis of signal-to-noise alone, it was observed that both the errors and RSD associated with the measurement of CL intensity increased as the sulphorhodamine 101 concentration increased to 1.0×10^{-5} M. For this reason the recommended sulphorhodamine 101 concentration for future use

was 1.0×10^{-6} M as this was shown to give a good signal-to-noise response with small errors and the lowest RSD (1.1%).

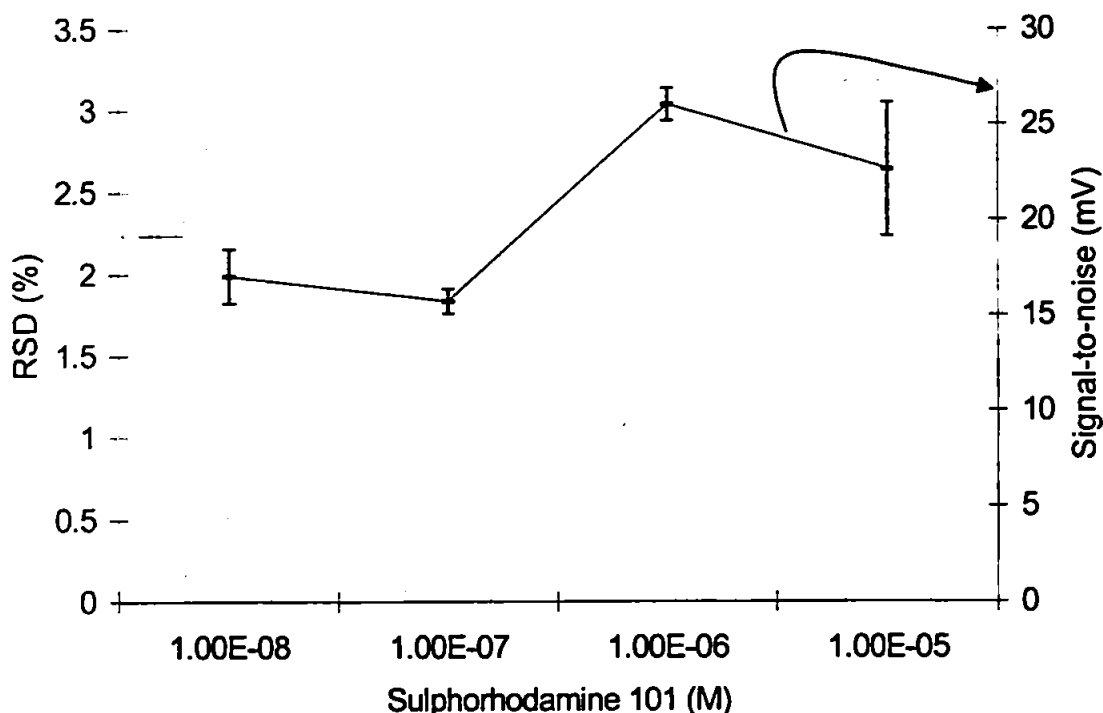


Figure 5.14. Effect of sulphorhodamine 101 concentration on the CL signal-to-noise (line chart, error bars = 3σ) and relative standard deviation (bar chart, $n = 5$).

Table 5.3 summarises the conditions used for the optimisation and the optimum parameters recommended for the sulphorhodamine 101 POCL determination of amines and these conditions were used for all subsequent analyses performed.

Table 5.3. Optimum conditions determined for detection of amines.		
Parameter	Range	Optimum Conc.
Mixing Coil	0 to 250 cm	150 cm
Mobile Phase	ACN/water (70/30) to ACN (100%)	ACN/water (90/10)
Hydrogen Peroxide	2.0×10^{-3} to 2.0×10^{-1} M	5.0×10^{-2} M
Sulphorhodamine 101	1.0×10^{-8} to 1.0×10^{-5} M	1.0×10^{-6} M
DNPO	5.0×10^{-5} to 5.0×10^{-3} M	5.0×10^{-4} M

From these results it is apparent that the concentration of hydrogen peroxide, mobile phase composition and length of mixing coil have the most significant influence on the CL

response. A simplex multivariate approach could also provide further optimisation of the reaction, although the above univariate approach has the advantage of highlighting the relative merits of optimising individual reaction conditions. These results are compared with reported values [91] in Table 5.4 and show good agreement. It is important to highlight that the aryl oxalate ester used in this investigation was DNPO rather than TDPO, although the concentration giving the best CL response was the same.

Table 5.4. Comparison of experimentally obtained reaction conditions with literature values [91].		
Parameter	Experimental conditions	Literature value
Mobile Phase	ACN/water (90/10)	ACN/water (95/5)
Hydrogen Peroxide	5.0×10^{-2} M	2.0×10^{-2} M
Sulphorhodamine 101	1.0×10^{-6} M	1.0×10^{-7} M
Aryl oxalate ester	5.0×10^{-4} M, (DNPO)	5.0×10^{-4} M, (TDPO)

5.3.3 Limits of detection

Using the optimum conditions shown in Table 5.3 for the FI investigation, limits of detection were obtained for selected amines. Ethylamine, diethylamine and triethylamine were chosen to represent a homologous series, imidazole was chosen because it is a known catalyst of the POCL reaction and dodecylamine was chosen because of its application as a detergent in fuels. Details about these amines are given in Table 5.5.

Table 5.5. Details of amines investigated.			
Amine	Formula	Mol. Wt.	Type
Ethylamine	$\text{CH}_3\text{CH}_2\text{NH}_2$	45.08	Primary
Diethylamine	$(\text{CH}_3\text{CH}_2)_2\text{NH}$	73.14	Secondary
Triethylamine	$(\text{CH}_3\text{CH}_2)_3\text{N}$	101.2	Tertiary
Imidazole		68.08	Cyclic
Dodecylamine	$\text{CH}_3(\text{CH}_2)_{11}\text{NH}_2$	185.34	Long chain primary

Table 5.6 shows the detection limits for the six amines in acetonitrile obtained by FI using sulphorhodamine 101 POCL detection. These were calculated as $\bar{y}_b + 3s_{y/x}$ where \bar{y}_b is the mean response of the blank and $s_{y/x}$ is the standard error of the y estimate [208].

Amine	LOD (mg l ⁻¹)	Gradient	Y-INTERCEPT	R ²	RANGE (mg l ⁻¹)
Imidazole	0.01 ± 0.01	1544.82	3.27	0.999	0 - 10
Ethylamine	0.01 ± 0.01	42.89	0.16	0.993	0 - 1
Diethylamine	0.21 ± 0.05	11.67	-0.09	0.999	0 - 10
Triethylamine	0.56 ± 0.04	11.61	1.93	0.998	0 - 10
Dodecylamine	1.03 ± 0.08	11.84	2.70	0.993	0 - 10

The results obtained have shown that the system used was able to detect amines at the ppm level. The sensitivity for the alkyl amines determined was independent of the alkyl chain length as shown by the similarity in gradient observed for diethylamine, triethylamine and dodecylamine. This was a particularly useful observation because performance enhancing additive compounds generally contain long and varying alkyl chain lengths rather than low molecular weight amines due to their higher solubility and greater stability.

The experimentally obtained detection limits were higher than those reported by Katayama *et al.* [91] (Table 5.7), due to the fact that DNPO has been used in place of TDPO. This is because DNPO is more readily available (there is no commercial source of TDPO) and relatively inexpensive and therefore more suitable for routine use.

Amine	Experimental (M)	Literature (M)
Imidazole	1.5×10^{-7}	2.0×10^{-10}
Ethylamine	2.2×10^{-7}	N/A
Diethylamine	2.9×10^{-6}	1.4×10^{-8}
Triethylamine	5.5×10^{-6}	7.0×10^{-7}
Dodecylamine	9.8×10^{-6}	N/A

5.3.3 Application to a diesel fuel matrix

The results discussed above have only dealt with amines in acetonitrile, which is a synthetic sample matrix. Diesel fuel however is by no means a simple matrix, because its composition is dependent on the source of crude oil from which the fuel is derived and the refining processes used to manufacture the fuel. This matrix would therefore potentially introduce interference problems, e.g. from other amine containing compounds naturally present and from other constituents able to participate in the POCL reactions.

A diesel fuel that had not been modified with any additive packages was investigated to determine the magnitude of the matrix interference. On injection of a diluted diesel sample a response was recorded that was off-scale and could therefore not be quantified. An investigation was conducted to determine which of the components of the raw diesel fuel were responsible for the large CL emissions recorded.

A homologous series of hydrocarbons were injected to determine which groups of compounds showed a response to the CL reagents within the system used. The hydrocarbons used for this investigation were hexane, cyclohexane, *o*-xylene 1-methylnaphthalene and phenanthrene. From these results it was observed that the diaromatics and tri+ aromatics reacted with the CL reagents. Unfortunately diesel fuel is comprised of massive quantities of these compounds and therefore extraction of the amine additives would have to be achieved before they could be quantified within the diesel matrix.

A second problem is that additives are introduced to a fuel as part of an additive package, which contains mixtures of compounds having broadly similar structures, rather than single chemical entities. Within any particular fuel there will exist any number of additive compounds that might show a response using the CL system described. A system whereby a particular compound, or group of compounds, can be isolated therefore needs to be investigated.

Solid Phase Extraction (SPE) is a technique that is used to separate and preconcentrate analytes from an interfering matrix. SPE has a number of advantages that would enable its use as part of a portable monitoring system;

- uses small volumes of common solvents
- requires very little laboratory skills
- allows rapid sample throughput
- does not require the use of highly specialized equipment
- can be easily automated

A typical sequence used in SPE has been summarised in Figure 5.15. It should be remembered however that there are several SPE modes that can be used, each having their own relative merits.

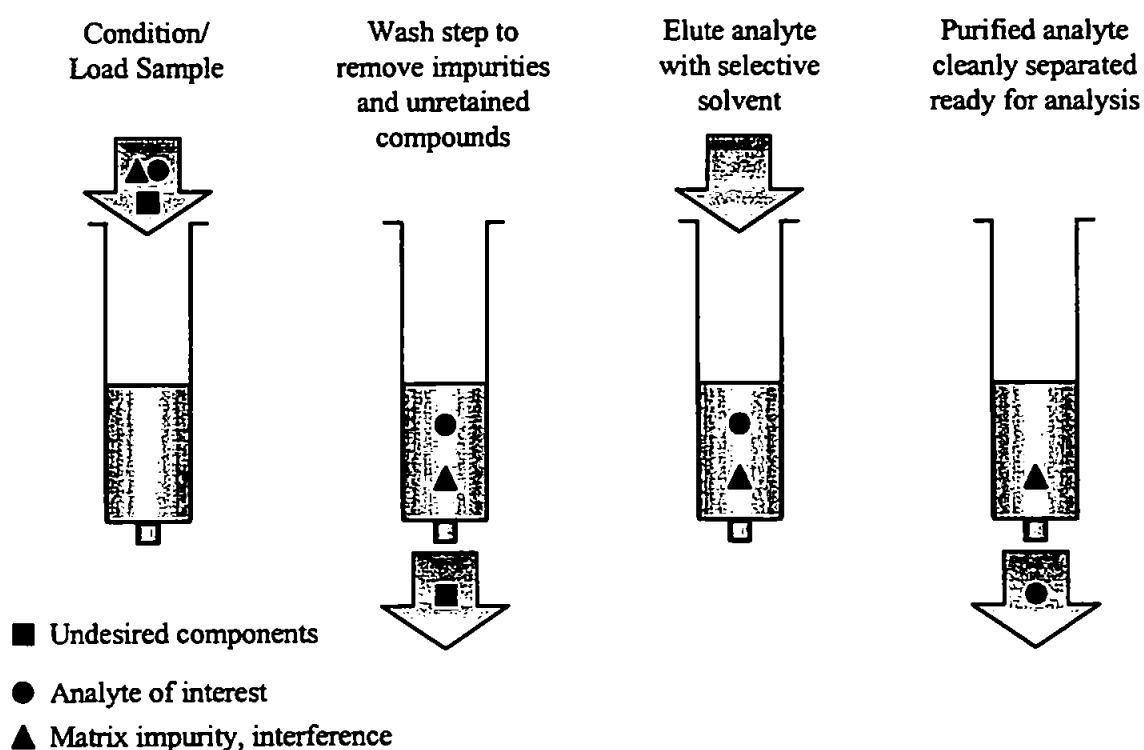


Figure 5.15. Typical SPE sequence.

The chromatographic characteristics of the phase will strongly influence which sample components will be retained on the phase and the strength of retention. Phase selection will be governed by the analytes to be extracted, sample matrix components and the sample solvent. Diesel fuel contains predominantly non-polar species. Dodecylamine is slightly polar and for this reason a polar SPE cartridges might be chosen for the separation and isolation from a fuel matrix. The non-polar species should travel straight through the polar cartridges, retaining only the polar species (including dodecylamine). Several types of polar cartridges are available and are shown in Figure 5.16.

—Si—OH	Silica (Si)
—Si—CH ₂ CH ₂ CH ₂ CN	Cyano (CN)
—Si—CH ₂ CH ₂ CH ₂ NH ₂	Amino (NH ₂)
—Si—CH ₂ CH ₂ CH ₂ NHCH ₂ CH ₂ NH ₂	Primary / Secondary amine (PSA)
—Si—CH ₂ CH ₂ CH ₂ OCH ₂ CHCH OHOH	Diol (2OH)

Figure 5.16. Commercially available polar SPE cartridges.

5.4 CONCLUSIONS

1. Hydrogen peroxide was shown to have significant influence on the CL signal obtained. Little deviation (± 0.02 M) from the 0.05 M optimum resulted in a 20% loss of signal-to-noise. Therefore the concentration needs to be maintained carefully between 0.04 M and 0.06 M in order to obtain greatest sensitivity.
2. The amount of water in the carrier stream also needs careful attention as this was shown to have a major influence on the signal obtained. This becomes particularly important when considering any chromatographic separation prior to detection. The recommended optimum of 10% water content should be maintained wherever possible.
3. Sulphorhodamine 101 and DNPO were shown to have little effect on the signal obtained over the concentration ranges investigated although optimum concentrations of 1.0×10^{-6} M and 5.0×10^{-4} M respectively were identified.
4. These experiments have shown that FI with POCL detection (using DNPO and sulphorhodamine 101) can be used for the quantification of primary amines (including dodecylamine) in the ppm range.
5. For the application of the method to diesel fuels however a sample clean up procedure using SPE would be required. It should be possible to include this step (once optimised) in a portable FI system for field deployment, e.g. at the garage forecourt.

CHAPTER 6

Conclusions and future work

6. CONCLUSIONS AND FUTURE WORK

6.1 GENERAL CONCLUSIONS

In addition to the specific conclusions discussed at the end of each experimental chapter, the following general conclusions can be drawn from the work described in this thesis;

- 1 Flow injection was shown to be a suitable technique for the determination of PAHs when coupled with FL and/or CL detection. After identification of optimum excitation and emission wavelengths, FL was shown to provide a very sensitive method for PAH detection. POCL detection was shown to provide an additional method for PAH detection, although, with the exception of perylene, was not found to provide quite the sensitivity of FL detection. It was also shown that the reaction parameters for POCL detection require careful optimisation if sensitivity is to be achieved. A comparison between DNPO and TCPO has shown that DNPO was more suitable for the detection of PAHs by POCL detection. The use of a low power (12 V) PMT based CL detector gave lower limits of detection than the PD based CL detector for the DNPO reaction. Detection limits for the PAHs investigated in this work using the low power (12 V) PMT based detector were in the pg range and broadly comparable with those reported elsewhere for CL detection using high power (1 kV) PMTs. This fundamental study has shown that FI techniques provide a reliable, robust sample delivery method for both FL and CL detection.
2. Reversed phase LC has been shown to provide a suitable method for the separation of PAH mixtures. From the three columns investigated (Spherisorb S5 PAH, LiChrospher PAH, and Envirosep-PP) it was shown that the LiChrospher PAH column provided the best separations of the 16 PAH test mixture. Wavelength programmed fluorescence detection has been shown to provide an excellent technique for the sensitive detection of PAHs after chromatographic separation and has shown good agreement with SRM1649 and SRM1650 certified values. Post column POCL detection has been applied to the analysis of PAHs after reversed phase and normal phase LC separations. It was observed that problems due to the water content of the mobile phase gradient for the reversed phase system severely hampered the detection of PAHs at environmentally significant levels. Normal phase chromatography (Hypersil Green PAH-2) was shown to offer some improvement for the analysis of

PAHs by LC using POCL detection because the absence of water from the mobile phase gradient provided a more stable baseline. As a laboratory based detector for LC, CL provides complementary information to that obtained with fluorescence detection and has the potential to be field deployable for PAH screening.

3. Multivariate calibration techniques enabled the quantification of PAHs using spectrophotometric data obtained for synthetic model systems. The three calibration techniques (PCR, PLS1 and PLS2) examined were all capable of an acceptable degree of precision (e.g. 10-15%). A procedure whereby individual spectra were 'glued' together before undergoing data analysis was investigated and the results obtained were shown to provide an improvement in the predictive accuracy of the calibration models constructed. When using FL detection the lowest prediction errors (4.8-10.6%) were achieved for anthracene, benzo[k]fluoranthene and benzo[a]pyrene, indicating that these PAHs could be accurately quantified in the 3-, 4- and 5-component systems. The predictive accuracies for fluoranthene and chrysene in the 4- and 5-component systems were significantly poorer however, since their fluorescence intensities are significantly lower in acetonitrile than anthracene, benzo[k]fluoranthene or benzo[a]pyrene.

A CCD based continuous flow system has been used to acquire full spectrum CL emission profiles and, in conjunction with multivariate calibration, was capable of a high degree of predictive accuracy (< 9%) for a synthetic two-component mixture of benzo[k]fluoranthene and benzo[a]pyrene in hexane. The combination of CL with CCD detection and multivariate calibration therefore has the potential to provide quantitative information in the field without the need for separation, as well as providing fundamental data that may be used for the study of the CL emission mechanism.

4. These experiments have shown that FI with aryl oxalate sulphorhodamine-101 CL can be used for the quantification of primary amines (including dodecylamine) in the ppm range. FI studies allowed the optimisation of the reaction conditions, highlighting hydrogen peroxide concentration, mobile phase composition and length of mixing coil as the most significant parameters for optimisation. Application of the method to a diesel fuel matrix has shown that before a field deployable system could be designed more attention to sample clean-up is needed.

6.2 SUGGESTIONS FOR FUTURE WORK

Possible directions for future work arising from this research can be divided into four separate areas;

Flow Injection

- The FI technique was shown to be an effective sample delivery method for the FL and CL detection systems. Advances in both instrumentation and more widely applicable CL chemistries would lead to more robust, easy to use systems for wider application within the industrial environment.

Liquid Chromatography

- The LC-CL approach has shown that in order to maximise the signal response obtained for a POCL system the gradient effects need careful attention and an investigation of mixing efficiency may provide a short term remedy to the problem.
- More longer term propositions include the development of novel CL reagents that are not significantly affected by changes in reversed phase gradient programmes. Another approach would be to further investigate the NP-LC approach with CL detection for the quantification of PAHs in non-aqueous matrices. This would include the evaluation of new NP column technologies and a full optimisation of the NP-LC-CL detection technique. Further validation of SRMs would be performed and a more comprehensive comparison between the FL and CL data would be investigated to show how the two techniques could be seen as being complementary in the information available.

Multivariate calibration

- Multivariate calibration routines have been shown to provide an approach that allows the quantification of PAH components in simple synthetic mixtures without prior separation methods being employed. The future of this technique would involve the detailed investigation of its use as a rapid screening method for the quantification of PAHs by classes e.g. ring size, analogues and nitro-PAH, rather than by individual components. This approach is far more realisable and would involve the building of larger data sets containing more components and levels. Ideally the calibration model would be applicable to a variety of typical matrices

from which sample extraction was performed and would be expandable as more data was collected and added to the model over time.

- Other mathematical algorithms, e.g. neural networks and non-linear chemometric techniques, might also provide useful approaches to increased quantification of samples.
- The process of spectral gluing could be investigated further to allow the maximum amount of information to be extractable from the collected data. Suggestions could include the gluing of FL and CL spectra and the gluing of spectra in differing solvents.

Other systems

- The realisation of a field deployable (e.g. petrol station forecourt) system for the quantification of dodecylamine in diesel fuel would be investigated using SPE coupled with CL detection. Automation of the technique using LabVIEW[®] might also be considered after suitable techniques for matrix removal had been achieved. Other functional groups within fuels would also be considered.

References

1. Web site: <http://www.bp.com/bpstats/pages/oil.htm>.
2. Freemantle, M., *Chemistry in Action*, Macmillan Press, London, 1994, pp 709-716.
3. Campbell, A. K., *Chemiluminescence*, Ellis Horwood, Chichester, 1988.
4. Schulman, S. G., (Ed), *Molecular Luminescence Spectroscopy, Methods and Applications, Part 1*, Wiley-Interscience, New York, 1985.
5. Schulman, S. G., (Ed), *Molecular Luminescence Spectroscopy, Methods and Applications, Part 2*, Wiley-Interscience, New York, 1988.
6. Barnett, N. W., and Evans, R. N., *Encyclopedia of Analytical Science* (Ed. Townshend, A.), Academic Press, London, 1995, Vol. 5, pp 2735-2749.
7. Gooijer, C., Velthorst, N. H., and Frei, R. W., *Trends Anal. Chem.*, 1984, 3, 259.
8. Hurtubise, R. J., *Phosphorimetry, Theory, Instrumentation and Applications*, VCH, New York, 1990.
9. Skoog, D. A., West, D. M., and Holler, F. J., *Fundamentals of Anal. Chem.*, 5th edn., Saunders College Publishing, New York, 1988, pp 534-538.
10. Blatchford, C., and Malcolm-Laws, D. J., *J. Chromatogr.*, 1985, 321, 227.
11. Blatchford, C., Humphreys, E., and Malcolm-Laws, D. J., *J. Chromatogr.*, 1985, 329, 281.
12. Hill, E., Humphreys, E., and Malcolm-Laws, D. J., *J. Chromatogr.*, 1986, 370, 427.
13. Hill, E., Humphreys, E., and Malcolm-Laws, D. J., *J. Chromatogr.*, 1988, 441, 394.
14. Robards, K., and Worsfold, P. J., *Anal. Chim. Acta*, 1992, 266, 147.
15. Nabi, A., and Worsfold, P. J., *Anal. Chim. Acta*, 1986, 111, 1321.
16. Worsfold, P. J., and Nabi, A., *Anal. Chim. Acta*, 1986, 179, 307.
17. *Photomultipliers and Accessories*, Thorn-EMI, Ruislip, 1993.
18. Campbell, A. K., *Chemiluminescence, Principles and Applications in Biology and Medicine*, Ellis Horwood, Chichester, 1989, pp 100.
19. Gachanja, A. N., and Worsfold, P. J., *Anal. Chim. Acta*, 1994, 290, 226.
20. Hemmi, A., Yagiuda, K., Funazaki, N., Ito, S., Asano, Y., Imato, T., Hayashi, K., and Karube, I., *Anal. Chim. Acta*, 1995, 316, 323.
21. Hayashi, K., Sasaki, S., Ikebukuro, K., and Karube, I., *Anal. Chim. Acta*, 1996, 329, 127.
22. Epperson, P. M., Sweedler, J. V., Bilhorn, R. B., Sims, G. R., and Denton, M. B., *Anal. Chem.*, 1988, 60, 327A.
23. Falkin, D., and Vosloo, M., *Spec. Europe*, 1993, 5, 16.
24. Stanley, P. E., *J. Biolumin. Chemilumin.* 1996, 11, 175.
25. Ruzicka, J., and Hansen, E.H., *Flow Injection Analysis*, 2nd edn., Wiley-Interscience., New York., 1988.

26. Ruzicka, J., and Hansen, E.H., *Anal. Chim. Acta*, 1975, 78, 145.
27. Ruzicka, J., and Hansen, E.H., *Anal. Chim. Acta*, 1978, 99, 178.
28. Various authors, Papers presented at the fifth International Conference of Flow Analysis, Kumamoto, Japan, *Anal. Chim. Acta*, 1992, 261, pp 1-581.
29. Various authors, Papers presented at the sixth International Conference of Flow Analysis, Toledo, Spain, *Anal. Chim. Acta*, 1995, 308, pp 1-472.
30. Valcarcel, M., and Luque de Castro, M. D., *Flow Injection Analysis - principles and applications*, Ellis Horwood, Chichester, 1987.
31. Karlberg, B., and Pacey, G., *Flow Injection Analysis - a practical guide*, Elsevier, Amsterdam, 1989.
32. Betteridge, D., *Anal. Chem.*, 1978, 50, 832A.
33. Ruzicka, J., *Anal. Chem.*, 1983, 55, 1041A.
34. Maugh II, T. H., *Science*, 1984, 224, 45.
35. Ruzicka, J., *Analyst*, 1994, 119, 1925.
36. Audunsson, G., *Anal. Chem.*, 1986, 58, 2714.
37. Van der Linden, W. E., *Anal. Chim. Acta*, 1983, 151, 359.
38. The Standing Committee of Analysts, DoE, *Flow Injection Analysis – An Essay Review and Analytical Methods 1990*, HMSO, London, 1991.
39. Luque de Castro, M. D., *Encyclopedia of Analytical Science* (Ed. Townshend, A.), Academic Press, London, 1995, Vol. 3, pp 1299-1300.
40. Trojanowicz, M., Worsfold, P.J., and Clinch, J.R., *Trends Anal. Chem.*, 1988, 7, 301.
41. Nickson, R. A., Hill, S. J., and Worsfold, P. J., *Anal. Proc.*, 1995, 32, 387.
42. Chen, G. N., Duan, J. P., and Hu, Q. F., *Mikrochimica Acta* 1994, 116, 227.
43. Lin, Q. X., Guiraum, A., Escobar, R., and Delarosa, F. F., *Anal. Chim. Acta*, 1993, 283, 379.
44. Makita, Y., Suzuki, T., Yamada, M., and Hobo, T., *Nippon Kagaku Kaishi*, 1994, 701.
45. Makita, Y., Umebayashi, H., Suzuki, T., Masuda, A., Yamada, M., and Hobo, T., *Chem. Lett.*, 1993, 1575.
46. Sunda, W. G., and Huntsman, S. A., *Mar. Chem.*, 1991, 36, 137.
47. Coale, K. H., Johnson, K. S., Stout, P. M., and Sakamoto, C. M., *Anal. Chim. Acta*, 1992, 266, 345.
48. Escobar, R., Lin, Q. X., Guiraum, A., and Delarosa, F.F., *Analyst*, 1993, 118, 643.
49. Nakano, S., Fukuda, M., Kageyama, S., Itabashi, H., and Kawashima, T., *Talanta*, 1993, 40, 75.
50. Gammelgaard, B., Jons, O., and Nielsen, B., *Analyst*, 1992, 117, 637.

51. Beere, H. G., and Jones, P., *Anal. Chim. Acta*, 1994, 293, 237.
52. Imdadullah, Fujiwara, T., and Kumamaru, T., *Anal. Chem.*, 1991, 63, 2348.
53. Imdadullah, Fujiwara, T., and Kumamaru, T., *Anal. Chem.*, 1993, 65, 421.
54. Imdadullah, *Bunseki Kagaku*, 1994, 43, 363.
55. Elrod, V. A., Johnson, K. S., and Coale, K. H., *Anal. Chem.*, 1991, 63, 893.
56. Obata, H., Karatani, H., and Nakayama, E., *Anal. Chem.*, 1993, 65, 1524.
57. Chapin, T. P., Johnson, K. S., and Coale, K. H., *Anal. Chim. Acta*, 1991, 249, 469.
58. Bowie, A. R., Fielden, P. R., Lowe, R. D., and Snook, R. D., *Analyst*, 1995, 120, 2119.
59. Imdadullah, Fujiwara, T., and Kumamaru, T., *Anal. Chim. Acta*, 1994, 292, 151.
60. Jones, P., and Beere, H. G., *Anal. Proc.*, 1995, 32, 169.
61. Alwarthan, A. A., Almuaibed, A., and Townshend, A., *Anal. Sci.*, 1991, 7, 623.
62. Ishii, M., Anazawa, Y., and Akai, T., *Nippon Kagaku Kaishi*, 1992, 1332.
63. Katayama, M., Takeuchi, H., and Taniguchi, H., *Anal. Lett.*, 1991, 24, 1005.
64. Rao, N. M., Hool, K., and Nieman, T. A., *Anal. Chim. Acta*, 1992, 266, 279.
65. Ishii, M., and Shirai, M., *Bunseki Kagaku*, 1992, 41, 125.
66. Ci, Y. X., Tie, J. K., Yao, F. J., Liu, Z. L., Lin, S., and Zheng, W. Q., *Anal. Chim. Acta*, 1993, 277, 67.
67. Preuschoff, F., Spohn, U., Blankenstein, G., Mohr, K. H., and Kula, M. R., *Fres. J. Anal. Chem.*, 1993, 346, 924.
68. Stigbrand, M., Ponten, E., and Irgum, K., *Anal. Chem.*, 1994, 66, 1766.
69. Price, D., Worsfold, P. J., and Mantoura, R. F. C., *Anal. Chim. Acta* 1994, 298, 121.
70. Tucker, D. J., Toivola, B., Pollema, C. H., Ruzicka, J., and Christian, G. D., *Analyst*, 1994, 119, 975.
71. Hu, X. C., Takenaka, N., Takasuna, S., Kitano, M., Bandow, H., Maeda, Y., and Hattori, M., *Anal. Chem.*, 1993, 65, 3489.
72. Niederlander, H. A. G., Dejong, M. M., Gooijer, C., and Velthorst, N. H., *Anal. Chim. Acta*, 1994, 290, 201.
73. Chung, H. K., Bellamy, H. S., and Dasgupta, P. K., *Talanta*, 1992, 39, 593.
74. Yan, B., Worsfold, P. J., and Robards, K., *Analyst*, 1991, 116, 1227.
75. Alwarthan, A. A., *Talanta*, 1994, 41, 1683.
76. Ishii, M., *Anal. Sci.*, 1991, 7, 703.
77. Lu, J. Z., Qin, W., Zhang, Z. J., Feng, M. L., and Wang, Y. J., *Anal. Chim. Acta*, 1995, 304, 369.
78. Sen, N. P., Baddoo, P. A., and Seaman, S. W., *J. Chromatog. A*, 1994, 673, 77.
79. Dunham, A. J., Barkley, R. M., and Sievers, R. E., *Anal. Chem.*, 1995, 67, 220.

80. Liu, R. M., Liu, D. J., Sun, A. L., and Liu, G. H., *Talanta*, 1995, 42, 437.
81. Aoki, T., and Wakabayashi, M., *Anal. Chim. Acta*, 1995, 308, 308.
82. Sakai, H., Fujiwara, T., and Kumamaru, T., *Anal. Chim. Acta*, 1995, 302, 173.
83. Huang, Y. L., Kim, J. M., and Schmid, R. D., *Anal. Chim. Acta*, 1992, 266, 317.
84. Paulls, D. A., and Townshend, A., *Analyst*, 1995, 120, 467.
85. Xie, X. F., Suleiman, A. A., Guilbault, G. G., Yang, Z. M., and Sun, Z.A., *Anal. Chim. Acta*, 1992, 266, 325.
86. Marshall, R. W., and Gibson, T. D., *Anal. Chim. Acta*, 1992, 266, 309.
87. Kondruweit, S., Dremel, B. A. A., and Schmid, R. D., *Anal. Lett.*, 1994, 27, 1489.
88. Sekine, Y., Suzuki, M., Takeuchi, T., Tamiya, E., and Karube, I., *Anal. Chim. Acta*, 1993, 280, 179.
89. Zhuang, H. S., Zhang, F., and Wang, Q. E., *Analyst*, 1995, 120, 121.
90. Worsfold, P. J., and Yan, B., *Anal. Chim. Acta*, 1991, 246, 447.
91. Katayama, M., Takeuchi H., Taniguchi H., *Anal. Chim. Acta*, 1993, 281, 111.
92. Hayashi J, Yamada, M., and Hobo, T., *Anal. Chim. Acta*, 1991, 247, 27.
93. Deftereos, N. T., Calokerinos, A. C., and Efstathiou, C. E., *Analyst*, 1993, 118, 627.
94. Hayashi, J., Yamada, M., and Hobo, T., *Anal. Chim. Acta*, 1992, 259, 67.
95. Ci, Y. X., Tie, J. K., Wang, Q. W., and Chang, W. B., *Anal. Chim. Acta*, 1992, 269, 109.
96. Preuschoff, F., Spohn, U., Weber, E., Unverhau, K., and Mohr, K. H., *Anal. Chim. Acta*, 1993, 280, 185.
97. Nakashima, K., Hayashida, N., Kawaguchi, S., Akiyama, S., Tsukamoto, Y., and Imai, K., *Anal. Sci.*, 1991, 7, 715.
98. Naslund, B., Arner, P., Bolinder, J., Hallander, L., and Lundin, A., *Anal. Biochem.*, 1991, 192, 237.
99. Suleiman, A. A., Villarta, R. L., and Guilbault, G. G., *Anal. Lett.*, 1993, 26, 1493.
100. Barnett, N. W., Rolfe, D. G., Bowser, T. A., and Paton, T. W., *Anal. Chim. Acta*, 1993, 282, 551.
101. Zhang, X. R., Baeyens, W. R. G., Vandenborre, A., Vanderweken, G., Calokerinos, A. C., and Schulman, S. G., *Analyst*, 1995, 120, 463.
102. Tie, J. K., Chang, W. B., and Ci, Y. X., *Anal. Chim. Acta*, 1995, 300, 215.
103. Delavalle, R., and Grayeski, M. L., *Anal. Biochem.*, 1991, 197, 340.
104. Kiba, N., Ueda, F., Saegusa, K., Goto, Y., Furusawa, M., and Yamane, T., *Anal. Chim. Acta*, 1993, 271, 47.
105. Tabata, M., Totani, M., and Endo, J., *Anal. Chim. Acta*, 1992, 262, 315.

106. Blankenstein, G., Preuschoff, F., Spohn, U., Mohr, K. H., and Kula, M. R., *Anal. Chim. Acta*, 1993, 271, 231.
107. Kiba, N., Koemado, H., and Furusawa, M., *Anal. Chim. Acta*, 1994, 290, 357.
108. Edwards, R., Townshend, A., and Stoddart, B., *Analyst*, 1995, 120, 117.
109. Alwarthan, A. A., *Analyst*, 1993, 118, 639.
110. Perezruiz, T., Martinezlozano, C., and Sanz, A., *Anal. Chim. Acta*, 1995, 308, 299.
111. Sato, K., Chiba, Y., and Tanaka, S., *Anal. Chim. Acta*, 1993, 277, 61.
112. Alwarthan, A. A., *Anal. Sci.*, 1994, 10, 919.
113. Perezruiz, T., Martinezlozano, C., Sanz, A., and Tomas, V., *Analyst*, 1994, 119, 1825.
114. Zhou, Y. K., Li, H., Liu, Y., and Liang, G. Y., *Anal. Chim. Acta*, 1991, 243, 127.
115. Ohno, Y., Hobo, T., Suyama, M., Tamura, R., and Ishii, M., *Anal. Sci.*, 1993, 9, 233.
116. Maeda, M., Tsuji, A., Ohshima, N., and Hukuoka, M., *J. Biolumin. Chemilumin.*, 1993, 8, 241.
117. Yoshimura, F., Suzuki, T., Yamada, M., and Hobo, T., *Bunseki Kagaku*, 1992, 41, 191.
118. Ahmed, T. E. A., and Townshend, A., *Anal. Chim. Acta*, 1994, 292, 169.
119. Psarellis, I. M., Deftereos, N. T., Sarantonis, E. G., and Calokerinos, A. C., *Anal. Chim. Acta*, 1994, 294, 27.
120. Perezruiz, T., Martinezlozano, C., Tomas, V., and Val, O., *Analyst*, 1995, 120, 471.
121. Psarellis, I. M., Sarantonis, E.G., and Calokerinos, A. C., *Anal. Chim. Acta*, 1993, 272, 265.
122. Ci, Y. X., Zheng, Y. G., Tie, J. K., and Chang, W. B., *Anal. Chim. Acta*, 1993, 282, 695.
123. Hu, X. C., Kitano, M., Takenaka, N., Bandow, H., Maeda, Y., and Zhang, D. I., *Bunseki Kagaku*, 1994, 43, 1077.
124. Alwarthan, A. A., Altamrah, S. A., and Alakel, A. A., *Anal. Sci.*, 1994, 10, 449.
125. Hansen, E. H., Norgaard, L., and Pedersen, M., *Talanta*, 1991, 38, 275.
126. Tabata, M., Totani, M., and Murachi, T., *Anal. Biochem.*, 1991, 193, 112.
127. Ishii, M., Ohno, Y., and Hobo, T., *Anal. Sci.*, 1991, 7, 873.
128. Fujimaki, T., Tani, T., Watanabe, S., Suzuki, S., and Nakazawa, H., *Anal. Chim. Acta*, 1993, 282, 175.
129. Perezruiz, T., Martinezlozano, C., Sanz, A., and Val, O., *Anal. Chim. Acta*, 1993, 284, 173.
130. Hansen, E. H., Winther, S. K., and Gundstrup, M., *Anal. Lett.*, 1994, 27, 1239.

131. Kishida, M., Makita, Y., Suzuki, T., Yamada, M., and Hobo, T., *Anal. Chem.*, 1991, 63, 2301.
132. Alwarthan, A. A., Altamrah, S. A., and Akel, A. A., *Anal. Chim. Acta*, 1993, 282, 169.
133. Deftereos, N. T., and Calokerinos, A. C., *Anal. Chim. Acta*, 1994, 290, 190.
134. Ishii, M., and Ito, K., *Bunseki Kagaku*, 1992, 41, 433.
135. Holeman, J. A., and Danielson, N. D., *Anal. Chim. Acta*, 1993, 277, 55.
136. Ohno, Y., Hobo, T., Tamura, R., and Ishii, M., *Bunseki Kagaku*, 1993, 42, 183.
137. Hu, X. C., Takenaka, N., Kitano, M., Bandow, H., Maeda, Y., and Hattori, M., *Analyst*, 1994, 119, 1829.
138. Scott, R. P. W., *Techniques and Practice of Chromatography*, Marcel Dekker, New York, 1995.
139. Poole, C. F., and Schuette, S. A., *Contemporary Practice of Chromatography*, Elsevier, Amsterdam, 1984.
140. Braithwaite, A., and Smith, F. J., *Chromatographic Methods*, 5th edn., Blackie Academic & Professional, London, 1996.
141. Scott, R. P. W., *Quantitative Analysis Using Chromatographic Techniques* (Ed. Katz, E.), John Wiley, Chichester, 1987.
142. Lawrence, J., *Organic Trace Analysis by Liquid Chromatography*, Academic Press, London, 1981.
143. Parris, N. A., *Instrumental Liquid Chromatography*, 2nd edn., Elsevier, Amsterdam, 1984, pp 193-220.
144. Ahuja, S., *Selectivity and Detectability Optimisations in HPLC*, Wiley-Interscience, New York, 1989, pp 87-91.
145. Ahuja, S., *Selectivity and Detectability Optimisations in HPLC*, Wiley-Interscience, New York, 1989, pp 161-173.
146. Hamilton, P. J., and Sewell, P. A., *Introduction to High-Performance Liquid Chromatography*, 2nd edn., Chapman and Hall, London, 1982, pp 33.
147. Braithwaite, A., and Smith, F. J., *Chromatographic Methods*, 5th edn., Blackie Academic & Professional, London, 1996, pp 37-40.
148. Scott, R. P. W., *Quantitative Analysis Using Chromatographic Techniques* (Ed. Katz, E.), John Wiley, Chichester, 1987, pp 8-9.
149. Braithwaite, A., and Smith, F. J., *Chromatographic Methods*, 5th edn., Blackie Academic & Professional, London, 1996, pp 26-30.
150. Braithwaite, A., and Smith, F. J., *Chromatographic Methods*, 5th edn., Blackie Academic & Professional, London, 1996, pp 30-37.

151. Ahuja, S., *Selectivity and Detectability Optimisations in HPLC*, Wiley-Interscience, New York, 1989, pp 3.
152. Braithwaite, A., and Smith, F. J., *Chromatographic Methods*, 5th edn., Blackie Academic & Professional, London, 1996, pp 288-290.
153. Yeung, E. S., *J. Chromatogr. Sci.*, 1989, 45, 117.
154. Fielden, P. R., *Chromatogr. Sci.*, 1992, 30, 45.
155. Slavin, W., Rhys Williams, R. T., and Adams, R. F., *J. Chromatogr.*, 1977, 134, 121.
156. Wheals, B. B., Vaughan, C. G., and Whitehouse, M. J., *J. Chromatogr.*, 1975, 106, 109.
157. Bowie, A. R., Sanders, M. G., and Worsfold, P. J., *J. Biolumin. Chemilumin.*, 1996, 11, 61.
158. Sanders, M. G., Andrew, K. N., and Worsfold, P. J., *Anal. Comm.*, 1997, 34, 13H.
159. Ishida J, Horike N, Yamaguchi M. *Anal. Chim. Acta*, 1995, 302, 61-7.
160. Tod, M., Legendre, J. Y., Chalom, J., Kouwatli, H., Poulou, M., Farinotti, R., and Mahuzier, G., *J. Chromatogr.*, 1992, 594, 386.
161. Ragab, G. H., Nohta, H., Kai, M., and Ohkura, Y., *Anal. Chim. Acta*, 1994, 298, 431.
162. Higashidate, S., and Imai, K., *Analyst*, 1992, 117, 1863.
163. Fu, C. G., Xu, H. D., and Wang, Z., *J. Chromatogr.*, 1993, 634, 221.
164. Fu, C. G., and Xu, H. D., *Analyst*, 1995, 120, 1147.
165. Katayama, M., Takeuchi, H., and Taniguchi, H., *Anal. Chim. Acta*, 1994, 287, 83.
166. Lee, W. Y., and Nieman, T. A., *J. Chromatogr.*, 1994, 659, 111.
167. Hanaoka, N., and Tanaka, H., *J. Chromatogr.*, 1992, 606, 129.
168. Sandmann, B. W., and Grayeski, M. L., *J. Chromatogr. B*, 1994, 653, 123.
169. Lewis, S. W., Worsfold, P. J., Lynes, A., and McKerrell, E. H., *Anal. Chim. Acta*, 1992, 266, 257.
170. Gachanja, A., and Worsfold, P. J., *Anal. Chim. Acta*, 1994, 290, 226.
171. Kwakman, P. J. M., Vanschaik, H. P., Brinkman, U. A. T., and Dejong, G. J., *Analyst*, 1991, 116, 1385.
172. Toyooka, T., Ishibashi, M., and Terao, T., *J. Chromatogr.*, 1992, 627, 75.
173. Tod, M., Prevot, M., Chalom, J., Farinotti, R., and Mahuzier, G., *J. Chromatogr.*, 1991, 542, 295.
174. Holeman, J. A., and Danielson, N. D., *J. Chromatogr. Sci.*, 1995, 33, 297.
175. Holeman, J. A., and Danielson, N. D., *J. Chromatogr.*, 1994, 679, 277.
176. Nishitani, A., Tsukamoto, Y., Kanda, S., and Imai, K., *Anal. Chim. Acta*, 1991, 251, 247.

177. Katayama, M., Taniguchi, H., Matsuda, Y., Akihama, S., Hara, I., Sato, H., Kaneko, S., Kuroda, Y., and Nozawa, S., *Anal. Chim. Acta*, 1995, 303, 333.
178. Sugiura, M., Kanda, S., and Imai, K., *Anal. Chim. Acta*, 1992, 266, 225.
179. Steijger, O. M., Dejong, G. J., Holthuis, J. J. M., and Brinkman, U. A. T., *J. Chromatogr.*, 1991, 557, 13.
180. Zhang, X. R., Baeyens, W. R. G., Vanderweken, G., Calokerinos, A. C., and Imai, K., *Anal. Chim. Acta*, 1995, 303, 137.
181. Uzu, S., and Imai, K., *Analyst*, 1991, 116, 1353.
182. Nakashima, K., Wada, M., Kuroda, N., Akiyama, S., and Imai, K., *J. Liq. Chromatogr.*, 1994, 17, 2111.
183. Nakashima, K., Maki, K., Kawaguchi, S., Akiyama, S., Tsukamoto, Y., and Imai, K., *Anal. Sci.*, 1991, 7, 709.
184. Capomacchia, A. C., Cho, J. K., Do, N. H., and Bunce, O. R., *Anal. Chim. Acta*, 1992, 266, 287.
185. Kwakman, P. J. M., Kamminga, D. A., Brinkman, U. A. T., and Dejong, G. J., *J. Chromatogr.*, 1991, 553, 345.
186. Abubaker, M. A., and Vonwandruszka, R., *Anal. Lett.*, 1991, 24, 93.
187. Niederlander, H. A. G., Nuijens, M. J., Dozy, E. M., Gooijer, C., and Velthorst, N. H., *Anal. Chim. Acta*, 1994, 297, 349.
188. Hayakawa, K., Kitamura, R., Butoh, M., Imaizumi, N., and Miyazaki, M., *Anal. Sci.*, 1991, 7, 573.
189. Maeda, M., Tsukagoshi, K., Murata, M., Takagi, M., and Yamashita, T., *Anal. Sci.*, 1994, 10, 583.
190. Hayakawa, K., Murahashi, T., Butoh, M., and Miyazaki, M., *Env. Sci. Tech.*, 1995, 29, 928.
191. Murahashi, T., Hayakawa, K., Iwamoto, Y., and Miyazaki, M., *Bunseki Kagaku*, 1994, 43, 1017.
192. Howard, A. L., Thomas, C. L. B., and Taylor, L. T., *Anal. Chem.*, 1994, 66, 1432.
193. Ryerson, T. B., Dunham, A. J., Barkley, R. M., and Sievers, R. E., *Anal. Chem.*, 1994, 66, 2841.
194. Chang, H. C. K., and Taylor, L. T., *Anal. Chem.*, 1991, 63, 486.
195. Kuroda, N., Nakashima, K., and Akiyama, S., *Anal. Chim. Acta*, 1993, 278, 275.
196. Fujinari, E. M., and Courthaudon, L. O., *J. Chromatogr.*, 1992, 592, 209.
197. Ikegawa, S., Hirabayashi, N., Yoshimura, T., Tohma, M., Maeda, M., and Tsuji, A., *J. Chromatogr. B*, 1992, 577, 229.

198. Kai, M., Ohkura, Y., Yonekura, S., and Iwasaki, M., *Anal. Chim. Acta*, 1994, 287, 75.
199. Skotty, D. R., and Nieman, T. A., *J. Chromatogr. B*, 1995, 665, 27.
200. Ishida, J., Sonezaki, S., Yamaguchi, M., and Yoshitake, T., *Analyst*, 1992, 117, 1719.
201. Fetzer, J. C., *Chemical Analysis of Polycyclic Aromatic Hydrocarbons*, (Ed. Vo-Dinh, T.), Wiley-Interscience, New York, 1989, pp 257-300.
202. Kwakman, P. J. M., and Brinkman, U. A. T., *Anal. Chim. Acta*, 1992, 266, 175.
203. Wise, S. A., Sander, L. C., and May, W. E., *J. Chromatog.*, 1993, 642, 329.
204. The Standing Committee of Analysts, DoE, *The Determination of 6 Specific Polynuclear Aromatic Hydrocarbons in Waters*, HMSO, London, 1985, pp 11.
205. Marriot, P. J., Carpenter, P. D., Brady, P. H., McCormick, M. J., Griffiths, A. J., Hatvani, T. S., and Rasdell, S. G., *J. Liq. Chromatog.*, 1993, 16, 3229.
206. Ahuja, S., *Selectivity and Detectability Optimisations in HPLC*, Wiley-Interscience, New York, 1989, pp 19-21.
207. Tucker, S. A., Acree, W. E., Cho, B. P., Harvey, R. G., and Fetzer, J. C., *Applied Spec.*, 45 (1991) 1699.
208. Miller, J. C., and Miller, J. N., *Statistics for Analytical Chemistry*, 3rd edn., Ellis Horwood, Chichester, 1993, pp 115-117.
209. Gachanja, A. N., PhD Thesis, University of Hull, Hull, 1991.
210. Chandross, E. A., *Tetrahedron Lett.*, 1963, 12, 761.
211. Rauhut, M. M., Bollyky, L. J., Roberts, B. G., Loy, M., Whitman, R. H., Iannota, A. V., Semsel, A. M., and Clarke, R. A., *J. Am. Chem. Soc.*, 1967, 89, 6515.
212. Rauhut, M. M., *Accounts of Chemical Research*, 1969, 2, 80.
213. Lechtken, P., and Turro, N. J., *Mol. Photochem.*, 1974, 6, 95.
214. Kwakman, P. J. M., Dejong, G. J., and Brinkman, U. A. T., *Trends Anal. Chem.*, 1992, 11, 232.
215. Schuster, G. B., *Acc. Chem. Res.*, 1979, 12, 366.
216. Koo, J. Y., and Schuster, G. B., *J. Am. Chem. Soc.*, 1977, 99, 6107.
217. McCapra, F., *Prog. Org. Chem.*, 1973, 8, 231.
218. Sigvardson, K. W., Kennish, J. M., and Birks, J. W., *Anal. Chem.*, 1984, 56, 1096.
219. Cordes, H. F., Richter, H. P., and Heller, C. A., *J. Am. Chem. Soc.*, 1969, 91, 7209.
220. DeCorpo, J. J., Baronavski, A., McDowell, M. V., and Saalfield, F. E., *J. Am. Chem. Soc.*, 1972, 94, 2879.
221. Hadd, A. G., and Birks, J. W., *Selective Detectors*, (Ed. Sievers, R. E.), John Wiley, Chichester, 1995, pp 213-221.

222. Givens, R. S., Jencen, D. A., Riley, C. M., Stobaugh, J. F., Chokshi, H., and Hanaoka, N., J., *Pharm. Biomed. Anal.*, 1990, 8, 477.
223. Honda, K., Miyaguchi, K., and Imai, K., *Anal. Chim. Acta*, 1985, 177, 103.
224. Imai, K., Nawa, H., Tanaka, M., and Ogata, H., *Analyst*, 1986, 111, 209.
225. Nakashima, K., Maki, K., Akiyama, S., Wang, W. H., Tsukamoto, Y., and Imai, K., *Analyst*, 1990, 114, 1413.
226. Mohan, A. G., and Turro, N. J., *J. chem. Educ.*, 1974, 51, 528.
227. Honda, K., Sekino, J., and Imai, K., *Anal. Chem.*, 1983, 55, 940.
228. Neuvonen, H., *J. Chem. Soc., Perkin Trans. 2*, 1994, 89.
229. Neuvonen, H., *J. Chem. Soc., Perkin Trans. 2*, 1995, 945.
230. Barnett, N. W., Bos, R., Lewis, S. W., Russell, R. A., *Analyst*, 1998, 123, 1239.
231. Stevani, C. V., Lima, D. F., Toscano, V. G., and Baader, W. J., *J. Chem. Soc. Perkin Trans. 2*, 1996, 989.
232. Jonsson, T., Emteborg, M., and Irgum, K., *Anal. Chim. Acta*, 1998, 361, 205.
233. Hadd, A. G., and Birks, J. W., *J. Org. Chem.*, 1996, 61, 2657.
234. Emteborg, M., Pontén, E., and Irgum, K., *Anal. Chem.*, 1997, 69, 2109.
235. Hadd, A. G., and Birks, J. W., *Selective Detectors*, (Ed. Sievers, R. E.), John Wiley, Chichester, 1995, pp 222-224.
236. Hadd, A. G., and Birks, J. W., *Selective Detectors*, (Ed. Sievers, R. E.), John Wiley, Chichester, 1995, pp 221-222.
237. Imai, K., and Weinberger, R., *Trends Anal. Chem.*, 1985, 4, 170.
238. Information Sheet, Camspec Limited, Cambridge, United Kingdom, 1996.
239. Gachanja, A. N., and Worsfold, P. J., *Anal. Proc.*, 1992, 29, 61.
240. Hamamatsu Photonics UK Limited, Enfield, United Kingdom, 1997.
241. Rauhut, M. M., *Acc. Chem. Res.*, 1969, 2, 80.
242. Gachanja, A. N., *Encyclopedia of Analytical Science* (Ed. Townshend A.), Academic Press, London, 1995, Vol. 7, pp 4047.
243. Badger, G. M., Buttery, R. G., Kimber, R. W. L., Lewis, G. E., Moritz, A. G., and Napier, I. M., *J. Chem. Soc.*, 1958, 2449.
244. Cook, J. W., Hewett, C. L., and Heiger, I., *J. Chem. Soc.*, 1933, 135, 395.
245. Alloway, B. J., and Ayres, D. C., *Chemical Principles of Environmental Pollution*, 2nd edn., Blackie Academic & Professional, London, 1997, pp 267-272.
246. Yang, S. K., Roller, P. P., and Gelboin, H. V., *Polynuclear Aromatic Hydrocarbons* (Ed. Jones, P. W. and Freudenthal, R. I.), Raven Press, New York, 1978, pp 285.
247. Gachanja, A. N., *Encyclopedia of Analytical Science* (Ed. Townshend A.), Academic Press, London, 1995, Vol. 7, pp 4045.

248. Pott, F., Oberdorster, B., Jacob, J., and Grimmer, G., *Environmental Carcinogens: Polycyclic Aromatic Hydrocarbons* (Ed. Grimmer, G.), CRC Press, Boca Raton, 1983, pp 139-142.
249. The Standing Committee of Analysts, DoE, *The Determination of 6 Specific Polynuclear Aromatic Hydrocarbons in Waters*, HMSO, London, 1985, pp 6.
250. Grimmer, G., Jacob, J., and Naujack, K. W., *Chemosphere*, 1997, 34, 2213.
251. Lee, M. L., Novotny, M., and Bartle, K.D., *Analytical Chemistry of Polycyclic Aromatic Compounds*, Academic Press, London, 1981, pp 156-187.
252. Wise, S. A., *Handbook of Polycyclic Aromatic Hydrocarbons* (Ed. Bjørseth, A., and Ramdahl T.), Marcel Dekker, New York, 1985, Vol. 2, pp 113-191.
253. Fell, A. F., Scott, H. P., Gill, R., and Moffat, A. C., *J. Chromatog.*, 1983, 282, 123
254. Amos, P., *J. Chromatog.*, 1981, 204, 469.
255. Sander, L. C., and Wise, S. A., *Advances in Chromatography* (Ed. Giddings, J. C., Grushka, E., Cazes, J., and Brown, P. R.), Marcel Dekker, New York, 1986, Vol. 25, pp 139.
256. Sander, L. C., and Wise, S. A., *Anal. Chem.*, 1984, 56, 505.
257. Sander, L. C., and Wise, S. A., *J. High Resolut. Chromatog.*, 1985, 8, 248.
258. Sander, L. C., and Wise, S. A., *J. High Resolut. Chromatog.*, 1988, 11, 383.
259. Sander, L. C., and Wise, S. A., *LC-GC*, 1990, 8(5), 378.
260. Wise, S. A., Benner, B. A., Chesler, S. N., Hilpert, L. R., Vogt, C. R., and May, W. E., *Anal. Chem.*, 1986, 58, 3067.
261. Jacob, J., *Quality assurance for Environmental Analysis*, (Ed. Quevauviller, Ph., Maier, E. A., and Griepink, B.), Elsevier, Amsterdam, 1995, pp 571-575.
262. Kowalski, B. R., *Chem. & Ind.*, 1978, November, 882.
263. Massart, D. L., Vandeginste, B. G. M., Deming, S. N., Michotte, Y., and Kaufman, L., *Chemometrics: A Textbook*, Elsevier, Amsterdam, 1988.
264. Brereton, R. G., *Analyst*, 1987, 112, 1635.
265. Kowalski, B. R., *Chemometrics: Theory and Applications*, ACS, Washington D. C., 1977.
266. Sharaf, M. A., Illman, D. L., and Kowalski, B. R., *Chemometrics*, Wiley-Interscience, New York, 1986.
267. Brereton, R. G., *Chemometrics: Applications of Mathematics and Statistics to Laboratory Systems*, Ellis Horwood, Chichester, 1990.
268. Haswell, S. J., *Practical Guide to Chemometrics*, Marcel Dekker, New York, 1992.
269. Adams, M. J., *Chemometrics in Analytical Spectroscopy*, Royal Society of Chemistry, Cambridge, 1995.

270. Beebe, K. R., and Kowalski, B. R., *Anal. Chem.*, 1987, 59, 1007A.
271. Martens, H., and Naes, T., *Multivariate Calibration*, Wiley, Chichester, 1989.
272. Pomeroy, R. S., Baker, M. E., Denton, M. B., and Dickson, A. G, *Applied Spec.*, 49 (1995) 1729.
273. Seasholtz, M. B., and Kowalski, B. R., *J. Chemometr.*, 1992, 6, 103.
274. Sanchez, E., and Kowalski, B. R., *J. Chemometr.*, 1988, 2, 247.
275. Howery, D. G., *Am. Lab.*, 1976, February, 14.
276. Wold, S., Esbensen, K., and Geladi, P., *Chemometr. Intell. Lab. Syst.*, 1987, 2, 37.
277. Meglen, R. R., *Marine. Chem.*, 1992, 39, 217.
278. Haaland, D. M., and Thomas, E. V., *Anal. Chem.*, 1988, 60, 1193.
279. Geladi, P., and Kowalski, B. R., *Anal. Chim. Acta*, 1986, 185, 1.
280. Höskuldsson, A., *J. Chemometr.*, 1988, 2, 211.
281. Blanco, M., Coello, J., Iturriaga, H., Maspoch, S., Redón, M., and Riba, J., *Anal. Chim. Acta*, 1992, 259, 219.
282. Lehrmann, R., Bürck, J., and Ache, H. J., *Process Qual Cont.*, 1993, 4, 139.
283. Lew, R., and Balke, S. T., *Applied Spec.*, 1993, 47, 1747.
284. Small, G. W., Arnold, M. A., and Marquardt, L. A., *Anal. Chem.*, 1993, 65, 3279.
285. Haaland, D. M., and Thomas, E. V., *Anal. Chem.*, 1988, 60, 1202.
286. Manne, R., *Chemometr. Intell. Lab. Syst.*, 1987, 2, 187.
287. Davies, A. M. C., *Spec. Europe*, 1998, 10(4), 28.
288. Davies, A. M. C., *Spec. Europe*, 1998, 10(6), 20.
289. Vo-Dinh, T., *Anal. Chem.*, 1978, 50, 396.
290. Vo-Dinh, T., *Applied Spec.*, 1982, 36, 576.
291. Horning, A. W. *Proceedings of the International Congress on Analytical Techniques in Environmental Chemistry*, (Ed. Albaiges, I.), Pergamon Press, Oxford, 1988 pp. 127-134.
292. MacLaurin, P., Worsfold, P. J., Townshend, A., Barnett, N. W., and Crane, M., *Analyst*, 1991, 116, 701.
293. Bundt, J., Herbei, W., Steinhart, H., Francke, W., and Franke, S., *J. High Res. Chromatogr.*, 1991, 14, 91.
294. Rawdon, M., *Encyclopedia of Analytical Science* (Ed. Townshend, A.), Academic Press, London, 1995, Vol. 3, pp1672-1679.
295. Braithwaite, A., and Smith, F. J., *Chromatographic Methods*, 5th edn., Blackie Academic & Professional, London, 1996, pp 278-286.
296. Scott, R. P. W., *Quantitative Analysis Using Chromatographic Techniques* (Ed. Katz, E.), John Wiley, Chichester, 1987, pp 65-70.

297. Jennings, R. N., and Capomacchia, A. C., *Anal. Chim. Acta*, 1988, 205, 207.
298. Orosz, G., and Dudar, E., *Anal. Chim. Acta*, 1991, 247, 141

Appendices

APPENDIX 1

Concentration (mg l^{-1}) data for the 2 component FL calibration and test set.

Sample number	Calibration set		Test set	
	Ant	B(k)F	Ant	B(k)F
1	2	2	4	0
2	0	0	1	0
3	4	2	3	3
4	3	2	1	3
5	0	1	3	1
6	4	0	2	0
7	1	4	0	0
8	4	1	4	4
9	3	0	3	4
10	2	3	1	1
11	0	3	-	-
12	0	2	-	-
13	4	3	-	-
14	0	4	-	-
15	3	1	-	-
16	1	3	-	-
17	4	4	-	-
18	2	0	-	-
19	2	4	-	-
20	3	4	-	-
21	3	3	-	-
22	1	0	-	-
23	2	1	-	-
24	1	2	-	-
25	1	1	-	-

APPENDIX 2

Concentration (mg l^{-1}) data for the 3 component FL calibration and test set.

Sample number	Calibration set			Test set		
	Ant	B(k)F	B(a)P	Ant	B(k)F	B(a)P
1	0	0	4	2	2	4
2	0	4	0	4	0	4
3	4	4	2	0	4	0
4	0	4	2	2	4	4
5	4	4	0	4	4	2
6	2	0	4	0	4	4
7	0	0	2	2	4	0
8	0	2	4	4	2	2
9	4	0	4	2	0	2
10	2	2	0	2	0	4
11	4	0	2	2	4	2
12	4	4	4	4	2	0
13	4	2	0	0	0	4
14	2	4	4	4	4	4
15	4	2	4	2	2	2
16	2	0	0	-	-	-
17	2	2	2	-	-	-
18	0	4	4	-	-	-
19	4	0	0	-	-	-
20	4	2	2	-	-	-
21	2	0	2	-	-	-
22	0	2	0	-	-	-
23	2	4	0	-	-	-
24	2	4	2	-	-	-
25	2	2	4	-	-	-
26	0	0	0	-	-	-
27	0	2	2	-	-	-

APPENDIX 3

Concentration (mg l^{-1}) data for the 4 component FL calibration and test set.

Sample number	Calibration set				Test set			
	Ant	B(k)F	B(a)P	Flu	Ant	B(k)F	B(a)P	Flu
1	4	4	0	0	1	1	3	3
2	0	0	4	4	3	3	1	3
3	4	4	4	4	3	3	3	3
4	4	0	0	0	3	3	1	1
5	0	0	4	0	3	1	3	1
6	4	0	0	4	1	3	3	1
7	4	0	4	4	1	1	1	1
8	0	4	0	0	1	3	1	1
9	4	4	0	4	1	3	3	3
10	4	4	4	0	3	1	3	3
11	4	0	4	0	3	1	1	3
12	0	4	4	0	1	3	1	3
13	0	4	4	4	1	1	3	1
14	0	4	0	4	3	3	3	1
15	0	0	0	4	3	1	1	1
16	0	0	0	0	1	1	1	3

APPENDIX 4

Concentration (mg l⁻¹) data for the 5 component FL calibration and test set.

Sample number	Calibration set				
	Ant	B(k)F	B(a)P	Flu	Chy
1	4	0	4	0	0
2	0	4	0	4	4
3	4	4	4	0	4
4	4	4	4	4	4
5	0	4	4	4	0
6	0	0	0	4	4
7	4	0	4	4	0
8	4	0	0	0	0
9	0	4	0	0	0
10	0	0	0	4	0
11	0	0	0	0	4
12	0	4	4	4	4
13	4	0	0	4	0
14	4	4	4	4	0
15	0	4	4	0	4
16	4	0	0	4	4
17	4	4	0	4	0
18	0	4	0	4	0
19	0	0	0	0	0
20	4	0	4	4	4
21	4	4	0	0	0
22	4	0	0	0	4
23	0	0	4	0	4
24	0	0	4	4	4
25	4	4	0	4	4
26	4	4	4	0	0
27	0	4	4	0	0
28	0	0	4	4	0
29	0	0	4	0	0
30	4	4	0	0	4
31	0	4	0	0	4
32	4	0	4	0	4

APPENDIX 4 continued

Sample number	Test set				
	Ant	B(k)F	B(a)P	Flu	Chy
1	3	3	1	3	1
2	1	1	1	3	1
3	1	3	1	1	3
4	3	1	1	3	3
5	3	1	1	3	1
6	1	1	1	1	1
7	1	1	3	1	3
8	3	3	1	1	3
9	3	1	1	1	1
10	3	3	3	1	3
11	3	3	3	3	3
12	1	1	1	1	3
13	3	1	3	1	1
14	1	3	3	1	3
15	3	1	3	1	3
16	3	3	1	1	1
17	3	1	3	3	3
18	3	1	1	1	3
19	1	3	3	3	1
20	1	3	1	1	1
21	1	1	1	3	3
22	3	3	1	3	3
23	1	1	3	3	1
24	3	3	3	3	1
25	1	1	3	1	1
26	1	3	1	3	3
27	3	1	3	3	1
28	1	1	3	3	3
29	1	3	3	1	1
30	3	3	3	1	1
31	1	3	3	3	3
32	1	3	1	3	1

APPENDIX 5

Concentration (mg l^{-1}) data for the 5 component sample simulation FL calibration and test set.

Sample number	Calibration set				
	Ant	B(k)F	B(a)P	Flu	Chy
1	3	0	3	50	0
2	3	3	3	50	0
3	0	3	0	0	0
4	3	0	0	50	20
5	0	0	0	50	0
6	0	3	3	0	0
7	3	3	3	50	20
8	3	0	3	0	20
9	3	0	0	0	20
10	3	0	0	0	0
11	0	3	3	50	20
12	0	0	3	0	20
13	3	3	0	50	0
14	3	3	3	0	0
15	0	0	0	0	20
16	3	0	3	0	0
17	0	3	3	0	20
18	0	3	0	50	0
19	0	3	3	50	0
20	3	0	3	50	20
21	0	0	3	50	20
22	0	0	0	0	0
23	0	3	0	50	20
24	0	0	0	50	20
25	0	0	3	0	0
26	0	3	0	0	20
27	0	0	3	50	0
28	3	3	0	0	0
29	3	3	0	50	20
30	3	0	0	50	0
31	3	3	3	0	20
32	3	3	0	0	20

APPENDIX 5 continued

Sample number	Test set				
	Ant	B(k)F	B(a)P	Flu	Chy
1	1	2	2	40	15
2	2	2	1	40	15
3	1	2	2	20	15
4	2	2	2	20	5
5	2	2	2	20	15
6	1	2	1	40	5
7	2	1	2	20	15
8	2	1	1	40	5
9	1	1	1	20	5
10	2	1	2	20	5
11	1	1	2	40	15
12	2	2	2	40	15
13	2	2	1	20	15
14	1	2	1	20	5
15	2	1	1	20	15
16	2	2	2	40	5
17	1	1	2	20	15
18	2	1	2	40	15
19	1	1	2	40	5
20	2	1	2	40	5
21	1	1	1	20	15
22	1	1	1	40	5
23	2	1	1	40	15
24	1	1	2	20	5
25	2	1	1	20	5
26	1	2	2	40	5
27	1	2	2	20	5
28	2	2	1	40	5
29	1	2	1	20	15
30	2	2	1	20	5
31	1	2	1	40	15
32	1	1	1	40	15

APPENDIX 6

Concentration (mg l^{-1}) data for the 2 component CL calibration and test set.

Sample number	Calibration set		Test set	
	B(a)P	B(k)F	B(a)P	B(k)F
1	0	0	1.7	0.1
2	0.5	0	0.9	0.2
3	1.0	0	1.1	0.9
4	1.5	0	1.5	0.7
5	2.0	0	0.5	1.5
6	0	0.5	0.8	2.0
7	0.5	0.5	0.9	0.6
8	1.0	0.5	1.0	0.8
9	1.5	0.5	1.3	0.6
10	2.0	0.5	0.5	0.2
11	0	1.0	-	-
12	0.5	1.0	-	-
13	1.0	1.0	-	-
14	1.5	1.0	-	-
15	2.0	1.0	-	-
16	0	1.5	-	-
17	0.5	1.5	-	-
18	1.0	1.5	-	-
19	1.5	1.5	-	-
20	2.0	1.5	-	-
21	0	2.0	-	-
22	0.5	2.0	-	-
23	1.0	2.0	-	-
24	1.5	2.0	-	-
25	2.0	2.0	-	-

APPENDIX 7

PUBLICATIONS

1. Bowie, A. R., Sanders, M. G., and Worsfold, P. J., Analytical applications of liquid phase chemiluminescence reactions – A review, *Journal of Bioluminescence and Chemiluminescence*, 1996, 11, 61-90.
2. Andrew, K. N., Sanders, M. G., Forbes, S., and Worsfold, P. J., Flow methods for the determination of polycyclic aromatic hydrocarbons using low power photomultiplier tube and charge coupled device chemiluminescence detection, *Analytica Chimica Acta*, 1997, 346, 113-120.
3. Sanders, M. G., Andrew, K. N., and Worsfold, P. J., Trends in chemiluminescence detection for liquid separations, *Analytical Communications*, 1997, 34, 13H-14H.

APPENDIX 8

PRESENTATIONS

1. *Simultaneous determination of polycyclic aromatic hydrocarbons by HPLC with fluorescence/chemiluminescence detection.* Poster presented at Research and Development Topics in Analytical Chemistry, University of Hull, July 1995.
2. *Peroxyoxalate chemiluminescence for the detection of polycyclic aromatic hydrocarbons.* Poster presented at Research and Development Topics in Analytical Chemistry, Nottingham Trent University, July 1996.
3. *The application of flow injection with aryl oxalate-sulphorhodamine 101 chemiluminescence for the determination of industrially important amine based compounds.* Poster presented at Research and Development Topics in Analytical Chemistry, University of Northumbria, July 1997.
4. *The determination of amines in non-aqueous media using flow injection analysis with chemiluminescence detection.* Poster presented at 24th Annual Conference of the Federation of Analytical Chemistry and Spectroscopy Societies, Providence, Rhode Island, USA, October 1997.

Regular lecture presentations at the University of Plymouth research seminars and at Shell Research and Technology Centre, Thornton were also given.

APPENDIX 9

CONFERENCES AND COURSES ATTENDED

1. Research and Development Topics in Analytical Chemistry, University of Hull, July 1995.
2. UK Chemometrics Discussion Group - PCR, PLS and Associated Techniques. Reading University, November 1995.
3. SIA '96. Wembley Exhibition and Conference Centre, April 1996.
4. Research and Development Topics in Analytical Chemistry, Nottingham Trent University, July 1996.
5. ERASMUS Eurocourse, Frontiers In Analytical Chemistry – Chemometrics, University of Antwerp (UIA), August 1996.
6. Analytical Science and the Environment, University of Northumbria, July 1997.
7. Research and Development Topics in Analytical Chemistry, University of Northumbria, July 1997.
8. 24th Annual Conference of the Federation of Analytical Chemistry and Spectroscopy Societies, Providence, Rhode Island, USA, October 1997.